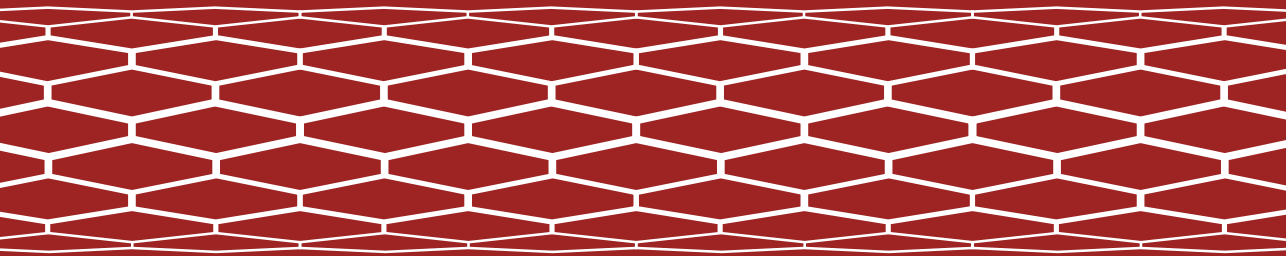


IMPROVING PERCUTANEOUS
CORONARY INTERVENTION
USING POST PROCEDURAL
PHYSIOLOGY AND
INTRAVASCULAR IMAGING



LAURENS J. C. VAN ZANDVOORT

ERASMUS UNIVERSITY
MEDICAL CENTER

Improving Percutaneous Coronary Intervention using Post Procedural Physiology and Intravascular Imaging

Improving Percutaneous Coronary Intervention using Post Procedural Physiology and Intravascular Imaging

Verbetering van een dotterprocedure door het gebruik van fysiologie en intravasculaire beeldvorming na een procedure

Thesis

to obtain the degree of Doctor from the
Erasmus University Rotterdam
by command of the
rector magnificus

prof. dr. R.C.M.E. Engels

and in accordance with the decision of the Doctorate Board.

The public defence shall be held on

Tuesday 24th of November at 15:30 hrs

by

Laurens Joannes Cornelis van Zandvoort

born in 's-Hertogenbosch, Netherlands.

Cover and lay-out design: Ton van Giessen | graphical designer

Printing: Proefschriftmaken | proefschriftmaken.nl

ISBN: 978-94-6423-045-1

©Laurens J.C. van Zandvoort, 2020

All rights reserved. No parts of this thesis may be reproduced or transmitted in any form or by any means, without prior permission of the author

ERASMUS UNIVERSITY ROTTERDAM



DOCTORAL COMMITTEE:

Promotor: Prof. dr. F. Zijlstra

Other members: Prof. dr. ir. H. Boersma
Prof. dr. N.M.D.A. van Mieghem
Prof. dr. J.J. Piek

Co-promotor: Dr. J. Daemen

*"What we call the beginning is often the end
And to make an end is to make a beginning."*

T.S. Eliot - Four Quartets

Financial support by the Dutch Heart Foundation for the publication of this thesis
is gratefully acknowledged

Table of contents

Chapter 1. **Introduction** 17

Part I - Value of Post PCI Physiology

Chapter 2. **Improving PCI outcomes using post procedural physiology and intravascular imaging** 35
van Zandvoort LJC, Ali Z, Kern M, van Mieghem NMDA, Mintz GS, Daemen J
(Submitted).

Chapter 3. **Routine fractional flow reserve measurement after percutaneous coronary intervention - The FFR-SEARCH study** 67
van Bommel RJ, Masdjedi K, Diletti R, Lemmert ME, van Zandvoort LJC, Wilschut J, Zijlstra F, de Jaegere PPT, Daemen J, van Mieghem NMDA
Circ Cardiovasc Interv. 2019;12(5):e007428

Chapter 4. **Predictors of post procedural fractional flow reserve – Insights from the FFR-SEARCH study** 89
van Zandvoort LJC, Masdjedi K, Neleman T, Tovar Forero MN, Wilschut J, den Dekker WK, de Jaegere PPT, Diletti R, Zijlstra F, van Mieghem NMDA, Daemen J
REC Interv Cardiol. 2020. (Accepted).

Chapter 5. **Impact of post-stenting fractional flow reserve on long term clinical outcomes – The FFR-SEARCH study** 105
Diletti R, Kanashka Masdjedi, Daemen J, van Zandvoort LJC, Neleman T, Wilschut J, den Dekker WK, Rutger J. van Bommel, Lemmert ME, Kardys I, Paul Cummins, de Jaegere PPT, Zijlstra F, van Mieghem NMDA
(Submitted).

Part II - Utility of (Post PCI) Intravascular Imaging

Chapter 6. **Predictors for clinical outcome of untreated stent edge dissections as detected by optical coherence tomography** 125
van Zandvoort LJC, Tomaniak M, Tovar Forero MN, Masdjedi K, Visseren L, Witberg K, Ligthart JMR, Kardys I, Lemmert ME, Diletti R, Wilschut J, de Jaegere PPT, Zijlstra F, van Mieghem NMDA, Daemen J
Circ Cardiovasc Interv. 2020;13(3):e008685.

Chapter 7. **Intravascular ultrasound findings of the Fantom sirolimuseluting bioresorbable scaffold at six- and nine-month follow-up: the FANTOM II study** 131
van Zandvoort LJC, Dudek D, Weber- Albers J, Abizaid A, Christiansen EH, Muller DWM, Kochman J, Kołtowski L, Flensted Lassen J, Wojdyla R, Wykrzykowska JJ, Onuma J, Daemen J
EuroIntervention. 2018;14(11):e1215-e23.

Chapter 8. **Serial invasive imaging follow-up of the first clinical experience with the Magmaris magnesium bioresorbable scaffold** 151
Tovar Forero MN, van Zandvoort LJC, Masdjedi K, Diletti R, Wilschut J, de Jaegere PPT, Zijlstra F, van Mieghem NMDA, Daemen J
Catheter Cardiovasc Interv. 2020;95(2):226-31.

Chapter 9. **References for left main stem dimensions: A cross sectional intravascular ultrasound analysis** 167
van Zandvoort LJC, Tovar Forero MN, Masdjedi K, Lemmert ME, Diletti R, Wilschut J, de Jaegere PPT, Zijlstra F, van Mieghem NMDA, Daemen J
Catheter Cardiovasc Interv. 2019;93(2):233-8.

Part III - Synergistic use of Intracoronary Imaging and Physiology

- Chapter 10. **Explanation of postprocedural fractional flow reserve below 0.85, a comprehensive ultrasound analysis of the FFR SEARCH registry** 183
van Zandvoort LJC, Masdjedi K, Witberg K, Ligthart JMR, Forero Tovar MN, Diletti R, Lemmert ME, Wilschut J, De Jaegere PPT, Boersma H, Zijlstra F, van Mieghem NMDA, Daemen J
Circ Cardiovasc Interv. 2019;12(2):e007030.
- Chapter 11. **Impact of intravascular ultrasound findings in patients with a post PCI fractional flow reserve ≤ 0.85 on 2 year clinical outcome** 207
van Zandvoort LJC, Masdjedi K, Neleman T, Tovar Forero MN, Wilschut J, den Dekker WK, de Jaegere PPT, Diletti R, Zijlstra F, van Mieghem NMDA, Daemen J
Int J Cardiol. 2020;317:33-36.
- Chapter 12. **FFR guided PCI optimization directed by high-definition IVUS versus standard of care: Rationale and study design of the prospective randomized FFR-REACT trial** 219
van Zandvoort LJC, Masdjedi K, Tovar Forero MN, Lenzen MJ, Ligthart JMR, Diletti R, Lemmert ME, Wilschut J, De Jaegere PPT, Zijlstra F, van Mieghem NMDA, Daemen J
Am Heart J. 2019;213:66-72.

Part IV - Innovations in Coronary Physiology

- Chapter 13. **Validation of 3-dimensional quantitative Coronary angiography based software to calculate vessel-fractional flow reserve: Fast Assessment of STenosis severity (FAST)-study** 239
Masdjedi K, van Zandvoort LJC, Balbi MM, Gijzen FJH, Ligthart JMR, Rutten MCM, Lemmert, Wilschut J, Diletti R, Zijlstra F, van Mieghem NMDA, Daemen J
EuroIntervention. 2019;EIJ-D-19-00466.
- Chapter 14. **Validation of novel 3-dimensional quantitative Coronary angiography based software to calculate vessel fractional flow reserve (vFFR) post stenting: fast assessment of stenosis severity post stenting, The FAST POST-study** 259
Masdjedi K, van Zandvoort LJC, Balbi MM, Ligthart JMR, Nuis RJ, Vermaire A, Lemmert ME, Wilschut J, Diletti R, De Jaegere PPT, Zijlstra F, van Mieghem NMDA, Daemen J
Catheter Cardiovasc Interv. (Accepted).
- Chapter 15. **Coronary physiology assessment in a cardiac transplant patient** 275
van Zandvoort LJC, Masdjedi K, Tovar Forero MN, Manintveld O, Daemen J
Neth Heart J. 2019;27(7-8):385-6.
- Chapter 16. **Validation of resting diastolic pressure ratio calculated by a novel algorithm and its correlation with distal coronary artery pressure to aortic pressure, instantaneous wave-free ratio, and fractional flow reserve, the dPR study** 279
Ligthart JMR*, Masdjedi K*, Witberg K, Mastik F, van Zandvoort LJC, Lemmert ME, Wilschut J, Diletti R, de Jaegere PPT, Zijlstra F, Kardys I, van Mieghem NMDA, Daemen J
Circ Cardiovasc Interv. 2018;11(12):e006911.

Chapter 17.	Validation of post procedural resting diastolic pressure ratio, its correlation with distal coronary artery pressure to aortic pressure, and fractional flow reserve	299
	Masdjedi K, van Zandvoort LJC, Neleman T, Tovar Forero MN, Kardys I, Ligthart JMR, den Dekker WK, Wilschut J, de Jaegere PPT, Diletti R, Zijlstra F, van Mieghem NMDA, Daemen J (Submitted).	

Part V - Innovations in Intravascular Polarimetry Assessment

Chapter 18.	Intravascular polarimetry in patients with coronary artery disease	321
	Otsuka K, Villiger M, Karanasos A, van Zandvoort LJC, Doradla P, Ren J, Lippok N, Daemen J, Diletti R, van Geuns RJ, Zijlstra F, van Soest G, Dijkstra J, Nadkarni SK, Regar E, Bouma BE <i>JACC Cardiovasc Imaging. 2020;13(3):790-801.</i>	
Chapter 19.	Intracoronary polarimetry of a honeycomb-like structure	349
	van Zandvoort LJC, Otsuka K, Bouma BE, Daemen J <i>EuroIntervention. 2019;EIJ-D-19-00431.</i>	
Chapter 20.	Polarimetric properties of coronary thrombus in patients with acute coronary syndrome	355
	van Zandvoort LJC, Otsuka K, Villiger M, Neleman T, Zijlstra F, van Mieghem NMDA, Bouma BE, Daemen J (Submitted).	
Chapter 21.	Summary & conclusion Samenvatting & conclusie	373
Epilogue	PhD portfolio	399
	List of publications	
	Acknowledgements Dankwoord	
	About the author	



INTRODUCTION

Chapter 1

A brief overview

A brief overview

Cardiovascular diseases and more specifically coronary artery disease (CAD) is a major cause of mortality and morbidity worldwide ¹.

CAD is the main cause for heart attacks, which occur when the arteries of the heart cannot deliver enough oxygen-rich blood to the heart. CAD or atherosclerosis is caused by the buildup of plaque, a waxy substance, inside the coronary arteries ^{2,3}. This buildup narrows the blood vessels of the heart which can intermittently prevent the heart muscle from receiving optimal blood supply. Atherosclerotic lesions typically form over the course of years to decades, making it one of the longest incubation periods among human diseases and are mainly comprised of fibrous tissue, lipids, calcium and inflammatory cells ².

Significant coronary artery disease typically presents as symptoms of chest pain, shortness of breath and fatigue. Stable CAD is categorized by complaints related to physical activity which may reduce in rest and is caused by the gradual increase in plaque burden in the coronary arteries. Acute coronary syndrome (ACS) on the other hand is associated with the sudden luminal narrowing of the coronary arteries, mostly due to the rupture of a plaque, resulting in a blood clot that may partially or completely occlude the artery. Complete coronary occlusion may cause cardiac muscle cells to go into apoptosis and result in a so called myocardial infarction.

The first line of treatment consists of drugs that stabilize the disease (lipid lowering therapies), reduce the myocardial oxygen demand (blood pressure lowering agents and vasodilators) and reduce the likelihood of the development of blood clots due to plaque rupture (antiplatelet agents) ⁵. In case of refractory symptoms of chest pain, a so called percutaneous coronary intervention (PCI) might be indicated ⁴. A PCI is performed by inserting a catheter (thin flexible tube) into the blood vessels through either the groin or the arm. Using a special type of X-ray called fluoroscopy, the catheter is advanced up until the ostium of the coronary artery ⁵. In order to fully visualize the coronary anatomy, a contrast medium is subsequently injected to visualize the artery, this is called angiography. In case of significant narrowing, a wire is used to cross the lesion and can then be used as a rail to advance small balloons or stents to treat the narrowing or occlusion ⁵. Once the plaque is compressed and the stent is in place, the balloon is deflated and withdrawn. The stent stays in the artery, holding it open. Stents primarily consist of metal. In contemporary clinical practice stents are covered by drugs to prevent inflammatory reactions by the body to the foreign metal in order

to prevent excessive tissue growth in the cell and subsequent new narrowing, a process called restenosis ⁶. In the past decades, several technical advancements were introduced, revolutionizing the field of interventional cardiology.

As such, progressive techniques to assess intracoronary anatomy and physiology (fractional flow reserve (FFR) were introduced ⁷. FFR is ratio of the distal coronary artery pressure (Pd) divided by the aortic pressure (Pa) under stress conditions induced by medication (hyperemia) (Figure 1). Intravascular imaging, comprised of intravascular ultrasound (IVUS) and optical coherence tomography (OCT) are small, tip based cameras, advanced into the coronaries based on either the reflection of sound or light respectively.

The implementation of FFR, IVUS and OCT in addition to quantitative coronary angiography, enables the operator to better plan, execute and reevaluate a coronary intervention ⁸. The latter techniques all moved away from the pure research setting and have been implemented in daily clinical practice.

Although percutaneous coronary interventions and pharmacologic therapies have improved the prognosis for patients with CAD, recurrent major adverse cardiovascular events still occur in a substantial proportion of cases. Physiological assessment and intravascular imaging to assist during a PCI have emerged as excellent tools to evaluate the status of a coronary artery. Nevertheless both technologies still have a relatively low uptake in daily clinical practice, specifically in a post PCI setting. This thesis aimed to provide the rationale for post PCI FFR and intravascular imaging and how the use of these conventional methods can be used in a post procedural setting to improve patient outcome.

Simultaneously new modalities have arisen to provide the operator with a more simplistic and faster method to assess the hemodynamic significance of a coronary lesion. In the current thesis we aimed to strengthen the body of evidence of the quantitative coronary angiography based vFFR and our own version of instantaneous free wave ratio (iFR): dPR.

Finally, we aimed to gain more insight in in-vivo plaque and thrombus vulnerability with the use of quantitative polarization properties, measured through standard intravascular OFDI catheters. The polarization features offer refined insight into intravascular tissue composition, consistent with our current understanding of the mechanisms involved in plaque and thrombus progression and destabilization.

A better understanding of intravascular physiology and imaging, combined with the knowledge on when to use it and how to interpret it, might be the key to improve patient outcome.

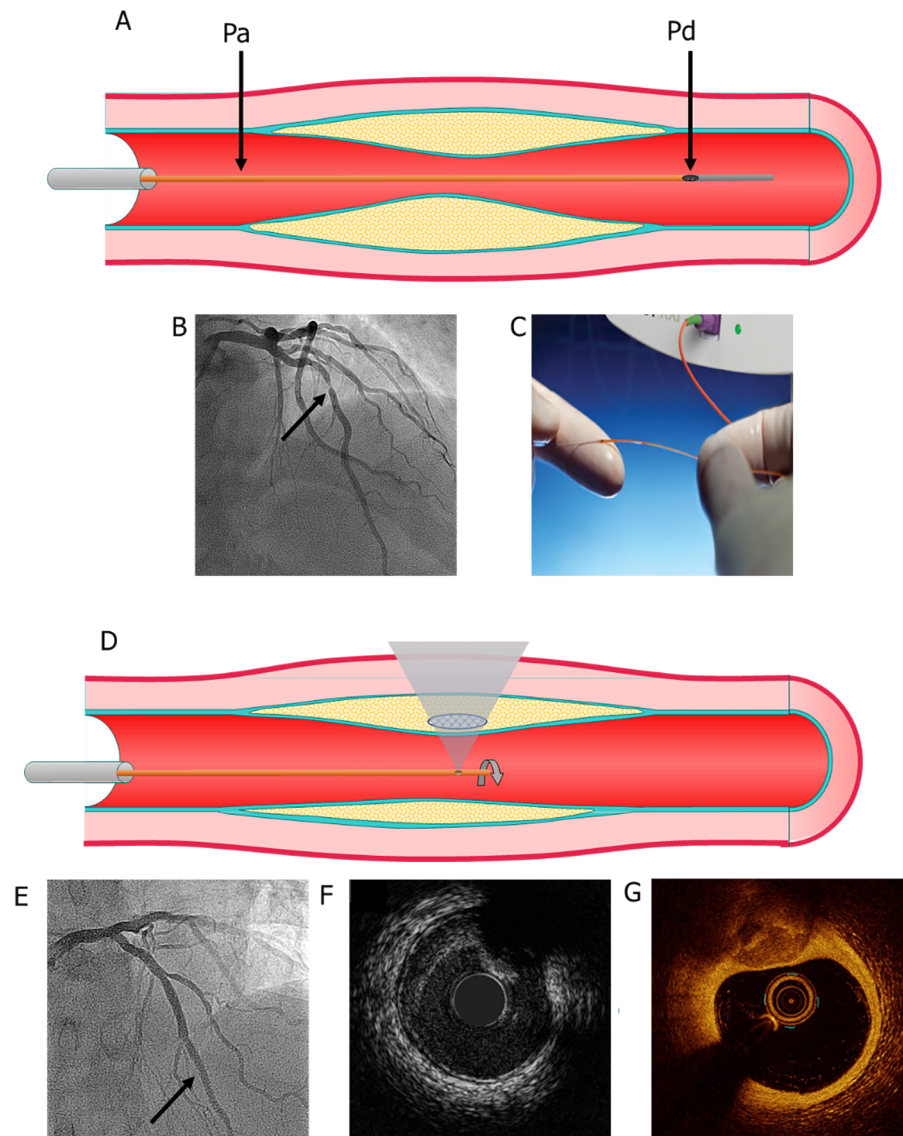


Figure 1. Intravascular diagnostic tools to evaluate coronary stenosis

A: schematic drawing of a significant coronary lesion with a microcatheter in place able to measure the pressure, the Pa is measured proximal of the lesion, the Pd is measured distal of the lesion (both under hyperemia); B: angiographic image of the location of interest; C: microcatheter which measures the pressure; D: schematic drawing of a non-significant calcified lesion with an imaging catheter in place; E: angiographic image of the location of interest; F: IVUS still frame with a calcified nodule at 1 o'clock; G: matched OCT still frame with a calcified nodule at 12 o'clock.

Outlines of the present thesis:

The use of coronary physiology is typically used to assess the hemodynamic significance of a coronary artery narrowing, providing valuable information on whether or not the individual lesion might warrant stenting. The technology however is barely used for post PCI evaluation. In PART I (Chapter 2 through 5) we will discuss the contemporary value of post PCI physiology

In Chapter 2 we begin with a broad overview of and history of post PCI physiology and intravascular imaging modalities in a state-of-the-art review format. Recent studies demonstrated that with the use of conventional intravascular imaging and physiology, clinical outcomes can be improved, while also newer modalities like angiography based fractional flow reserve (FFR) and hybrid imaging catheters are entering the stage. With the use of these modalities, several vessel and stent related predictors of major adverse cardiac events (MACE) can be found and we will discuss their impact on outcome and when additional treatment is required.

FFR is the current gold standard to determine the hemodynamic severity of an angiographically intermediate coronary stenosis. Post procedural evaluation is typically performed by angiographic guidance alone and much less is known about the prognostic effects FFR measured directly after a PCI. Therefore the Chapter 3 to 5 will focus on the use FFR directly measured after coronary stenting. These chapters are based on the FFR SEARCH registry, the largest prospective post PCI FFR registry to date including up to 1000 patients. In Chapter 3 the initial demographic and descriptive findings of the FFR SEARCH trial will be discussed, including the 30 day outcome figures.

In the next chapter, Chapter 4, we will provide the readers with a dedicated analysis, answering the question, what are the predictors of post procedural FFR values. The study describes several patient and vessel characteristics which will substantially contribute to the post procedural value measured.

In Chapter 5, the primary endpoint of the FFR SEARCH registry, the two year clinical outcomes will be evaluated. The study uses a cut-off value for the definition of sub-optimal FFR (FFR <0.90) already hypothesized in the FAME 1 and FAME 2 trials and supported by large meta-analyses but never evaluated in a prospective fashion.

In PART II (chapter 6 through 9) the utility of (post PCI) intravascular imaging will be discussed and we will take a closer look at the specifics and merits of intravascular imaging to improve patient outcome.

First, stent implantation for the treatment of coronary artery disease can cause unintended tearing at the site of vessel wall adjacent to the stent struts resulting in a stent edge dissection (SED). Prior research indicated that SEDs increase the risk of stent thrombosis and MACE in the short- to mid-term follow-up⁹⁻¹³. SEDs can be assessed with the use of angiography, however the likelihood to spot one can be increased with use of IVUS and even more with optical coherence tomography (OCT)¹⁴⁻²⁰. Although SEDs increase the risk of adverse events, not all SEDs visualized by OCT warrant additional treatment. Therefore, the aim in Chapter 6 was to provide a detailed morphometric characterization of SEDs and define predictors for outcome in patients with untreated SEDs. Additionally, we assessed the healing patterns of SEDs by serial OCT.

In Chapter 7, we aimed to investigate the luminal integrity 6 to 9 months after implantation of the Fantom bioresorbable scaffold (BRS) with the use of IVUS. The sirolimus-eluting Fantom BRS is a novel technology that is characterized by its thin struts, rapid and broad expansion capability, and most uniquely, its high radiopacity^{21, 22}. The angiographic and clinical results from the first cohort, demonstrated that the Fantom scaffold is capable of treating non-complex de novo native coronary artery lesions with low late lumen loss and MACE at 6 months²². With a backbone that is designed to be absorbed within 4 to 5 years, minimal loss of radial strength is essential to prevent high obstruction volumes²¹. The 6 and 9 months IVUS derived dimensions will therefore provide additional more detailed information on the performance and safety of this novel device.

In Chapter 8, as part of a single center experience, we aimed to assess the performance of another bioresorbable scaffold, the commercially available Magmaris sirolimus-eluting BRS, at different time points with the use of OCT.

Finally, a high risk patient subset that might benefit in particular from the use of intracoronary imaging to guide stent implantation is the cohort of patients with left-main stem disease. Although stenting of the left main artery has become a valid alternative to coronary artery bypass grafting, patients presenting with left main coronary artery stenosis are known to be at significantly increased risk for future major adverse cardiac events. The 2018 ESC guidelines provide a class IIa recommendation for IVUS-guided assessment of unprotected left main disease. In Chapter 9, the normal dimension of left main coronaries will be discussed as measured with IVUS. While clear guidelines exist on what threshold of minimal lumen area should be treated, no data was yet available on the dimensions that should be aimed for.

PART III (chapter 10 through 12) focusses on the integration of both post

procedural FFR and high definition IVUS with the aim to identify specific patient populations and vessel characteristic as assessed with IVUS to improve patient outcome.

First, a sub-study of the FFR SEARCH trial is discussed in Chapter 10. A dedicated high definition intravascular ultrasound (HD-IVUS) analysis was performed in a subgroup of 95 patients 100 vessels with a post PCI FFR ≤ 0.85 and 20 patients with an FFR > 0.85 . The study provides a quantitative in-depth IVUS and quantitative coronary angiography (QCA) analysis of vessels with a suboptimal post procedural FFR in order to find a rationale for the low FFR values.

Second, the subsequent sub-study of FFR SEARCH, Chapter 11, focusses on the two year outcome figures in the latter IVUS cohort. We discuss the event rates between groups of patients with and without luminal abnormalities as seen on IVUS.

While post procedural FFR proved to predict long-term adverse events, little is known on whether additional post procedural optimization based on a low post PCI FFR improves outcome.

The latter question resulted in the design of the FFR REACT trial, of which the design is described in Chapter 12. In this chapter the specifics of the single center randomized control trial are evaluated and substantiated while going into depth to discuss the detailed procedural methods of an IVUS guided optimization after a suboptimal post procedural FFR (< 0.90).

PART IV (chapter 13 through 17) evolves around novel physiology indices and recent innovations in this field. The introduction of FFR enabled the physician for the first time to evaluate the coronary arteries in vivo^{7, 23}. FFR and the instantaneous free wave ratio (iFR) both moved away from the pure research setting and have been implemented in daily clinical practice, however implementation in daily clinical practice has been low²⁴. At the moment, there is a need for faster and easier physiologic assessments. First, in Chapter 13, we will discuss the validation of a novel 3D-QCA based software tool to calculate FFR without the use of a pressure wire or microcatheter: vFFR. Through a pre-clinical technical validation model, we aimed to correlate vFFR with computational fluid dynamics and invasively measured flow parameters. Additionally, we investigated the agreement and diagnostic value of vFFR as compared to invasively measured FFR using a dedicated pressure wire under maximum hyperemia. Finally, we assessed the inter-observer variability of the vFFR computation.

Chapter 14 describes an observational cohort study including patients who

underwent a successful PCI and who received a post PCI FFR measurement with the Navvus microcatheter. The aim of the study was to assess the feasibility of the vFFR software in a post PCI setting and measure the correlation and agreement between vFFR and invasively measured FFR. In addition, we assessed the ability of vFFR to identify post PCI FFR values <0.90 , since this might be a clinically relevant cut-off to predict further MACE²⁵.

In Chapter 15, we will show how vFFR might play a future role in lesion assessment in patients with a potential impaired microvascular dysfunction. We illustrate this using a clinical case from the Erasmus University Medical Center (Erasmus MC).

In contrast to FFR, and recently validated in large randomized trials, iFR provides the operator with a resting index in a coronary vessel without the need for a hyperemic agent^{26, 27}. However, the conventional iFR wire and algorithm are owned by a single vendor (Phillips, Volcano Corporation), therefore the aim of Chapter 16 was to develop and assess the feasibility of a generic non-hyperemic ratio: dPR. In this section we discuss the substitutable value of dPR towards IFR, Pd/Pa and pressure wire derived FFR. In Chapter 17 we assessed the feasibility of this novel index in a post PCI setting. We investigated the correlation of post PCI dPR and FFR in order to identify vessels and patients at risk for future events without the need for hyperemic agents.

The final part of this dissertation, PART V (chapter 18-20), will focus on innovations in intravascular polarimetry assessment and its potential applicability in daily clinical practice.

Intravascular OCT and optical frequency domain imaging (OFDI) currently offer the highest spatial resolution for invasive coronary imaging²⁸. The latter modalities construct a series of cross-sectional images by using a near-infrared spectrum light to measure the echo time delay and the intensity of the backscattered light²⁹. Despite the merits of contemporary intravascular imaging such as OFDI and OCT, there remains a demand to improve plaque morphology characterization. In Chapter 18 we will describe the first-in-man cohort study to use the novel imaging modality, developed at the Massachusetts General Hospital in Boston. The polarization sensitive (PS) OFDI allows automatic co-registration of polarimetric measurements along with the standard intensity data, using a conventional OFDI catheter³⁰. Tissue with fibrillar architecture, such as collagen or arterial smooth muscle cells, exhibit birefringence, an optical property that results in a differential delay, or retardation, between light polarized parallel to the tissue fibrillar components and light having a perpendicular polarization. Depolarization corresponds to a randomization of the detected polarization states

and complements birefringence for the polarimetric characterization of tissue³⁰. The study in chapter 18 discusses the results from the OPTICS study performed in Rotterdam, Erasmus MC. In this study, a total of 30 patients presenting with stable angina underwent a PS-OFDI pullback before or after a coronary intervention. We will describe the birefringence and depolarization properties in different plaque types as well as a dedicated cap analysis on thick and thin cap lipid rich plaques.

In 2018 we started the POLARIS-I study, a single center study to assess the merits of PS-OFDI, focusing on patients presenting with an acute coronary syndrome.

One case from the POLARIS-I registry was specifically interesting since the right coronary artery of a patient presenting with a non-ST elevation myocardial infarction displayed a not so often seen honeycomb-like structure on the PS-OFDI. In Chapter 19, we will discuss this particular case and include a potential rationale for the observed polarimetric distribution.

Finally in Chapter 20, we will dive deeper into the POLARIS-I study and investigate the polarimetric properties of thrombus containing lesions in patients presenting with an acute coronary syndrome.

REFERENCES

1. Roth GA, Johnson C, Abajobir A, Abd-Allah F, Abera SF, Abyu G, et al. Global, Regional, and National Burden of Cardiovascular Diseases for 10 Causes, 1990 to 2015. *Journal of the American College of Cardiology*. 2017;70(1):1-25.
2. Libby P. Mechanisms of acute coronary syndromes and their implications for therapy. *N Engl J Med*. 2013;368(21):2004-13.
3. Stary HC, Blankenhorn DH, Chandler AB, Glagov S, Insull W, Jr., Richardson M, et al. A definition of the intima of human arteries and of its atherosclerosis-prone regions. A report from the Committee on Vascular Lesions of the Council on Arteriosclerosis, American Heart Association. *Circulation*. 1992;85(1):391-405.
4. Cram P, House JA, Messenger JC, Piana RN, Horwitz PA, Spertus JA. Indications for percutaneous coronary interventions performed in US hospitals: a report from the NCDR®. *American heart journal*. 2012;163(2):214-21.e1.
5. Neumann F-J, Sousa-Uva M, Ahlsson A, Alfonso F, Banning AP, Benedetto U, et al. 2018 ESC/EACTS Guidelines on myocardial revascularization. *European Heart Journal*. 2018;ehy394-ehy.
6. Partida RA, Yeh RW. Contemporary Drug-Eluting Stent Platforms: Design, Safety, and Clinical Efficacy. *Cardiology clinics*. 2017;35(2):281-96.
7. Pijls NH, van Son JA, Kirkeeide RL, De Bruyne B, Gould KL. Experimental basis of determining maximum coronary, myocardial, and collateral blood flow by pressure measurements for assessing functional stenosis severity before and after percutaneous transluminal coronary angioplasty. *Circulation*. 1993;87(4):1354-67.
8. Maehara A, Matsumura M, Ali ZA, Mintz GS, Stone GW. IVUS-Guided Versus OCT-Guided Coronary Stent Implantation: A Critical Appraisal. *JACC Cardiovasc Imaging*. 2017;10(12):1487-503.
9. Biondi-Zoccai GGL, Agostoni P, Sangiorgi GM, Airoidi F, Cosgrave J, Chieffo A, et al. Incidence, predictors, and outcomes of coronary dissections left untreated after drug-eluting stent implantation†. *European Heart Journal*. 2006;27(5):540-6.
10. Choi S-Y, Witzenbichler B, Maehara A, Lansky AJ, Guagliumi G, Brodie B, et al. Intravascular Ultrasound Findings of Early Stent Thrombosis After Primary Percutaneous Intervention in Acute Myocardial Infarction A Harmonizing Outcomes With Revascularization and Stents in Acute Myocardial Infarction (HORIZONS-AMI) Substudy. *Circulation-Cardiovascular Interventions*. 2011;4(3):239-47.
11. Cutlip DE, Baim DS, Ho KK, Popma JJ, Lansky AJ, Cohen DJ, et al. Stent thrombosis in the modern era: a pooled analysis of multicenter coronary stent clinical trials. *Circulation*. 2001;103(15):1967-71.
12. Cheneau E, Leborgne L, Mintz GS, Kotani J, Pichard AD, Satler LF, et al. Predictors of subacute stent thrombosis - Results of a systematic intravascular ultrasound study. *Circulation*. 2003;108(1):43-7.
13. Rogers JH, Lasala JM. Coronary artery dissection and perforation complicating percutaneous coronary intervention. *J Invasive Cardiol*. 2004;16(9):493-9.
14. Kobayashi N, Mintz GS, Witzenbichler B, Metzger DC, Rinaldi MJ, Duffy PL, et al. Prevalence, Features, and Prognostic Importance of Edge Dissection After Drug-Eluting Stent Implantation: An ADAPT-DES Intravascular Ultrasound Substudy. *Circ Cardiovasc Interv*. 2016;9(7):e003553.
15. Kume T, Okura H, Miyamoto Y, Yamada R, Saito K, Tamada T, et al. Natural History of Stent Edge Dissection, Tissue Protrusion and Incomplete Stent Apposition Detectable Only on Optical Coherence Tomography After Stent Implantation - Preliminary Observation. *Circulation Journal*. 2012;76(3):698-703.
16. Chamie D, Bezerra HG, Attizzani GF, Yamamoto H, Kanaya T, Stefano GT, et al. Incidence, Predictors, Morphological Characteristics, and Clinical Outcomes of Stent Edge Dissections Detected by Optical Coherence Tomography. *Jacc-Cardiovascular Interventions*. 2013;6(8):800-13.
17. Liu X, Tsujita K, Maehara A, Mintz GS, Weisz G, Dangas GD, et al. Intravascular Ultrasound Assessment of the Incidence and Predictors of Edge Dissections After Drug-Eluting Stent Implantation. *JACC: Cardiovascular Interventions*. 2009;2(10):997-1004.
18. Kawamori H, Shite J, Shinke T, Otake H, Matsumoto D, Nakagawa M, et al. Natural consequence of post-intervention stent malapposition, thrombus, tissue prolapse, and dissection assessed by optical coherence tomography at mid-term follow-up. *European Heart Journal Cardiovascular Imaging*. 2013;14(9):865-75.
19. Bouki KP, Sakkali E, Toutouzas K, Vlad D, Barmperis D, Phychari S, et al. Impact of coronary artery stent edge dissections on long-term clinical outcome in patients with acute coronary syndrome: an optical coherence tomography study. *Catheter Cardiovasc Interv*. 2015;86(2):237-46.
20. Ali ZA, Maehara A, Genereux P, Shlofmitz RA, Fabbicocchi F, Nazif TM, et al. Optical coherence tomography compared with intravascular ultrasound and with angiography to guide coronary stent implantation (ILUMIEN III: OPTIMIZE PCI): a randomised controlled trial. *Lancet*. 2016;388(10060):2618-28.
21. Costa JdR, Abizaid A, Chamie D, Lansky A, Kochman J, Koltowski L. INITIAL RESULTS OF THE FANTOM 1 TRIAL: A FIRST-IN-MAN EVALUATION OF A NOVEL, RADIOPAQUE SIROLIMUS-ELUTING BIORESORBABLE VASCULAR SCAFFOLD. *Journal of the American College of Cardiology*. 2016;67(13 Supplement):232.
22. Abizaid A, Carrié D, Frey N, Lutz M, Weber-Albers J, Dudek D, et al. 6-Month Clinical and Angiographic Outcomes of a Novel Radiopaque Sirolimus-Eluting Bioresorbable Vascular Scaffold. *JACC: Cardiovascular Interventions*. 2017;10(18):1832.
23. Potkin BN, Bartorelli AL, Gessert JM, Neville RF, Almagor Y, Roberts WC, et al. Coronary artery imaging with intravascular high-frequency ultrasound. *Circulation*. 1990;81(5):1575-85.
24. Gotberg M, Cook CM, Sen S, Nijjer S, Escaned J, Davies JE. The Evolving Future of Instantaneous Wave-Free Ratio and Fractional Flow Reserve. *J Am Coll Cardiol*. 2017;70(11):1379-402.
25. Wolfrum M, Fahrni G, de Maria GL, Knapp G, Curzen N, Kharbada RK, et al. Impact of impaired fractional flow reserve after coronary interventions on outcomes: a systematic review and

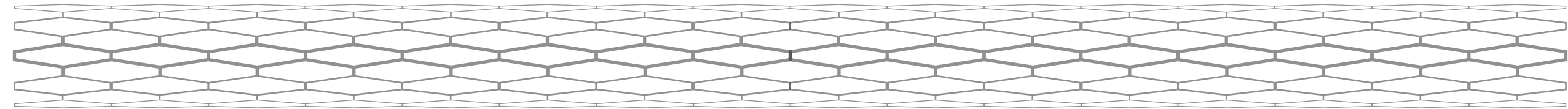
- meta-analysis. *BMC Cardiovascular Disorders*. 2016;16(1):177.
26. Gotberg M, Christiansen EH, Gudmundsdottir IJ, Sandhall L, Danielewicz M, Jakobsen L, et al. Instantaneous Wave-free Ratio versus Fractional Flow Reserve to Guide PCI. *N Engl J Med*. 2017.
27. Davies JE, Sen S, Dehbi HM, Al-Lamee R, Petraco R, Nijjer SS, et al. Use of the Instantaneous Wave-free Ratio or Fractional Flow Reserve in PCI. *N Engl J Med*. 2017;376(19):1824-34.
28. Villiger M, Otsuka K, Karanasos A, Doradla P, Ren J, Lippok N, et al. Repeatability Assessment of Intravascular Polarimetry in Patients. *IEEE Trans Med Imaging*. 2018;37(7):1618-25.
29. Jang IK, Tearney GJ, MacNeill B, Takano M, Moselewski F, Iftima N, et al. In vivo characterization of coronary atherosclerotic plaque by use of optical coherence tomography. *Circulation*. 2005;111(12):1551-5.
30. Villiger M, Otsuka K, Karanasos A, Doradla P, Ren J, Lippok N, et al. Coronary Plaque Microstructure and Composition Modify Optical Polarization: A New Endogenous Contrast Mechanism for Optical Frequency Domain Imaging. *JACC Cardiovasc Imaging*. 2018.

Abbreviations

ACS	Acute Coronary Syndrome	MLA	Minimal Lumen Area
BMI	Body Mass Index	MLD	Minimal Lumen Diameter
BRS	Bioresorbable Scaffold	MSA	Minimal Stent/Scaffold Area
BVS	Bioresorbable Vascular Scaffold (Absorb)	NC	Non-Compliant
CABG	Coronary Artery Bypass Graft	NHPR	Non-Hyperemic Pressure Ratios
CAD	Coronary Artery Disease	NSD	Normalized Standard Deviation
CTO	Chronic Total Occlusion	NSTEMI	Non ST Elevated Myocardial Infarction
CV	Variance Coefficient	nTAV	normalized Total Atheroma Volume
CVD	Cardiovascular Disease	OCT	Optical Coherence Tomography
DAT	Desaminotyrosine	OFDI	Optical Frequency Domain Imaging
DES	Drug Eluting Stent	OR	Odds Ratio
DOCE	Device Orientated Cardiovascular Event	PAV	Percent Atheroma Volume
dPR	diastolic Pressure Ratio	PCI	Percutaneous Coronary Intervention
DS	Diameter Stenosis	Pd/Pa	the Pressure in the Distal coronary artery to the Pressure in the Aorta ratio
EEM	External Elastic Membrane	PR	Plaque Rupture
FC	Fibro-Calcified plaque	PS-OFDI	Polarization-Sensitive Optical Frequency Domain Imaging
FCT	Fibrous Cap thickness	QCA	Quantitative Coronary Angiography
FFR	Fractional Flow Reserve	QFR	Quantitative Flow Ratio
FP	Fibrous Plaque	R ²	Squared Pearson Correlation Coefficient
GEE	Generalized Estimating Equation	RCA	Right Coronary Artery
GM	Geographical Miss	ROI	Region Of Interest
HD	High Definition	RVD	Reference Vessel Diameter
HR	Hazard Ratio	SA	Stent/Scaffold Area
iFR	instantaneous Wave Free Ratio	SAP	Stable Angina Pectoris
IQR	Inter Quartile Range	SD	Standard Deviation
ISA	Incomplete Strut Apposition	SED	Stent Edge Dissection
IVUS	Intravascular Ultrasound	SEM	Standard Error of the Mean
LA	Lumen Area	SE-MEA	Scaffold Expansion according to Manufacturer's Expected Area
LAD	Left Anterior Descending Artery	SE-RVA	Scaffold Expansion according to Reference Vessel Area
LCX	Left Circumflex Artery	STEMI	ST segment Elevation Myocardial Infarction
LLL	Late Lumen Loss	TCFA	Thin Cap Fibroatheroma
LME-model	Linear Mixed Effects Model	ThCFA	Thick Cap Fibroatheroma
MACE	Major Adverse Cardiac Event	TLF	Target Lesion Failure
MI	Myocardial Infarction	TVF	Target Vessel Failure
		VA	Vessel Area
		vFFR	Vessel Fractional Flow Reserve

PART I

VALUE OF POST
PCI PHYSIOLOGY



Chapter 3



Routine Fractional Flow Reserve Measurement after Percutaneous Coronary Intervention – The FFR-SEARCH Study

van Bommel RJ, Masdjedi K, Diletti R, Lemmert ME, van Zandvoort LJC, Wilschut J, Zijlstra F, de Jaegere PPT, Daemen J, van Mieghem NMDA

*Erasmus University Medical Center, Thoraxcenter, Department of cardiology,
Rotterdam, the Netherlands*

Circ Cardiovasc Interv. 2019;12(5):e007428

ABSTRACT

Background: Fractional flow reserve (FFR) is the current gold standard to determine hemodynamic severity of angiographically intermediate coronary lesions. Much less is known about the prognostic effects of FFR measured directly after percutaneous coronary intervention (PCI). The aims of this study were to evaluate post-PCI FFR values, identify predictors for a low post-PCI FFR, and to investigate whether a relationship between postprocedural FFR and outcome during 30-day follow-up exists.

Methods and Results: The FFR-SEARCH (Fractional Flow Reserve—Stent Evaluated at Rotterdam Cardiology Hospital) is a prospective registry in which FFR measurements were performed after PCI in 1000 consecutive patients. All FFR measurements were performed under maximum hyperemia with intravenous adenosine with the Navvus RXi system (ACIST Medical Systems, Eden Prairie, MN). The clinical end point was defined as a composite of death, target vessel revascularization, or nonfatal myocardial infarction at 30-day follow-up. Measurement of post-PCI FFR was successful in 959 patients (96%), and a total of 1165 lesions were assessed. There were no complications related to the microcatheter. A total of 322 ST-segment–elevation myocardial infarction patients with 371 measured lesions were excluded leaving 637 patients with 794 measured lesions for the final analysis. Overall post-PCI FFR was 0.90 ± 0.07 . In 396 lesions (50%), post-PCI FFR was >0.90 . A total of 357 patients (56%) had ≥ 1 lesion(s) with a post-PCI FFR ≤ 0.90 , and 73 patients (11%) had ≥ 1 lesion(s) with a post-PCI FFR ≤ 0.80 with post-PCI FFR ≤ 0.80 in 78 lesions (9.8%). Complex lesion characteristics, use of multiple stents and smaller reference vessel diameter was associated with post-PCI FFR ≤ 0.90 . During follow-up, 11 patients (1.8%) reached the clinical end point. There was no significant relationship between post-PCI FFR and the clinical end point at 30-day follow-up ($P=0.636$).

Conclusion: Routine measurement of post-PCI FFR using a monorail microcatheter is safe and feasible. Several lesion and patient characteristics were associated with a low post-PCI FFR. Post-PCI FFR did not correlate with clinical events at 30 days.

WHAT IS KNOWN

Fractional flow reserve (FFR) is the current gold standard to determine the hemodynamic severity of angiographically intermediate coronary lesions.

Previous studies, using mainly pressure wires, suggested a relationship between low FFR after coronary stenting and future adverse cardiac events but were either small in sample-size or used selected patients.

WHAT THE STUDY ADDS

Routine measurement of FFR after coronary stenting using a dedicated monorail microcatheter is safe and feasible.

Both lesion and patient characteristics are associated with a low FFR after coronary stenting.

Low FFR after coronary stenting is not associated with clinical events at 30-day follow-up.

INTRODUCTION

Fractional flow reserve (FFR) is the current gold standard to determine hemodynamic severity of angiographically intermediate coronary lesions. Large randomized studies have established the superiority of FFR and even demonstrated beneficial effects on long-term outcome (death, myocardial infarction [MI], and repeat revascularization) in patients treated with FFR-guided percutaneous coronary intervention (PCI) as compared to angiography-guided PCI alone ¹⁻³. As a result, the use of FFR in patients with intermediate coronary lesions and no previously documented ischemia has been given a class I recommendation in current European Society of Cardiology guidelines ⁴. Although it has been widely established that angiographic evaluation is not consistent with the hemodynamic severity of a lesion, coronary physiology is not used to assess PCI results. Several previous studies suggested a relationship between low post-PCI FFR and future adverse cardiac events (mainly repeat target vessel revascularization), but most of them were retrospective by nature, contained only limited numbers of selected patients and were inconsistent in reporting an optimal cutoff value for post-PCI FFR ⁵⁻¹¹. Also, most of these studies used selected cases with stable, intermediate coronary lesions in which also pre-PCI FFR was performed. Subsequently, the aims of the current study were (1) to prospectively evaluate FFR values after angiographically successful PCI in a large cohort of consecutive patients, (2) to identify predictors of a low post-PCI FFR, and (3) to investigate whether there is a relationship between postprocedural FFR and clinical outcome during 30-day follow-up.

METHODS

The data that support the findings of this study are available from the corresponding author on reasonable request.

Patient population and study protocol

The FFR-SEARCH (Fractional Flow Reserve—stent Evaluated at Rotterdam Cardiology Hospital) is a prospective registry in which FFR measurements were performed after angiographically successful PCI in 1000 consecutive patients. Post-PCI FFR was measured in all patients, regardless of the clinical presentation or whether FFR or intravascular imaging was performed before PCI. However, patients presenting with cardiogenic shock, high-risk PCI with mechanical circulatory support or an estimated vessel size <2.25 mm were excluded.

PCI was performed according to standard techniques and in accordance with

the European Society of Cardiology guidelines. Unfractionated heparin (70–100 U/kg) was used to achieve an activated clotting time >250 seconds. Coronary artery lesion characteristics were classified according to the American College of Cardiology/American Heart Association lesion classification ¹². The decision to perform a diagnostic hemodynamic assessment with instantaneous free wave ratio or FFR, pre-intravascular or post-intravascular imaging, thrombus aspiration, predilatation or postdilatation was left at the discretion of the operator.

All FFR measurements were performed with the Navvus RXi system (ACIST Medical Systems, Eden Prairie, MN). This rapid exchange monorail microcatheter uses fiber optic-based sensor technology to assess FFR and is compatible with all standard 0.014 inches guidewires ^{13,14}. The microcatheter technology allows easy access over any coronary guidewire which makes it particularly useful for assessment of post-PCI FFR. In addition, it permits multiple pullbacks while maintaining wire access to the vessel. After angiographically successful PCI, the Navvus RXi was inserted over the previously used coronary guidewire to \approx 20 mm distal of the most distal stent edge, this location was defined as P1, Figure 1. Then, hyperemia was achieved with a continuous intravenous infusion of adenosine at a rate of 140 μ g/kg per minute through an antecubital vein. Post-PCI FFR values were measured under hyperemia after a minimum of 2 minutes of intravenous adenosine infusion. The lowest value of hyperemic Pd/Pa of any single beat was used.

Next, the microcatheter was pulled back to the most distal stent edge, this location was defined as P2, Figure 1 and the FFR value at that location was noted. The microcatheter was then pulled back to the most proximal stent edge, defined as P3 and again the FFR value at that location was noted. Finally, the microcatheter was pulled back to the ostium to check for pressure drift, this location was named P4, Figure 1. Using the FFR values at these 4 locations, pressure drop gradients were calculated from 3 segments; the distal segment (Δ FFR P2–P1), the stented segment (Δ FFR P3–P2), and the proximal segment (Δ FFR P4–P3). A significant pressure drop was defined as a Δ FFR >0.05.

For all later lesion and patient comparisons, only the FFR values measured 20 mm distal of the most distal stent edge (P1) were used.

Irrespective of the final post-PCI FFR value, and as directed by the study protocol, no further treatment was performed. The latter was directed in order not to bias the predictive value of post-PCI FFR on future adverse cardiac events. All angiograms and FFR pullbacks were checked to confirm protocol adherence. Based on previous studies, comparisons were made between lesions (and patients with lesions) with a low post-PCI FFR \leq 0.90 versus a high post-PCI FFR >0.90 ¹¹.

For this specific study, patients who presented with ST-segment-elevation myocardial infarction (STEMI) were excluded from further analysis as measuring FFR in patients with STEMI can be considered unreliable, mainly caused by incomplete hyperemia because of endothelial dysfunction and microvascular injury and obstruction in STEMI¹⁵⁻¹⁷. Consequently, patients with STEMI are more likely to have a high-FFR value which does not necessarily reflect a better procedural result or outcome. Specific analysis on FFR-SEARCH patients with STEMI will be presented separately.

The study was performed in accordance with the Declaration of Helsinki. The study protocol was approved by the local ethics committee. All patients provided written informed consent for the procedure and the use of anonymous data sets for research purposes in alignment with the Dutch Medical Research Act.

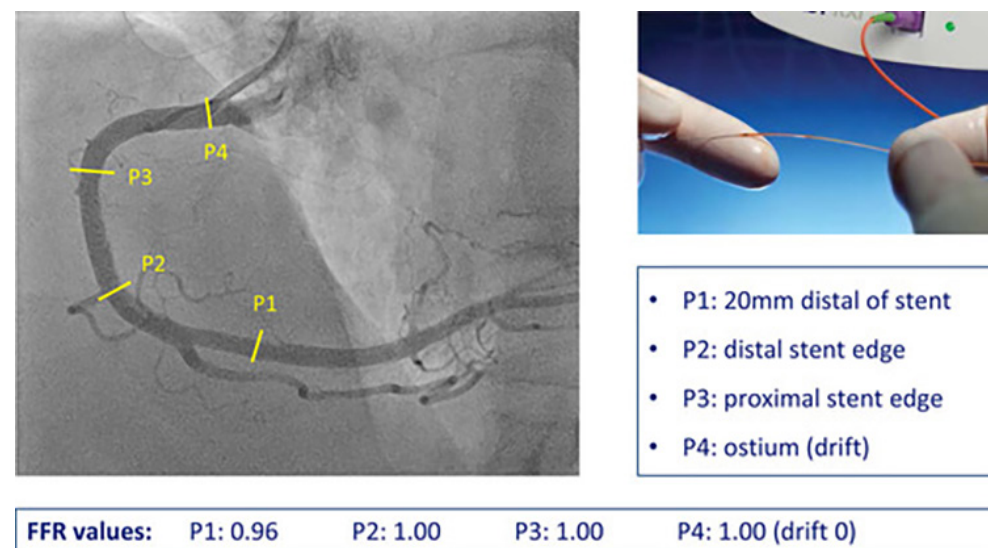


Figure 1. Example of post-percutaneous coronary intervention (PCI) fractional flow reserve (FFR) measurements as performed in FFR-SEARCH (Fractional Flow Reserve—Stent Evaluated at Rotterdam Cardiology Hospital), in this case in the right coronary artery in a patient presenting with a non-ST-segment-elevation myocardial infarction (NSTEMI).

After successful PCI, the Navvus RXi was inserted over the previously used coronary guidewire (upper right). Then post-PCI FFR measurements were collected 20 mm distal of the most distal stent edge (P1), the distal stent edge (P2), the proximal stent edge (P3), and finally at the ostium (P4) to check for signal drift (left). The values for this case are shown in the bar below.

Quantitative coronary angiography

Two-dimensional quantitative coronary angiography analysis was performed pre-stent and post-stent implantation in all treated lesions. An angiographic view with minimal foreshortening of the lesion and minimal overlap with others vessels was selected, and similar angiographic views were used pre-stent and post-stent implantation. Measurements included lesion length, reference diameter, minimal lumen diameter, and diameter stenosis. In case of preprocedural total occlusion of the treated lesion (in patients presenting with STEMI or a chronic total occlusion), the minimal lumen diameter value was considered 0% and stenosis 100%. Reference diameter and lesion length were calculated from the first angiographic view with restored flow.

Follow-up and outcome analysis

Clinical follow-up data were obtained from electronic medical records of the hospital, general practitioner, and the municipal civil records databases. In addition, all patients were contacted personally by letter or telephone contact. The clinical end point was defined as a composite of cardiac death, nonfatal MI, or target vessel revascularization at 30 days. Clinical events including all-cause mortality, cardiac mortality, MI, target lesion revascularization and target vessel revascularization, any revascularization, stent thrombosis, stroke, and bleeding were collected. Target lesion revascularization was defined as repeat PCI or bypass grafting for restenosis at the lesion treated during the index procedure. Target vessel revascularization was defined as repeat PCI or bypass grafting for a stenosis outside the stented area of the index procedure.

Statistical analysis

Continuous data are presented as mean±SD. Categorical data are presented as numbers and percentages. Comparison of data between lesions and patient groups was performed using the independent samples t test for continuous data. Fisher exact tests or χ^2 tests were used as appropriate to compare categorical data. All analyses were performed with SPSS statistics for Windows, version 24.0 (SPSS, Chicago, IL). All statistical tests were 2-sided. A $P < 0.05$ was considered statistically significant.

RESULTS

Patient characteristics and procedural results

Baseline characteristics of the patient population are presented in Table 1. A total of 1000 patients were included in the study. In 28 patients, the microcatheter was not able to cross the treated lesion, in 11 patients there was another technical issue and in 2 patients a severe response to the intravenous adenosine occurred, leaving 959 patients (96%) with at least 1 successfully treated and FFR assessed lesion. In these 959 patients, a total of 1348 lesions were treated. In 14 of these lesions, the microcatheter was not able to cross and in 1 there was another technical issue. Furthermore, in 109 lesions, the distal vessel was considered too small for the microcatheter. In 9 lesions, the patient was too unstable to administer intravenous adenosine, in 22 cases the operator decided not to perform the FFR measurement. Finally, in 28 cases post-PCI FFR measurement was not performed for other reasons, leaving 1165 successfully treated and measured lesions (Figure 2). Out of these 959 patients with 1165 lesions, 322 STEMI patients with 371 measured lesions were excluded leaving a total of 637 patients with 794 measured lesions for the final analysis.

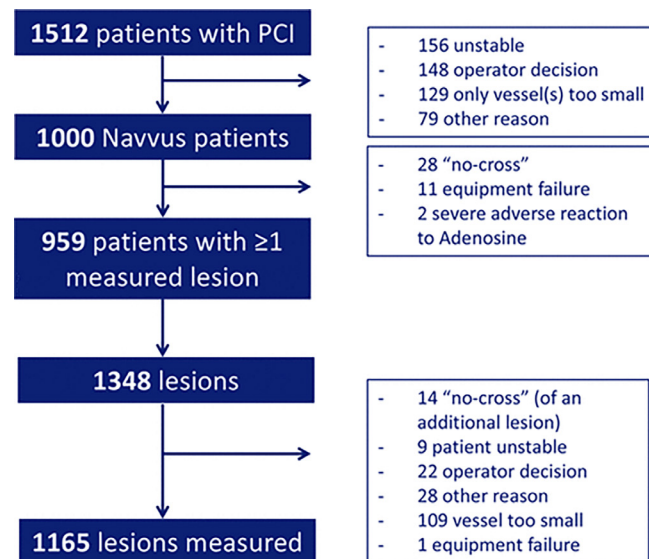


Figure 2. Flowchart showing all included and excluded patients and lesions in FFR-SEARCH (Fractional Flow Reserve—Stent Evaluated at Rotterdam Cardiology Hospital).

Measurement of ≥ 1 post-percutaneous coronary intervention (PCI) FFR was successful in 959 patients (96%).

Table 1. Patient baseline characteristics

	n=1000
Age, y	64.6±11.8
Male sex, n (%)	725 (73)
Hypertension, n (%)	515 (52)
Hypercholesterolemia, n (%)	451 (45)
Diabetes mellitus, n (%)	191 (19)
Smoking history, n (%)	499 (50)
Prior stroke, n (%)	77 (8)
Peripheral artery disease, n (%)	76 (8)
Prior myocardial infarction, n (%)	203 (20)
Prior PCI, n (%)	264 (26)
Prior CABG, n (%)	57 (6)
Hb level, mmol/L	8.7±1.0
Creatinine, μ mol/L	92±51
<u>Indication for PCI, n (%)</u>	
Stable angina	304 (30)
Unstable angina/NSTEMI	367 (37)
Acute myocardial infarction	329 (33)
No. of lesions treated	1.40±0.6
No. of lesions measured	1.21±0.5

CABG indicates coronary artery bypass graft; Hb, hemoglobin; NSTEMI, non-ST-segment-elevation myocardial infarction; and PCI, percutaneous coronary intervention.

FFR results

The mean time to perform post-PCI FFR was 5.0±1.4 minutes per lesion. No complications related to the microcatheter occurred. The mean Pd/Pa in resting condition was 0.96±0.04, while the mean post-PCI FFR under maximal hyperemia was 0.90±0.07 (as measured at P1). The mean post-PCI FFR at P2 was 0.95±0.05 and mean post-PCI FFR at P3 was 0.98±0.04. Finally, mean drift at P4 was 0.011±0.014 with 50 lesions (6.3%) having a significant drift >0.03, Figure 3. This resulted in an Δ FFR 0.04±0.05 along the distal segment, an Δ FFR 0.03±0.04 over the stented segment, and finally an Δ FFR 0.02±0.04 along the proximal segment. Interestingly, a significant pressure drop (>0.05) was observed in 32% of the distal segments, in 18% of the stented segments, and finally in 15% of the proximal segments.

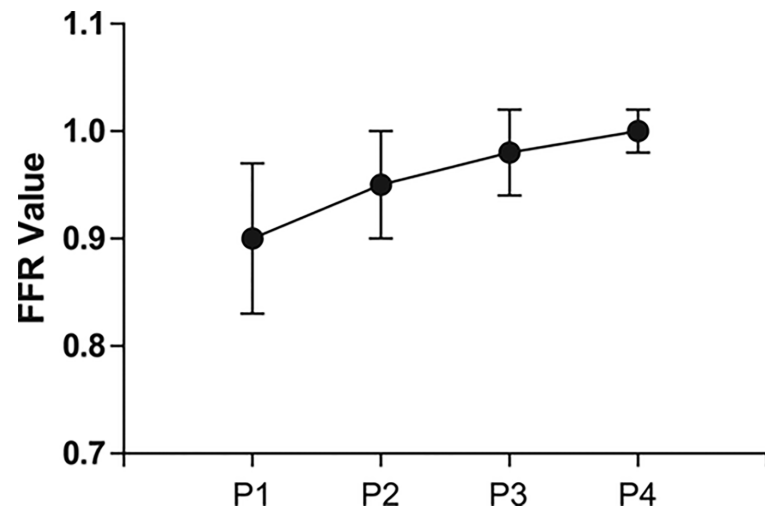


Figure 3. Mean post-percutaneous coronary intervention fractional flow reserve (FFR) values as measured at the 4 different locations in the coronary artery.

Distribution of post-PCI FFR values at P1 is shown in Figure 4. Although a satisfactory angiographic result was achieved in all cases, post-PCI FFR remained ≤ 0.80 in 78 lesions (9.8%). Conversely, post-PCI FFR was >0.90 in 396 lesions (50%). Comparison of post-PCI FFR in 3 predefined subgroups revealed no differences in men and women (0.89 ± 0.07 versus 0.90 ± 0.06 , $P=0.134$) or in patients presenting with a non-STEMI versus stable angina (0.90 ± 0.06 versus 0.89 ± 0.07 , $P=0.100$), but did show a significant difference in patients with diabetes mellitus and patients without diabetes mellitus (0.88 ± 0.07 versus 0.90 ± 0.06 , $P=0.027$).

Characteristics of lesions with a post-PCI ≤ 0.90 versus lesions with a post-PCI FFR >0.90 are displayed in Table 2. Lesions with a post-PCI ≤ 0.90 were more complex lesions and more frequently included bifurcation lesions (18% versus 10%, $P=0.002$) or calcified lesions (47% versus 35%, $P=0.001$). Conversely, lesions with a post-PCI FFR >0.90 were more frequently thrombotic lesions (14% versus 7%, $P=0.001$), had a higher stenosis grade pre ($63 \pm 20\%$ versus $57 \pm 19\%$, $P<0.001$), higher reference diameter pre (2.7 ± 0.5 versus 2.5 ± 0.5 mm, $P<0.001$), and smaller minimal lumen diameter pre (1.0 ± 0.6 versus 1.1 ± 0.5 mm, $P=0.044$). Furthermore, postdilatation was more frequently performed in lesions with a post-PCI FFR ≤ 0.90 (68% versus 57%, $P=0.001$). Also, intravascular ultrasound was more frequently used in lesions with a post-PCI FFR ≤ 0.90 (16% versus 6%, $P<0.001$). In lesions with a post-PCI FFR ≤ 0.90 more stents were used (1.5 ± 0.7 versus 1.3 ± 0.6 , $P=0.022$), with a smaller mean diameter (3.1 ± 0.4 versus 3.2 ± 0.5 mm, $P<0.001$), and a greater stent length (31 ± 19 versus 28 ± 16

mm, $P=0.015$). Finally, lesions with a post-PCI FFR >0.90 had a higher reference diameter post (2.7 ± 0.5 versus 2.5 ± 0.5 mm, $P<0.001$) and larger minimal lumen diameter post (2.7 ± 0.5 versus 2.5 ± 0.5 mm, $P<0.001$). Of note, in lesions with a post-PCI FFR ≤ 0.90 , a significant pressure drop (>0.05) was observed in 57% of the distal segments, in 33% of the stented segments, and finally in 29% of the proximal segments (as compared to 9% of the distal segments, 4% of the stented segments, and 3% of the proximal segments in lesions with post-PCI FFR >0.90).

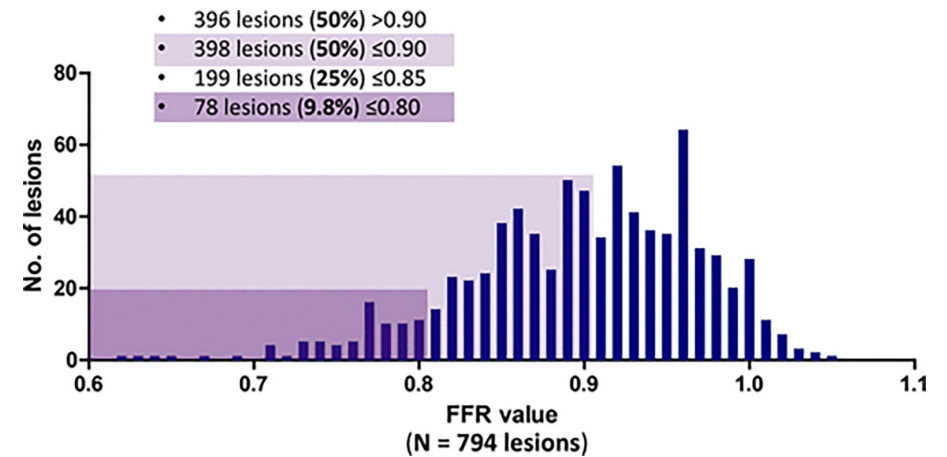


Figure 4. Post-percutaneous coronary intervention (PCI) fractional flow reserve (FFR) results on lesion level.

In 398 lesions (50%), a post-PCI FFR ≤ 0.90 was found (light purple box), while in 78 lesions (9.8%), the post-PCI FFR was even ≤ 0.80 (dark purple box).

Table 2. Lesion characteristics with FFR ≤0.90 versus FFR >0.90

	All Lesions (n=794)	FFR ≤0.90 (n=398)	FFR >0.90 (n=396)	p value
<u>Lesion type, n (%)</u>				0.003
A	100 (13)	35 (9)	65 (16)	
B1	163 (21)	78 (20)	85 (21)	
B2	232 (29)	132 (33)	100 (25)	
C	299 (37)	153 (38)	146 (37)	
Bifurcation, n (%)	109 (14)	70 (18)	39 (10)	0.002
Calcified, n (%)	328 (41)	188 (47)	140 (35)	0.001
In-stent restenosis, n (%)	30 (4)	19 (5)	11 (3)	0.140
Thrombus, n (%)	81 (10)	26 (7)	55 (14)	0.001
Stent thrombosis, n (%)	5 (1)	3 (1)	2 (1)	0.658
Ostial, n (%)	84 (11)	37 (9)	47 (12)	0.239
CTO, n (%)	39 (5)	25 (6)	14 (4)	0.073
Stenosis pre, %	60±20	57±19	63±20	<0.001
Ref diameter pre, mm	2.6±0.6	2.5±0.5	2.7±0.5	<0.001
Length pre, mm	21±11	20±11	21±12	0.631
MLD pre, mm	1.0±0.5	1.1±0.5	1.0±0.6	0.044
Predilatation, n (%)	553 (70)	289 (73)	264 (67)	0.068
Postdilatation, n (%)	499 (63)	272 (68)	227 (57)	0.001
IVUS, n (%)	87 (11)	65 (16)	22 (6)	<0.001
Stenosis post, %	3.5±14	2.8±14	4.2±13	0.153
Ref diameter post, mm	2.7±0.5	2.5±0.5	2.7±0.5	<0.001
Length post, mm	24±14	24±14	23±14	0.345
MLD post, mm	2.6±0.5	2.5±0.5	2.7±0.5	<0.001
No. of stent, n	1.4±0.7	1.5±0.7	1.3±0.6	0.022
Stent length, mm	29±18	31±19	28±16	0.015
Stent diameter, mm	3.1±0.5	3.1±0.4	3.2±0.5	<0.001

CTO indicates chronic total occlusion; FFR, fractional flow reserve; IVUS, intravascular ultrasound; and MLD, minimum luminal diameter.

Patients With all measured post-PCI FFR >0.90 versus any FFR ≤0.90

In a total of 280 patients (44%), all measured lesions had a post-PCI FFR >0.90. There were 357 patients (56%) with ≥1 lesion ≤0.90, 182 patients (29%) with ≥1 lesion ≤0.85, and 73 patients (11%) with ≥1 lesion ≤0.80 despite an angiographically satisfactory result of the procedure. Baseline and procedural characteristics of patients with ≥1 lesion ≤0.90 versus patients with all lesions >0.90 are shown in Table 3. Patients with ≥1 lesion ≤0.90 were more likely to have diabetes mellitus (28% versus 19%, P=0.007) or peripheral arterial disease (11% versus 6%, P=0.038) as compared to patients with all lesions >0.90. Conversely, patients with all lesions >0.90 more frequently had prior coronary artery bypass graft (12% versus 5%, P=0.002). Finally, patients with ≥1 lesion ≤0.90 had more lesions treated (1.59±0.7 versus 1.31±0.6, P<0.001) and measured (1.36±0.6 versus 1.11±0.4, P<0.001) as compared to patients with all lesions >0.90.

Table 3. Patient baseline characteristics with any FFR ≤0.90 versus FFR >0.90

	FFR ≤0.90 (n=357)	FFR >0.90 (n=280)	p value
Age, y	65.8±10.6	65.6±12.1	0.878
Male sex, n (%)	261 (73)	185 (66)	0.054
Hypertension, n (%)	215 (60)	164 (59)	0.684
Hypercholesterolemia, n (%)	202 (57)	145 (52)	0.476
Diabetes mellitus, n (%)	99 (28)	52 (19)	0.007
Smoking history, n (%)	152 (43)	131 (47)	0.303
Prior stroke, n (%)	35 (10)	17 (6)	0.088
Peripheral artery disease, n (%)	40 (11)	18 (6)	0.038
Prior myocardial infarction, n (%)	92 (26)	69 (25)	0.745
Prior PCI, n (%)	113 (32)	95 (34)	0.543
Prior CABG, n (%)	18 (5)	33 (12)	0.002
Hb level, mmol/L	8.6±1.0	8.5±1.1	0.519
Creatinine, μmol/L	99±75	92±32	0.192
<u>Indication for PCI, n (%)</u>			0.243
Stable angina	167 (47)	118 (42)	
Unstable angina/NSTEMI	190 (53)	162 (58)	
No. of lesions treated	1.59±0.7	1.31±0.6	<0.001
No. of lesions measured	1.36±0.6	1.11±0.4	<0.001

CABG indicates coronary artery bypass graft; FFR, fractional flow reserve; Hb, hemoglobin; NSTEMI, non-ST-segment-elevation myocardial infarction; and PCI, percutaneous coronary intervention.

Follow-up

Clinical follow-up at 30 days was available in 618 patients (97%). In total, 11 patients (1.8%) experienced a clinical end point. All separate end points and corresponding incidences are displayed in Table 4. No significant difference was found for the occurrence of the combined end point between the groups (2.0% in patients with ≥ 1 lesion ≤ 0.90 versus 1.5% in the patients with all lesions > 0.90 , $P=0.636$), or in any of the separate end points. Finally, no differences were found in event rates between men and women (2.0% versus 1.1%, $P=0.385$), patients with or without diabetes mellitus (2.7% versus 1.5%, $P=0.316$) and patients presenting with a non-STEMI versus patients with stable angina (2.7% versus 0.7%, $P=0.064$).

Table 4. Thirty-day clinical outcome

	All Patients (n=618)	FFR ≤ 0.90 (n=350)	FFR > 0.90 (n=268)	p value
Combined end point, n (%)	11 (1.8)	7 (2.0)	4 (1.5)	0.636
All-cause mortality, n (%)	5 (0.8)	4 (1.1)	1 (0.4)	0.290
Cardiac mortality, n (%)	4 (0.6)	3 (0.9)	1 (0.4)	0.457
Nonfatal MI, n (%)	4 (0.6)	4 (1.1)	0 (0)	0.079
TLR, n (%)	1 (0.2)	1 (0.3)	0 (0)	0.380
TVR, n (%)	2 (0.3)	1 (0.3)	1 (0.4)	0.851
Any revascularization, n (%)	7 (1.1)	4 (1.1)	3 (1.1)	0.978
Stent thrombosis, n (%)	1 (0.2)	1 (0.3)	0 (0)	0.380
Stroke, n (%)	0 (0)	0 (0)	0 (0)	1.000
Bleeding, n (%)	1 (0.2)	1 (0.3)	0 (0)	0.380

FFR indicates fractional flow reserve; MI, myocardial infarction; TLR, target lesion revascularization; and TVR, target vessel revascularization.

DISCUSSION

The main findings of FFR-SEARCH at 30-day follow-up can be summarized as follows: (1) Routine measurement of post-PCI FFR is safe and feasible. (2) Mean post-PCI FFR was 0.90 ± 0.07 , with 73 patients (11%) having ≥ 1 lesion(s) with a post-PCI FFR ≤ 0.80 despite angiographically successful PCI and 357 patients (56%) having a low post-PCI FFR ≤ 0.90 . (3) A significant pressure drop (> 0.05) was found in 32% of the segments distal of the stent, while only in 18% of the stented segments and 15% of the proximal segments. (4) Several factors were associated with a low post-PCI FFR, including bifurcations or calcified lesions. Furthermore, patients with diabetes mellitus or peripheral arterial disease were

more likely to have ≥ 1 lesion with a post-PCI FFR ≤ 0.90 . (5) Finally, no significant relationship was found between post-PCI FFR and the combined clinical end point at 30-day follow-up.

Since the beginning of coronary angioplasty, interventional cardiologists have been on an evercontinuing search to further optimize outcome in patients undergoing PCI. In the last decade, intracoronary physiological assessment with FFR has become an established diagnostic tool to measure the hemodynamic importance of intermediate coronary lesions and guide the need for revascularization¹⁻³. However, FFR is only rarely used to assess the functional result after PCI. The angiographic result after PCI does not correlate with FFR post-PCI^{5-8,10, 18}. Pijls et al¹⁹ studied 750 patients with post-PCI FFR measurements and a total of 44 patients (6%) had an FFR < 0.80 . In our study, more complex lesion phenotypes like bifurcations lesion or extensive calcification were associated with a post-PCI FFR ≤ 0.90 . Furthermore, balloon postdilatation and invasive imaging were more frequently performed in lesions with a post-PCI FFR ≤ 0.90 .

On a patient level, diabetes mellitus and peripheral arterial disease were more prevalent in patients with ≥ 1 lesion with a post-PCI FFR ≤ 0.90 .

Currently, no substantial data on the exact mechanism of a suboptimal result after PCI (as measured with FFR) exist. There are several potential explanations for a low FFR value after PCI, including incomplete stent deployment, underexpansion or malapposition, protruding struts in bifurcations, small edge dissection or plaque shift proximally or distally to the stent and remaining nontreated atherosclerotic disease throughout the coronary artery. In the present study, a significant pressure drop (> 0.05) was found almost twice as often in the segments distal of the stent, as compared to the stented segments and the proximal segments (32% versus 18% and 15%, respectively). In patients with post-PCI FFR ≤ 0.90 , a significant pressure drop was found in over 57% of the distal segments as compared to only 30% of the stented and proximal segments. This could be indicative that diffuse atherosclerotic disease distal to the stent may play an important role in low FFR after PCI. Although this is currently hypothetical, invasive imaging may complement conventional coronary angiography to help elucidate the etiopathology of low FFR post-PCI.

In the DOCTORS trial (Does Optical Coherence Tomography Optimize Results of Stenting), which randomized 240 patients to either optical coherence tomography (OCT)-guided PCI or angiography-guided PCI²⁰, post-PCI OCT revealed stent under expansion in 42% of patients, stent malapposition in 32%, incomplete lesion coverage in 20%, and edge dissection in 37.5%. This resulted in more

frequent use of postdilatation in the OCT-guided group versus the angiography-guided group (43% versus 12.5%, $P < 0.0001$). More importantly, the mean post-PCI FFR in the OCT-guided group was significantly higher as compared to the angiography-guided group (0.94 ± 0.04 versus 0.92 ± 0.05 , $P = 0.005$). These findings are consistent with data from the earlier ILUMIEN I study (Observational Study of Optical Coherence Tomography in Patients Undergoing Fractional Flow Reserve and Percutaneous Coronary Intervention)²¹. In this specific study, OCT and FFR were performed pre-PCI and post-PCI in 418 patients with stable or unstable angina or non-STEMI. Not only did post-PCI OCT uncover 14.5% malapposition, 7.6% under expansion, and 2.7% edge dissection, but it resulted in further stent optimization in 25% of patients with additional postdilatation in 81% of the cases and placement of additional stents in 12%. As a result, post-PCI FFR values improved from 0.86 ± 0.07 to 0.90 ± 0.10 after optimization.

From this data, it may be concluded that post-PCI FFR could signal a suboptimal PCI result, unnoticeable by angiography alone. The most important question raised by these findings is: "can post-PCI FFR be used to detect and optimize procedural results and consequently improve patient outcome?" Agarwal et al²² demonstrated in 574 consecutive patients with stable angina that 143 of the 664 treated lesions (21%) had an FFR of ≤ 0.80 despite optimal angiographic PCI results (mean post-PCI FFR 0.87 ± 0.08). After optimization of these lesions (42% received further postdilatation of the implanted stent, 33% additional stenting, and 18% underwent additional stenting and postdilatation), 80 lesions (56%) improved to an FFR > 0.80 , leaving 63 lesions (9.5%) with a persistently ischemic FFR of ≤ 0.80 . A final post-PCI FFR > 0.86 was considered as the optimal cutoff, and this was associated with improved outcome (major adverse cardiovascular event) during a mean follow-up of for 31 ± 16 months. As the percentage of patients in this optimal post-PCI FFR group increased from 60% to 74% after the additional optimization, the authors concluded these subsequent interventions not only improved the overall functional outcome as measured with FFR but also likely reduced major adverse cardiovascular event during follow-up. As this study was a retrospective nonrandomized study, it remains unclear whether routine FFR assessment, followed by additional optimization in case of low post-PCI FFR may actually improve patient outcome. This hypothesis is currently studied in the FFR-REACT trial (Dutch trial register: NTR6711) that will randomize 290 patients with post-PCI FFR < 0.90 to intravascular ultrasound-guided PCI optimization or control.

Limitations

Some limitations of the study need to be addressed. First, this is a single-center, observational study and, therefore, reflects local practice. Second, pressure measurements were performed with the Navvus microcatheter. The microcatheter may enhance luminal narrowing and thus affect coronary flow and result in a lower FFR as compared to wire-based FFR^{23,24}. However, in FFR-SEARCH coronary physiology was assessed after successful PCI which makes the obstructive effect of the microcatheter less relevant, especially because only vessels > 2.25 mm were eligible. Nonetheless, in $\approx 8\%$ of the cases, the distal vessel was considered too small for the microcatheter. In addition, in 3.4% of the attempted lesions, the microcatheter was not able to cross the stented segment. Finally, this analysis was restricted to a 30-day clinical follow-up. The association of post-PCI FFR with clinical events may only appear during longer-term follow-up. The primary clinical end point of FFR-SEARCH is, therefore, set at 2 years.

CONCLUSION

Routine measurement of post-PCI FFR using a monorail microcatheter is safe and feasible. Mean post-PCI FFR was 0.90 ± 0.07 , with 73 patients (11%) having ≥ 1 lesion(s) with a post-PCI FFR ≤ 0.80 despite angiographically successful PCI. Post-PCI FFR did not correlate with clinical events at 30 days.

REFERENCES

1. De Bruyne B, Pijls NH, Kalesan B, Barbato E, Tonino PA, Piroth Z, Jagic N, Möbius-Winkler S, Mobius-Winckler S, Rioufol G, Witt N, Kala P, MacCarthy P, Engström T, Oldroyd KG, Mavromatis K, Manoharan G, Verlee P, Frobert O, Curzen N, Johnson JB, Jüni P, Fearon WF; FAME 2 Trial Investigators. Fractional flow reserve-guided PCI versus medical therapy in stable coronary disease. *N Engl J Med*. 2012; 367:991–1001.
2. De Bruyne B, Fearon WF, Pijls NH, Barbato E, Tonino P, Piroth Z, Jagic N, Mobius-Winckler S, Rioufol G, Witt N, Kala P, MacCarthy P, Engström T, Oldroyd K, Mavromatis K, Manoharan G, Verlee P, Frobert O, Curzen N, Johnson JB, Limacher A, Nüesch E, Jüni P; FAME 2 Trial Investigators. Fractional flow reserve-guided PCI for stable coronary artery disease. *N Engl J Med*. 2014; 371:1208–1217.
3. Tonino PA, De Bruyne B, Pijls NH, Siebert U, Ikeno F, van' t Veer M, Klauss V, Manoharan G, Engström T, Oldroyd KG, Ver Lee PN, MacCarthy PA, Fearon WF; FAME Study Investigators. Fractional flow reserve versus angiography for guiding percutaneous coronary intervention. *N Engl J Med*. 2009; 360:213–224.
4. Windecker S, Kolh P, Alfonso F, Collet JP, Cremer J, Falk V, Filippatos G, Hamm C, Head SJ, Juni P, Kappetein AP, Kastrati A, Knuuti J, Landmesser U, Laufer G, Neumann FJ, Richter DJ, Schauerte P, Sousa Uva M, Stefanini GG, Taggart DP, Torracca L, Valgimigli M, Wijns W, Witkowski A, Authors/Task Force members. 2014 ESC/EACTS guidelines on myocardial revascularization: The Task Force on Myocardial Revascularization of the European Society of Cardiology (ESC) and the European Association for Cardio-Thoracic Surgery (EACTS) Developed with the special contribution of the European Association of Percutaneous Cardiovascular Interventions (EAPCI). *Eur Heart J*. 2014; 35:2541–2619.
5. Ishii H, Kataoka T, Kobayashi Y, Tsumori T, Takeshita H, Matsumoto R, Shirai N, Nishioka H, Hasegawa T, Nakata S, Shimada Y, Ehara S, Muro T, Yoshiyama M. Utility of myocardial fractional flow reserve for prediction of restenosis following sirolimus-eluting stent implantation. *Heart Vessels*. 2011; 26:572–581.
6. Nam CW, Hur SH, Cho YK, Park HS, Yoon HJ, Kim H, Chung IS, Kim YN, Kim KB, Doh JH, Koo BK, Tahk SJ, Fearon WF. Relation of fractional flow reserve after drug-eluting stent implantation to one-year outcomes. *Am J Cardiol*. 2011; 107:1763–1767.
7. Agarwal SK, Kasula S, Almomani A, Hacioglu Y, Ahmed Z, Uretsky BF, Hakeem A. Clinical and angiographic predictors of persistently ischemic fractional flow reserve after percutaneous revascularization. *Am Heart J*. 2017; 184:10–16.
8. Doh JH, Nam CW, Koo BK, Lee SY, Choi H, Namgung J, Kwon SU, Kwak JJ, Kim HY, Choi WH, Lee WR. Clinical relevance of poststent fractional flow reserve after drug-eluting stent implantation. *J Invasive Cardiol*. 2015; 27:346–351.
9. Kimura Y, Tanaka N, Okura H, Yoshida K, Akabane M, Takayama T, Hirayama A, Tada T, Kimura T, Takano H, Mizuno K, Inami T, Yoshino H, Yamashina A. Characterization of real-world patients with low fractional flow reserve immediately after drug-eluting stents implantation. *Cardiovasc Interv Ther*. 2016; 31:29–37.
10. Leesar MA, Satran A, Yalamanchili V, Helmy T, Abdul-Waheed M, Wongpraparut N. The impact of fractional flow reserve measurement on clinical outcomes after transradial coronary stenting. *EuroIntervention*. 2011; 7:917–923.
11. Wolfrum M, Fahrni G, de Maria GL, Knapp G, Curzen N, Kharbada RK, Fröhlich GM, Banning AP. Impact of impaired fractional flow reserve after coronary interventions on outcomes: a systematic review and meta-analysis. *BMC Cardiovasc Disord*. 2016; 16:177.
12. Ryan TJ, Faxon DP, Gunnar RM, Kennedy JW, King SB, Loop FD, Peterson KL, Reeves TJ, Williams DO, Winters WL. Guidelines for percutaneous transluminal coronary angioplasty. a report of the American College of Cardiology/American Heart Association Task Force on Assessment of Diagnostic and Therapeutic Cardiovascular Procedures (Subcommittee on Percutaneous Transluminal Coronary Angioplasty). *Circulation*. 1988; 78:486–502.
13. Diletti R, van Mieghem NMDA, Valgimigli M, Karanasos A, Everaert BR, Daemen J, van Geuns RJ, de Jaegere PP, Zijlstra F, Regar E. Rapid exchange ultra-thin microcatheter using fibre-optic sensing technology for measurement of intracoronary fractional flow reserve. *EuroIntervention*. 2015; 11:428–432.
14. Menon M, Jaffe W, Watson T, Webster M. Assessment of coronary fractional flow reserve using a monorail pressure catheter: the first-in-human ACCESS-NZ trial. *EuroIntervention*. 2015; 11:257–263.
15. Rezkalla SH, Kloner RA. No-reflow phenomenon. *Circulation*. 2002; 105:656–662.
16. Bulluck H, Foin N, Tan JW, Low AF, Sezer M, Hausenloy DJ. Invasive assessment of the coronary microcirculation in reperfused ST-segment-elevation myocardial infarction patients: where do we stand? *Circ Cardiovasc Interv*. 2017; 10:e004373.
17. Cuculi F, De Maria GL, Meier P, Dall'Armellina E, de Caterina AR, Channon KM, Prendergast BD, Choudhury RP, Choudhury RC, Forfar JC, Kharbada RK, Banning AP. Impact of microvascular obstruction on the assessment of coronary flow reserve, index of microcirculatory resistance, and fractional flow reserve after ST-segment elevation myocardial infarction. *J Am Coll Cardiol*. 2014; 64:1894–1904.
18. Tonino PA, Johnson NP. Why is fractional flow reserve after percutaneous coronary intervention not always 1.0? *JACC Cardiovasc Interv*. 2016; 9:1032–1035.
19. Pijls NH, Klauss V, Siebert U, Powers E, Takazawa K, Fearon WF, Escaned J, Tsurumi Y, Akasaka T, Samady H, De Bruyne B; Fractional Flow Reserve (FFR) Post-Stent Registry Investigators. Coronary pressure measurement after stenting predicts adverse events at follow-up: a multicenter registry. *Circulation*. 2002; 105:2950–2954.
20. Meneveau N, Souteyrand G, Motreff P, Caussin C, Amabile N, Ohlmann P, Morel O, Lefrançois Y, Descotes-Genon V, Silvain J, Braik N, Chopard R, Chatot M, Ecartot F, Tauzin H, van Belle E, Belle L, Schiele F. Optical coherence tomography to optimize results of percutaneous coronary intervention in patients with non-ST-elevation acute coronary syndrome: results of

- the multicenter, randomized DOCTORS Study (Does Optical Coherence Tomography Optimize Results of Stenting). *Circulation*. 2016; 134:906–917.
21. Wijns W, Shite J, Jones MR, Lee SW, Price MJ, Fabbicchi F, Barbato E, Akasaka T, Bezerra H, Holmes D. Optical coherence tomography imaging during percutaneous coronary intervention impacts physician decision-making: ILUMIEN I study. *Eur Heart J*. 2015; 36:3346–3355.
 22. Agarwal SK, Kasula S, Hacıoglu Y, Ahmed Z, Uretsky BF, Hakeem A. Utilizing post-intervention fractional flow reserve to optimize acute results and the relationship to long-term outcomes. *JACC Cardiovasc Interv*. 2016; 9:1022–1031.
 23. Wijntjens GW, van de Hoef TP, Kraak RP, Beijk MA, Sjauw KD, Vis MM, Madera Cambero MI, Brinckman SL, Plomp J, Baan J, Koch KT, Wykrzykowska JJ, Henriques JP, de Winter RJ, Piek JJ. The IMPACT Study (Influence of Sensor-Equipped Microcatheters on Coronary Hemodynamics and the Accuracy of Physiological Indices of Functional Stenosis Severity). *Circ Cardiovasc Interv*. 2016; 9:e004645.
 24. Pouillot C, Fournier S, Glasenapp J, Rambaud G, Bougrini K, Vi Fane R, Geyer C, Adjedj J. Pressure wire versus microcatheter for FFR measurement: a head-to-head comparison. *EuroIntervention*. 2018; 13:e1850–e1856.

Chapter 4



Predictors of post procedural fractional flow reserve – Insights from the FFR-SEARCH study

van Zandvoort LJC, Masdjedi K, Neleman T, Tovar Forero MN, Wilschut J, den Dekker WK, de Jaegere PPT, Diletti R, Zijlstra F, van Mieghem NMDA, Daemen J

*Erasmus University Medical Center, Thoraxcenter, Department of cardiology,
Rotterdam, the Netherlands*

REC Interv Cardiol. 2020. (Accepted)

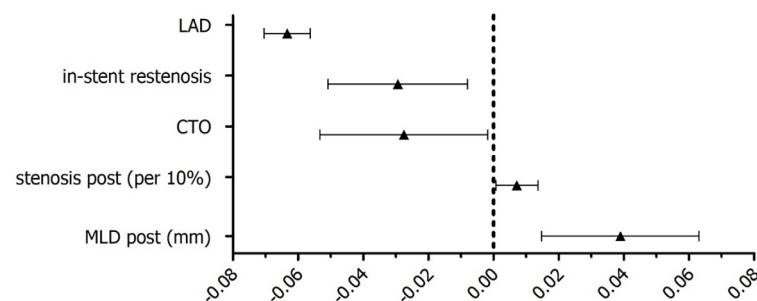
ABSTRACT

Introduction and objective: Patients with a low post percutaneous coronary intervention (PCI) fractional flow reserve (FFR) are at increased risk for future adverse cardiac events. The aim of the current study was to assess specific patient and procedural predictors of post PCI FFR.

Methods: The FFR SEARCH study is a prospective single center registry including 1000 consecutive all-comer patients that underwent FFR evaluation after angiographic successful PCI using a dedicated microcatheter. Mixed-effects models were used to search for independent predictors of post PCI FFR.

Results: Mean post PCI Pd/Pa (distal pressure divided by the aortic pressure) was 0.96 ± 0.04 and mean post PCI FFR was 0.91 ± 0.07 . Adjusting for independent predictors of post PCI FFR, left anterior descending artery as measured vessel was the strongest predictor (adjusted $\beta = -0.063$; 95%CI [-0.070 to -0.056]; $P < .0001$), followed by post procedural minimal lumen diameter (adjusted $\beta = 0.039$; 95%CI [0.015 - 0.065]; $P = .002$). Additionally, male sex, in-stent restenosis, chronic total occlusions and pre- and post-dilatation were negatively correlated to the post procedural FFR. Conversely, type A lesions, thrombus containing lesions, post procedural percentage stenosis and stent diameter positively correlated to the post procedural FFR. The R^2 for the complete model was 53%.

Conclusion: Multiple independent patient and vessel related predictors for post procedural FFR were identified, including gender, LAD as measured vessel and post procedural MLD.



Central illustration. Forest plot of most important predictor of the post PCI FFR

Adjusted beta values with 95% confidence intervals. The Figure includes all significant predictors from the multivariate generalized mix model which predicts post PCI FFR, excluding categorical variables with a beta < 0.02 . LAD = left anterior descending artery; CTO = chronic total occlusion; MLD = minimal lumen diameter.

What is known about the topic?

Fractional flow reserve (FFR) has proven to be a useful technique to address coronary physiology and the haemodynamic significance of coronary segments both pre- and post-intervention. Moreover, FFR after stenting has proven to be a strong and independent predictor of major adverse cardiac events up to 2 years. Unfortunately, at present, there is lack of data on independent predictors of post PCI FFR.

What does this study add?

The present study is the largest report to date focusing on predictors of post PCI FFR. Based on data derived from the FFR SEARCH registry, we were able to identify several patient and procedural predictors of post PCI FFR. The main predictors included gender, LAD vessels and post procedural lumen dimensions. The latter will help to further interpret post PCI FFR values and rightfully identify those vessels prone for future events.

INTRODUCTION

Limitations of accurate estimation of the hemodynamic significance of coronary artery lesions by angiographic guidance alone are well known¹. Fractional flow reserve (FFR) instead has proven to be a useful technique to address coronary physiology and the haemodynamic significance of coronary segments both pre- and post-intervention²⁻⁴. Moreover, FFR after stenting has proven to be a strong and independent predictor of major adverse cardiac events up to 2 years³⁻⁵.

While FFR primarily takes into account the relative luminal narrowing and the amount of viable myocardium perfused by a specific vessel, several factors have been shown to impact pre percutaneous coronary intervention (PCI) FFR values. As such, longer lesion length, high syntax scores, calcifications and tortuosity are associated with significantly lower FFR values while the presence of microvascular dysfunction, chronic kidney disease and female gender have been associated with higher FFR values⁶⁻¹¹.

At present, there is lack of data on independent predictors of post PCI FFR. Therefore, the aim of the present study was to assess both patient and procedural characteristics associated with low post PCI FFR in an all-comer patient population.

METHODS

The FFR SEARCH study is a prospective single center registry in which all consecutive patients underwent routine Pd/Pa (distal pressure divided by the aortic pressure) and FFR evaluation after angiographic successful PCI with the primary aim to study the impact of post PCI FFR on major adverse cardiac event rates at 2 years. Accordingly, no further actions were taken to improve post PCI FFR. The study was performed in accordance with the Declaration of Helsinki. The study protocol was approved by the local ethics committee. All patients provided written informed consent for the procedure and the use of anonymous datasets for research purposes in alignment with the Dutch Medical Research Act. A total of 1512 patients treated between March 2016 and May 2017 at the Erasmus Medical Center were available for our study. Among them, 504 patients were excluded due to either haemodynamic instability ($n = 156$), distal outflow being too small ($n = 129$), operator's decision not to proceed with post PCI hemodynamic assessment ($n = 148$) or other reasons ($n = 79$). A total of 1000 patients were included in the study. The microcatheter was not able to cross the treated lesion in 28 patients, technical issues with the catheter prohibited post PCI assessment in 11 patients and in 2 patients post PCI FFR assessment had to be aborted prematurely due to adenosine intolerance, leaving 959 patients in which post PCI FFR was assessed in at least 1 angiographically successfully treated lesion.

Quantitative coronary angiography

Pre procedural lesion type was defined according to the ACC/AHA guidelines and divided in 4 categories: A, B1, B2 and C¹². Comprehensive quantitative coronary angiography (QCA) analyses were performed pre and post stent implantation in all treated lesions. An angiographic view with minimal foreshortening of the lesion and minimal overlap with others vessels was selected. Similar angiographic views were used pre and post stent implantation. Measurements included: pre and post procedural percent diameter stenosis; reference vessel diameter; lesion length and minimal luminal diameter (MLD). In case of a total occlusion (in patients presenting with ST elevation myocardial infarction (STEMI) or a chronic total occlusion (CTO), the MLD was considered zero and percent diameter stenosis 100%. Reference vessel diameter and lesion length were calculated from the first angiographic view with restored flow. All measurements were performed using CAAS for Windows, version 2.11.2 (Pie Medical Imaging, Maastricht, The Netherlands).

FFR measurements

All FFR measurements were performed using the Navvus RXi system (ACIST Medical Systems, Eden Prairie, MN, USA), a dedicated FFR microcatheter with optical pressure sensor technology^{13,14}. Measurements were performed after an intracoronary bolus of nitrates (200 μg). The catheter was advanced over the previously used coronary guidewire approximately 20 mm distal to the most distal stent edge. FFR was defined as mean distal coronary artery pressure divided by mean aortic pressure during maximum hyperaemia achieved by continuous intravenous infusion of adenosine at a rate of 140 $\mu\text{g}/\text{kg}/\text{min}$ through an antecubital vein. No vessels in this study were evaluated using admission of intracoronary adenosine.

Statistical analysis

Baseline, categorical variables are reported as counts (percentage) and continuous variables are reported as mean \pm standard. In order to evaluate independent predictors for post PCI FFR, all patient and vessel characteristics were primarily univariately tested using a mixed-effects model (LME-model) with a random effect for patients and a fixed effect for post PCI FFR. All variables were subsequently inserted in a multivariate LME-model using the enter method, resulting in all significant independent predictors for post PCI FFR values. A forest plot was developed to depict all variables with the corresponding 95% confidence intervals. Beta (β) values indicate the average in-or decrease in FFR in case of a dichotomous variable or the increment per unit increase in case of continuous variables. Statistical analyses were performed by using R (version 3.5.1, packages: Hmisc, lme4 and nlme, RStudio Team (2020), Boston, MA).

RESULTS

Demographic characteristics

Mean age was 64.6 ± 11.8 years and 72.5% were males. In 959 patients at least one lesion was measured with a total of 1165 successfully treated and measured lesions. Patient demographics and baseline characteristics are depicted in Table 1. Up to 70% of patients presented with an acute coronary syndrome (ACS), while 18% had confirmed thrombus on angiography. Intravascular imaging was used in 9.6% to guide the procedure. Overall, 1.4 ± 0.6 lesions were treated per patient and in 1.2 ± 0.5 lesions per patient post PCI FFR was successfully assessed. The average total stented length per vessel was 29 ± 17 mm with an average diameter stent of 3.2 ± 0.5 mm.

Mean post PCI FFR was 0.91 ± 0.07 and 7.7% of vessels had a post PCI FFR ≤ 0.80 . In the LME-model, adjusting for independent predictors of post PCI FFR, LAD as measured vessel was the strongest predictor (adjusted $\beta = -0.063$, 95%CI, -0.070 to -0.056; $P < .0001$), followed by the post procedural MLD (adjusted $\beta = 0.039$, 95%CI, 0.015- 0.065]; $P = .002$). Additionally, male gender, in-stent restenosis, chronic total occlusions (CTO) and pre- and post-dilatation were negatively correlated to the post procedural FFR. Conversely, type A lesions, thrombus containing lesions, post procedural percentage diameter stenosis and stent diameter positively correlated to the post procedural FFR. The R^2 for the complete model was 53%. Figure 1 illustrates all significant and non-significant adjusted predictors that were put in the LME-model and Table 2 depicts all adjusted and unadjusted predictors with corresponding β values and 95% confidence intervals. The central illustrations depicts the most important predictors.

Table 1. Baseline patient and vessel characteristics

Patient characteristics	Total FFR SEARCH registry (n = 1000)
Age	64.6±11.8
Gender, male	725 (73)
Hypertension	515 (52)
Hypercholesterolemia	451 (45)
Diabetes	191 (19)
Smoking history	499 (50)
Prior Stroke	77 (8)
Peripheral arterial disease	76 (8)
Prior myocardial infarction	203 (20)
Prior PCI	264 (26)
Prior CABG	57 (6)
Indication for PCI	
Stable angina	304 (30)
NSTEMI	367 (37)
STEMI	329 (33)
Vessel characteristics (n = 1165)	
Lesion type	
A	125 (11)
B1	233 (20)
B2	379 (33)
C	428 (37)
LAD	593 (51)
Bifurcation	138 (12)
Calcified	402 (35)
In-stent restenosis	39 (3)
Thrombus	214 (18)
Stent thrombosis	14 (1)
Ostial	97 (8)
CTO	42 (4)
Stenosis Pre	69±22
Ref diameter Pre (mm)	2.6±0.6
Length Pre (cm)	21±11
MLD Pre (mm)	0.9±0.6
Predilatation	769 (66)
Post dilatation	691 (59)
Stenosis Post (per 10%)	4.4±13
Ref diameter Post (mm)	2.7±0.5
Length Post (cm)	24±13
MLD Post (mm)	2.6±0.5
No. Stent	1.4±0.6
Stent length (cm)	29±17
Stent diameter (mm)	3.2±0.5
Mean post PCI Pd/Pa	0.96 ± 0.04
Mean post PCI FFR	0.91 ± 0.07

Values are mean \pm SD or n (%). PCI = percutaneous coronary intervention; CABG = coronary artery bypass graft; NSTEMI = non elevated ST segment myocardial infarction; STEMI = ST elevated myocardial infarction; Pd/Pa = Pressure in the Distal coronary artery to the Pressure in the Aorta ratio; FFR = Fractional Flow Reserve.

Table 2: predictors for post PCI FFR

Patient characteristics	Unadjusted p value	Adjusted β (95% CI)	p value	β (95% CI)
Male gender	0.214	-0.006 (-0.015 - 0.003)	0.001	-0.013 (-0.021 - -0.005)
Age (per 10 years)	0.976	0.000 (-0.03 - 0.03)	0.724	0.001 (-0.002 - 0.003)
Hypertension	0.013	-0.010 (-0.018 - -0.002)	0.610	0.002 (-0.006 - 0.010)
Hypercholesterolemia	<0.001	-0.019 (-0.027 - -0.011)	0.287	-0.004 (-0.012 - 0.004)
Diabetes	<0.001	0.018 (0.008 - 0.042)	0.081	-0.008 (-0.017 - 0.001)
Smoking history	0.007	0.020 (0.010 - 0.019)	0.054	0.007 (-0.0001 - 0.014)
Prior Stroke	0.831	-0.002 (-0.017 - 0.013)	0.342	0.006 (-0.0007 - 0.019)
Peripheral arterial disease	0.022	-0.017 (-0.032 - -0.003)	0.460	-0.005 (-0.018 - 0.008)
Prior myocardial infarction	0.002	-0.016 (-0.026 - -0.006)	0.137	-0.008 (-0.019 - 0.003)
Prior PCI	<0.001	-0.016 (-0.025 - -0.007)	0.569	-0.032 (-0.014 - 0.008)
Prior CABG	0.896	-0.001 (-0.019 - 0.017)	0.166	-0.011 (-0.014 - 0.004)
Indication for PCI				
Stable angina	<0.001	-0.025 (-0.034 - -0.016)	0.563	-0.002 (-0.011 - 0.005)
STEMI	<0.001	0.032 (0.025 - 0.041)	0.171	0.006 (-0.003 - 0.015)
Vessel characteristics				
Lesion type				
A	<0.001	0.022 (0.009 - 0.035)	0.040	0.012 (0.0005 - 0.023)
C	0.045	-0.008 (-0.016 - -0.0002)	0.172	-0.006 (-0.014 - 0.002)
LAD	<0.001	-0.070 (-0.077 - -0.064)	<0.001	-0.063 (-0.070 - -0.056)
Bifurcation	<0.001	-0.024 (-0.036 - -0.012)	0.883	0.001 (-0.010 - 0.011)
Calcified	<0.001	-0.025 (-0.033 - -0.017)	0.409	-0.003 (-0.011 - 0.005)
In-stent restenosis	0.006	-0.031 (-0.053 - -0.009)	0.007	-0.029 (-0.051 - -0.008)
Thrombus	<0.001	0.031 (0.021 - 0.042)	0.026	0.012 (-0.001 - 0.023)
Stent thrombosis	0.920	0.002 (-0.034 - 0.038)	0.362	0.019 (-0.022 - 0.060)
Ostial	0.181	-0.010 (-0.024 - -0.005)	0.165	-0.010 (-0.024 - 0.004)
CTO				
Stenosis Pre (per 10%)	0.002	-0.034 (-0.056 - -0.013)	0.036	-0.027 (-0.053 - -0.002)
Ref diameter Pre (mm)	<0.001	0.007 (0.005 - 0.009)	0.105	0.004 (-0.0009 - 0.009)
Length Pre (cm)	<0.001	0.030 (0.023 - 0.037)	0.704	0.002 (-0.008 - 0.011)
MLD Pre (mm)	0.900	-0.00002 (-0.004 - 0.003)	0.101	0.004 (0.0008 - 0.009)
Predilatation	<0.001	-0.015 (-0.022 - -0.008)	0.638	0.004 (-0.014 - 0.023)
Post dilatation	<0.001	-0.019 (-0.027 - -0.011)	0.002	-0.012 (-0.020 - -0.005)
Stenosis Post (per 10%)	<0.001	0.027 (-0.035 - -0.019)	0.015	-0.009 (-0.016 - -0.002)
Ref diameter Post (mm)	0.077	0.003 (-0.0003 - 0.006)	0.029	0.01 (0.0007 - 0.01)
Length Post (cm)	<0.001	0.035 (0.027 - 0.042)	0.067	-0.022 (-0.045 - 0.002)
MLD Post (mm)	0.312	-0.002 (-0.005 - 0.001)	0.086	0.001 (-0.0007 - 0.001)
No. Stent	<0.001	0.032 (0.024 - 0.040)	0.002	0.039 (0.015 - 0.063)
Stent length (cm)	<0.001	-0.012 (-0.018 - -0.006)	0.620	-0.002 (-0.012 - 0.007)
Stent diameter (mm)	<0.001	0.019 (0.009 - 0.041)	0.286	-0.003 (-0.009 - 0.002)
	<0.001	0.033 (0.025 - 0.042)	0.026	0.012 (0.001 - 0.022)

Beta (β) values indicate the average in-or decrease in FFR in case of a dichotomous variable or the increment per unit increase in case of continuous variables. STEMI = ST elevated myocardial infarction; CABG = coronary artery bypass graft, LAD = left anterior descending artery, CTO = chronic total occlusion, MLD = minimal lumen diameter

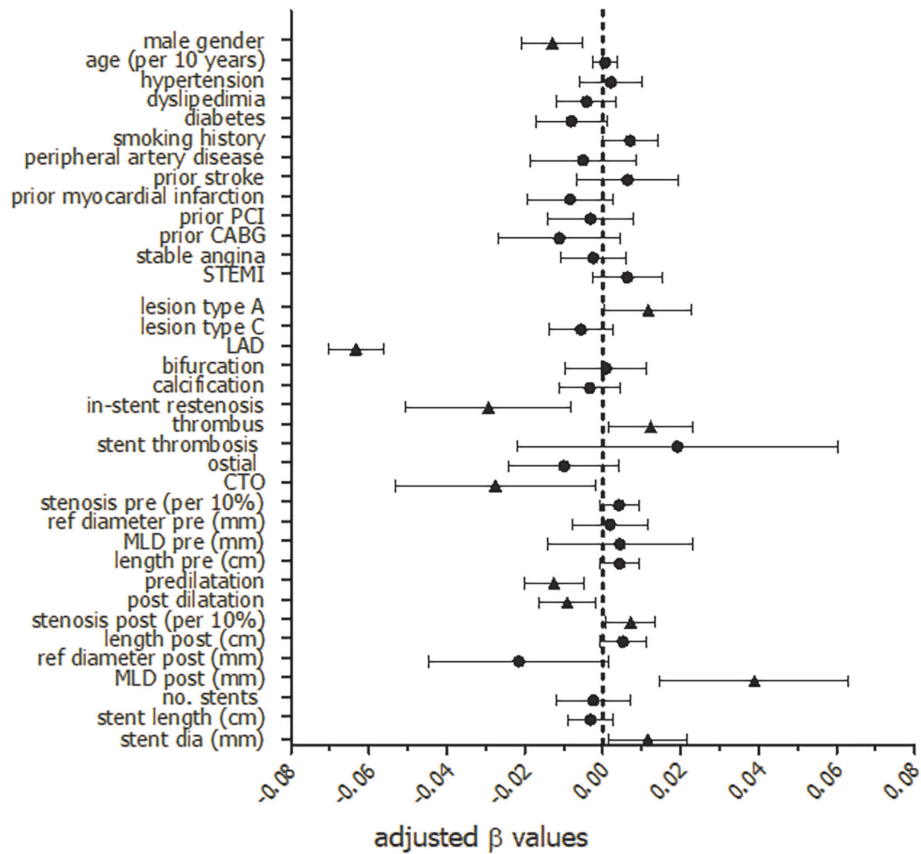


Figure 1. Forest plot of independent predictors for post PCI FFR. Adjusted beta values with 95% confidence intervals. Triangles indicate non-significant predictors, while circles indicate significant predictors in the multivariate generalized mix model to predict post PCI FFR. ACS, acute coronary syndrome; PCI, percutaneous coronary intervention; STEMI, ST-elevation myocardial infarction; LAD, left anterior descending artery; CTO, chronic total occlusion; MLD, minimal lumen diameter.

DISCUSSION

The present study is the largest report to date focusing on predictors of post PCI FFR. Based on data derived from the FFR SEARCH registry, we were able to identify several patient and procedural predictors of post PCI FFR. These predictors will help to further interpret post PCI FFR values and rightfully identify those vessels prone for future events. At first, male gender appeared to be negatively correlated to post procedural FFR. The latter finding extends the findings previous studies

focusing on the impact of gender on pre PCI FFR measurement ^{6, 11, 15, 16}. Males are known to have a lower prevalence of microvascular dysfunction as compared to females ^{8, 17}. The concept of FFR is based on drug induced maximal hyperemia in order to minimize microvascular resistance. Microvascular dysfunction may hamper this vasodilator response and consequently result in a dampened flow response and elevated FFR ¹⁵. Subsequently, males have on average a larger myocardial mass and thus, larger myocardial perfusion territories as compared to females ^{18, 19}. The importance of the latter can be illustrated by the second and strongest predictor of post PCI FFR in the present study, measurement of FFR in the LAD. FFR values are associated with myocardial mass and outflow territory of the measured vessel. As such, the LAD, the vessel with the largest perfusion area, has previously been correlated to lower pre and post procedural FFR values ²⁰⁻²².

Stent diameters of implanted stents in the RCA are, on average larger, even though the outflow territory of the LAD is larger ²³. The discrepancy between luminal dimensions and myocardial mass might explain why optimal improvement of the FFR in the LAD is hard to achieve ²³.

Third, larger stent diameters and larger post PCI MLD were associated with higher post PCI FFR, however, higher post procedural percentage stenosis was also correlated to higher post PCI FFR values. While these findings might seem contradictory, also in the DEFINE PCI study post procedural percentage stenosis was not correlated to post PCI physiology ²⁴.

In the intravascular ultrasound sub-study of the FFR SEARCH registry van Zandvoort et al. demonstrated that clear signs of residual luminal narrowing, including focal lesions, underexpansion and malapposition, were present in a significant amount of vessels with a post PCI FFR ≤ 0.85 , findings that could not linked not readily apparent on QCA ²⁵. Percent diameter stenosis was 20% in both the cohort of patients with a post PCI ≤ 0.85 and >0.85 ²⁶.

Next to the latter predictors of post PCI FFR, we identified several other predictors.

A dedicated analysis on 26 CTO's recently illustrated that post procedural FFR values initially are typically low; however appeared to increase at 4 months follow-up. The initial low post PCI FFR is hypothesized to be due to microvascular dysfunction in the recently opened vessel, a phenomena which improves after several months ²⁷. In-stent restenosis and pre- and post-dilatation were associated with lower post PCI values. The latter is in line with previous studies demonstrating that complex lesions in general were associated with lower post PCI FFR values ^{20, 21, 26, 28}.

Of interest was also the impact of the clinical presentation on post PCI FFR in the study population in which the majority of patients presented with ACS. In contrast to previous studies questioning the validity of invasive hyperemic physiological indices in patients presenting with ACS, we were not able to confirm an impact of clinical presentation on post PCI FFR. The identification of thrombus however, often present after a plaque rupture in ACS patients, was associated with significantly higher FFR values. Despite the restoration of epicardial flow by the PCI, a relatively large proportion of patients with STEMI have abnormal myocardial perfusion at the end of the procedure²⁹. This phenomenon is thought to be related to microvascular obstruction due to distal embolization (reperfusion injury) and tissue inflammation due to myocyte necrosis^{30, 31}. The latter might explain the significantly higher post PCI FFR values in patients presenting with thrombus containing lesions as compared to those without. Conversely, our findings also illustrate that in patients without thrombus containing lesions post PCI FFR might be a valuable diagnostic tool to identify those patients with an elevated risk for future adverse cardiac events.

Limitations

The current study was performed with the Navvus microcatheter, a dedicated rapid-exchange microcatheter with a mean diameter of 0.022" that proved to result in a slight but significant underestimation of FFR as compared to the conventional 0.014" pressure wires³². The latter withholds us from direct extrapolation of the current findings towards wire based FFR devices¹⁴. Based on the study protocol, no further action was taken in case of a low post PCI FFR. The Target FFR and FFR REACT study (NCT03259815 & NTR6711) should provide more information concerning post-PCI FFR and the potential of further actions intended to improve post PCI FFR and clinical outcomes^{33, 34}. The latter studies should also focus on the trade-off of potential benefits and harm when performing additional interventions in order to improve the final FFR values.

CONCLUSION

In this substudy of the FFR SEARCH registry, the largest real world post PCI FFR registry thus far, we identified gender, LAD vessels, post procedural MLD and several other independent predictors for post procedural FFR.

REFERENCES

1. Topol EJ, Nissen SE. Our preoccupation with coronary luminology. The dissociation between clinical and angiographic findings in ischemic heart disease. *Circulation*. 1995;92(8):2333-42.
2. De Bruyne B, Fearon Wf Fau - Pijls NHJ, Pijls Nh Fau - Barbato E, Barbato E Fau - Tonino P, Tonino P Fau - Piroth Z, Piroth Z Fau - Jagic N, et al. Fractional flow reserve-guided PCI for stable coronary artery disease. *N Engl J Med*. 2014(1533-4406 (Electronic)).
3. Wolfrum M, Fahrni G, de Maria GL, Knapp G, Curzen N, Kharbanda RK, et al. Impact of impaired fractional flow reserve after coronary interventions on outcomes: a systematic review and meta-analysis. *BMC Cardiovascular Disorders*. 2016;16(1):177.
4. Rimac G, Fearon WF, De Bruyne B, Ikeno F, Matsuo H, Piroth Z, et al. Clinical value of post-percutaneous coronary intervention fractional flow reserve value: A systematic review and meta-analysis. *Am Heart J*. 2017;183:1-9.
5. Kasula S, Agarwal SK, Hacıoglu Y, Pothineni NK, Bhatti S, Ahmed Z, et al. Clinical and prognostic value of poststenting fractional flow reserve in acute coronary syndromes. *Heart*. 2016;102(24):1988-94.
6. Sareen N, Baber U, Kezbor S, Sayseng S, Aquino M, Mehran R, et al. Clinical and angiographic predictors of haemodynamically significant angiographic lesions: development and validation of a risk score to predict positive fractional flow reserve. *EuroIntervention*. 2017;12(18):e2228-e35.
7. Baranauskas A, Peace A, Kibarskis A, Shannon J, Abraitis V, Bajoras V, et al. FFR result post PCI is suboptimal in long diffuse coronary artery disease. *EuroIntervention*. 2016;12(12):1473-80.
8. Crystal GJ, Klein LW. Fractional flow reserve: physiological basis, advantages and limitations, and potential gender differences. *Curr Cardiol Rev*. 2015;11(3):209-19.
9. Ahmadi A, Leipsic J, Ovrehus KA, Gaur S, Bagiella E, Ko B, et al. Lesion-Specific and Vessel-Related Determinants of Fractional Flow Reserve Beyond Coronary Artery Stenosis. *JACC Cardiovasc Imaging*. 2018.
10. Tebaldi M, Biscaglia S, Fineschi M, Manari A, Menozzi M, Secco GG, et al. Fractional Flow Reserve Evaluation and Chronic Kidney Disease: Analysis From a Multicenter Italian Registry (the FREAK Study). *Catheter Cardiovasc Interv*. 2016;88(4):555-62.
11. Fineschi M, Guerrieri G, Orphal D, Palmerini E, Münzel T, Warnholtz A, et al. The impact of gender on fractional flow reserve measurements. *EuroIntervention*. 2013;9.
12. Ryan TJ, Faxon DP, Gunnar RM, Kennedy JW, King SB, 3rd, Loop FD, et al. Guidelines for percutaneous transluminal coronary angioplasty. A report of the American College of Cardiology/American Heart Association Task Force on Assessment of Diagnostic and Therapeutic Cardiovascular Procedures (Subcommittee on Percutaneous Transluminal Coronary Angioplasty). *Circulation*. 1988;78(2):486-502.
13. Diletti R, van Mieghem NMDA, Valgimigli M, Karanasos A, Everaert BR, Daemen J, et al. Rapid exchange ultra-thin microcatheter using fibre-optic sensing technology for measurement of intracoronary fractional flow reserve. *EuroIntervention*. 2015;11(4):428-32.

14. Menon M, Jaffe W, Watson T, Webster M. Assessment of coronary fractional flow reserve using a monorail pressure catheter: the first-in-human ACCESS-NZ trial. *EuroIntervention*. 2015;11(3):257-63.
15. van de Hoef TP, Meuwissen M, Escaned J, Davies JE, Siebes M, Spaan JA, et al. Fractional flow reserve as a surrogate for inducible myocardial ischaemia. *Nat Rev Cardiol*. 2013;10(8):439-52.
16. Kim HS, Tonino PA, De Bruyne B, Yong AS, Tremmel JA, Pijls NH, et al. The impact of sex differences on fractional flow reserve-guided percutaneous coronary intervention: a FAME (Fractional Flow Reserve Versus Angiography for Multivessel Evaluation) substudy. *JACC Cardiovasc Interv*. 2012;5(10):1037-42.
17. Reis SE, Holubkov R, Lee JS, Sharaf B, Reichek N, Rogers WJ, et al. Coronary flow velocity response to adenosine characterizes coronary microvascular function in women with chest pain and no obstructive coronary disease. Results from the pilot phase of the Women's Ischemia Syndrome Evaluation (WISE) study. *J Am Coll Cardiol*. 1999;33(6):1469-75.
18. Iqbal MB, Shah N, Khan M, Wallis W. Reduction in myocardial perfusion territory and its effect on the physiological severity of a coronary stenosis. *Circ Cardiovasc Interv*. 2010;3(1):89-90.
19. Lin FY, Devereux RB, Roman MJ, Meng J, Jow VM, Jacobs A, et al. Cardiac chamber volumes, function, and mass as determined by 64-multidetector row computed tomography: mean values among healthy adults free of hypertension and obesity. *JACC Cardiovasc Imaging*. 2008;1(6):782-6.
20. Nam CW, Hur SH, Cho YK, Park HS, Yoon HJ, Kim H, et al. Relation of fractional flow reserve after drug-eluting stent implantation to one-year outcomes. *Am J Cardiol*. 2011;107.
21. Doh JH, Nam CW, Koo BK, Lee SY, Choi H, Namgung J, et al. Clinical Relevance of Poststent Fractional Flow Reserve After Drug-Eluting Stent Implantation. *J Invasive Cardiol*. 2015;27.
22. Agarwal SK, Kasula S, Hacioglu Y, Ahmed Z, Uretsky BF, Hakeem A. Utilizing Post-Intervention Fractional Flow Reserve to Optimize Acute Results and the Relationship to Long-Term Outcomes. *JACC Cardiovasc Interv*. 2016;9(10):1022-31.
23. Kimura Y, Tanaka N, Okura H, Yoshida K, Akabane M, Takayama T, et al. Characterization of real-world patients with low fractional flow reserve immediately after drug-eluting stents implantation. *Cardiovascular intervention and therapeutics*. 2016;31(1):29-37.
24. Jeremias A, Davies JE, Maehara A, Matsumura M, Schneider J, Tang K, et al. Blinded Physiological Assessment of Residual Ischemia After Successful Angiographic Percutaneous Coronary Intervention: The DEFINE PCI Study. *JACC: Cardiovascular Interventions*. 2019;12(20):1991-2001.
25. van Zandvoort LJC, Masdjedi K, Witberg K, Ligthart JMR, Tovar Forero MN, Diletti R, et al. Explanation of Postprocedural Fractional Flow Reserve Below 0.85. *Circ Cardiovasc Interv*. 2019;12(2):e007030.
26. Zandvoort van LJC MK, Witberg K, Ligthart JMR., Tovar Forero M.N., Diletti R., Lemmert M., Wilschut J., Jaegere de P.T., Boersma E., Zijlstra F, Mieghem van N., Daemen J.. Explanation of post procedural fractional flow reserve below 0.85: a comprehensive ultrasound analysis of the FFR Search registry. CRT meeting. 2018.
27. Karamasis GV, Kalogeropoulos AS, Mohdnazri SR, Al-Janabi F, Jones R, Jagathesan R, et al. Serial Fractional Flow Reserve Measurements Post Coronary Chronic Total Occlusion Percutaneous Coronary Intervention. *Circ Cardiovasc Interv*. 2018;11(11):e006941.
28. Pijls NH, Klauss V, Siebert U, Powers E, Takazawa K, Fearon WF, et al. Coronary pressure measurement after stenting predicts adverse events at follow-up: a multicenter registry. *Circulation*. 2002;105.
29. Stone GW, Webb J, Cox DA, Brodie BR, Qureshi M, Kalynych A, et al. Distal microcirculatory protection during percutaneous coronary intervention in acute ST-segment elevation myocardial infarction: a randomized controlled trial. *Jama*. 2005;293(9):1063-72.
30. Shah NR, Al-Lamee R, Davies J. Fractional flow reserve in acute coronary syndromes: A review. *Int J Cardiol Heart Vasc*. 2014;5:20-5.
31. Cuculi F, De Maria GL, Meier P, Dall'Armellina E, de Caterina AR, Channon KM, et al. Impact of microvascular obstruction on the assessment of coronary flow reserve, index of microcirculatory resistance, and fractional flow reserve after ST-segment elevation myocardial infarction. *J Am Coll Cardiol*. 2014;64(18):1894-904.
32. Pouillot C, Fournier S, Glasenapp J, Rambaud G, Bougrini K, Vi Fane R, et al. Pressure wire versus microcatheter for FFR measurement: a head-to-head comparison. *EuroIntervention*. 2018;13(15):e1850-e6.
33. van Zandvoort LJC, Masdjedi K, Tovar Forero MN, Lenzen MJ, Ligthart JMR, Diletti R, et al. Fractional flow reserve guided percutaneous coronary intervention optimization directed by high-definition intravascular ultrasound versus standard of care: Rationale and study design of the prospective randomized FFR-REACT trial. *Am Heart J*. 2019;213:66-72.
34. Collison D, McClure JD, Berry C, Oldroyd KG. A randomized controlled trial of a physiology-guided percutaneous coronary intervention optimization strategy: Rationale and design of the TARGET FFR study. *Clin Cardiol*. 2020.

Chapter 5



Impact of post-stenting fractional flow reserve on long term clinical outcomes – the FFR-SEARCH study

Diletti R*¹, Kanashka Masdjedi*¹, Daemen J¹, van Zandvoort LJC¹, Neleman T¹, Wilschut J¹, den Dekker WK¹, Rutger J. van Bommel², Lemmert ME³, Kardys I¹, Paul Cummins¹, de Jaegere PPT¹, Zijlstra F¹, van Mieghem NMDA¹

¹*Erasmus University Medical Center, Thoraxcenter, Department of cardiology, Rotterdam, the Netherlands*

²*Department of Cardiology, Tergooi Hospital, Tergooi, the Netherlands*

³*Department of Cardiology, Isala Hospital, Zwolle, the Netherlands*

**These two authors contributed equally to this study*

Circ Cardiovasc Interv. (Accepted)

ABSTRACT

Background: Fractional flow reserve (FFR) guided treatment has been demonstrated to improve percutaneous coronary intervention (PCI) results. However, little is known on the long-term impact of low post PCI FFR

Methods: This is a large prospective all comers study evaluating the impact of post-PCI FFR on clinical outcomes. All patients undergoing successful PCI were eligible for enrollment. FFR measurements were performed immediately after PCI when the operator considered the angiographic result acceptable and final. No further action was undertaken based on the post-PCI result. Suboptimal post-PCI FFR was defined as $FFR < 0.90$. The primary endpoint was major adverse cardiac events (MACE), a composite of cardiac death, any myocardial infarction or any revascularization at 2-year follow-up. Secondary end-points were target vessel revascularizations (TVR) and stent thrombosis (ST) and the separate components of the primary endpoint.

Results: A total of 1000 patients were enrolled. Post PCI FFR was successfully measured in 1165 vessels from 959 patients. A post-stenting $FFR < 0.90$ was observed in 440 vessels (37.8%). A total of 399 patients had at least 1 vessel with $FFR < 0.90$ post-PCI. At 2-year follow-up, a patient level analysis showed no association between post PCI FFR and MACE (HR1.08 [95%CI, 0.73-1.60], $p=0.707$), cardiac death (HR1.55 [95%CI, 0.72-3.36], $p=0.261$), any myocardial infarction (HR1.53 [95%CI, 0.78-3.02], $p=0.217$). A vessel level analysis showed a higher rate of TVR (HR1.91 [95%CI, 1.06-3.44], $p=0.030$) and a tendency towards higher rate of ST (HR2.89 [95%CI, 0.88-9.48], $p=0.081$) with final post-PCI $FFR < 0.90$.

Conclusion: Suboptimal Post-PCI FFR has only a moderate impact on MACE but coronary arteries with a post-PCI $FFR < 0.90$ have a higher rate of TVR.

INTRODUCTION

Fractional flow reserve (FFR) is a reliable index of functional severity for epicardial vessel stenosis ¹. This diagnostic tool facilitates the correct identification of hemodynamically significant coronary artery disease, translating into increased intervention appropriateness and improved clinical outcomes ^{2, 3}. Therefore, the ESC/EACTS guidelines on myocardial revascularization formulated strong recommendations towards FFR guidance for percutaneous coronary interventions (PCI) ⁴.

Conversely, the significance of FFR immediately after stenting to assess the impact of the treatment on coronary flow and the possible residual stenosis has been poorly investigated and data on this specific FFR application are sparse ⁵. In particular, a relationship between post-PCI FFR and clinical outcomes has mainly been derived from retrospective studies and post-hoc analyses of randomized studies, with unclear results in terms of optimal cut-off values for the identification and definition of sub-optimal post-stenting FFR ⁶⁻⁸. Given this background, we performed the FFR-SEARCH prospective study, to investigate the clinical impact of post-PCI FFR values on long terms clinical outcomes using a cut-off value for the definition of sub-optimal FFR ($FFR < 0.90$) already hypothesized in the FAME 1 and FAME 2 trials ^{7, 9} and supported by large meta-analyses ¹⁰ but never evaluated in a prospective fashion.

METHODS

Patient population

The FFR-SEARCH (Fractional Flow Reserve Stent Evaluated at Rotterdam Cardiology Hospital) is a large prospective, open label, all comers study evaluating the impact of post stenting FFR on long-term clinical outcomes.

Consecutive patients undergoing coronary intervention with stent implantation, irrespectively of the clinical presentation were considered for the study. Culprit lesions in patients presenting with ST- elevation or non ST-elevation acute coronary syndromes were included in the analysis. Exclusion criteria comprised age < 18 years, cardiogenic shock, high-risk PCI with mechanical circulatory support, vessel size < 2.25 mm by visual estimation, uncertain neurological outcome after cardiopulmonary resuscitation, planned CABG as a staged procedure (hybrid) within 12 months of the index procedure.

Post stenting FFR measurements and analysis

Functional assessments were performed at the end of the procedure when the operator considered the angiographic result acceptable and final.

The Guide-wire access to the vessel was maintained and was used to advance a monorail micro-catheter with an optical pressure FFR sensor technology (Navvus RXi, ACIST Medical Systems, Eden Prairie, MN ¹¹).

For post-stenting FFR values the microcatheter sensor was positioned in the mid-distal segment of the investigated vessel and at least 20 mm distal of the most distal stent edge and hyperaemia was induced with a continuous intravenous infusion of adenosine at 140 µg/kg/minute for at least 2 minutes.

As per study protocol and in order not to bias the predictive value of post-PCI FFR no additional interventions were performed regardless of the final post-PCI FFR value ¹².

Based on previous reports, comparisons in terms of long-term clinical outcomes were made using a post-PCI FFR cut-off value of 0.90 ^{7, 10}. In the patient-level analysis, patients were stratified based on the presence at least one post-PCI FFR value <0.90. Therefore, for the patient-level analysis the patients were divided into two groups: 1) at least one FFR<0.90 and 2) No any FFR<0.90.

In addition, a vessel level analysis was performed. The study was performed in accordance with the Declaration of Helsinki. The study protocol was approved by the local ethics committee. All patients provided written informed consent for the procedure and the use of anonymous data-sets for research purposes in alignment with the Dutch Medical Research Act.

Quantitative Coronary Angiography

Two-dimensional quantitative coronary angiography (2D-QCA) was performed for descriptive purposes, pre- and post-stent implantation in all treated lesions, using angiographic projections with minimal foreshortening of the lesion and minimal overlap with others coronary vessels. Analyses were performed with a dedicated quantitative coronary angiography (QCA) analysis software (CAAS Workstation, Pie Medical Imaging, Maastricht, the Netherlands). QCA measurements included lesion length, reference diameter, minimal lumen diameter, and diameter stenosis. In case of totally occluded vessels either acutely or chronically the minimal lumen diameter value was considered 0% and diameter stenosis 100% in the pre-stenting analysis and reference vessel diameter and lesion length were calculated from the first angiographic view with restored flow.

Clinical Follow-up and definitions

Clinical follow-up was obtained for each patient from electronic medical records of the hospital, general practitioner, and the municipal civil records databases. In addition, all patients were contacted personally by letter or telephone. Clinical events including all-cause mortality, cardiac mortality, any spontaneous myocardial infarction, target vessel revascularization, any revascularization and stent thrombosis, were collected.

The primary endpoint was major adverse cardiac events (MACE), defined as a composite of cardiac death, any spontaneous myocardial infarction or any revascularization. The secondary end-points were target vessel revascularizations (TVR), stent thrombosis (ST) and the separate components of the primary endpoint. Cardiac death was defined as any death in which a cardiac cause could not be excluded ¹³. Myocardial infarction was defined according to the fourth universal definition of myocardial infarction ¹⁴. Target vessel revascularization (TVR) was defined as a re-intervention driven by any lesion located in the same epicardial vessel. Stent thrombosis was defined according to the ARC 2 definitions ¹³. Event adjudication was performed by two independent cardiologists unaware of the final physiological assessment.

Statistical analysis

Baseline, categorical variables are reported as counts and percentages and compared using the Chi Squared test on patient level and generalized linear mixed models (GLMM) with random intercepts on vessel level. Baseline, continuous data are presented as mean with standard deviation for normally distributed variables and as medians with interquartile range for variable that were not normally distributed. Differences between both groups for continuous data were assessed using the independent t-test on patient level and GLMM with random intercepts on vessel level.

The Kaplan-Meier method was applied to show the cumulative incidence of clinical endpoints. The association between post PCI FFR and clinical endpoints was analysed by Cox proportional hazard regression analysis. First the analysis was performed univariably. Then the analysis was adjusted for potential confounders. To identify potential confounders, univariable associations of baseline characteristics with the clinical endpoints were examined, and variables with a univariable p value <0.1 were entered into the multivariate models. In the 'patient level' analyses the associations of post PCI FFR with MACE, cardiac death, MI and any revascularization were consequently adjusted for gender,

hypertension, dyslipidaemia, diabetes, smoking, peripheral arty disease, prior PCI, prior infarction, prior CABG, STEMI, NSTEMI and stable angina.

For the analysis on a vessel level, Cox regression with robust standard errors was used to account for the correlation between the vessels in case multiple vessels were assessed within one patient. In these analyses, the associations of post PCI FFR with TVR and stent thrombosis were adjusted for bifurcation, severe calcification, in-stent restenosis, thrombotic culprit lesion in STEMI, CTO and stented region located in the left anterior descending artery. Data are presented as Hazard-Ratios (HRs) with 95% confidence intervals (CI 95%).

All tests were two-tailed and a P value <0.05 was considered statistically significant. Statistical analyses were performed using SPSS statistics for Windows, version 24.0 (SPSS, Chicago, IL, USA) and R (version 3.4.1).

RESULTS

A total of 1512 patients were screened and 1000 patients with 1207 treated vessels were included. Post-PCI FFR measurement was successfully performed in 959 patients and 1165 vessels (Table 1, Table 2, Figure 1). No complications related to the use of the FFR microcatheter were observed (Table 3). A post-PCI FFR <0.90 was reported in 440 vessels (37.8%), and ≤ 0.80 in 90 (7.7%) vessels (Figure 2). Baseline clinical characteristics are reported in Table 1. In brief the mean age was 64.6 ± 11.8 years, 19% of patients had diabetes, 70% of the coronary lesions were B2 (33%), or C (37%) with a median stent length of 23mm (IQR 15-36) and a median post-stenting MLD of 2.6mm (IQR 2.25-2.93). Patients with a final post-stenting FFR <0.90 more frequently had hypertension (58% vs 49%, $p=0.005$), hypercholesterolemia (52% vs 42%, $p=0.001$), diabetes, (24% vs 16%, $p=0.001$). Patients with a final post-stenting FFR ≥ 0.90 presented more often with a STEMI (20% vs 41%, $p < 0.001$) (Table 1). Vessels with a final post-stenting FFR <0.90 were more often calcified (45% vs 28%, $p < 0.001$) and less frequently thrombotic (11% vs 23%, $p < 0.001$).

Vessels with post-stenting FFR ≥ 0.90 showed a smaller pre-intervention MLD of 0.9mm (IQR 0.4-1.3) vs 1.0 (IQR 0.7-1.4), $p < 0.001$ by QCA, but a larger post-procedure MLD (median 2.7 vs 2.5mm, $p < 0.001$).

Complete 2-year follow-up was available in 849 patients (88.5%), 39 had at least 1-year follow-up, 59 patient had follow up between 1-365 days, 12 patients were lost at follow up.

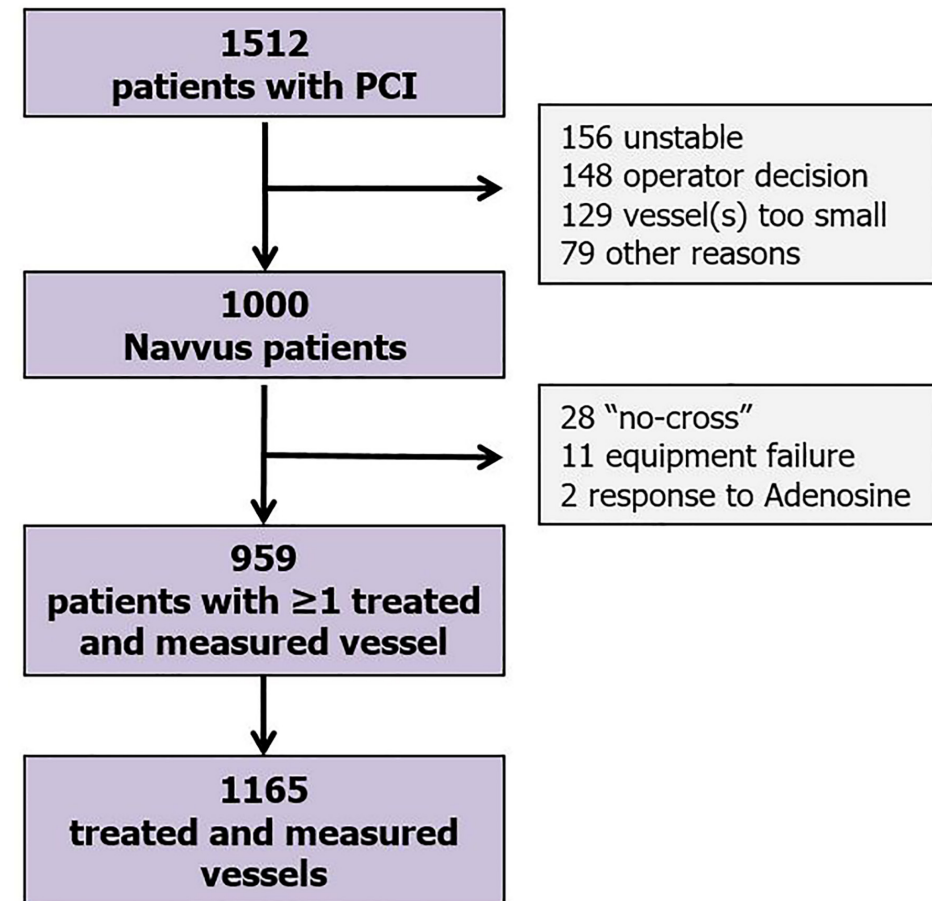


Figure 1. Study flow-chart

At 2-year follow-up at the univariate analysis and after adjustment for confounders, in the patient level analysis, no associations were found between post PCI FFR and MACE (HR 1.08, [95% CI, 0.73-1.60] $p=0.707$), cardiovascular death (HR 1.55 [95% CI, 0.72-3.36] $p=0.261$) and any myocardial infarction (HR 1.53 [95% CI, 0.78-3.02] $p=0.217$) (Table 4, Figure 3).

In the individual vessel level analysis, a higher rate of TVR (HR 1.91, [95%CI, 1.06-3.44], $p=0.030$) and a tendency towards higher rate of ST (HR 2.89, [95%CI, 0.88-9.48], $p=0.081$) was observed with a final post-stenting FFR <0.90 (Table 4, Figure 4).

Table 1. Baseline clinic characteristics

Patient characteristics	All patients (n=959)	FFR <0.90 (n=399)	FFR ≥0.90 (n=560)	p value
Age (years)	64.6±11.8	64.7±11.3	64.2±12.4	0.335
Male gender (n)	725 (76)	301 (75)	424 (75)	0.090
<u>Cardiovascular risk factors, n (%)</u>				
Hypertension	515 (54)	228 (57)	287 (51)	0.005
Hypercholesterolemia	451 (447)	206 (52)	245 (44)	0.001
Diabetes	191 (20)	97 (24)	94 (17)	0.001
Current smoker	499 (52)	184 (46)	315 (56)	0.056
Prior stroke	77 (8)	37 (9)	40 (7)	0.128
Peripheral art. Disease	76 (8)	42 (11)	34 (6)	0.004
<u>Comorbidity, n (%)</u>				
Prior myocardial infarction	203 (21)	100 (25)	103 (18)	0.002
Prior PCI	264 (28)	120 (30)	144 (28)	0.032
Prior CABG	57 (6)	17 (4)	40 (7)	0.110
Hb level (mmol/L), mean±SD	8.7±1.0	8.6±1.0	8.7±1.0	0.568
Creatinine (µmol/L), median (IQR)	84 (72-99)	85 (73-98)	83 (71-99)	0.030
<u>Presentation, n (%)</u>				
Stable angina	304 (32)	151 (38)	153 (27)	<0.001
Unstable angina / NSTEMI	367 (38)	167 (42)	200 (36)	0.006
STEMI	329 (34)	81 (20)	248 (44)	<0.001

BMI= body mass index; CABG= coronary artery bypass graft; Hb= haemoglobin; IQR= Interquartile range; (N)STEMI= (non) ST-elevation myocardial infarction; PCI= percutaneous coronary intervention.

Table 2. Procedural Characteristics

	All vessels with post-PCI FFR (n=1165)	FFR <0.90 (n=440)	FFR ≥0.90 (n=725)	p value
<u>Lesion type, n (%)</u>				
A	125 (11)	34 (8)	91 (13)	0.012
B1	233 (20)	84 (19)	149 (21)	0.557
B2	379 (33)	150 (34)	229 (32)	0.380
C	428 (37)	172 (39)	256 (35)	0.198
Bifurcation	138 (12)	78 (18)	60 (8)	<0.001
Calcified	402 (35)	196 (45)	206 (28)	<0.001
In-stent restenosis	39 (3)	24 (6)	15 (2)	0.003
Thrombus	214 (18)	47 (11)	167 (23)	<0.001
Stent thrombosis	14 (1)	7 (1)	7 (1)	0.351
Ostial	97 (8)	38 (9)	59 (8)	0.783
CTO	42 (4)	24 (6)	18 (3)	0.011
<u>Measured vessel, n (%)</u>				
Right coronary artery	331 (28)	57 (5)	274 (24)	<0.001
Left Main	19 (2)	12 (1)	7 (1)	0.029
Left anterior descending artery	593 (51)	339 (29)	254 (35)	<0.001
Left circumflex artery	211 (18)	32 (3)	179 (15)	<0.001
Coronary Artery Bypass Graft	10 (1)	0 (0)	10 (1)	*
<u>2D-QCA measurements; median (IQR)</u>				
Stenosis Pre, %	63 (50-78)	56 (44-70)	67 (53-86)	<0.001
Stenosis Post, %	4 (-4-13)	4 (-5-13)	5 (-3-13)	0.190
MLD Pre, mm	0.92 (0.56-1.34)	1.0 (0.7-1.4)	0.9 (0.4-1.3)	<0.001
MLD Post, mm	2.60 (2.25-2.93)	2.5 (2.2-2.8)	2.7 (2.3-3.0)	<0.001
Stent length, mm	23 (15-36)	26 (15-40)	22 (15-35)	0.004
Stent diameter, mm	3 (3-4)	3 (2.75-3.5)	3 (2-5)	<0.001
No. of Stents, n mean±SD	1.4±0.6	1.4±0.7	1.3±0.6	0.007
Pre-dilation, n (%)	769 (66)	328 (75)	441 (38)	<0.001
Post-dilation, n (%)	691 (59)	305 (69)	386 (53)	<0.001
FFR, mean±SD	0.91±0.07	0.84±0.05	0.95±0.03	<0.001

Vessel-based analysis: CTO= chronic total occlusion; IQR= Interquartile range; MLD= minimum luminal diameter; *Not tested due to complete separation. Data are reported as mean ± SD or median and IQR

Table 3. Post-stenting FFR measurements and microcatheter performance

All vessels (n=1165)	
Successful post-PCI FFR, mean±SD	96.5% (1165)
Average Pd/Pa 20mm distal of stent, mean±SD	0.96 ± 0.04
Average FFR value 20mm distal of stent, mean±SD	0.91 ± 0.07
Average FFR value distal stent edge, mean±SD	0.95 ± 0.06
Average FFR value proximal stent edge, mean±SD	0.98 ± 0.04
Average drift value, median (IQR)	0.01 (0.00-0.02)
Average time per lesion (minutes), mean±SD	5.0 ± 1.4
FFR microcatheter related complications, n (%)	0 (0)

Table 4. Clinical outcomes at 2-year follow-up

	FFR <0.90 vs FFR ≥0.90	
	Univariate HR [95% CI] p value	Multivariate HR [95% CI] p value
Patient-based analysis		
MACE	1.17 [0.81-1.70] p=0.397	1.08 [0.73-1.60] p=0.707
Cardiovascular Death	1.58 [0.77-3.23] p=0.212	1.55 [0.72-3.36] p=0.261
Any Myocardial Infarction	1.72 [0.91-3.27] p=0.095	1.53 [0.78-3.02] p=0.217
Any Revascularization	1.23 [0.81-1.88] p=0.33	1.10 [0.71-1.73] p=0.666
Vessel-based analysis		
TVR	1.71 [0.98-2.99] p=0.061	1.91 [1.06-3.44] p=0.030
Stent thrombosis	2.71 [0.99-7.46] p=0.054	2.89 [0.88-9.48] p=0.081

Data are presented as Hazard ratio (HR) [95% Confidence Interval (CI)] p-value. MACE= Composite endpoint of cardiac death, myocardial infarction and any revascularization. Extended Cox regression with time-dependent covariate modelling was performed. Data are reported as mean ± SD or median and IQR

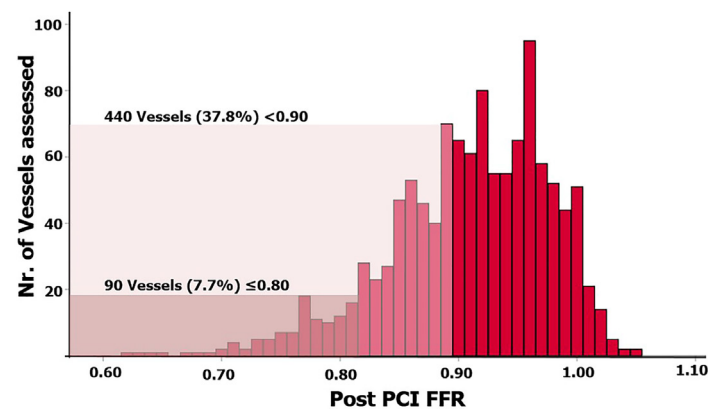


Figure 2. Vessels distribution per 0.01 FFR increment

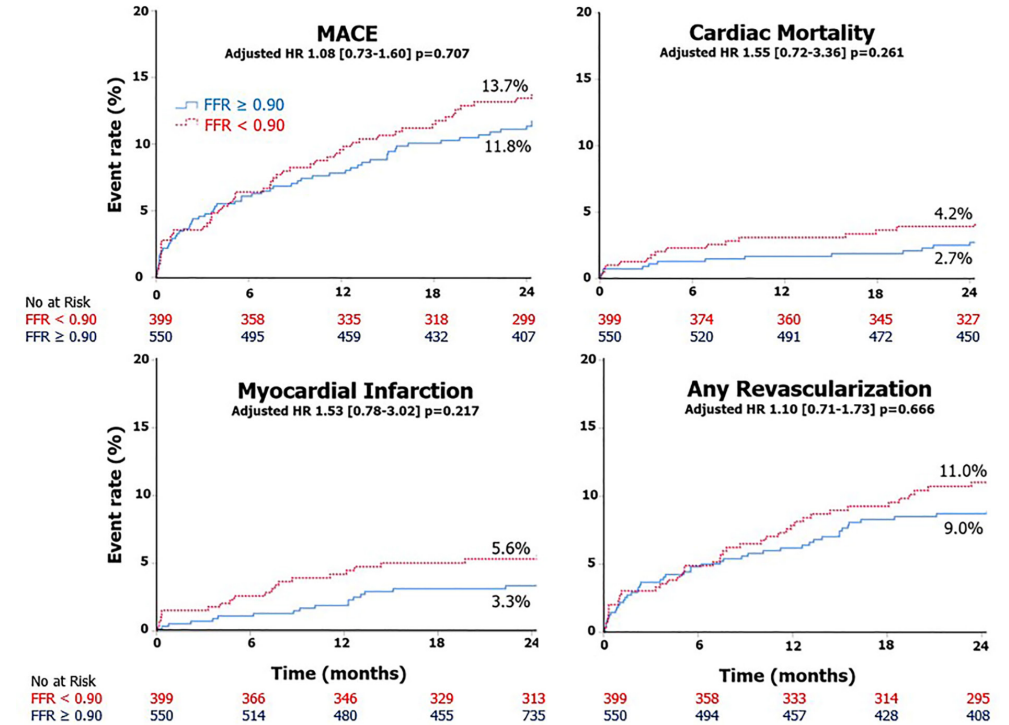


Figure 3. Kaplan-Meier curves for MACE, cardiovascular mortality, myocardial infarction and any revascularization. Patient-based analysis.

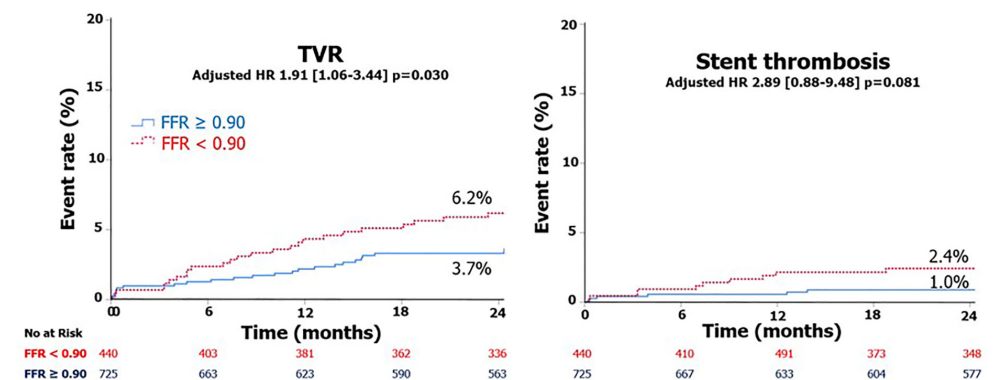


Figure 4. Kaplan-Meier curves for target vessel revascularization and stent thrombosis. Vessel-level analysis.

DISCUSSION

FFR SEARCH is the largest prospective study to date evaluating the impact of post-stenting FFR on long-term clinical outcomes. The main findings of our study are: 1) post-stenting FFR is safe, feasible and can be easily performed when using a rapid exchange microcatheter maintaining wire access. 2) Impaired coronary physiology expressed by FFR < 0.90 was common (37.8% of patients). 3) Post PCI FFR < 0.90 was not associated with overall MACE. But on a vessel level analysis FFR < 0.90 post PCI resulted into a higher rate of target vessel revascularizations and a trend towards higher rate of stent thrombosis during a follow up of 2 years.

A large body of evidence has cemented FFR as the standard for invasive ischemia detection in the catheterization laboratory and both American and European clinical guidelines have formulated strong recommendations for FFR evaluation in intermediate coronary stenosis ^{4, 15}. Conversely, not much is known about the relevance of coronary physiology to address PCI results.

Post-PCI FFR with a rapid exchange microcatheter appeared safe and easy to execute over the coronary guidewire that was previously used for PCI mitigating the need for additional wire manipulations and concomitant risk of wire passage behind stent struts and coronary dissections ¹¹.

The FFR cut-off < 0.90 was derived from a post-hoc analysis of the FAME Trials ⁹ and was supported by a large meta-analysis ¹⁰, however, never tested in a prospective fashion. Using this threshold more than one third of the final results judged as acceptable by angiography were categorized as sub-optimal, highlighting its clinical relevance. On the other hand we cannot exclude that lower cut-off values might have a similar or even higher association with clinical events.

The comparison of clinical outcomes on a patient-level analysis showed a consistent numerical, although non-statistically significant, increase in clinical events in subjects with suboptimal post-PCI FFR values. Such results are in line with previous retrospective studies or post-hoc analyses suggesting a moderate impact of sub-optimal post PCI FFR on hard clinical end-points and a more relevant impact on vessel-specific end-points ^{7, 8}. Piroth Z. and colleagues, comparing the 2-year outcome of lower and upper tertiles of post-PCI FFR reported a significant increase of the vessel oriented composite end point (VOCE), defined as the composite of vessel-related cardiovascular death, vessel-related spontaneous (nonperiprocedural) MI, and ischemia-driven target vessel revascularization (9.2% vs. 3.8%, p=0.037) ⁷. Lee J.M. showed in patients with low post-PCI FFR a higher risk of 2-year TVF compared with those with high post-PCI FFR (9.1% vs.

2.6%, p = 0.006) ⁸. Importantly, lesions with FFR <0.90 post PCI was associated with more TVR and a numerical increase of definite stent thrombosis, this analysis might be able to better capture the real impact of a single post-stenting FFR values on a specific vessel.

From a mechanistic point of view, post-stenting FFR indicates residual flow impairment during maximal hyperaemia ⁷. Various factors that may not be appreciated by conventional angiography might contribute to the flow impairment, such as proximal or distal residual focal stenosis, stent underexpansion, or diffuse atherosclerotic disease ¹⁶⁻¹⁸. Invasive coronary imaging may help elucidate the pathophysiologic mechanism of impaired coronary flow and guide corrective measures including high-pressure balloon post-dilation, additional stenting or drug eluting balloon therapy.

Optimization of a suboptimal post PCI FFR may be challenging and FFR pullbacks can help identifying focal drops or more gradual decreases ^{1, 19}. Still, FFR pullbacks are not devoid of limitations, such as the absence of a clear threshold ²⁰, the need for prolonged adenosine infusion, with possible patients discomfort and unstable hyperaemia, the occurrence of pressure recovery affecting pressure gradients and often increasing the proportion of focal lesion identification ^{19, 21} and finally cases with no clear FFR drop but a diffuse pressure loss indicating a diffuse disease, particularly challenge to treat with local therapies ²⁰. therefore, intravascular coronary imaging may complement post PCI FFR.

In this context, the currently on-going FFR REACT Trial (NTR6711) ²² is randomizing patients with a post PCI FFR <0.90 to either standard of care (no additional intervention) or intravascular ultrasound (IVUS) directed optimization. The primary end point is the composite of cardiac death, target vessel MI and clinically driven target vessel revascularisation (target vessel failure) at 1 year.

Limitations

FFR SEARCH is a single centre study. The sample size is limited and might be not sufficient to highlight differences in terms of hard clinical outcomes. Given the observational nature of the analysis, the results do not evaluate the clinical benefit of additional intervention in vessels with sub-optimal post-PCI FFR. No direct comparisons between microcatheter based and wire based FFR was performed in terms of stented lesion crossability. Further large randomized trials are needed to fully investigate the relation between sub-optimal post-PCI FFR and clinical events and to elucidate PCI optimization strategies.

CONCLUSION

FFR < 0.90 occurs in approximately one third of patients post stenting. Suboptimal Post-PCI FFR has only a moderate impact on MACE. Post PCI FFR < 0.90 is associated with a higher rate of target vessel revascularizations.

REFERENCES

1. Pijls NH, De Bruyne B, Peels K et al. Measurement of fractional flow reserve to assess the functional severity of coronary-artery stenoses. *N Engl J Med* 1996;334:1703-8.
2. Tonino PA, De Bruyne B, Pijls NH et al. Fractional flow reserve versus angiography for guiding percutaneous coronary intervention. *N Engl J Med* 2009;360:213-24.
3. Xaplanteris P, Fournier S, Pijls NHJ et al. Five-Year Outcomes with PCI Guided by Fractional Flow Reserve. *N Engl J Med* 2018;379:250-259.
4. Neumann FJ, Sousa-Uva M, Ahlsson A et al. 2018 ESC/EACTS Guidelines on myocardial revascularization. *Eur Heart J* 2019;40:87-165.
5. Hakeem A, Uretsky BF. Role of Postintervention Fractional Flow Reserve to Improve Procedural and Clinical Outcomes. *Circulation* 2019;139:694-706.
6. Agarwal SK, Kasula S, Hacioglu Y, Ahmed Z, Uretsky BF, Hakeem A. Utilizing Post-Intervention Fractional Flow Reserve to Optimize Acute Results and the Relationship to Long-Term Outcomes. *JACC Cardiovasc Interv* 2016;9:1022-31.
7. Piroth Z, Toth GG, Tonino PAL et al. Prognostic Value of Fractional Flow Reserve Measured Immediately After Drug-Eluting Stent Implantation. *Circ Cardiovasc Interv* 2017;10.
8. Lee JM, Hwang D, Choi KH et al. Prognostic Implications of Relative Increase and Final Fractional Flow Reserve in Patients With Stent Implantation. *JACC Cardiovasc Interv* 2018;11:2099-2109.
9. Pijls NH, Klauss V, Siebert U et al. Coronary pressure measurement after stenting predicts adverse events at follow-up: a multicenter registry. *Circulation* 2002;105:2950-4.
10. Rimac G, Fearon WF, De Bruyne B et al. Clinical value of post-percutaneous coronary intervention fractional flow reserve value: A systematic review and meta-analysis. *Am Heart J* 2017;183:1-9.
11. Diletti R, van Mieghem NMDA, Valgimigli M et al. Rapid exchange ultra-thin microcatheter using fibre-optic sensing technology for measurement of intracoronary fractional flow reserve. *EuroIntervention* 2015;11:428-32.
12. van Bommel RJ, Masdjedi K, Diletti R et al. Routine Fractional Flow Reserve Measurement After Percutaneous Coronary Intervention. *Circ Cardiovasc Interv* 2019;12:e007428.
13. Garcia-Garcia HM, McFadden EP, Farb A et al. Standardized End Point Definitions for Coronary Intervention Trials: The Academic Research Consortium-2 Consensus Document. *Eur Heart J* 2018;39:2192-2207.
14. Thygesen K, Alpert JS, Jaffe AS et al. Fourth universal definition of myocardial infarction (2018). *Eur Heart J* 2019;40:237-269.
15. Patel MR, Calhoon JH, Dehmer GJ et al. ACC/AATS/AHA/ASE/ASNC/SCAI/SCCT/STS 2017 Appropriate Use Criteria for Coronary Revascularization in Patients With Stable Ischemic Heart Disease: A Report of the American College of Cardiology Appropriate Use Criteria Task Force, American Association for Thoracic Surgery, American Heart Association, American Society of Echocardiography, American Society of Nuclear Cardiology, Society for Cardiovascular

- Angiography and Interventions, Society of Cardiovascular Computed Tomography, and Society of Thoracic Surgeons. *J Am Coll Cardiol* 2017;69:2212-2241.
16. van Zandvoort LJC, Masdjedi K, Witberg K et al. Explanation of Postprocedural Fractional Flow Reserve Below 0.85. *Circ Cardiovasc Interv* 2019;12:e007030.
 17. Baranauskas A, Peace A, Kibarskis A et al. FFR result post PCI is suboptimal in long diffuse coronary artery disease. *EuroIntervention* 2016;12:1473-1480.
 18. Wolfrum M, De Maria GL, Benenati S et al. What are the causes of a suboptimal FFR after coronary stent deployment? Insights from a consecutive series using OCT imaging. *EuroIntervention* 2018;14:e1324-e1331.
 19. Collet C, Sonck J, vandelloo B et al. Measurement of Hyperemic Pullback Pressure Gradients to Characterize Patterns of Coronary Atherosclerosis. *J Am Coll Cardiol* 2019;74:1772-1784.
 20. Tonino PA, Johnson NP. Why Is Fractional Flow Reserve After Percutaneous Coronary Intervention Not Always 1.0? *JACC Cardiovasc Interv* 2016;9:1032-5.
 21. Davies JE, Sen S, Dehbi HM et al. Use of the Instantaneous Wave-free Ratio or Fractional Flow Reserve in PCI. *N Engl J Med* 2017;376:1824-1834.
 22. van Zandvoort LJC, Masdjedi K, Tovar Forero MN et al. Fractional flow reserve guided percutaneous coronary intervention optimization directed by high-definition intravascular ultrasound versus standard of care: Rationale and study design of the prospective randomized FFR-REACT trial. *Am Heart J* 2019;213:66-72.

PART II



UTILITY OF
(POST PCI)
INTRAVASCULAR
IMAGING

Chapter 6



Predictors for clinical outcome of untreated stent edge dissections as detected by optical coherence tomography

van Zandvoort LJC, Tomaniak M, Tovar Forero MN, Masdjedi K, Visseren L, Witberg K, Ligthart JMR, Kardys I, Lemmert ME, Diletti R, Wilschut J, de Jaegere PPT, Zijlstra F, van Mieghem NMDA, Daemen J

Erasmus University Medical Center, Thoraxcenter, Department of cardiology, Rotterdam, the Netherlands

Circ Cardiovasc Interv. 2020;13(3):e008685

Stent implantation for the treatment of coronary artery disease can cause unintended tearing at the site of vessel wall adjacent to the stent struts resulting in a stent edge dissection (SED). At present, limited data is available on the exact optical coherence tomography (OCT) characteristics and extent of SEDs that might warrant further treatment. Given this background, we aimed to study the morphometric features and impact of untreated SEDs on clinical outcomes and assess dissection healing by serial OCT.

We retrospectively identified 295 untreated SEDs in 261 patients from a dedicated local database containing all OCT recordings from January 2009 to August 2017. Patients were eligible in case they underwent a percutaneous coronary intervention with stent implantation and post procedural OCT evaluation. SEDs were defined as tearing of the vessel luminal surface within 5 mm of the proximal or distal stent border. Selected pullbacks with untreated SEDs were quantitatively analysed using dedicated software (Rubo DICOM viewer 2.0, Rubo Medical Imaging, Aerdenhout, The Netherlands).

The plaque type at the site of the SED was categorized into fibrous, fibroatheroma, lipid or necrotic core, superficial calcium or deep calcium. The following morphometric characteristics of each dissection were measured: longitudinal length, circumferential extension, cavity depth, maximal thickness of the dissection flap, minimal lumen area and area stenosis in the SED, dissection area and reference lumen area. The severity of each dissection was further characterized based on its extend to either subintimal or submedial and the presence of an intramural hematoma or thrombus¹. Finally, in the subset of 51 patients (53 SEDs) with follow-up OCT imaging, the presence of late persisting SEDs on OCT was evaluated stratified per follow-up timeframe, (1-7 days, 7 days-6 months, 6-12 months and > 1 year). The primary endpoint of the study was a device-oriented composite endpoint (DOCE) at one year, defined as a composite of cardiac death, target lesion myocardial infarction (MI) or target lesion revascularization. In order to evaluate independent predictors for DOCE at follow-up, all patients, vessel and SED characteristics were first tested univariately using a Cox proportional hazards model which accounted for the multilevel nature of the data. Subsequently, variables with a $p < 0.05$ were inserted into the model. For the stratified analysis of distal and proximal SEDs, only univariate hazard ratios (HR) were examined since not enough events occurred for a multivariate analysis. The data and analytical methods used in this study will be made available to other researchers for the purposes of replicating the procedure or reproducing the results.

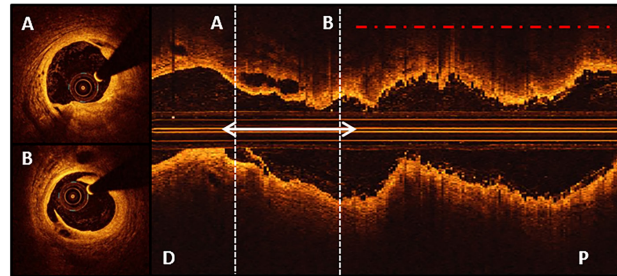
The study population consisted of 71% males, 22% of the patients had diabetes and 25% presented with an ST-segment elevation MI. The overall median SED length was $2.0 \pm (1.4-3.0)$ mm with an median angle of $54 \pm (34-92)^\circ$. The minimal lumen areas in the proximal and distal SEDs were $6.4 \pm (4.5-8.3)$ mm² and $4.3 \pm (3.1-5.8)$ mm² respectively. Clinical follow-up was available for 89% of the patients and at one year the cumulative incidence of the DOCE was 6.7%. Only SED length (adjusted HR 1.17; 95% CI 1.02-1.34) was associated with an increased risk of DOCE. For distal SEDs, cavity depth in mm was the only predictor of 1-year DOCE (HR 1.029; 95% CI 1.012-1.047), whereas reference area in mm² (adjusted HR 0.63; 95% CI 0.45-0.87) was the only predictor for 1-year DOCE in patients with proximal SEDs (Figure 1). Within the first week post procedure, all (8/8) of the SEDs were still visible on OCT. Between 1 week and 6 months, SEDs remained visible in up to 15% (2/13) while between 6 and 12 months 16% (3/19) were still visible. No remaining SEDs were visible after one year (median follow-up 22 months) (0/13).

The incidence of the DOCE in the present study was significantly lower as compared to previous studies reporting on the outcome of patients with SEDs 2-4. The latter might be due to an overall lower risk of the present study population and follow-up truncation at 1 year. The CLI-OPCI ACS and CLI-OPCI II used an arbitrary cut-off for flap thickness of 0.20 mm and found this to be a significant predictor for DOCE^{2, 3}. In contrast, we found dissection length (best cut-off for DOCE at 3.55mm) to be the only independent predictor of the DOCE at one year. Almost 85% of the SEDs were no longer visible at 6 months while after 1 year, none of them were still visible. The latter is in line with previous research reporting SEDs were still visible in 10% of cases at 12 months follow-up⁵.

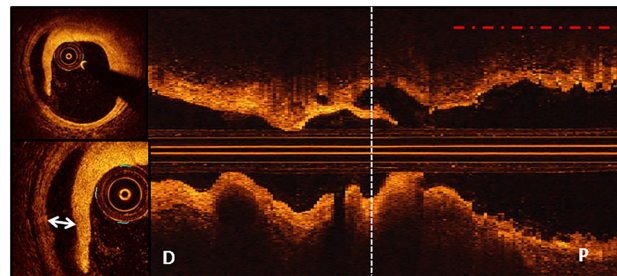
In conclusion, this is the largest cohort of patients with SEDs to date, demonstrating a 6.7% risk of 1-year cardiac events potentially linked to untreated dissections. In patients with SEDs, dissection length, cavity depth and proximal reference area were identified as predictors of the DOCE.

Predictors for the DOCE at 1 year in patients with untreated stent edge dissections

All stent edge dissections:
Dissection length



Distal stent edge dissections:
Cavity depth



Proximal stent edge dissections:
Proximal reference lumen area

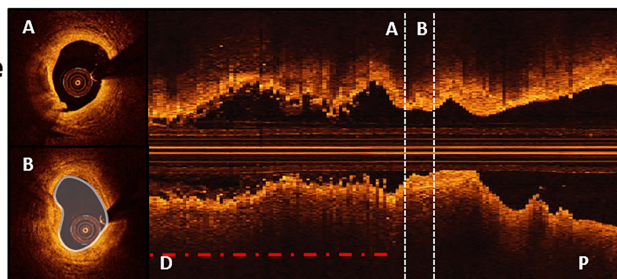


Figure 1. Independent morphometric predictors of device-oriented clinical endpoint (DOCE) at 1 year in patient with stent edge dissections detected by optical coherence tomography

Upper figure: Dissection length is an independent predictor for DOCE at 1 year in all stent edge dissections (SED), cross-section A and B refer to the corresponding location on the longitudinal view. The combination of highest sensitivity and specificity for SED length indicated that the best cut-off for DOCE at one year was at 3.55mm (Youden’s index = 0.22, area under the curve = 0.56). D and P denote distal and proximal respectively. Middle figure: cavity depth is an independent predictor for DOCE at 1 year for distal SEDs, the cross-sections correspondent to the dashed line on the longitudinal view. Lower figure: proximal reference lumen area is an independent predictor for DOCE at 1 year for proximal SEDs, cross-section A and B refer to the corresponding location on the longitudinal view. Cross-section B denotes the proximal reference lumen area in white. The red dash-dot lines denote the stented segment.

REFERENCES

1. Tearney GJ, Regar E, Akasaka T, Adriaenssens T, Barlis P, Bezerra HG, et al. Consensus Standards for Acquisition, Measurement, and Reporting of Intravascular Optical Coherence Tomography Studies A Report From the International Working Group for Intravascular Optical Coherence Tomography Standardization and Validation. *Journal of the American College of Cardiology*. 2012;59(12):1058-72.
2. Prati F, Romagnoli E, Burzotta F, Limbruno U, Gatto L, La Manna A, et al. Clinical Impact of OCT Findings During PCI The CLI-OPCI II Study. *Jacc-Cardiovascular Imaging*. 2015;8(11):1297-305.
3. Prati F, Romagnoli E, Gatto L, La Manna A, Burzotta F, Limbruno U, et al. Clinical Impact of Suboptimal Stenting and Residual Intrastent Plaque/Thrombus Protrusion in Patients With Acute Coronary Syndrome: The CLI-OPCI ACS Substudy (Centro per la Lotta Contro L’Infarto-Optimization of Percutaneous Coronary Intervention in Acute Coronary Syndrome). *Circ Cardiovasc Interv*. 2016;9(12).
4. Chamie D, Bezerra HG, Attizzani GF, Yamamoto H, Kanaya T, Stefano GT, et al. Incidence, Predictors, Morphological Characteristics, and Clinical Outcomes of Stent Edge Dissections Detected by Optical Coherence Tomography. *Jacc-Cardiovascular Interventions*. 2013;6(8):800-13.
5. Radu MD, Räber L, Heo JH, Gogas BD, Jørgensen E, Kelbæk H, et al. Natural history of optical coherence tomography-detected non-flow-limiting edge dissections following drug-eluting stent implantation. *EuroIntervention*. 2014;9(9):1085-94.

Chapter 7



Intravascular ultrasound findings of the Fantom sirolimus-eluting bioresorbable scaffold at six- and nine-month follow-up: the FANTOM II study

van Zandvoort LJC¹, Dudek D², Weber-Albers J³, Abizaid A⁴, Christiansen EH⁵, Muller DWM⁶, Kochman J⁷, Koltowski L⁷, Flensted Lassen J⁸, Wojdyla R⁹, Wykrzykowska JJ¹⁰, Onuma J^{1, 11}, Daemen J¹

¹ *Erasmus University Medical Center, Thoraxcenter, Department of cardiology, Rotterdam, the Netherlands*

² *Department of cardiology, University Hospital, Krakow, Poland*

³ *Cardiac research GmbH, St.-Johannes-Hospital, Dortmund, Germany*

⁴ *Cardiology institute, Dante Pazzanese, São Paulo, Brazil*

⁵ *Department of cardiology, Aarhus University Hospital, Aarhus, Denmark*

⁶ *Department of cardiology, St Vincent's Hospital, Sydney, Australia*

⁷ *Department of cardiology, Medical University of Warsaw, Poland*

⁸ *Department of cardiology, The Heart Centre Rigshospitalet, Copenhagen, Denmark*

⁹ *Department of cardiology, St. Raphael Hospital, Kraków, Poland*

¹⁰ *Department of cardiology, Academic Medical Center Amsterdam, Amsterdam, the Netherlands*

¹¹ *Clinical Core Laboratory, Cardialysis, Rotterdam The Netherlands*

ABSTRACT

Aims: FANTOM II is a prospective multicenter trial assessing the safety and efficacy of the Fantom Sirolimus-Eluting Bioresorbable Coronary Scaffold (BRS). The present substudy focuses on the 6 and 9 months IVUS findings.

Methods and results: A total of 240 patients with de novo coronary artery lesions presenting with stable or unstable disease were included in 2 sequential cohorts (cohort A (n=117) and B (n=123) in which angiographic follow-up was performed at either 6 or 9 months respectively. Matched IVUS data was available for 35 paired cases in cohort A and 26 paired cases in cohort B.

At 6 months, mean and minimum scaffold area (SA) decreased from $6.09 \pm 1.08 \text{mm}^2$ to $5.88 \pm 1.07 \text{mm}^2$, $p=0.009$ and $5.27 \pm 0.99 \text{mm}^2$ to $5.05 \pm 0.99 \text{mm}^2$, $p=0.01$ respectively. At 9 months, no significant change in mean scaffold and minimum scaffold area was observed ($6.46 \pm 1.11 \text{mm}^2$ to $6.38 \pm 0.96 \text{mm}^2$; $p=0.35$ and $5.45 \pm 1.00 \text{mm}^2$ to $5.36 \pm 0.86 \text{mm}^2$; $p=0.32$ respectively). Neointimal hyperplasia area was low at both 6 ($0.11 \pm 0.12 \text{mm}^2$) and 9 months ($0.20 \pm 0.21 \text{mm}^2$) as was in-scaffold obstruction volume ($1.94 \pm 2.25\%$ at 6 months and $3.40 \pm 4.11\%$ at 9 months).

Conclusion: The use of the Fantom BRS in stable coronary artery disease was associated with low rates of neointimal hyperplasia volume and in-scaffold volume obstruction at both 6 and 9 months.

INTRODUCTION

Bioresorbable scaffolds (BRS) were developed to address problems associated with the use of permanent drug eluting metallic stents (DES) like vascular inflammation, neoatherosclerosis, thrombosis, jailing of side-branches and impairment of future surgical revascularization options^{1,2}. Up until today, multiple types of BRS have been studied for their in vivo performance with varying degrees of success²⁻⁶.

The Fantom BRS (REVA Medical, San Diego, California) is a desaminotyrosine-derived polycarbonate sirolimus-eluting BRS with improved radiopacity and a strut thickness of around 125micron⁷. The device is primarily made from iodinated polycarbonate copolymer of tyrosine analogs (DAT) and biocompatible hydroxyl-esters⁸⁻¹⁰. Due to the iodine atoms, the scaffold has a similar radio-opacity to cobalt chromium DES precluding the need for additional tantalum or platinum radiopaque markers¹¹. The polycarbonate is degraded by hydrolysis in I₂DAT, CO₂ and water. This initial degradation phase is followed by a resorption process that last 4 to 5 years¹².

The device was first assessed in the Fantom I pilot study, followed by the Fantom II study, in the which the use of the scaffold was associated with a major adverse cardiac event rate of 2.6% along with a late lumen loss of $0.25 \pm 0.40 \text{mm}$ in 117 patients included in cohort A with 6 month follow-up^{11,13}. The present report contains the intravascular Ultrasound (IVUS) findings of patients enrolled in the Fantom II study at baseline and either 6 or 9 months.

METHODS

Fantom II is a non-randomized prospective multicenter trial, enrolling patients in 35 sites from Australia, Belgium, Brazil, Denmark, France, Germany, The Netherlands and Poland, assessing the safety and efficacy of the Fantom BRS¹¹. In brief, the study enrolled patients with stable or unstable angina and single de novo coronary artery lesions with an average reference vessel diameter between 2.5mm and 3.5mm and an estimated lesion length of less than 20 mm. The use of intravascular imaging including either IVUS and/or optical coherence tomography (OCT) was optional though encouraged at baseline, and mandatory at follow-up when performed at baseline. A total of 240 patients were enrolled in 2 cohorts (cohort A with 6 and 24 months angiographic follow-up and cohort B with 9 and 48 months angiographic follow-up).

The present study reports the baseline and follow-up (6 and 9 months) IVUS findings of patients enrolled in cohort A and B respectively. Only paired analyses were assessed resulting in 35 paired cases in cohort A and 26 cases in cohort B (Figure 1).

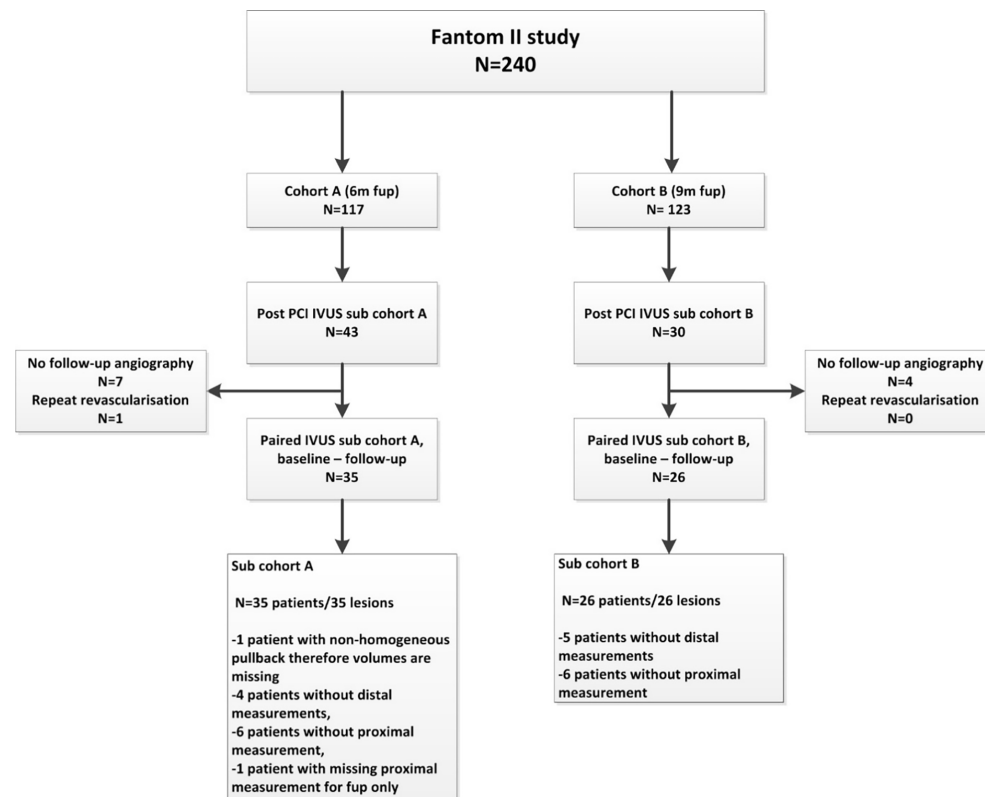


Figure 1. Fantom II inclusion flowchart

QCA analyses

Procedural and follow-up angiograms were assessed at an independent angiographic core laboratory (Yale Cardiovascular Research Group). In-scaffold late lumen loss (LLL) at 6 and 9 months follow-up, as assessed by quantitative coronary angiography (QCA), was defined as the difference between the post procedural minimal lumen diameter (MLD) and the MLD at follow-up. In-scaffold acute recoil was defined as $(A-B)/A$. A was the mean diameter of the stent delivery balloon at the highest pressure A or in case of post dilatation was used, the mean diameter of the post dilatation balloon at the highest pressure. B was the mean luminal diameter post procedural.

IVUS analyses

In 10 from the 35 sites, post procedural IVUS pullbacks were performed. Motorized IVUS pullbacks were performed after an intracoronary bolus of 200µg nitroglycerine at 40MHz (Boston Scientific, Natick, MA, USA or InfraReDx, Burlington, MA, USA) with a pullback speed of 0.5mm/sec. The catheter was positioned distally to the stented segment, at least 10mm from the distal stent edge. The automated pullback acquired footage from the distal reference segment to at least 10mm proximal to the proximal scaffold edge. At follow-up IVUS pullback was repeated in the same coronary segment, which was matched with post-procedural IVUS pullback using the fiducial anatomical landmarks. In case of a required TLR, pre-procedural IVUS acquisitions was used for follow-up analyses.

All IVUS pullbacks were analysed by an independent core lab (Cardialysis BV, Rotterdam, the Netherlands). The region of interest beginning 5 mm distal to and extending 5 mm proximal to the treated segment was examined and analysed¹⁴. Three contours were delineated on IVUS: The endoluminal contour (lumen area, LA), the leading edge of the struts (scaffold area, SA) and the external elastic membrane (EEM) area (vessel area, VA). Accordingly, four areas were quantified and assessed: the luminal area, the neointimal area between the lumen and the scaffold contours ($= SA - LA$), the plaque behind the struts area ($= VA - SA$) and the vessel area. The total plaque area was defined as: $VA - LA$ ¹⁵. Incomplete apposition was defined as one or more scaffold struts separated from the vessel wall. An illustrative figure of angiographic and IVUS footage at baseline, 6 and 9 months follow-up is shown in Figure 2

Underexpansion or expansion rate was measured according to the MUSIC criteria and was defined as $MSA / \text{mean reference LA} * 100$ ¹⁶. The manufactured expected expansion rate was defined as $MSA / (\text{Manufactured radius} * 2\pi) * 100$ ¹⁷. The acute recoil was defined as $(\text{maximal balloon diameter on angiography} - MSA) / \text{maximal balloon diameter on angiography} * 100$ ¹⁸.

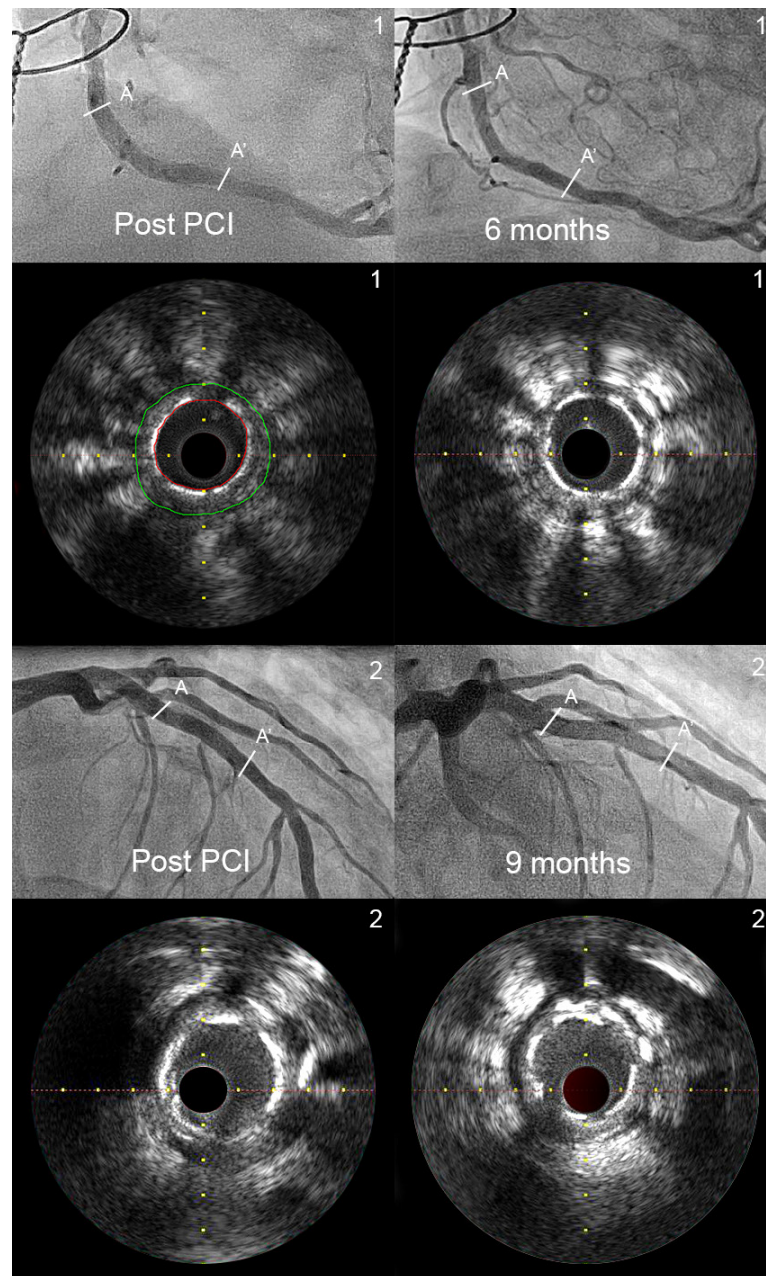


Figure 2. Angiographic and IVUS footage of baseline, 6 and 9 months in two patients

The struts of the Fantom BRS are still clearly visible at 6 months (patient 1) and 9 months follow-up (patient 2). A refers to the proximal stent edge while A' refers to the distal stent edge. The green line in the upper right IVUS still frame indicates the external elastic membrane area. The red line indicates the lumen area.

Statistical Analysis

Statistical analyses were performed by using SPSS (version 21.0, SPSS Inc, Chicago Ill). Categorical variables are expressed as counts and percentages. Differences in categorical variables between allocated cohorts are evaluated by applying chi-square tests, or Fisher's exact tests. Continuous variables are described as mean \pm one standard deviation. Differences in continuous variables between allocated treatment groups are evaluated by applying Student's t-tests. For the main analysis a paired sample t test was used.

RESULTS

Mean age was 59.7 years, 75.4% were male. Diabetes was present in 19.7%. Baseline characteristics did not differ between the cohorts (Table 1).

As compared to cohort A, patients included in cohort B had a slightly longer scaffold length (19.4mm vs. 18.0mm, $p=0.002$), underwent more frequent post dilatation (96.2% vs. 74.3%, $p=0.023$) and average maximum balloon diameter was larger (3.38mm vs. 3.20mm, $p=0.034$) (Table 1).

Pre-procedural QCA analyses of the entire cohort were available for 238 patients, while angiographic follow-up was available in 100 and 105 patients in cohorts A and B respectively. Preprocedural RVD was 2.71 ± 0.37 mm, MLD 0.82 ± 0.31 mm, percentage diameter stenosis was $69.5 \pm 11.0\%$ and acute recoil $4.0 \pm 8.3\%$. In scaffold mean LLL was 0.25 ± 0.40 mm at 6 months in cohort A and 0.33 ± 0.36 mm at 9 months in cohort B.

IVUS cohort A (6 months follow-up)

As compared to baseline, vessel area remained unchanged. At 6 months, mean scaffold area (SA) and minimum scaffold area (MSA) slightly decreased as compared to baseline (mean SA baseline: 6.09 ± 1.08 mm² vs. 5.88 ± 1.07 mm², $p=0.009$; baseline MSA : 5.27 ± 0.99 mm² vs. 5.05 ± 0.99 mm², $p=0.01$). Neointimal hyperplasia area was 0.11 ± 0.12 mm² resulting in an in-scaffold obstruction volume of $1.94 \pm 2.25\%$. Mean and minimum lumen area decreased from baseline to 6 months by 0.32 mm² ($p= 0.005$) and 0.40 mm² ($p=0.006$) respectively (Table 2).

IVUS cohort B (9 months follow-up)

At 9 months follow-up, struts were still visually recognizable on IVUS as highly echogenic material (Figure 2). Mean scaffold area (SA) and minimum scaffold area (MSA) remained unchanged as compared to baseline (mean SA baseline: 6.46 ± 1.11 mm² vs. 6.38 ± 0.96 mm², $p=0.35$; MSA baseline: 5.45 ± 1.00 mm²

vs. $5.36 \pm 0.86 \text{ mm}^2$, $p=0.32$). Neointimal hyperplasia area was $0.20 \pm 0.21 \text{ mm}^2$ resulting in an in-scaffold obstruction volume of $3.40 \pm 4.11\%$. Mean and minimum lumen area decreased from baseline to 9 months by 0.27 mm^2 and 0.49 mm^2 ($p < 0.01$) respectively (Table 3).

Comparative IVUS baseline findings of cohort A and B respectively

Expansion rates, manufacturer expected expansion rates and acute recoil did not significantly differ between the cohorts and expansion rates did not change between baseline and follow-up in both cohorts. However, as compared to cohort B, a lower in segment MLA at baseline was found in cohort A, a discrepancy which was no longer visible at follow-up (6 and 9 months compared) (supplemental Table 1).

Table 1. Baseline and procedure characteristics of IVUS cohort A and B

	Cohort A & B (n=61)	Cohort A (n=35)	Cohort B (n=26)	p value Cohort A vs B
Mean age (years)	59.8±9.4	60.5±7.2	58.8±11.8	0.52
Male (%)	75.4	77.1	73.1	0.72
Diabetes (%)	19.7	20.0	19.2	0.94
Hypertension (%)	78.7	80.0	76.9	0.78
Dyslipidemia (%)	83.6	85.7	80.8	0.61
Family history of coronary artery disease (%)	44.3	45.7	42.3	0.79
Renal impairment at baseline (%)	0.0	0.0	0.0	-
Peripheral vascular disease (%)	3.3	2.9	3.8	0.83
Current smoker	19.7	20.0	19.2	0.94
Prior PCI (%)	39.3	40.0	38.5	0.90
Prior CABG (%)	4.9	8.6	0.0	0.13
Prior MI (%)	31.1	31.4	30.8	0.96
LAD (%)	54.1	48.6	61.5	0.32
LCX (%)	23.0	25.7	19.2	0.55
RCA (%)	21.3	22.9	19.2	0.73
Nominal scaffold diameter (mm)	2.94±0.16	2.93±0.18	2.96±0.14	0.43
Scaffold length (mm)	18.59±1.8	18.0±0.0	19.39±2.58	0.002
Post dilatation (%)	83.6	74.3	96.2	0.023
Max balloon diameter (mm)	3.29±0.30	3.20±0.33	3.38±0.24	0.034

Data are shown as mean ± SD or percentage (%). LAD = left anterior descending artery; LCX = left circumflex artery; PCI = percutaneous coronary intervention; RCA = right coronary artery.

Table 2. Summary table Cohort A: Paired grayscale IVUS measurements per lesion

	Post-Procedure n = 35	6 months n = 35	Δ6 months vs post (95% CI)	p value 6 months vs post
Reference analysis				
- Reference vessel area (mm ²)	13.83±3.44	13.38±3.61	-0.45 [-0.67, 0.97]	0.086
- Reference lumen area (mm ²)	6.66±1.66	6.25±1.64	-0.41 [-0.01, 0.82]	0.057
- Reference plaque area (mm ²)	7.20±2.75	7.15±2.89	-0.05 [-0.35, 0.45]	0.794
In-segment analysis				
- Mean vessel area (mm ²)	14.21±2.88	14.20±3.05	-0.01 [-0.30, 0.33]	0.914
- Mean lumen area (mm ²)	6.25±1.13	5.93±1.13	-0.32 [0.12, 0.51]	0.003
- Minimal lumen area (mm ²)	4.67±1.24	4.53±1.19	-0.14 [-0.23, 0.52]	0.439
- Total plaque area (mm ²)	8.25±3.01	8.25±2.32	0.00 [-0.61, 0.62]	0.991
- Vessel volume (mm ³)	374.85±83.81	380.12±88.86	5.27 [-17.25, 9.67]	0.571
- Lumen volume (mm ³)	165.98±37.66	160.08±36.97	-5.90 [-1.41, 13.71]	0.107
- Total plaque volume (mm ³)	208.67±60.60	220.04±64.04	11.37 [-18.58, -2.38]	0.013
In-scaffold analysis				
- Mean vessel area (mm ²)	14.34±2.83	14.47±2.99	0.13 [-0.56, 0.19]	0.405
- Mean scaffold area (mm ²)	6.09±1.08	5.88±1.07	-0.21 [-0.37, -0.06]	0.0086
- Minimum scaffold Area (mm ²)	5.27±0.99	5.05±0.99	-0.22 [-0.40, -0.05]	0.0131
- Mean lumen area (mm ²)	6.09±1.08	5.77±1.06	-0.32 [-0.48, -0.15]	0.0005
- Minimal lumen area (mm ²)	5.26±0.97	4.86±1.00	-0.40 [-0.61, -0.18]	0.0006
- Total plaque area (mm ²)	8.25±2.20	8.70±2.27	0.45 [0.19, 0.71]	0.0014
- expansion rate (%)	81.29±14.56	83.29±17.54	2.00 [-6.46, 2.45]	0.367
- Neointimal hyperplasia area (mm ²)		0.11±0.12		
- Mal-apposition area (mm ²)	0.00±0.02#	0.00±0.00#	-0.00 [-0.01, 0.00]	0.3950
- Scaffold volume (mm ³)	116.35±29.03	114.61±26.51*	-2.15 [-8.22, 3.91]	0.4751
- Lumen volume (mm ³)	116.20±28.98	112.69±26.18*	-3.93 [-10.06, 2.21]	0.2019
- Total plaque volume (mm ³)	156.21±43.42	169.83±49.32*	12.60 [4.47, 20.73]	0.0034
- In-scaffold obstruction volume (%)		1.94±2.25*		
- Acute recoil (%)†		3.45±10.13		

Data are shown as mean ± SD, differences as mean and 95% confidence limits (CI) (except post dilation). IVUS= Intravascular ultrasound; ISA=Incomplete strut apposition; # In 2 patients malapposition was present at baseline, while at follow-up malapposition was present in 8 patients. *1 patient had a lesion with non-homogeneous pullback at follow-up therefore volumes are missing for this patient, and only 34 lesions remain. †Acute recoil is measured using QCA

Table 3. Summary table Cohort B: Paired grayscale IVUS measurements per lesion

	Post-Procedure n = 26	9 months n = 26	A9 months vs post (95% CI)	p value 9 months vs post
Reference analysis				
- Reference vessel area (mm ²)	14.05±4.07	13.81±4.31	-0.24 [-0.18, 0.67]	0.250
- Reference lumen area (mm ²)	7.40±2.10	7.22±2.18	-0.18 [-0.21, 0.57]	0.351
- Reference plaque area (mm ²)	6.65±2.51	6.46±2.88	-0.19 [-0.22, 0.60]	0.347
In-segment analysis				
- Mean vessel area (mm ²)	14.64±3.15	14.52±3.10	-0.12 [-0.17, 0.41]	0.401
- Mean lumen area (mm ²)	6.70±1.21	6.48±1.09	-0.22 [0.05, 0.40]	0.014
- Minimal lumen area (mm ²)	5.34±1.01	5.09±1.15	-0.25 [-0.05, 0.56]	0.103
- Total plaque area (mm ²)	7.88±2.44	8.04±2.25	0.16 [-0.12, 0.44]	0.254
- Vessel volume (mm ³)	403.97±107.75	392.38±97.61	-11.59 [-6.33, 29.51]	0.195
- Lumen volume (mm ³)	185.54±48.40	176.17±46.62	-9.37 [1.79, 16.95]	0.017
- Total plaque volume (mm ³)	216.55±72.14	216.21±61.21	-0.34 [-12.12, 12.79]	0.956
In-scaffold analysis				
- Mean vessel area (mm ²)	14.83±3.11	14.76±3.01	-0.07 [-0.24, 0.39]	0.635
- Mean scaffold area (mm ²)	6.46±1.11	6.38±0.96	-0.08 [-0.25, 0.09]	0.3512
- Minimum scaffold Area (mm ²)	5.45±1.00	5.36±0.86	-0.09 [-0.27, 0.09]	0.3185
- Mean lumen area (mm ²)	6.50±1.15	6.24±1.09	-0.27 [-0.45, -0.08]	0.0064
- Minimal lumen area (mm ²)	5.47±1.01	4.98±1.15	-0.49 [-0.82, -0.17]	0.0045
- Total plaque area (mm ²)	8.33±2.37	8.52±2.24	0.19 [-0.10, 0.49]	0.1849
- expansion rate (%)	76.82±16.08	79.18±20.25	2.36 [-8.65, 3.96]	0.450
- Neointimal hyperplasia area (mm ²)	0.20±0.21	0.20±0.21		
- Mal-apposition area (mm ²)	0.05±0.12#	0.04±0.15#	-0.01 [-0.04, 0.03]	0.7265
- Scaffold volume (mm ³)	137.04±33.16	132.80±27.50	-4.24 [-11.53, 3.04]	0.2417
- Lumen volume (mm ³)	137.61±33.98	129.29±28.40	-8.32 [-15.38, -1.25]	0.0228
- Total plaque volume (mm ³)	177.73±62.20	177.92±51.26	0.20 [-11.88, 12.27]	0.9737
- In-scaffold obstruction volume (%)	3.40±4.11			
- Acute recoil (%)*	5.25±7.35			

Data are shown as mean ± SD, differences as mean and 95% confidence limits (CI) (except post dilation). IVUS= Intravascular ultrasound; ISA=Incomplete strut apposition; # In 10 patients malapposition was present at baseline, while at follow-up malapposition was present in 7 patients.* Acute recoil is measured using QCA

DISCUSSION

The present IVUS substudy of the FANTOM II study confirms the efficacy of the Fantom BRS in patients with stable coronary artery disease by successfully inhibiting neointimal hyperplasia at 6 and 9 months as assessed by IVUS. With a backbone that is designed to be absorbed within 4 to 5 years, our results show obstruction volumes of 1.9% and 3.4% at 6 and 9 months respectively, strengthening the recently published clinical and angiographic findings with late loss of 0.25 mm¹¹. Although the Fantom II study only represents the performance of the scaffold in highly selected cases, the obstruction volumes found are comparable to contemporary metallic DES like Resolute Onyx with reported obstruction volumes of 6.9% at 8 months follow-up¹⁹.

A slight decrease in mean SA and MSA was observed in cohort A (0.21mm² (3.45%) and 0.22mm² (4.17%) respectively) at 6 months, which was not seen in cohort B at 9 months in which mean SA and MSA remained unchanged. Although the apparent decrease in mean SA on IVUS in cohort A was merely 3.45% and expansion rates did not significantly differ between cohorts, post dilatation was more often performed in cohort B (p=0.023) and larger balloon diameters were used for post dilatation (p=0.034), resulting in a 0.18mm² larger MSA and 0.37mm² mean SA at baseline in cohort B as compared to cohort A – despite identical mean labelled nominal scaffold diameters. The latter supports the use of aggressive post dilatation with high pressure balloons²⁰.

Irrespective of the minor differences between both cohorts in the present study the performance of the Fantom BRS appeared comparable to earlier published findings on the Absorb BVS (Abbott Vascular, Santa Clara, California, USA) and superior to the data on the Dreams 2G (Biotronik, Bülach, Switzerland)^{4, 6}. Following BVS implantation, both mean SA and minimal SA decreased over a period of 6 months after implantation (MSA: -0.27 mm² (4.9%) and mean SA -0.14 mm² (2.1%)) while following implantation of the Dreams 2G, MSA decreased by 0.79 mm² (14.6%) (mean SA remained unchanged 0.03mm² (0.05%))⁴. Interestingly, in the 12-month results of Absorb BVS, both MSA and minimum SA were back at baseline levels (-0.04 mm² (0.08%) and +0.04 mm² (0.06%) respectively) and at 3 years, mean SA even increased further with 0.65mm² (10.1%) as compared to baseline, whereas the MSA remained unchanged¹⁵. A similar late increase in mean SA was seen 12 months after implantation of the DESolve BRS (Elixir Medical Corporation, Sunnyvale, California, USA) in which mean SA increased by 0.93mm² (15.7%)²¹. Conversely, this late restoration of scaffold dimensions was not seen 12 months after implantation of the magnesium Dreams 2G BRS in which a persistent

decrease in minimal SA (-0.93 mm², 16.1%) and mean SA (-0.34 mm², 5.2%) (p=ns) as assessed by IVUS was found^{5, 22}. Unfortunately, in the latter studies, no information on the aggressiveness of post dilatation and/or post dilatation balloon diameters was provided. Prior in vitro research demonstrated 60-70% molecular weight loss after 6-9 months post implantation²³. In the present study, on IVUS, scaffold struts were still well visible at both 6 and 9 months follow-up without any apparent change in strut echogenicity (Figure 2). Although the latter might be due to the typical character of the materials, longer-term follow-up is needed to confirm the integrity of the Fantom scaffold at 2 and 4 years.

Limitations

Several limitations need to be mentioned. First, the results of the present study should be considered to be applicable to a highly selected patient population with stable or unstable coronary artery disease and non-complex coronary artery lesions. The external validity might not be as strong due to the strict in- and exclusion criteria of the study as well as the fact that not all participating sites included patients for the IVUS analysis. Second, although the use of intravascular imaging was encouraged, there was no predefined number of IVUS cases resulting in a relatively small number of IVUS cases with matched baseline and follow-up imaging. Third, the matching of post PCI and follow-up IVUS frames are prone to error and we cannot ascertain for discrepancies that might have arisen. Finally, we hypothesized that the non-significant difference in baseline mean scaffold area and MSA in the subgroup of patients with baseline and follow-up IVUS was driven by more aggressive post dilatation in cohort B. However, in the total Fantom cohort no difference in post dilatation strategy was found between both cohorts. The latter might suggest a play of chance. In addition, the comparison between follow-up dimensions in supplement Table 1 between cohorts should be interpreted with caution given the differences in follow-up duration.

CONCLUSION

The use of the Fantom BRS in stable coronary artery disease was effective with low rates of neointimal hyperplasia volume and in-scaffold volume obstruction at both 6 and 9 months as assessed by IVUS.

Impact on daily practice

The present findings strengthen and extend the recently published main clinical safety and efficacy data of the use of the Fantom Sirolimus-Eluting Bioresorbable Coronary Scaffold in patients with stable coronary artery disease at 6 and 9 months

follow-up. The use of the Fantom BRS was associated with in-scaffold obstruction volumes of 3.40% at 9 months, comparable to contemporary metallic DES. These results support the safe use of the Fantom BRS with aggressive post dilatation in daily practice in appropriate patients. Longer-term clinical and invasive imaging data are needed to confirm the current findings.

Supplement table 1. Summary table Cohort A and B compared: Paired grayscale IVUS measurements per lesion

	Post-Procedure cohort A (n=35)	Post-Procedure cohort B (n=26)	p value baseline	6 months follow-up cohort A (n=35)	9 months follow-up cohort B (n=26)	p value follow-up
Reference analysis						
Reference vessel area (mm ²)	13.83±3.44	14.05±4.07	0.818	13.38±3.61	13.81±4.31	0.675
- Reference lumen area (mm ²)	6.66±1.66	7.40±2.10	0.130	6.25±1.64	7.22±2.18	0.508
- Reference plaque area (mm ²)	7.20±2.75	6.65±2.51	0.054	7.15±2.89	6.46±2.88	0.447
In-segment analysis						
- Mean vessel area (mm ²)	14.21±2.88	14.64±3.15	0.582	14.20±3.05	14.52±3.10	0.683
- Mean lumen area (mm ²)	6.25±1.13	6.70±1.21	0.141	5.93±1.13	6.48±1.09	0.082
- Minimal lumen area (mm ²)	4.67±1.24	5.34±1.01	0.040	4.53±1.19	5.09±1.15	0.090
- Total plaque area (mm ²)	8.25±3.01	7.88±2.44	0.610	8.25±2.32	8.04±2.25	0.718
- Vessel volume (mm ³)	374.85±83.81	403.97±107.75	0.240	380.12±88.86	392.38±97.61	0.614
- Lumen volume (mm ³)	165.98±37.66	185.54±48.40	0.081	160.08±36.97	176.17±46.62	0.141
- Total plaque volume (mm ³)	208.67±60.60	216.55±72.14	0.648	220.04±64.04	216.21±61.21	0.816
In-scaffold analysis						
- Mean vessel area (mm ²)	14.34±2.83	14.83±3.11	0.520	14.47±2.99	14.76±3.01	0.713
- Mean scaffold area (mm ²)	6.09±1.08	6.46±1.11	0.194	5.88±1.07	6.38±0.96	0.062
- Minimum scaffold Area (mm ²)	5.27±0.99	5.45±1.00	0.487	5.05±0.99	5.36±0.86	0.196
- Mean lumen area (mm ²)	6.09±1.08	6.50±1.15	0.149	5.77±1.06	6.24±1.09	0.098
- Total plaque area (mm ²)	5.26±0.97	5.47±1.01	0.410	4.86±1.00	4.98±1.15	0.680
- Total plaque volume (mm ³)	8.25±2.20	8.33±2.37	0.899	8.70±2.27	8.52±2.24	0.759
- Neointimal hyperplasia area (mm ²)				0.11±0.12	0.20±0.21	0.082
- Mal-apposition area (mm ²)	0.00±0.02	0.05±0.12	0.065	0.00±0.00	0.04±0.15	0.159
- Scaffold volume (mm ³)	116.35±29.03	137.04±33.16	0.012	114.61±26.51*	132.80±27.50	0.012
- Lumen volume (mm ³)	116.20±28.98	137.61±33.98	0.010	112.69±26.18*	129.29±28.40	0.022
- Total plaque volume (mm ³)	156.21±43.42	177.73±62.20	0.117	169.83±49.32*	177.92±51.26	0.539
In-scaffold obstruction volume (%)						
- In-scaffold obstruction volume (follow-up baseline)				1.94±2.25*	3.40±4.11	0.080
Difference minimal scaffold area (follow-up baseline)				-0.21±0.45	-0.08±0.42	0.246
Increased mean scaffold area (%)				-0.22±0.51	-0.09±0.044	0.279
Increased minimal scaffold area (%)				40.0	50.0	0.437
Expansion rate (%)				31.4	46.2	0.241
Manufactured expected expansion rate (%)	81.29±14.56	76.82±16.08	0.267	83.29±17.54	79.18±20.25	0.404
Acute recoil (%)*	78.56±14.68	78.89±12.23	0.927			
	3.45±10.13	5.25±7.35	0.524			

Data are shown as mean ± SD, differences as mean and 95% confidence limits (CI) (except post dilatation). IVUS= Intravascular ultrasound, ISA=Incomplete strut apposition; * Acute recoil is measured using QCA

REFERENCES

1. Joner M, Finn AV, Farb A, Mont EK, Kolodgie FD, Ladich E, Kutys R, Skorija K, Gold HK, Virmani R. Pathology of drug-eluting stents in humans: delayed healing and late thrombotic risk. *J Am Coll Cardiol*. 2006;48(1):193-202.
2. Iqbal J, Onuma Y, Ormiston J, Abizaid A, Waksman R, Serruys P. Bioresorbable scaffolds: rationale, current status, challenges, and future. *Eur Heart J*. 2014;35(12):765-76.
3. Stone GW. Bioresorbable Vascular Scaffolds: More Different Than Alike? *JACC Cardiovasc Interv*. 2016(1876-7605).
4. Haude M, Ince H, Abizaid A, Toelg R, Lemos PA, von Birgelen C, Christiansen EH, Wijns W, Neumann FJ, Kaiser C, Eeckhout E, Lim ST, Escaned J, Garcia-Garcia HM, Waksman R. Safety and performance of the second-generation drug-eluting absorbable metal scaffold in patients with de-novo coronary artery lesions (BIOSOLVE-II): 6 month results of a prospective, multicentre, non-randomised, first-in-man trial. *Lancet*. 2016;387(10013):31-9.
5. Serruys PW, Onuma Y, Dudek D, Smits PC, Koolen J, Chevalier B, de Bruyne B, Thuesen L, McClean D, van Geuns RJ, Windecker S, Whitbourn R, Meredith I, Dorange C, Veldhof S, Hebert KM, Sudhir K, Garcia-Garcia HM, Ormiston JA. Evaluation of the second generation of a bioresorbable everolimus-eluting vascular scaffold for the treatment of de novo coronary artery stenosis: 12-month clinical and imaging outcomes. *J Am Coll Cardiol*. 2011;58(15):1578-88.
6. Serruys PW, Onuma Y, Ormiston JA, de Bruyne B, Regar E, Dudek D, Thuesen L, Smits PC, Chevalier B, McClean D, Koolen J, Windecker S, Whitbourn R, Meredith I, Dorange C, Veldhof S, Miquel-Hebert K, Rapoza R, Garcia-Garcia HM. Evaluation of the second generation of a bioresorbable everolimus drug-eluting vascular scaffold for treatment of de novo coronary artery stenosis: six-month clinical and imaging outcomes. *Circulation*. 2010;122(22):2301-12.
7. Simonsen J, Holck E, Carrié D, Frey N, Lutz M, Weber-Albers J, Dudek D, Chevalier B, Dijkstra J, Lassen JF, Anderson J, Christiansen E, Abizaid A, Holm N. TCT-29 Performance and healing patterns after implantation of a novel sirolimus eluting bioresorbable scaffold. Six-month follow-up by optical coherence tomography in the FANTOM II study. *Journal of the American College of Cardiology*. 2016;68(18, Supplement):B12.
8. Tangpasuthadol V, Pendharkar SM, Kohn J. Hydrolytic degradation of tyrosine-derived polycarbonates, a class of new biomaterials. Part I: Study of model compounds. *Biomaterials*. 2000;21(23):2371-8.
9. Abramson S B, LeveneH, Simon J,Kohn J.Small. Small changes in polymer structure can dramatically increase degradation rates: the effect of free carboxylate groups on the properties of tyrosine-derived polycarbonates. In: *Transactions of the Sixth World Biomaterials Congress: May 15-20, 2000 Minneapolis, MN: Society for Biomaterials, 2000.*
10. Pendharkar S.M.J.K. KJ. Iodinated derivatives of tyrosine-based polycarbonates: new radioopaque degradable biomaterials. SB Goodman (Ed), *Society for Biomaterials Transactions: Twenty-Fourth Annual Meeting of the Society for Biomaterials*. 1998;Society for Biomaterial, Minneapolis.
11. Abizaid A, Carrié D, Frey N, Lutz M, Weber-Albers J, Dudek D, Chevalier B, Weng S-C, Costa RA, Anderson J, Stone GW. 6-Month Clinical and Angiographic Outcomes of a Novel Radiopaque Sirolimus-Eluting Bioresorbable Vascular Scaffold. *JACC: Cardiovascular Interventions*. 2017;10(18):1832.
12. Leibundgut PDMG. Tyrocore: a proprietary polymer uniquely designed for vascular scaffolds. EuroPCR presentation. 2018:1-14.
13. Costa JdR, Abizaid A, Chamie D, Lansky A, Kochman J, Koltowski L. INITIAL RESULTS OF THE FANTOM 1 TRIAL: A FIRST-IN-MAN EVALUATION OF A NOVEL, RADIOPAQUE SIROLIMUS-ELUTING BIORESORBABLE VASCULAR SCAFFOLD. *Journal of the American College of Cardiology*. 2016;67(13 Supplement):232.
14. Mintz GS, Nissen SE, Anderson WD, Bailey SR, Erbel R, Fitzgerald PJ, Pinto FJ, Rosenfield K, Siegel RJ, Tuzcu EM, Yock PG. American College of Cardiology Clinical Expert Consensus Document on Standards for Acquisition, Measurement and Reporting of Intravascular Ultrasound Studies (IVUS). A report of the American College of Cardiology Task Force on Clinical Expert Consensus Documents. *J Am Coll Cardiol*. 2001;37(5):1478-92.
15. Serruys PW, Onuma Y, Garcia-Garcia HM, Muramatsu T, van Geuns RJ, de Bruyne B, Dudek D, Thuesen L, Smits PC, Chevalier B, McClean D, Koolen J, Windecker S, Whitbourn R, Meredith I, Dorange C, Veldhof S, Hebert KM, Rapoza R, Ormiston JA. Dynamics of vessel wall changes following the implantation of the absorb everolimus-eluting bioresorbable vascular scaffold: a multi-imaging modality study at 6, 12, 24 and 36 months. *EuroIntervention*. 2014;9(11):1271-84.
16. de Jaegere P, Mudra H, Figulla H, Almagor Y, Doucet S, Penn I, Colombo A, Hamm C, Bartorelli A, Rothman M, Nobuyoshi M, Yamaguchi T, Voudris V, DiMario C, Makovski S, Hausmann D, Rowe S, Rabinovich S, Sunamura M, van Es GA. Intravascular ultrasound-guided optimized stent deployment. Immediate and 6 months clinical and angiographic results from the Multicenter Ultrasound Stenting in Coronaries Study (MUSIC Study). *Eur Heart J*. 1998;19(8):1214-23.
17. He Y, Maehara A, Mintz GS, Bharaj H, Castellanos C, Kesanakurthy S, Wu X, Guo N, Choi SY, Leon MB, Stone GW, Mehran R, Rabbani LE, Moses JW. Intravascular ultrasound assessment of cobalt chromium versus stainless steel drug-eluting stent expansion. *Am J Cardiol*. 2010;105(9):1272-5.
18. Aziz S, Morris JL, Perry RA, Stables RH. Stent expansion: a combination of delivery balloon underexpansion and acute stent recoil reduces predicted stent diameter irrespective of reference vessel size. *Heart*. 2007;93(12):1562-6.
19. Price MJ, Shlofmitz RA, Spriggs DJ, Haldis TA, Myers P, Popma Almonacid A, Maehara A, Dauler M, Peng Y, Mehran R. Safety and efficacy of the next generation Resolute Onyx zotarolimus-eluting stent: Primary outcome of the RESOLUTE ONYX core trial. *Catheter Cardiovasc Interv*. 2017.
20. Anadol R, Lorenz L, Weissner M, Ullrich H, Polimeni A, Munzel T, Gori T. Characteristics and

- outcome of patients with complex coronary lesions treated with bioresorbable scaffolds Three years follow-up in a cohort of consecutive patients. *EuroIntervention*. 2017.
21. Abizaid A, Costa RA, Schofer J, Ormiston J, Maeng M, Witzendichler B, Botelho RV, Costa JR, Jr., Chamie D, Abizaid AS, Castro JP, Morrison L, Toyloy S, Bhat V, Yan J, Verheye S. Serial Multimodality Imaging and 2-Year Clinical Outcomes of the Novel DESolve Novolimus-Eluting Bioresorbable Coronary Scaffold System for the Treatment of Single De Novo Coronary Lesions. *JACC Cardiovasc Interv*. 2016;9(6):565-74.
 22. Haude M, Ince H, Abizaid A, Toelg R, Lemos PA, von Birgelen C, Christiansen EH, Wijns W, Neumann FJ, Kaiser C, Eeckhout E, Lim ST, Escaned J, Onuma Y, Garcia-Garcia HM, Waksman R. Sustained safety and performance of the second-generation drug-eluting absorbable metal scaffold in patients with de novo coronary lesions: 12-month clinical results and angiographic findings of the BIOSOLVE-II first-in-man trial. *Eur Heart J*. 2016;37(35):2701-9.
 23. Abizaid DA. First Report for the 12-month clinical outcomes of the Fantom sirolimus-eluting bioresorbable scaffold. *EuroPCR presentation*. 2017:1-23.

Chapter 8



Serial invasive imaging follow-up of the first clinical experience with the Magmaris magnesium bioresorbable scaffold

Tovar Forero MN, van Zandvoort LJC, Masdjedi K, Diletti R, Wilschut J, de Jaegere PPT, Zijlstra F, van Mieghem NMDA, Daemen J

Erasmus University Medical Center, Thoraxcenter, Department of cardiology, Rotterdam, the Netherlands

Catheter Cardiovasc Interv. 2020;95(2):226-31.

ABSTRACT

Objectives: To assess the performance of the commercially available Magmaris sirolimus-eluting bioresorbable scaffold (BRS) with invasive imaging at different time points.

Background: Coronary BRS with a magnesium backbone have been recently studied as an alternative to polymeric scaffolds, providing enhanced vessel support and a faster resorption rate. We aimed to assess the performance of the commercially available Magmaris sirolimus-eluting BRS at different time points.

Methods: A prospective, single-center, nonrandomized study was performed at the Thoraxcenter, Erasmus Medical Center, Rotterdam, The Netherlands. Six patients with stable de novo coronary artery lesions underwent single-vessel revascularization with the Magmaris sirolimus-eluting BRS. Invasive follow-up including intravascular imaging using optical coherence tomography (OCT) was performed at different time points.

Results: At a median of 8 months (range 4–12 months) target lesion failure occurred in one patient. Angiography revealed a late lumen loss of 0.59 ± 0.39 mm, a percentage diameter stenosis of $39.65 \pm 15.81\%$, and a binary restenosis rate of 33.3%. OCT showed a significant reduction in both minimal lumen area (MLA) and scaffold area at the site of the MLA by 43.44 ± 28.62 and $38.20 \pm 25.74\%$, respectively. A fast and heterogeneous scaffold degradation process was found with a significant reduction of patent struts at 4–5 months.

Conclusion: Our findings show that the latest iteration of magnesium BRS suffers from premature dismantling, resulting in a higher than expected decrease in MLA.

INTRODUCTION

Bioresorbable scaffolds (BRS) provide short-term vessel scaffolding while avoiding long-term consequences of metallic drug-eluting stents (DES). Recent studies demonstrated higher rates of clinical events with polymeric BRS as compared to contemporary metallic DES ¹. In order to improve BRS performance, alternative backbone materials such as magnesium are currently under investigation. First generations of absorbable magnesium scaffolds (AMS-1 and AMS-2; Biotronik, Berlin, Germany) failed to maintain vessel support due to rapid degradation process ². Later iterations of the device (DREAMS and DREAMS 2G; Biotronik AG, Bülach, Switzerland) demonstrated safety and efficacy in the BIOSOLVE I and BIOSOLVE II trials ^{3,4}. The Magmaris sirolimus-eluting BRS (Biotronik AG) represents the latest generation and is currently being tested in the BIOSOLVE III and IV studies.

We present the findings of clinical and intravascular imaging at different time points following the commercial use of the Magmaris sirolimus-eluting BRS.

MATERIALS AND METHODS

All commercial cases treated with the Magmaris BRS (six cases) in the Thoraxcenter of the Erasmus Medical Center, Rotterdam, The Netherlands, from September 2016 to April 2017 were included in the analysis. Angiographic follow-up was available for all patients at a median of 8 months (range 4–12 months). Quantitative coronary analysis (QCA) and optical coherence tomography (OCT) imaging analysis were performed offline. In-device measurements are reported and presented as mean \pm 1 standard deviation (SD) or percentages. Wilcoxon's signed rank test was used to analyze paired comparisons between continuous values. The coefficient of correlation of Pearson (*r*) was used to determine the linear relationship between quantitative variables. A value of $p < .05$ was considered statistically significant. Statistical analysis was conducted using SPSS for Windows version 21 (SPSS Inc., Chicago, IL) (see Supporting Information, Methods).

RESULTS

All patients presented with stable angina and noncomplex single-vessel coronary artery disease. Mean age was 57.2 years and 50% were male. One scaffold per patient was implanted; mean BRS diameter and length were 3.08 ± 0.20 and 20.00 ± 4.47 mm, respectively. High-pressure predilatation and post-dilatation was implemented in all cases using noncompliant (NC) balloons. (see Tables S1 and S2).

OCT post-procedure was performed in five cases. Procedural and device success was 100%. Patients were discharged on dual antiplatelet therapy (DAPT) for at least 12 months along with high-intensity statin treatment.

Offline pre-percutaneous coronary intervention (pre-PCI) QCA revealed a lesion length of 16.50 ± 4.61 mm, percentage diameter stenosis (%DS) of $61.95 \pm 5.30\%$, and a reference vessel diameter (RVD) of 2.75 ± 0.25 . Pre-dilatation balloon diameter/RVD ratio was 1.10 ± 0.10 . BRS diameter/RVD ratio was 1.13 ± 0.10 , and post-dilatation balloon diameter/BRS diameter ratio was 1.14 ± 0.10 . Residual %DS was $22.41 \pm 8.13\%$. Acute recoil was $5.34 \pm 3.99\%$. Offline post-percutaneous coronary intervention (post-PCI) OCT showed a minimal lumen area (MLA) of 5.64 ± 1.47 mm² and a minimal scaffold area (MSA) of 5.62 ± 1.60 mm². Scaffold expansion (SE) according to reference vessel area (SE-RVA) was $91.04 \pm 18.13\%$ and scaffold expansion according to manufacturer's expected area (SE-MEA) was $73.84 \pm 16.33\%$. Eccentricity index and symmetry index were 0.88 ± 0.01 and 0.32 ± 0.08 , respectively. Incomplete strut apposition was $3.16 \pm 4.22\%$ (Table 1). No edge dissections were found.

At a median of 8 months (minimum 4 months, maximum 12 months), all patients were under DAPT and target lesion failure occurred in one patient (patient #5, see Figure S1) based on severe constrictive remodeling. All other patients remained asymptomatic.

Offline QCA of the invasive follow-up procedure revealed a late lumen loss (LLL) of 0.59 ± 0.39 mm, %DS of $39.65 \pm 15.81\%$, and a binary restenosis rate of 33.3%. Offline OCT at follow-up demonstrated a decrease in MLA by $43.44 \pm 28.62\%$ ($p = .042$), along with a significant decrease in scaffold area (SA) at the site of the MLA by $38.20 \pm 25.74\%$ ($p = .043$) (Figure 1 and Table 1).

Table 1. QCA and OCT measurements

	Post-PCI	Follow-up	Absolute difference	Relative difference (%)	p value
QCA measurements¹					
Lesion length (mm)	19.79 ± 4.48	20.12 ± 4.64	-0.33 ± 0.41	-1.59 ± 1.97	0.116
Reference vessel diameter (mm)	2.92 ± 0.26	2.74 ± 0.39	0.18 ± 0.21	6.47 ± 7.05	0.080
Minimal lumen diameter (mm)	2.25 ± 0.20	1.66 ± 0.48	0.59 ± 0.39	26.33 ± 19.52	0.028
Mean lumen diameter (mm)	2.67 ± 0.23	2.30 ± 0.35	0.37 ± 0.22	14.00 ± 8.79	0.028
In device diameter stenosis (%)	22.41 ± 8.13	39.65 ± 15.81	-17.24 ± 16.48	-99.88 ± 103.13	0.046
Acute recoil (%)	5.34 ± 3.99	NA	NA	NA	NA
OCT measurements					
MLA (mm ²) ²	5.64 ± 1.47	3.24 ± 1.85	2.41 ± 1.51	43.44 ± 28.62	0.042
Mean lumen area (mm ²) ²	7.03 ± 1.91	6.82 ± 3.79	0.22 ± 2.64	5.49 ± 36.04	0.686
MSA (mm ²)	5.62 ± 1.60	NA	NA	NA	NA
Mean SA (mm ²)	6.87 ± 1.73	NA	NA	NA	NA
SA at MLA site (mm ²) ³	6.06 ± 1.70	3.76 ± 1.77	2.30 ± 1.48	38.20 ± 25.74	0.043
ISA (%) ⁴	3.16 ± 4.22	0.44 ± 0.88	2.72 ± 3.37	70.25 ± 47.68	0.109
SE-RVA (%)	91.04 ± 18.13	NA	NA	NA	NA
SE-MEA (%)	73.84 ± 16.36	NA	NA	NA	NA
Eccentricity index	0.88 ± 0.01	NA	NA	NA	NA
Symmetry index	0.32 ± 0.08	NA	NA	NA	NA
Maximum attenuation values ²	16.4 ± 2.63	8.71 ± 5.38	7.70 ± 5.74	46.62 ± 30.7	0.080
Maximum backscattering values ²	8.97 ± 0.33	8.13 ± 0.59	0.84 ± 0.68	9.23 ± 7.22	0.080

Paired comparison of the pooled data measurements at baseline post-intervention (post-PCI) and at a median follow-up of 8 months by QCA and OCT. Data area expressed as mean ± SD.

Abbreviations: ISA, incomplete strut apposition; MLA, minimal lumen area; MSA, minimal scaffold area; OCT, optical coherence tomography; post-PCI, post-percutaneous coronary intervention; QCA, quantitative coronary analysis; SA, scaffold area; SE-MEA, scaffold expansion according to manufacturer's expected area; SE-RVA, scaffold expansion according to reference vessel area.

1 Comparison made for six patients.; 2 Comparison made for five patients; 3 Comparison made for five patients with the SA at baseline and follow-up matching the same cross-sectional area; 4 Comparison made for four patients.

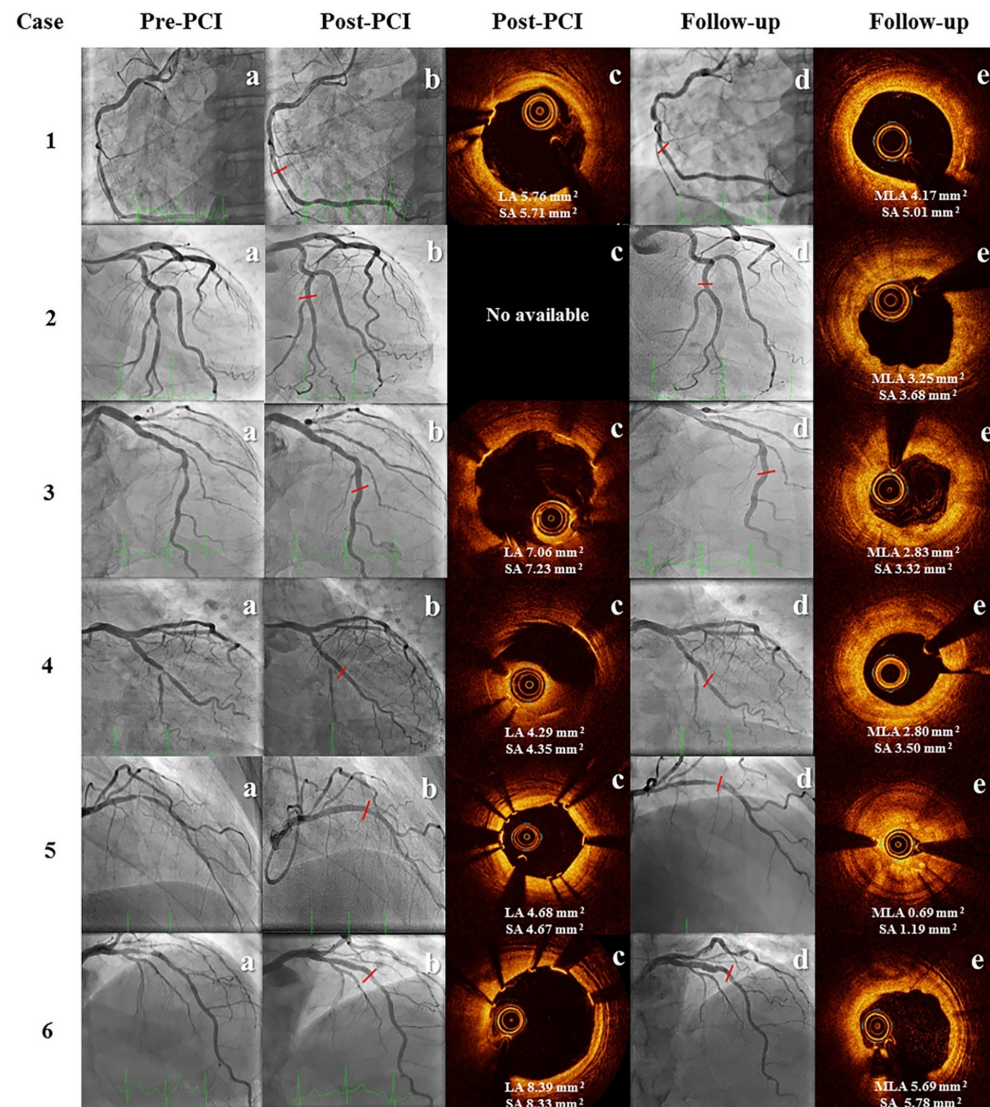


Figure 1. Angiography and OCT imaging at baseline and follow-up

Angiography imaging available for six patients showing target vessel at baseline before intervention (pre-PCI), post-intervention (post-PCI) and at invasive control (follow-up). OCT imaging available for five patients at post-intervention (post-PCI) and for six patients at invasive control (follow-up). Comparison of cross-sectional image at follow-up with the MLA matched with the same cross-sectional image at baseline. LA, lumen area; MLA, minimal lumen area; OCT, optical coherence tomography; post-PCI, post-percutaneous coronary intervention; pre-PCI, pre-percutaneous coronary intervention; SA, scaffold area

Percentage lumen area (%LA) stenosis was 56.64% with a binary restenosis rate of 83.3%.

In a per-scaffold subsegment analysis, a strong linear correlation between SA at baseline and %LA reduction at follow-up was found ($r = -.87$, $p = .001$). Furthermore, a similar correlation was present between SE at baseline and %LA reduction at follow-up according to both RVA and MEA ($r = -.86$, $p = .001$ and $r = -.85$, $p = .002$, respectively) (see Figure S2a–c). Attenuation and backscattering analysis demonstrated a numerical reduction of maximum indices that correspond with strut degradation. Yet, both high and low values were within the same scaffolded segment at follow-up illustrating a heterogeneous strut degradation process (see Figures S3 and S4). No evidence of edge dissection or thrombosis was found.

DISCUSSION

Sufficient radial force to overcome elastic recoil and plaque resistance is an essential feature of contemporary stents. The mechanical properties of coronary stents are influenced by backbone/polymer material, geometry, and strut thickness⁵; recently, with the advent of BRS, the resorption time was also added to this equation. Driven by the presentation of case #5 with severe early scaffold collapse at 4 months, and the recent data on adverse events related to Absorb Bioresorbable vascular scaffold (BVS), our hospital institutional board mandated us to call back all previous cases treated with the commercially available Magmaris BRS and to perform invasive control in order to assess the performance of this device. This resulted in imaging assessment at different follow-up time points.

The Magmaris BRS starts its degradation process as soon as 3 months and completes at 12 months.⁶ Our results revealed a significant decrease in patent struts with a heterogeneous resorption pattern as soon as 4–5 months postimplantation; the latest was demonstrated by an important reduction of attenuation and backscattering indices; this is in line with a serial OCT imaging analysis performed in the BIOSOLVE II trial, showing a significant decrease in MLA of 28.3% at 6 months, and reduction of attenuation and backscattering values with fewer struts remnants visible^{3, 7}. A rapid bioresorption rate might induce nonuniform vessel support and loss of radial strength, which has been corroborated with the first generation of Absorb BVS and magnesium BRS^{2, 8}. The present report suggests that the most recent version of magnesium BRS also suffers from premature dismantling.

Whether the high LA reduction as found in our study could be attributed to a

lower radial strength secondary to rapid bioresorption, an excessive neointimal formation, or both, is yet to be proven. Complete SA and neointimal volumes throughout the scaffolded segment could not be determined due to the difficulty in recognizing patent struts; however, when the SA was analyzable, a significant reduction of SA was found compared to the postimplantation result at the same location. These findings are in line with seven recently published case reports on severe lumen reduction and scaffold collapse after Magmaris BRS implantation⁹⁻¹⁵. Furthermore, acute recoil was only 5.3%, in line with current generation metallic DES and BVS^{16, 17}. Preclinical data have suggested that increased local inflammation is responsible for the higher LLL obtained during the Magmaris degradation process, and a switch to a progressive positive vessel remodeling once the bioresorption is completed might be expected¹⁸. The latest warrants for serial invasive evaluation of the vessel response beyond 12 months. Nevertheless, vessel constrictive remodeling occurs between 1 and 6 months after PCI; therefore, assuring optimal radial support for at least 6 months after device implantation seems to be crucial¹⁹.

Although careful lesion preparation and systematic high-pressure post-dilatation with NC balloons were routinely performed in all cases, a trend toward enhanced lumen loss in the distal scaffold edges was noticed. The latter appeared to be strongly linked to the post-procedural SA and lower SE at the most distal scaffold subsegments, compared to the middle and proximal subsegments. This discrepancy could be explained by the presence of smaller vessel diameter in the distal subsegments leading to scaffold oversizing, and potentially less aggressive post-dilatation due to the challenge in visualizing the tantalum markers. OCT assessment of magnesium BRS has shown an increase of lumen volume loss when expansion index is >1 ,²⁰ and previous data on Absorb BVS have correlated implantation in small vessel diameter with a higher rate of in-device restenosis,²¹ eccentricity, and asymmetry²². Performing pre-procedural intracoronary imaging for vessel sizing and lesion characterization might help to further improve lesion/device selection²³. On the other hand, increasing device visibility under fluoroscopy for future BRS generations could boost expansion optimization.

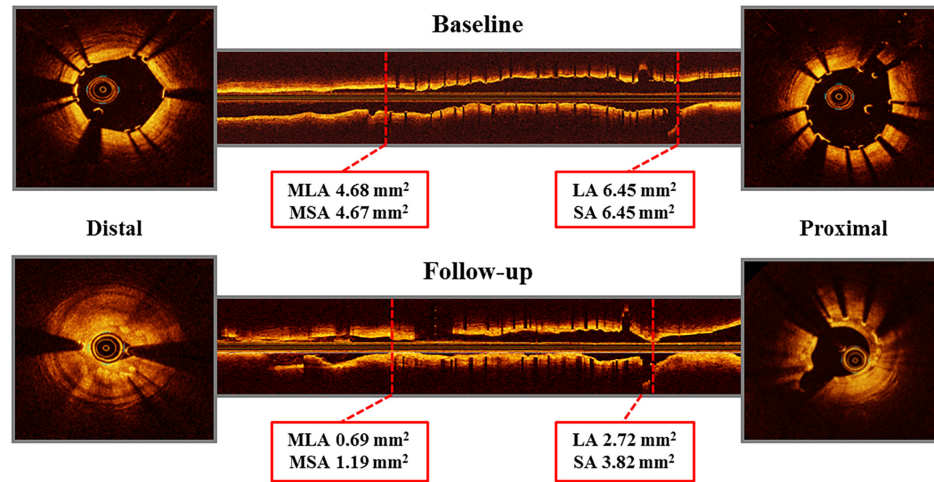
Study limitations

This is a nonrandomized single-center study with small sample size. Patient and lesion selection was at the operator's discretion. Pre-PCI intracoronary imaging was not systematically performed. The heterogeneity of the invasive follow-up time points might have resulted in high SD caused by extreme values, and the lack of serial invasive imaging after 12 months prohibited statements on potential

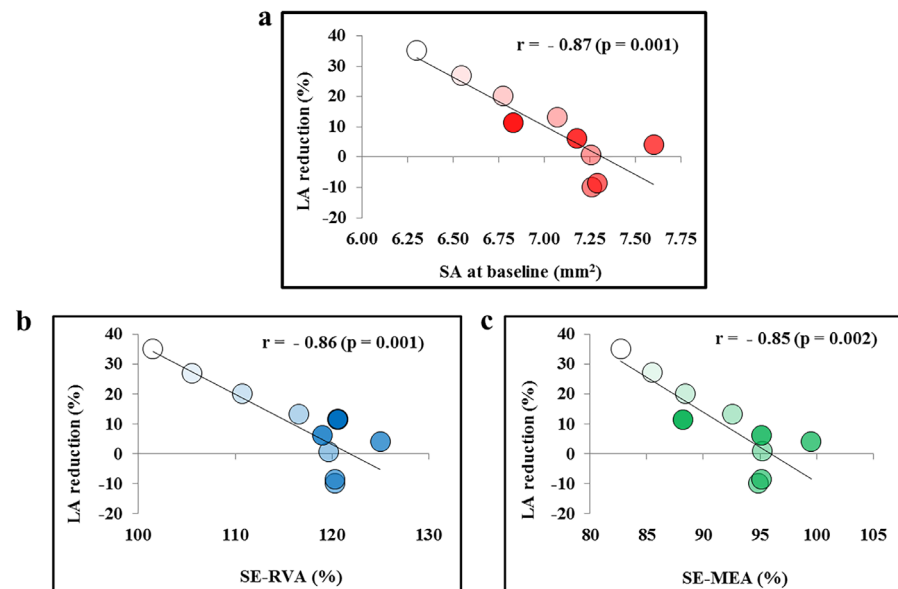
long-term lumen enlargement. The difficulty of identifying patent struts at follow-up did not allow us to perform methodical analysis of the entire scaffold and precluded any detailed analyses on neointimal hyperplasia volumes.

CONCLUSION

The latest magnesium BRS iteration suffers from premature dismantling with subsequent loss of vessel support; together with incomplete distal device expansion, could have contributed to a higher than expected lumen loss. While our findings need to be confirmed in a randomized fashion, it seems imperative to follow the European working group recommendations on BRS and limiting their use to clinical trials or registries with adequate follow-up²⁴. Finally, our results suggest that clinical and angiographic follow-up alone might not be sufficient to establish the safety and long-term efficacy of new BRS, and warrants the use of serial invasive coronary imaging at baseline and follow-up.

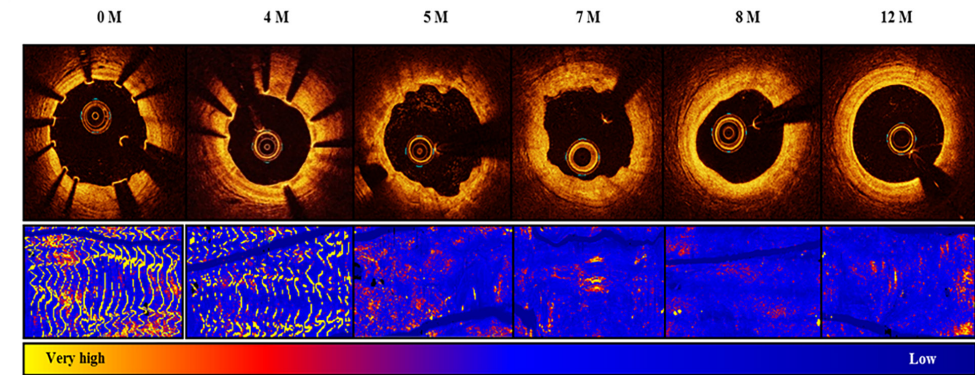


Supplementary Figure 1. Severe scaffold collapse at 4 months post-implantation of Magmaris BRS. Optical coherence tomography imaging at baseline and follow-up at the same cross-section sites illustrating proximal and distal constrictive remodeling and scaffold severe recoil. Lumen Area (LA); Minimal Lumen Area (MLA); Minimal Scaffold Area (MSA); Scaffold Area (SA).



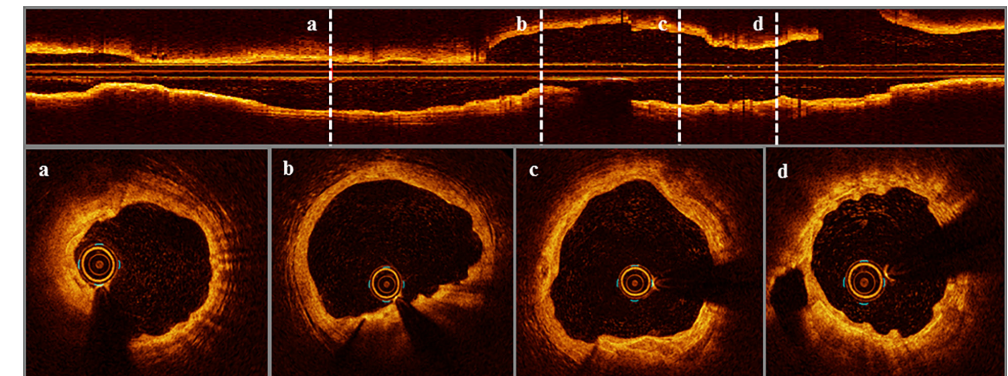
Supplementary Figure 2. Per scaffold 10-subsegment serial changes in OCT measurements

Per scaffold subsegment correlation between SA at baseline and LA reduction at follow-up (a). Per scaffold subsegment correlation between SE-RVA at baseline and LA reduction at follow-up (b). Per scaffold subsegment correlation between SE-MEA at baseline and LA reduction at follow-up. Most distal subsegments (light color). Most proximal subsegments (dark color). Scaffold Area (SA); Lumen Area (LA); Scaffold Expansion according to Manufacturer Expected Area (SE-MEA); Scaffold Expansion according to Reference Vessel Area (SE-RVA).



Supplementary Figure 3. OCT of Magmaris degradation from baseline to 12 months

Upper row shows OCT representation of the degradation process of different scaffolds visualized at different follow-up time points. The bottom row shows attenuation values of the scaffolded segment. Attenuation values reduce from very high to low with struts bioresorption; higher attenuation values correspond to patent struts, middle attenuation values correspond to struts undergoing degradation. Lower attenuation values correspond to absence of struts remains. Optical Coherence Tomography (OCT).



Supplementary Figure 4. In-scaffold heterogeneous strut degradation

Optical coherence tomography longitudinal view (first row) and cross-section images of one Magmaris BRS illustrating different stages of strut degradation at 5-month follow-up in patient #6.

Supplementary Table 1. Baseline clinical and angiographic characteristics

Case number	#1	#2	#3	#4	#5	#6
Age (years)	47	63	67	56	49	61
Gender	Male	Female	Male	Female	Female	Male
Hypertension	Yes	Yes	Yes	Yes	No	Yes
Smoking	Current	Former	No	No	No	Current
Diabetes mellitus	Yes	No	No	No	No	Yes
IDDM	Yes	No	No	No	No	No
Dyslipidemia	Yes	Yes	Yes	Yes	Yes	Yes
Family history of CAD	No	No	No	No	Yes	No
Previous myocardial infarction	Yes	No	No	No	No	No
Previous PCI	No	No	No	Yes	No	No
Previous CABG	No	No	No	No	No	No
Chronic renal failure	No	No	No	No	No	No
LVEF	Normal	Severely reduced	Normal	Unknown	Normal	Normal
P2Y12 inhibitor at discharge	Clopidogrel	Clopidogrel	Clopidogrel	Clopidogrel	Clopidogrel	Clopidogrel
Vessel disease	1	1	1	1	1	1
Chronic total occlusion present	No	No	No	No	No	No
Target vessel	RCA	LCX	LAD	LCX	LAD	LAD
Lesion type (ACC/AHA)	B1	B1	B1	B1	C	B1
Moderate-severe calcification	No	No	No	No	No	No
Moderate-severe tortuosity	No	No	No	No	No	No
Ostial lesion	No	No	No	No	No	No
Bifurcation with a major branch	No	No	No	No	No	No
Angiographic follow-up (months)	12	8	8	7	4	5

Cardiovascular disease (CVD); Coronary artery bypass graft (CABG); Insulin-dependent diabetes mellitus (IDDM); Left ventricular ejection fraction (LVEF); Percutaneous coronary intervention (PCI).

Supplementary Table 2. Baseline procedural characteristics

Case number	#1	#2	#3	#4	#5	#6	Mean ± SD
MLD (mm)	0.98	0.92	1.36	1.00	0.97	1.04	1.04 ± 0.16
Lesion length (mm)	20.07	18.23	12.91	11.90	23.06	12.81	16.50 ± 4.61
RVD (mm)	2.95	2.61	2.91	2.36	2.69	3.0	2.75 ± 0.25
DS (%)	66.78	64.75	53.26	57.63	63.94	65.33	61.95 ± 5.30
Scaffold diameter (mm)	3.0	3.0	3.0	3.0	3.0	3.5	3.08 ± 0.20
Scaffold length (mm)	25	20	15	15	25	20	20.00 ± 4.47
Scaffold inflation pressure (Atm)	12	12	16	18	14	16	14.67 ± 2.42
Pre-dilatation NC Balloon diameter (mm)	3.0	3.0	3.0	3.0	3.0	3.0	3.0 ± 0.0
Pre-dilatation NC Balloon length (mm)	15	15	8	8	15	8	11.50 ± 3.83
Pre-dilatation maximum pressure (Atm)	16	14	12	12	14	20	14.67 ± 3.01
Post-dilatation NC Balloon diameter (mm)	3.0	3.0	3.0	3.0	3.25	3.5	3.13 ± 0.21
Post-dilatation NC Balloon length (mm)	20	15	8	8	15	15	13.50 ± 4.68
Post-dilatation maximum pressure (Atm)	20	18	22	20	16	20	19.33 ± 2.07

Diameter Stenosis (DS); Minimal Lumen Diameter (MLD); Reference vessel diameter (RVD); Non-compliance (NC); Atmospheres (Atm).

REFERENCES

1. Sorrentino S, Giustino G, Mehran R, et al. Everolimus-eluting bioresorbable scaffolds versus everolimus-eluting metallic stents. *J Am Coll Cardiol*. 2017; 69(25): 3055- 3066.
2. Erbel R, Di Mario C, Bartunek J, et al. Temporary scaffolding of coronary arteries with bioabsorbable magnesium stents: a prospective, non-randomised multicentre trial. *Lancet*. 2007; 369(9576): 1869- 1875.
3. Haude M, Ince H, Abizaid A, et al. Sustained safety and performance of the second-generation drug-eluting absorbable metal scaffold in patients with de novo coronary lesions: 12-month clinical results and angiographic findings of the BIOSOLVE-II first-in-man trial. *Eur Heart J*. 2016; 37(35): 2701- 2709.
4. Haude M, Erbel R, Erne P, et al. Safety and performance of the drug-eluting absorbable metal scaffold (DREAMS) in patients with de-novo coronary lesions: 12 month results of the prospective, multicentre, first-in-man BIOSOLVE-I trial. *Lancet*. 2013; 381(9869): 836- 844.
5. Chichareon P, Katagiri Y, Asano T, et al. Mechanical properties and performances of contemporary drug-eluting stent: focus on the metallic backbone. *Expert Rev Med Devices*. 2019; 16(3): 211- 228. Sotomi Y, Onuma Y, Collet C, et al. Bioresorbable scaffold: the emerging reality and future directions. *Circ Res*. 2017; 120(8): 1341- 1352.
6. Garcia-Garcia HM, Haude M, Kuku K, et al. In vivo serial invasive imaging of the second-generation drug-eluting absorbable metal scaffold (Magmaris—DREAMS 2G) in de novo coronary lesions: insights from the BIOSOLVE-II first-in-man trial. *Int J Cardiol*. 2018; 255: 22- 28.
7. Ormiston JA, Serruys PW, Regar E, et al. A bioabsorbable everolimus-eluting coronary stent system for patients with single de-novo coronary artery lesions (ABSORB): a prospective open-label trial. *Lancet*. 2008; 371(9616): 899- 907.
8. Cubero-Callego H. Early collapse of a magnesium Bioresorbable scaffold. *J Am Coll Cardiol Interv*. 2017; 10(18): e171- e172.
9. Barkholt TO, Neghabat O, Terkelsen CJ, Christiansen EH, Holm NR. Restenosis in a collapsed magnesium bioresorbable scaffold. *Circ Cardiovasc Interv*. 2017; 10: e005677.
10. Garcia-Blas S, Minana G, Sanchis J. Optical coherence tomography of magnesium bioresorbable scaffold restenosis. *Rev Esp Cardiol (Engl Ed)*. 2018; 71: 1069.
11. Yang H, Zhang F, Qian J, Chen J, Ge J. Restenosis in Magmaris stents due to significant collapse. *JACC Cardiovasc Interv*. 2018; 11(10): e77- e78.
12. Roa-Garrido J, Cardenal-Piris RM, El Amrawy AM, Gomez-Menchero A, Camacho Freire S, Diaz-Fernandez JF. Optical coherence tomographic image pattern of metallic bioresorbable vascular scaffold restenosis. *JACC Cardiovasc Interv*. 2018; 11(7): 707- 708.
13. Marynissen T, McCutcheon K, Bennett J. Early collapse causing stenosis in a resorbable magnesium scaffold. *Catheter Cardiovasc Interv*. 2018; 92(2): 310- 312.
14. Mitomo S, Demir OM, Giannini F, Latib A, Colombo A. Magmaris Bioresorbable scaffold—possible dismantling 2 months after implantation on intravascular ultrasound. *Circ J*. 2018. <https://doi.org/10.1253/circj.CJ-18-0795>
15. Onuma Y, Serruys PW, Gomez J, et al. Comparison of in vivo acute stent recoil between the bioresorbable everolimus-eluting coronary scaffolds (revision 1.0 and 1.1) and the metallic everolimus-eluting stent. *Catheter Cardiovasc Interv*. 2011; 78(1): 3- 12.
16. van Bommel RJ, Lemmert ME, van Mieghem NMDA, van Geuns RJ, van Domburg RT, Daemen J. Occurrence and predictors of acute stent recoil—a comparison between the xience prime cobalt chromium stent and the promus premier platinum chromium stent. *Catheter Cardiovasc Interv*. 2018; 91: E21- E28.
17. Waksman R, Zumstein P, Pritsch M, et al. Second-generation magnesium scaffold Magmaris: device design and preclinical evaluation in a porcine coronary artery model. *EuroIntervention*. 2017; 13(4): 440- 449.
18. Kimura T, Kaburagi S, Tamura T, et al. Remodeling of human coronary arteries undergoing coronary angioplasty or atherectomy. *Circulation*. 1997; 96(2): 475- 483.
19. Ozaki Y, Garcia-Garcia HM, Hideo-Kajita A, et al. Impact of procedural characteristics on coronary vessel wall healing following implantation of second-generation drug-eluting absorbable metal scaffold in patients with de novo coronary artery lesions: an optical coherence tomography analysis. *Eur Heart J Cardiovasc Imaging*. 2018. <https://doi.org/10.1093/ehjci/jey210>
20. Baquet M, Nef H, Gori T, et al. Restenosis patterns after bioresorbable vascular scaffold implantation: angiographic substudy of the GHOST-EU registry. *Catheter Cardiovasc Interv*. 2018; 92(2): 276- 282.
21. Suwannasom P, Sotomi Y, Ishibashi Y, et al. The impact of post-procedural asymmetry, expansion, and eccentricity of bioresorbable Everolimus-eluting scaffold and metallic Everolimus-eluting stent on clinical outcomes in the ABSORB II trial. *JACC Cardiovasc Interv*. 2016; 9(12): 1231- 1242.
22. Ali ZA, Karimi Galougahi K, Shlofmitz R, et al. Imaging-guided pre-dilatation, stenting, post-dilatation: a protocolized approach highlighting the importance of intravascular imaging for implantation of bioresorbable scaffolds. *Expert Rev Cardiovasc Ther*. 2018; 16(6): 431- 440.
23. Byrne RA, Stefanini GG, Capodanno D, et al. Report of an ESC-EAPCI task force on the evaluation and use of bioresorbable scaffolds for percutaneous coronary intervention: executive summary. *Eur Heart J*. 2017; 39: 1591- 1601.

Chapter 9



References for left main stem dimensions: A cross sectional intravascular ultrasound analysis

van Zandvoort LJC, Tovar Forero MN, Masdjedi K, Lemmert ME, Diletti R,
Wilschut J, de Jaegere PPT, Zijlstra F, van Mieghem NMDA, Daemen J

*Erasmus University Medical Center, Thoraxcenter, Department of cardiology, Rotterdam,
the Netherlands*

Catheter Cardiovasc Interv. 2019;93(2):233-8.

ABSTRACT

Background: Angiographic assessment of left main coronary artery (LMCA) lesions remains challenging and limited data is available on reference diameters and length of non-obstructive LMCA dimensions. Our aim was to provide insights in the dimensions of non-obstructive LMCA and to find a possible correlation with gender and patient habitus.

Methods: This retrospective single centre study was performed in a consecutive cohort of patients who underwent Intravascular Ultrasound (IVUS) guided percutaneous coronary interventions of the left coronary system including complete pullbacks of a non-obstructive LMCA (n=254).

Results: Mean LMCA length as measured with IVUS was 7.37 ± 4.2 mm and mean lumen area (LA) was 15.63 ± 4.76 mm² corresponding to a mean lumen diameter (LD) of 4.41 ± 0.67 mm. An IVUS derived mean LD of >4 mm was present in 71.7%, >4.5 mm in 43% and >5 mm in 19% of patients. LMCA mean LA was significantly smaller in women as compared to men (14.1 ± 4.1 mm² and 16.2 ± 4.8 mm², $p < 0.01$). Multivariable analysis identified weight of the patient as the sole significant predictor for LMCA length while height of the patient and LMCA length were predictors of LMCA mean LA. Correlation coefficients of determination for all independent predictors were low ($R^2 < 0.1$ for all).

Conclusion: The current study demonstrated that the mean LD of a non-obstructive LMCA is 4 mm or greater in the majority of patients, with a mean LMCA length of 7.4 mm. Women have smaller luminal dimension than men. No clinically relevant predictors were found for both LMCA length and mean LA.

INTRODUCTION

Limitations of the angiographic assessment of left main coronary arteries (LMCA) lesions have been well-documented¹⁻³. Instead, intravascular ultrasound (IVUS) has proven to be a reliable tool to more precisely determine LMCA luminal dimensions⁴⁻¹⁰. Multiple studies provide IVUS criteria for revascularization based on minimal lumen diameters (MLD) or minimal lumen areas (MLA) for diseased LMCAs. An MLD below 2.8 mm and MLAs smaller than 4.5 mm² to 7.5 mm² were significantly correlated to late adverse events^{7, 8, 11-17}. Although numerous studies focussed on diseased LMCAs, no data is available on reference dimensions of LMCA as measured using IVUS and their potential relationship with patient characteristics.

METHODS

Study population

This study consists of all consecutive patients undergoing percutaneous coronary intervention (PCI) in combination with IVUS for suspected or confirmed coronary artery disease in the Thoraxcenter, Erasmus Medical Centre, Rotterdam, The Netherlands, between January 2010 and December 2016. Patients were included if IVUS images from either the left anterior descending artery (LAD) or the left circumflex artery (LCX) were available. Patients were excluded if only IVUS images from the right coronary artery (RCA), or a graft vessel were present, or in case stenting of the LMCA was scheduled due to obstructive atherosclerotic disease.

IVUS analysis

Targeted segments were examined with an IVUS system with automatic pullback at 0.5 mm/s (OptiCross, Boston Scientific, Natick, MA, USA; Eagle Eye, Volcano Corp, Rancho Cordova, CA, USA; TVC Insight, InfraReDx, Burlington, MA, USA) or 2.5 mm/sec (Kodama, Acist Medical, Eden Prairie, MN, USA). IVUS images were digitally stored and analysed offline. Volumetric analysis of the region of interest was performed in fixed 0.5 mm intervals between the LMCA ostium and its distal bifurcation using dedicated software (QCU-CMS, CMS, Leiden University Medical Centre, LKEB, Division of Image Processing, version 4.69). The proximal border of the LMCA, the ostium, was defined as the first frame which contained a 360 degrees luminal border of the LMCA. Whenever the transition from aorta to LMCA ostium was not seen because of a too deeply engaged guiding catheter, the patient was excluded. The distal border was defined as the last frame that contained a complete LMCA before an asymmetric lumen indicating the start of the bifurcation.

Furthermore, the external elastic membrane (EEM) had to be completely visible within the IVUS image. Morphometric analysis included EEM measurements, lumen measurements, and percent intima-and-media measurements (area stenosis; calculated as EEM minus lumen divided by EEM). Two volumetric intima-and-media indices, normalized total atheroma volume (nTAV) and percent atheroma volume (PAV), were also derived from these measurements. These indices have been used in coronary atherosclerosis regression studies and are defined as follows:

$$nTAV = \frac{\sum(EEM_{area} - lumen_{area})}{no. of analyzed images in the pullback} \times median no. of analyzed images in this cohort$$

and:

$$PAV = \frac{\sum(EEM_{area} - lumen_{area})}{\sum EEM_{area}} \times 100$$

where EEM_{area} is the cross-sectional EEM area and $lumen_{area}$ is the cross-sectional LA¹⁸.

Statistical analysis

Statistical analyses were performed in SPSS (version 21.0, SPSS Inc., Chicago IL, USA). Categorical variables are reported percentages. Continuous variables are reported as mean \pm standard deviation (SD). For the calculation of body mass index (BMI) the following formula was used: . Whenever one of the two variables of this formula was missing (<10% of the cases), it was imputed using the mean of 5 multiple imputations within the multivariable regression analysis. The variance coefficient (CV) was calculated with the following formula:

For the univariate analysis the Pearson correlation coefficient was used when two continuous variables were compared. The Pearson correlation coefficient R was squared in order to demonstrate the proportion of variance in the dependent variable that is predictable from the independent variable. In order to investigate the difference of continuous variables between binary groups, in this case gender, the independent t test was used. The Chi-Square test was used in case of two categorical variables.

Finally, a multivariable regression model with a stepwise exclusion method was used in order to estimate the best predictive model.

RESULTS

A total of 1197 IVUS pullbacks were performed in patients with supposedly non-obstructive LMCA's between 2010 and 2016, 946 patients were excluded because of incomplete footage of the LMCA (n=543) or other reasons (n=403) (Figure 1). The mean length of the LMCA as measured by IVUS was 7.3 \pm 4.2 mm. Mean LA was 15.7 \pm 4.7 mm², MLA was 12.7 \pm 4.6 mm² and IVUS derived mean LD was 4.4 \pm 0.7 mm. A mean LD >4 mm was present in 71.7% of patients, while 43% and 19% of the patients had IVUS derived mean LD >4.5 mm and >5 mm respectively. All the luminal dimensions as measured by IVUS are depicted in Table 2. The percentage CV for all luminal dimension displayed in Table 2 ranged between 12.5% and 44.9% with the exception of length of the LMCA which demonstrated a percentage CV of 57.5%.

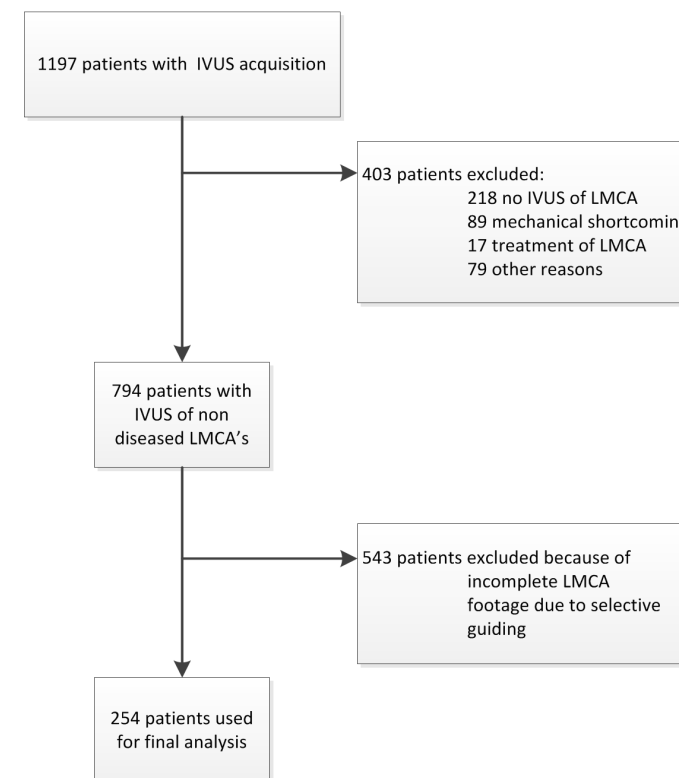


Figure 1. Patient inclusion flowchart

A total of 254 patients were used for the final analysis. The study population consisted of 197 males (78%) and 57 females (22%), mean age was 63 \pm 11 years and mean BMI was 27.27 \pm 4.46 kg/m². Baseline characteristics of the study population are depicted in Table 1.

Table 1. Baseline characteristics

All patients (n=254)	
Age, years (±SD)	64±11
Male, n (%)	197 (78)
Length, cm (±SD)	175.0±9.2
Weight, kg (±SD)	83.8±15.9
BMI, kg/m ² (±SD)	27.27±4.46
DM, n (%)	53 (21)
Hypertension, n (%)	141 (56)
Hypercholesterolemia, n (%)	115 (45)
Family history, n (%)	96 (38)
Current smoking, n (%)	70 (28)

Table 2. Quantitative IVUS dimensions analysis

All patients (n=254)	
Mean lumen area mm ² (±SD)	15.7±4.7
Mean lumen diameter mm (±SD)	4.4±0.7
Mean plaque burden mm ² (±SD)	9.4±3.4
Minimal lumen area mm ² (±SD)	12.7±4.6
Mean vessel diameter mm (±SD)	4.0±0.7
Minimal lumen diameter mm (±SD)	3.95±0.7
Length of the LMCA mm (±SD)	7.3±4.2
nTAV mm ² ±SD	62.1±27.9
PAV % (±SD)	37.7±10.2

nTAV = normalized total atheroma volume, PAV = percent atheroma volume.

Univariate analysis identified weight and BMI as positive significant predictors for LMCA length ($\beta=0.51$, CI(0.017:0.085), $p=0.003$ $R^2=0.04$ and $\beta=0.16$, CI(0.037:0.028), $p=0.011$ $R^2=0.03$ respectively). Both height and weight of the patient were positive predictors of LMCA mean LA ($\beta=0.09$, CI(0.03:0.16), $p=0.006$ $R^2=0.03$ and $\beta=0.04$, CI(0.004:0.08), $p=0.031$ $R^2=0.02$ respectively) while length of the LMCA was negatively correlated to LMCA mean LA ($\beta=-0.26$, CI(0.03:0.16), $p=0.006$ $R^2=0.03$) (Table 3 and Figure 2).

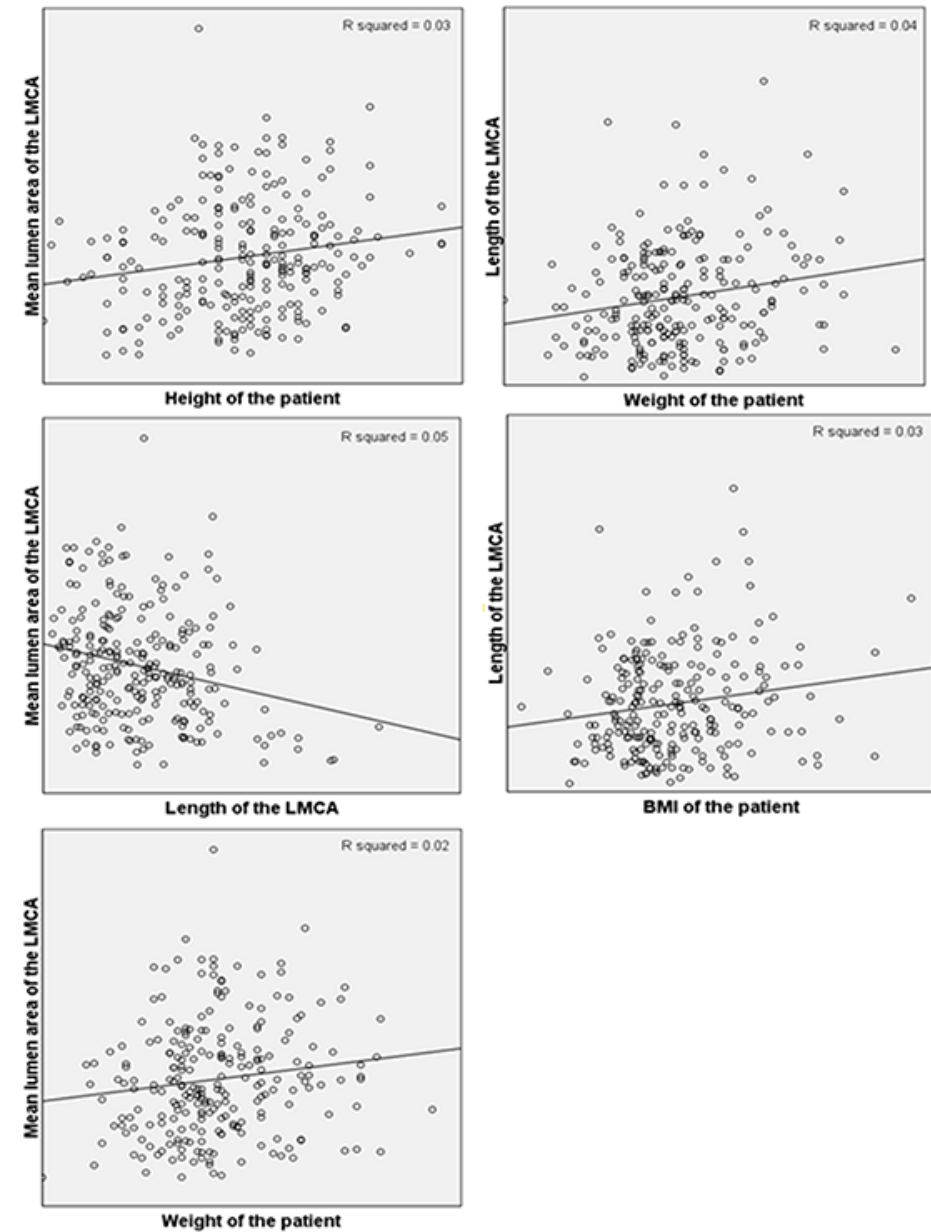


Figure 2. Correlation plots of significant predictors for LMCA properties

LMCA mean LA was significantly smaller in women as compared to men (14.1±4.1 mm² vs. 16.2±4.8 mm² respectively ($p<0.01$)) as were IVUS derived mean LD (4.2±0.6 mm and 4.5±0.7 mm respectively ($p<0.01$)) (Figure 3).

Table 3. Univariate Pearson regression analysis and multivariable regression analysis

	Predictors	β , CI	R ²	p value
<u>Univariate analysis</u>				
LMCA length	Weight of the patient BMI of the patient	0.51, 0.017:0.085 0.16, 0.037:0.28	0.04 0.03	0.003 0.011
LMCA mean LA	Height of the patient Length of the LMCA Weight of the patient	0.09, 0.03:0.16 -0.26, -0.39:-0.12 0.04, 0.004:0.08	0.03 0.05 0.02	0.006 <0.001 0.031
<u>Multivariable analysis</u>				
LMCA length	+ Weight of the patient	0.14, 0.017:0.085	0.04	0.003
LMCA mean LA	+ Height of the patient - Length of the LMCA	0.20, 0.04:0.17 -0.25, -0.41:-0.14	0.09	0.002 <0.001

β = correlation slope, CI = confidence interval, R² = squared Pearson correlation coefficient, LA = lumen area

LMCA mean LA was significantly smaller in women as compared to men (14.1±4.1 mm² vs. 16.2±4.8 mm² respectively (p<0.01)) as were IVUS derived mean LD (4.2±0.6 mm and 4.5±0.7 mm respectively (p<0.01)) (figure 3). IVUS derived LMCA mean LD were >4 mm in 76% of the men, this percentage was significantly smaller among women (56%; p=0.003). LMCA mean LD was >5 mm in 23% of men and 7% of women (p=0.008). No significant differences were found in LMCA length between both sexes.

Multivariable regression analyses identified weight as the only independent predictor of LMCA length (β =0.14, CI(0.017:0.085), p=0.003, R²=0.04) while patient height and length of the LMCA were the only independent predictors of LMCA mean LA (β =0.20, CI(0.04:0.17), p=0.002 and β =-0.25, CI(-0.41:-0.14), p<0.001, R²=0.09 respectively) (Table 3).

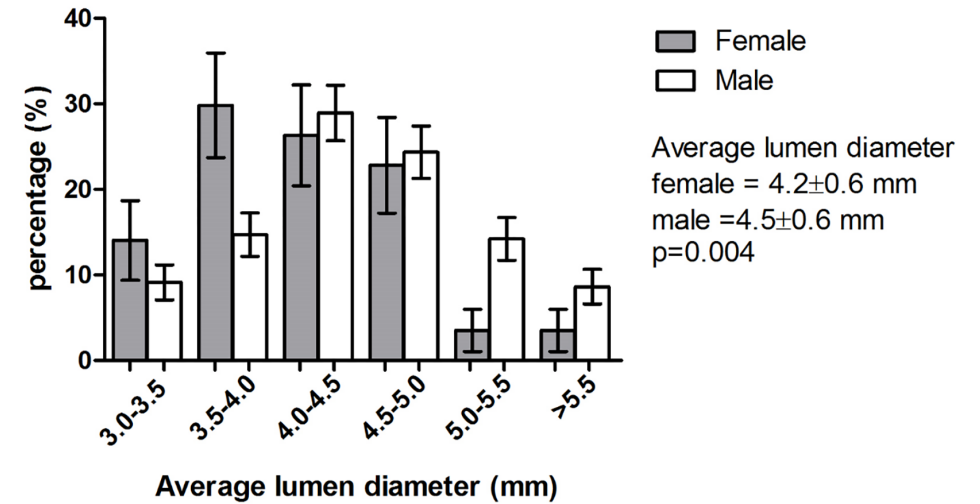


Figure 3. IVUS derived average lumen diameters according to gender
Error bars: standard error of the mean (SEM)

DISCUSSION

By using quantitative IVUS analysis we were able to assess the luminal dimension of non-obstructive LMCA in a large real world cohort. We demonstrated for the first time how non-diseased LMCA dimensions and length vary within the population and how women display smaller luminal dimension compared to men. No clinically relevant predictors were found for both LMCA mean LA and length as correlation coefficients were low.

These findings might guide physicians in deciding on stent- and post dilatation balloon sizing, and support the use of intravascular imaging in LMCA stenting ¹⁹. Given the structural undersizing based on QCA, IVUS helps in correctly identifying the exact LMCA length and area and thereby improves outcomes of complex LMCA PCI ¹⁹⁻²¹. More specifically, we demonstrated that 19% of the patients presented with IVUS derived mean luminal dimensions of >5 mm, requiring post dilatation with balloons up to 5 mm along with the use of stents with sufficient post dilatation margins. In real world clinical practice, the multicentre DELTA I registry demonstrated that the mean diameter of stents used for LMCA stenting was merely 3.51 mm along with a maximal post dilatation balloon diameter of 3.88 ± 0.58 mm for mid-shaft and ostial treatment and 3.59 ± 0.54 mm for distal LMCA treatment ²². Also in the NOBLE trial, comparing PCI and CABG for LMCA revascularization, only half of the LMCA stents in the PCI group were post dilated with balloons larger than 4 mm ²³. The authors of the NOBLE trial even argued that underexpansion and malapposition might have contributed to a higher revascularisation risk in the PCI group. Our study makes this hypothesis even more likely since we demonstrated that IVUS derived LMCA mean LD were 4.4 mm and 71.7% of LMCAs have a mean LD >4 mm.

Finally, LMCA LA appeared to be significantly smaller in women as compared to men (Figure 3). While IVUS derived LMCA mean LD were >4 mm in 76% of the men, this percentage was significantly smaller among women (56%). While multivariable analysis revealed several other predictors for both LMCA length and LMCA mean LA, the overall correlation appeared poor for all predictors suggesting a limited clinical applicability of these parameters.

Limitations

Despite the large sample of IVUS pullbacks eligible for our study (n=1197) a significant amount of cases had to be excluded due to either incomplete footage of the LMCA or mechanical shortcomings. Although the lack of coverage by the model we presented is low, the relatively low percentage CV might not have changed substantially by enlarging our sample size.

Nevertheless we were able to provide a complete quantitative IVUS assessment of 254 non-obstructive LMCAs. The latter, therefore, still represents the largest sample reported in the literature thus far. Finally, no additional steps were taken to reduce structural multicollinearity.

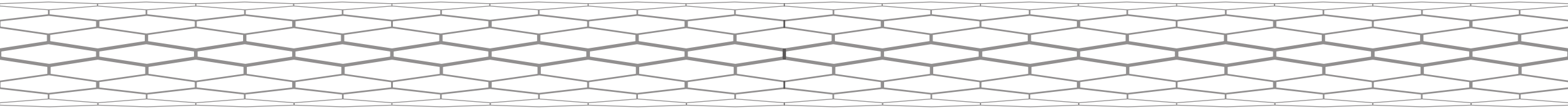
CONCLUSION

The current study demonstrated that the mean luminal diameter of a non-obstructive LMCA is 4 mm or greater in the majority of patients, with a mean LMCA length of 7.4 mm. Women proved to have smaller luminal dimension compared to men. No clinically relevant predictors were found for both LMCA mean LA and length.

REFERENCES

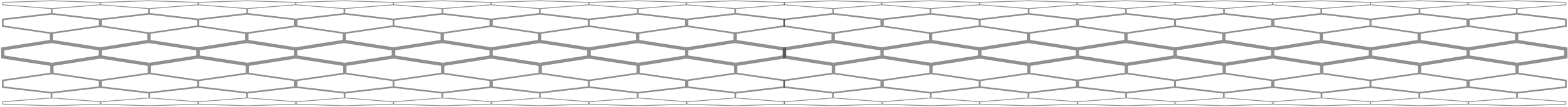
1. Fisher LD, Judkins MP, Lesperance J, Cameron A, Swaye P, Ryan T, et al. Reproducibility of coronary arteriographic reading in the coronary artery surgery study (CASS). *Cathet Cardiovasc Diagn.* 1982;8(6):565-75.
2. Arnett EN, Isner JM, Redwood DR, Kent KM, Baker WP, Ackerstein H, et al. Coronary artery narrowing in coronary heart disease: comparison of cineangiographic and necropsy findings. *Ann Intern Med.* 1979;91(3):350-6.
3. Cameron A, Kemp HG, Jr., Fisher LD, Gosselin A, Judkins MP, Kennedy JW, et al. Left main coronary artery stenosis: angiographic determination. *Circulation.* 1983;68(3):484-9.
4. Sano K, Mintz GS, Carlier SG, de Ribamar Costa J, Jr., Qian J, Missel E, et al. Assessing intermediate left main coronary lesions using intravascular ultrasound. *Am Heart J.* 2007;154(5):983-8.
5. Gerber TC, Erbel R, Gorge G, Ge J, Rupprecht HJ, Meyer J. Extent of atherosclerosis and remodeling of the left main coronary artery determined by intravascular ultrasound. *Am J Cardiol.* 1994;73(9):666-71.
6. Wolfhard U, Gorge G, Konorza T, Haude M, Ge J, Piotrowski JA, et al. Intravascular ultrasound (IVUS) examination reverses therapeutic decision from percutaneous intervention to a surgical approach in patients with alterations of the left main stem. *Thorac Cardiovasc Surg.* 1998;46(5):281-4.
7. Abizaid AS, Mintz GS, Abizaid A, Mehran R, Lansky AJ, Pichard AD, et al. One-year follow-up after intravascular ultrasound assessment of moderate left main coronary artery disease in patients with ambiguous angiograms. *J Am Coll Cardiol.* 1999;34(3):707-15.
8. Fassa AA, Wagatsuma K, Higano ST, Mathew V, Barsness GW, Lennon RJ, et al. Intravascular ultrasound-guided treatment for angiographically indeterminate left main coronary artery disease: a long-term follow-up study. *J Am Coll Cardiol.* 2005;45(2):204-11.
9. de la Torre Hernandez JM, Ruiz-Lera M, Fernandez-Friera L, Ruisanchez C, Sainz-Laso F, Zueco J, et al. [Prospective use of an intravascular ultrasound-derived minimum lumen area cut-off value in the assessment of intermediate left main coronary artery lesions]
10. Aplicacion prospectiva de un valor de corte de area luminal minima por ecografia intravascular en la evaluacion de lesiones intermedias del tronco. *Rev Esp Cardiol.* 2007;60(8):811-6.
11. Okabe T, Mintz GS, Lee SY, Lee B, Roy P, Steinberg DH, et al. Five-year outcomes of moderate or ambiguous left main coronary artery disease and the intravascular ultrasound predictors of events. *J Invasive Cardiol.* 2008;20(12):635-9.
12. Kassimis G, de Maria GL, Patel N, Tushar R, Scott P, Kharbanda RK, et al. Assessing the left main stem in the cardiac catheterization laboratory. What is "significant"? Function, imaging or both? *Cardiovasc Revasc Med.* 2017.
13. Jasti V, Ivan E Fau - Yalamanchili V, Yalamanchili V Fau - Wongpraparut N, Wongpraparut N Fau - Leesar MA, Leesar MA. Correlations between fractional flow reserve and intravascular ultrasound in patients with an ambiguous left main coronary artery stenosis. *Circulation.* 2004(1524-4539 (Electronic)).
14. de la Torre Hernandez JM, Hernandez Hernandez F, Alfonso F, Rumoroso JR, Lopez-Palop R, Sadaba M, et al. Prospective application of pre-defined intravascular ultrasound criteria for assessment of intermediate left main coronary artery lesions results from the multicenter LITRO study. *J Am Coll Cardiol.* 2011;58(4):351-8.
15. Park SJ, Ahn JM, Kang SJ, Yoon SH, Koo BK, Lee JY, et al. Intravascular ultrasound-derived minimal lumen area criteria for functionally significant left main coronary artery stenosis. *JACC Cardiovasc Interv.* 2014;7(8):868-74.
16. Ricciardi MJ, Meyers S, Choi K, Pang JL, Goodreau L, Davidson CJ. Angiographically silent left main disease detected by intravascular ultrasound: a marker for future adverse cardiac events. *Am Heart J.* 2003;146(3):507-12.
17. Kang SJ, Lee JY, Ahn JM, Song HG, Kim WJ, Park DW, et al. Intravascular ultrasound-derived predictors for fractional flow reserve in intermediate left main disease. *JACC Cardiovasc Interv.* 2011;4(11):1168-74.
18. Stone GW, Sabik JF, Serruys PW, Simonton CA, Genereux P, Puskas J, et al. Everolimus-Eluting Stents or Bypass Surgery for Left Main Coronary Artery Disease. *N Engl J Med.* 2016;375(23):2223-35.
19. Mintz GS, García-García HM, Nicholls S, Weissman NJ, Bruining N, Crowe T, et al. Clinical expert consensus document on standards for acquisition, measurement and reporting of intravascular ultrasound regression/progression studies. *EuroIntervention.* 2011;6(9):1123-30.
20. Escaned J, Collet C, Ryan N, De Maria GL, Walsh S, Sabate M, et al. Clinical outcomes of state-of-the-art percutaneous coronary revascularization in patients with de novo three vessel disease: 1-year results of the SYNTAX II study. *Eur Heart J.* 2017;38(42):3124-34.
21. Tu S, Xu L, Lighthart JMR, Xu B, Witberg K, Sun Z, et al. In vivo comparison of arterial lumen dimensions assessed by co-registered three-dimensional (3D) quantitative coronary angiography, intravascular ultrasound and optical coherence tomography. *Int J Cardiovasc Imaging.* 2012;28(6):1315-27.
22. Mazhar J, Shaw E, Allahwala UK, Figtree GA, Bhandi R. Comparison of two dimensional quantitative coronary angiography (2D-QCA) with optical coherence tomography (OCT) in the assessment of coronary artery lesion dimensions. *Int J Cardiol Heart Vasc.* 2015;7:14-7.
23. Naganuma T, Chieffo A, Meliga E, Capodanno D, Park SJ, Onuma Y, et al. Long-term clinical outcomes after percutaneous coronary intervention versus coronary artery bypass grafting for ostial/midshaft lesions in unprotected left main coronary artery from the DELTA registry: a multicenter registry evaluating percutaneous coronary intervention versus coronary artery bypass grafting for left main treatment. *JACC Cardiovasc Interv.* 2014;7(4):354-61.
24. Makikallio T, Holm NR, Lindsay M, Spence MS, Erglis A, Menown IB, et al. Percutaneous coronary angioplasty versus coronary artery bypass grafting in treatment of unprotected left main stenosis (NOBLE): a prospective, randomised, open-label, non-inferiority trial. *Lancet.* 2016;388(10061):2743-52.

PART III



SYNERGISTIC
USE OF
INTRACORONARY
IMAGING AND
PHYSIOLOGY

Chapter 10



Explanation of Postprocedural Fractional Flow Reserve Below 0.85, A Comprehensive Ultrasound Analysis of the FFR SEARCH Registry

van Zandvoort LJC, Masdjedi K, Witberg K, Ligthart JMR, Forero Tovar MN, Diletti R, Lemmert ME, Wilschut J, De Jaegere PPT, Boersma H, Zijlstra F, van Mieghem NMDA, Daemen J

Erasmus University Medical Center, Thoraxcenter, Department of cardiology, Rotterdam, the Netherlands

Circ Cardiovasc Interv. 2019;12(2):e007030.

ABSTRACT

Background: Fractional flow reserve (FFR) after percutaneous coronary intervention (PCI) is a predictor of adverse cardiovascular events during follow-up. However the rationale for low post procedural FFR values remains often elusive based on angiographic findings alone.

Methods and Results: FFR SEARCH is a prospective single center registry in which post PCI FFR was assessed in 1.000 consecutive all-comer patients. FFR measurements were performed with a microcatheter ± 20 mm distal to the most distal stent edge. In 100 vessels with a post procedural FFR ≤ 0.85 , and 20 vessels > 0.85 high definition intravascular ultrasound analysis (IVUS) was performed.

In 100 vessels with a post PCI FFR ≤ 0.85 , mean post procedural FFR was 0.79 ± 0.05 . Minimal lumen area was 2.19 ($1.81-3.19$) mm^2 , mean lumen area was 5.95 ($5.01-7.03$) mm^2 and minimal stent area was 4.01 ($3.09-5.21$) mm^2 . Significant residual focal proximal lesions were found in 29% of the assessed vessels while focal distal lesions were found in 30% of the vessels. Stent underexpansion and malapposition were found in 74% and 22% of vessels respectively. Clear focal signs of luminal narrowing were found in 54% of the vessels analysed. While incidences of focal lesions, underexpansion and malapposition were similar between both cohorts, minimal stent area was significantly smaller in vessels with a post PCI FFR ≤ 0.85 as compared to those with an FFR > 0.85 .

Conclusion: In patients with a post procedural FFR ≤ 0.85 , IVUS revealed focal signs of luminal narrowing in a significant number of cases.

Clinical perspective

What's known?

FFR after stenting is a strong and independent predictor of major adverse cardiac events.

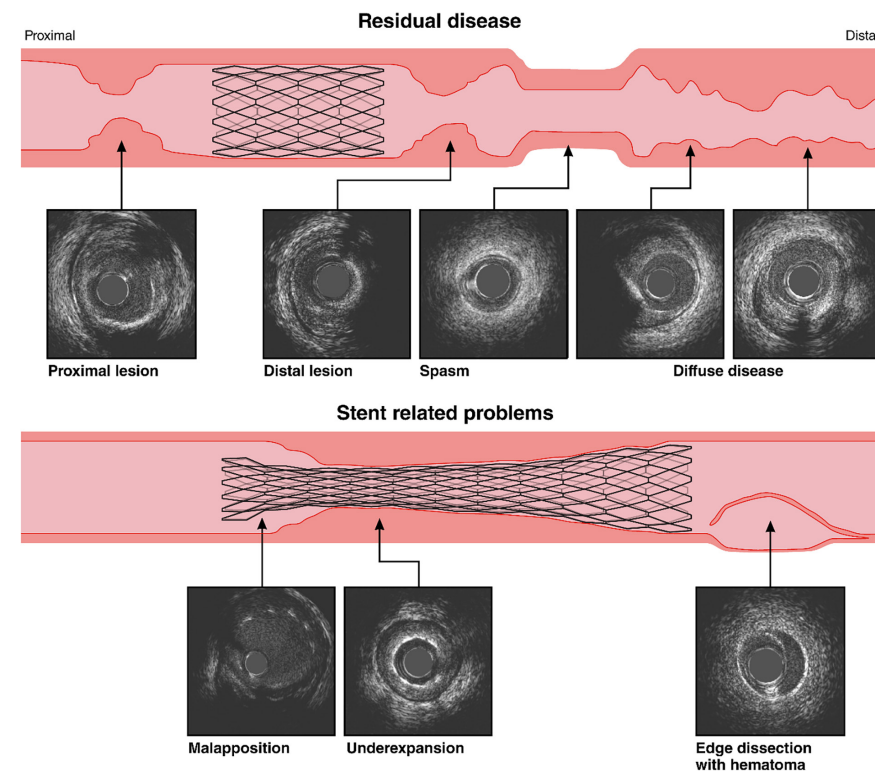
Unfortunately, the rationale for low post procedural FFR values often remains elusive based on angiographic findings alone.

What the study adds?

Residual treatable lesions or lumen compromising hematomas were present in 54% in vessels with a post PCI FFR ≤ 0.85 .

Underexpansion was present in 75% of the treated vessel

More data on the use of post-PCI FFR values, their association with intravascular findings and potential further treatment in order to improve clinical outcome is warranted.



Central illustration. IVUS detected causes of post PCI FFR ≤ 0.85

INTRODUCTION

In order to overcome the limitations of angiographic lesion assessment, fractional flow reserve (FFR) has proven to be a useful tool to identify the hemodynamic impact of a coronary artery stenosis ¹. Several randomized trials have demonstrated that a routine pre-procedural FFR measurement in patients with multivessel coronary artery disease undergoing percutaneous coronary intervention (PCI) significantly reduces the composite endpoint of death, nonfatal myocardial infarction, and repeat revascularization at 1 year as compared to angiographic guidance alone ². More recently, FFR after stenting has proved to be a strong and independent predictor of major adverse cardiac events (MACE) up to 2 years ³⁻⁵. The actual scope of the problem of low post PCI FFR was illustrated by recent work from our group demonstrating that in up to 43% of the cases, post PCI FFR values ≤ 0.90 were found while in 20% of the cases post PCI FFR even dropped below 0.85 ⁶.

Unfortunately, the rationale for low post procedural FFR values often remains elusive based on angiographic findings alone, warranting further assessment using an FFR pullback or additional intravascular imaging ⁷⁻¹¹. The primary objective of the current study was to look for morphological reasons for a post procedural FFR ≤ 0.85 in a real world patient cohort with the help of high definition intravascular ultrasound (HD-IVUS).

METHODS

Patient selection

The FFR SEARCH (Stent Evaluated at Rotterdam Cardiology Hospital) study is a prospective, all comer registry, enrolling 1512 consecutive patients who underwent successful PCI between March 2016 and May 2017. Among them, 512 patients were excluded due to several reasons (156 were unstable, in 129 patients the treated vessel was too small, in 148 cases it was operators decision not to perform an FFR and in 79 cases for other reasons). In a total of 1000 patients after angiographic confirmation of treatment success, FFR was measured. In 41 cases, no FFR measurements were performed because of failure of the microcatheter to cross the stented segment, equipment failure or the occurrence of an adverse reaction to adenosine. Finally, FFR was measured in at least one lesion in a total of 959 patients. A total of 1165 post PCI FFR measurements were performed. For the present prespecified subgroup analysis, IVUS analysis were performed in 100 consecutive vessels with a post procedural FFR ≤ 0.85 as well as 20 consecutive vessels with a post procedural FFR > 0.85 between August 2016 and October 2017 in respectively 95 and 20 patients. No complications due to FFR

measurements were encountered. The study was performed in accordance with the Declaration of Helsinki. The study protocol was approved by the local ethics committee. All patients provided written informed consent for the procedure and the use of anonymous datasets for research purposes in alignment with the Dutch Medical Research Act. The data, analytic methods, and study materials will not be made available to other researchers for purposes of reproducing the results or replicating the procedure.

FFR and IVUS acquisition

After angiographic confirmation of treatment success, post procedural FFR measurements were performed using the Navvus rapid exchange monorail microcatheter (ACIST Medical Systems, Inc., Eden Prairie, MN, USA). Measurements were performed in all stented segments after an intracoronary bolus of nitrates (200 μg). Results were based on single FFR measurement performed at approximately 20 mm distal to the distal stent edge as well as single measurements at the distal stent edge, proximal stent edge and ostium. Whenever multiple vessels were treated, this method was performed in all treated vessels. Pd/Pa was defined as the ratio of mean distal coronary artery pressure to mean aortic pressure in the resting state during the whole cardiac cycle. FFR was defined as mean distal coronary artery pressure divided by mean aortic pressure during maximum hyperemia achieved by continuous intravenous infusion of adenosine at a rate of 140 $\mu\text{g}/\text{kg}/\text{min}$ through an antecubital vein. Pullback analyses were performed under hyperemic conditions measuring FFR at the distal stent edge, proximal stent edge and the ostium to test for drift.

IVUS imaging was performed with the multi frequency HD-IVUS Kodama catheter (ACIST Medical Systems, Inc., Eden Prairie, MN, USA) at 60Mhz with a pullback speed of 2.5 mm/sec (24 frames per mm). Imaging assessment was performed off-line every 0.5 mm using dedicated software (QCU-CMS, Leiden University Medical Centre, LKEB, Division of Image Processing, version 4.69) by three dedicated academic intravascular imaging specialists, blinded to the final FFR results. Focal lesions were manually detected and defined as treatable lesions with an appropriate landing zone either proximal or distal to the stented segment. Proximal focal lesions were defined as lesions proximal to the stented segment with a minimal lumen area (MLA) $< 4.0 \text{ mm}^2$ or $< 6.0 \text{ mm}^2$ in case of left main (LM) lesions. Additionally, the MLA at the residual proximal stenosis had to be smaller than the distal reference external elastic membrane (EEM) diameter ^{12, 13} (Figure 1).

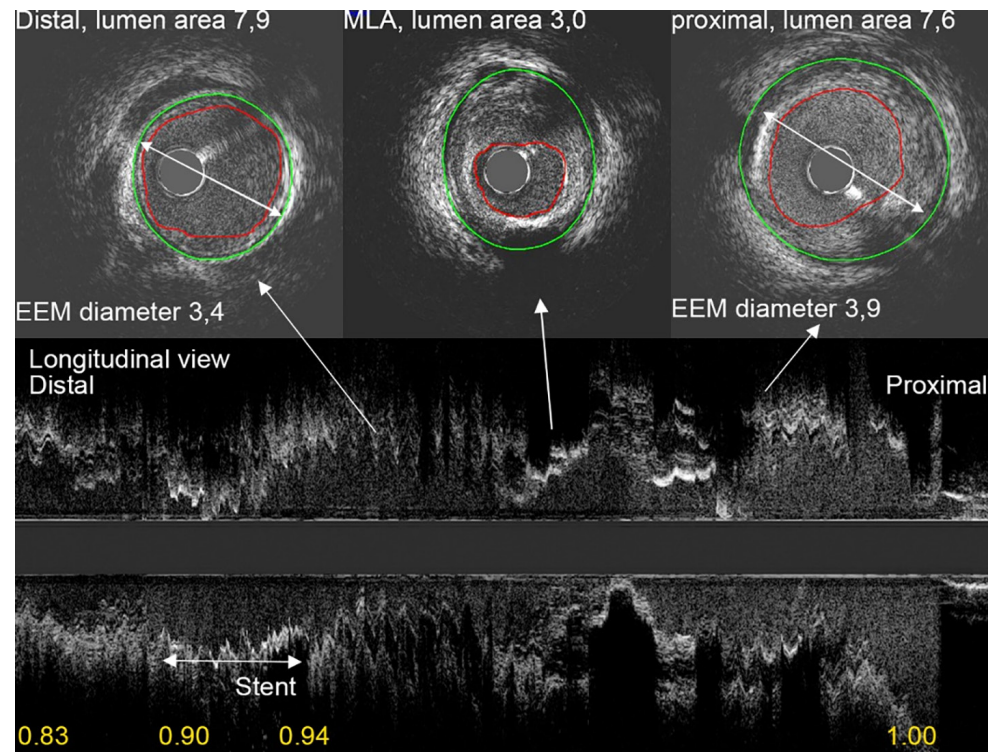


Figure 1. IVUS analysis of a focal lesion

Lumen areas are in mm² and diameters are in mm. EEM = External Elastic Membrane. MLA = minimum luminal area. The EEM, distal of the MLA, is smaller than the MLA, therefore, the luminal narrowing in this example can be categorised as a focal lesion. Values in yellow at the bottom of the figure represent the FFR measurements, from left to right: 15mm distal, distal stent edge, proximal stent edge and ostium respectively.

Distal focal lesions were assessed based solely on the criteria involving the size of the distal reference EEM diameter^{12, 13}. Underexpansion, according to the MUSIC criteria, was defined as an in-stent MLA <90% of the average reference lumen area (LA)¹⁴. Reference LAs were measured 5 mm proximal and 5 mm distal to the implanted stent. If one of these locations could not be accounted for as a reference lumen due to a bifurcation, it was excluded and only one reference area was used. Stent malapposition was defined as incomplete strut apposition of at least one strut to the lumen wall, without involvement of side branches, thus permitting blood to flow between the struts and the underlying wall¹⁵.

An intramural hematoma was defined as a severe lumen narrowing due to a intravascular stent edge dissection filled with blood within the medial space, displacing the internal elastic membrane inward and the external elastic membrane

outward¹⁵. Non flow-limiting edge dissections were not assessed in this study.

Coronary vasospasm was defined as severe diffuse intimal thickening and a thick media, often accompanied by negative remodelling, even in the absence of a significant coronary stenosis^{16, 17}.

Quantitative coronary angiography

Angiographic success was assessed, offline, with the use of quantitative coronary angiography (QCA) (CAAS workstation 8.0, Pie Medical Imaging, Maastricht, The Netherlands). The treated vessels were divided into four segments: proximal segment (ostium to proximal stent edge); stented segment (in-stent analysis); stented segment with (including an additional 5 mm proximal and 5 mm distal to stent edges; in-segment analysis); the distal segment (distal stent edge to position where FFR was measured, at least 20mm from distal stent edge). If multiple stents were implanted with a gap of more than 10 mm in-between, the gap segment was considered as a proximal segment. For each segment, length, minimal diameter (mm), diameter stenosis (%), reference diameter (mm), maximal diameter (mm) and mean diameter (mm) were calculated.

Statistical analysis

Statistical analyses were performed by using R (version 3.5.1, packages: Hmisc, lme4 and nlme). Baseline, categorical variables are reported as either counts or percentages and compared using the Chi Squared test on patient level. Normality for continuous variables was assessed using the Shapiro-Wilk test. Normally distributed continuous variables are reported as mean ± standard deviation (SD), Non-Gaussian variables are reported as median (interquartile range (IQR)). Normally distributed continuous variable were compared using a generalized linear mixed-effects model with a random effect for patients and a fixed effect for FFR groups, non-Gaussian variable were log transformed preparatory to the generalized linear mixed-effects model.

RESULTS

Patient demographics and baseline characteristics are depicted in Table 1.

In the cohort of patients with a post PCI $FFR_{\leq 0.85}$, mean age was 65 ± 12 years and 85% of the patients were male. Clinical presentation was stable angina in 42%, unstable angina or non ST elevated myocardial infarction (NSTEMI) in 45% and ST segment elevation myocardial infarction (STEMI) in 13% of the patients. In the vessels assessed an average of 1.6 ± 0.8 stents were used with a median stent diameter of 3 (2.75-3.25) mm. Median total stented length was 28 (15-46) mm.

Comparable baseline characteristics were observed in the >0.85 cohort, with the exception of a lower total stented length. Mean post procedural Pd/Pa and FFR were 0.91 ± 0.04 and 0.79 ± 0.05 in the ≤ 0.85 cohort and 0.96 ± 0.03 and 0.90 ± 0.03 in patients with a post PCI $FFR > 0.85$ respectively.

IVUS analysis in the post PCI $FFR \leq 0.85$ cohort

IVUS analyses showed a mean LA of 5.95 (5.01 - 7.03) mm^2 with an MLA of 2.19 (1.81 - 3.19) mm^2 and minimal stent area was 4.01 (3.09 - 5.21) mm^2 (Table 2).

Significant focal lesions proximal or distal to the stented segment were found in 29% and 30% of the vessels respectively. With an average of 1.6 ± 0.8 stents implanted, a total of 115 nonadjacent stented segments were analysed. According to the MUSIC criteria stent underexpansion was present in 88% of these segments (74% of the vessels). Mean stent expansion rate in the segments was 78.7%. Malapposition was found in 21% of the segments (23% of the vessels). In 54% of the vessels clear focal signs of luminal narrowing were found due to residual focal lesions or lumen compromising hematoma (3%). Spasm was present in 9% of the vessels analysed and in 8% of the vessels diffuse disease was present.

In 87% of the vessels, either a focal lesion, underexpansion, a lumen compromising hematoma or malapposition were present.

A dedicated sub-analysis on vessels with FFR values ≤ 0.75 and ≤ 0.80 can be found in Table 3.

Table 1. Baseline characteristic

	FFR ≤ 0.85 (n=95) (100 vessels)	FFR > 0.85 (n=20) (20 vessels)	p value
Age, years	65 \pm 12	66 \pm 12	0.67
Gender, male	81 (85)	19 (95)	0.29
Hypertension	58 (61)	14 (70)	0.40
Hypercholesterolemia	50 (53)	50 (53)	0.29
Diabetes	24 (25)	6 (30)	0.57
Smoking history	39 (41)	6 (30)	0.32
Prior stroke	11 (12)	0 (0)	0.23
Peripheral art. disease	6 (6)	1 (5)	0.86
Prior PCI	29 (31)	7 (35)	0.66
Prior CABG	3 (3)	1 (5)	0.65
Indication			
Stable angina	41 (43)	9 (45)	0.80
Unstable angina or NSTEMI	41 (43)	8 (40)	0.68
STEMI	13 (14)	3 (15)	0.81
Target vessel			
Left anterior descending artery (LAD)	81 (81)	12 (60)	0.24
Left circumflex artery (LCX)	7 (7)	3 (15)	0.25
Left main artery (LM)	3 (3)	1 (5)	0.65
Right coronary artery (RCA)	9 (9)	4 (20)	0.16
Predilatation	74 (74)	10 (50)	0.04
High pressure post dilatation (NC balloon)	74 (74)	13 (65)	0.41
Mean post PCI Pd/Pa	0.91 \pm 0.04	0.96 \pm 0.03	<0.001
Mean post PCI FFR	0.79 \pm 0.05	0.90 \pm 0.03	<0.001
No. of vessels with a post PCI $FFR \leq 0.80$	56 (56)		
No. of vessels with a post PCI $FFR \leq 0.75$	22 (22)		
No. of stents	1 (1-2)	1 (1-1)	<0.001
Mean stent diameter, mm	3 (2.75-3.25)	3.25 (3.0-3.5)	0.13
Total stent length, mm	28 (15-46)	21 (16-25)	0.12

Values are n (%), mean \pm SD or median (IQR), PCI = Percutaneous Coronary Artery and CABG = Coronary Artery Bypass Grafting, NSTEMI = non ST elevated myocardial infarction, STEMI =ST elevated myocardial infarction. NC = non compliant, Pd/Pa = the Pressure in the Distal coronary artery to the Pressure in the Aorta ratio, FFR = Fractional Flow Reserve under maximum hyperemia.

Table 2. IVUS findings in 100 vessels with an FFR ≤0.85 and 20 vessels >0.85

	FFR ≤0.85 (n=100)	FFR >0.85 (n=20)	p value
Mean lumen area, mm ²	5.95 (5.01-7.03)	6.24 (5.12-8.10)	0.15
Minimal lumen area, mm ²	2.19 (1.81-3.19)	2.92 (1.96-4.10)	0.02
Minimal stent area, mm ²	4.01 (3.09-5.21)	5.11 (3.05-7.41)	0.01
Focal lesion (proximal)	29 (29)	3 (15)	0.78
MLA at proximal lesion, mm ²	2.98 (2.24-3.36)	2.60 (2.30-2.60)	0.98
Focal lesion (distal)	30 (30)	6 (30)	1.00
MLA at distal lesion, mm ²	2.01 (1.68-2.12)	2.51 (1.88-3.26)	0.02
Lumen compromising hematoma	3 (3)	0 (0)	0.69
MLA lumen compromising hematoma, mm ²	1.97 (1.22-1.97)	-	-
Underexpansion	74 (74)	15 (75)	0.93
Malapposition	23 (23)	1 (5)	0.1
Spasm	9 (9)	0 (0)	0.31
Diffuse diseased	8 (8)	0 (0)	0.68
Any focal lesion	51 (51)	9 (45)	0.63
Any focal lesion or lumen compromising hematoma	54 (54)	9 (45)	0.37
Any focal lesion, underexpansion, lumen compromising hematoma or malapposition	84 (84)	18 (90)	0.99

Values are n (%) or median (IQR)

Table 3. IVUS findings according to incrementing groups of post PCI FFR

	FFR ≤0.75 (n=22)	FFR ≤0.80 (n=56)	FFR ≤0.85 (n=100)	FFR >0.85 (n=20)
Mean lumen area, mm ²	5.99 (4.53-6.78)	5.79 (4.68-6.95)	5.95 (5.01-7.03)	6.24 (5.12-8.10)
Minimal lumen area, mm ²	2.04 (1.49-2.92)	2.14 (1.59-3.17)	2.19 (1.81-3.19)	2.92 (1.96-4.10)
Minimal stent area, mm ²	3.59 (4.53-6.78)	3.87 (2.83-4.94)	4.01 (3.09-5.21)	5.11 (3.05-7.41)
Focal lesion (proximal)	10 (46)	18 (32)	29 (29)	3 (15)
MLA at proximal lesion, mm ²	3.12 (2.26-4.83)	3.00 (2.26-3.51)	2.98 (2.24-3.36)	2.60 (2.30-2.60)
Focal lesion (distal)	3 (14)	13 (23)	30 (30)	6 (30)
MLA at distal lesion, mm ²	1.71 (1.40-1.71)	2.03 (1.54-2.28)	2.01 (1.68-2.12)	2.51 (1.88-3.26)
Lumen compromising hematoma	0 (0)	1 (1.8)	3 (3)	0 (0)
MLA lumen compromising hematoma, mm ²	-	1.22	1.97 (1.22-1.97)	-
Underexpansion	18 (82)	40 (71)	74 (74)	15 (75)
Malapposition	6 (27)	17 (23)	23 (23)	1 (5)
Spasm	2 (9)	8 (14)	9 (9)	0 (0)
Diffuse diseased	2 (9)	6 (11)	8 (8)	0 (0)
Any focal lesion	11 (50)	27 (48)	51 (51)	9 (45)
Any focal lesion or lumen compromising hematoma	11 (50)	28 (50)	54 (54)	9 (45)
Any focal lesion, underexpansion, lumen compromising hematoma or malapposition	19 (86)	49 (88)	84 (84)	18 (90)

Values are median (IQR) or absolute numbers (%). MLA is minimal lumen area

IVUS analysis in the post FFR PCI > 0.85 cohort

IVUS analysis of the 20 vessels with a post PCI FFR >0.85 showed a median LA 6.24 (5.12-8.10) mm² with an MLA of 2.92 (1.96-4.10) mm² and minimal stent area was 5.11 (3.05-7.41) mm² (Table 2). Significant focal lesions proximal or distal to the stented segment were found in 15% and 30% of the vessels respectively. With an average of 1.0±0.0 stent implanted. According to the MUSIC criteria stent underexpansion was present in 75% of the vessels with a mean stent expansion rate of 79.6%. Malapposition was found in 1 vessel (5%). In 45% of the vessels clear focal signs of luminal narrowing were found due to residual focal lesions or lumen compromising hematoma (0 instances). Spasm and diffuse disease were not present in this cohort.

Pressure drops per segment in the total cohort

FFR pullback data were available for 107/120 vessels. A significantly higher pressure drop over the proximal segment was found in vessels with residual proximal focal lesions as compared to segments with no residual proximal focal lesions (0.06±0.09 vs 0.03±0.06 respectively, p=0.004). No significant differences in FFR drop were found in case of residual distal lesions (0.06±0.05 in the presence of a distal lesion vs. 0.05±0.06 in the absence of a distal lesion, p=0.92) or malapposition (0.06±0.06 with malapposition vs 0.05±0.06 without malapposition, p=0.22)(Figure 2).

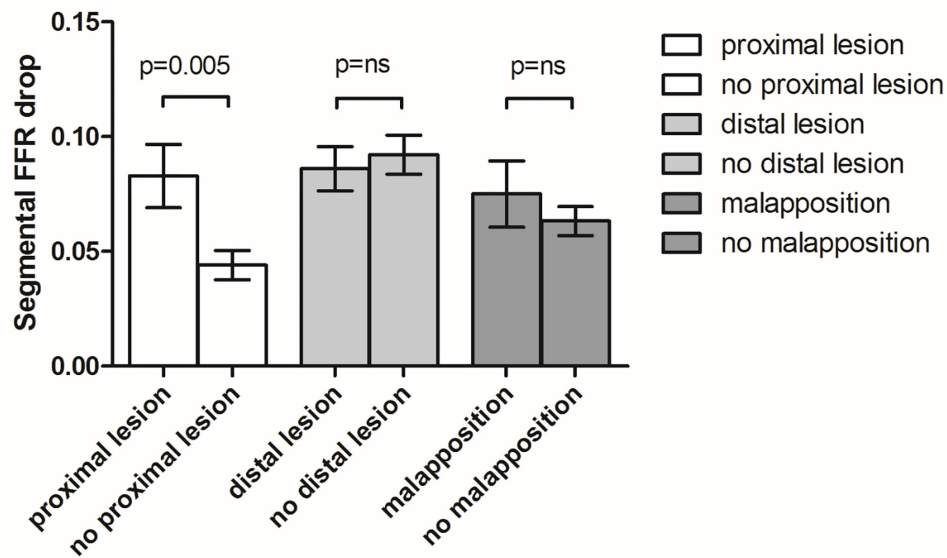


Figure 2. FFR drop by presence of residual lesions or malapposition
Values are means with error bars of the standard error of the mean

No significant changes in pressure drops over the stented segment were found in case of underexpansion according to either the MUSIC criteria or criteria with modified underexpansion limits, however, a trend was observed towards higher pressure drops along with more severe underexpansion rates (Figure 3).

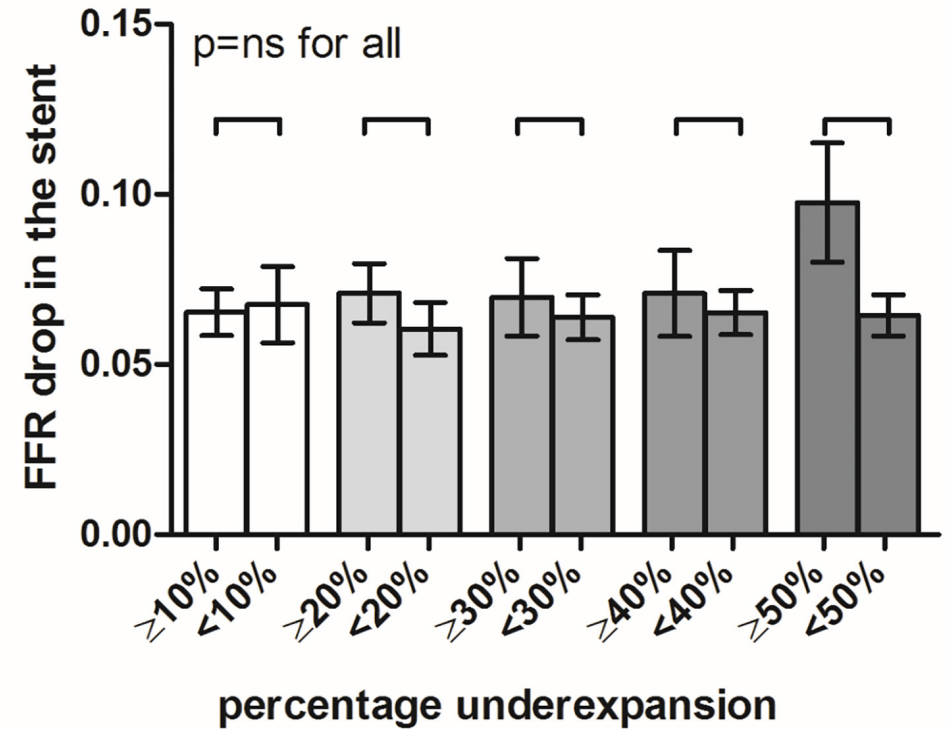


Figure 3. FFR drop by % of underexpansion
Values are means with error bars of the standard error of the mean

QCA analysis

A total of 103 proximal segments, 123 stented segments and 109 distal segments were analysed with QCA (Table 4).

Table 4. Quantitative coronary angiography of the proximal and distal segment as well as in-segment and in-stent analysis.

Proximal segment						
	FFR ≤0.85 (n=87)	FFR >0.85 (n=16)	p value	Proximal lesion* (n=31)	No proximal lesion* (n=72)	p value
Length, mm	17.20 (11.43-27.70)	16.31 (12.01-30.77)	0.99	27.01 (12.90-39.58)	15.42 (9.02-24.74)	0.19
Minimal diameter, mm	2.38 (1.97-2.99)	2.43 (2.22-2.94)	0.90	1.98 (1.67-2.21)	2.52 (2.27-3.02)	<0.001
Diameter stenosis, %	20 (11-30)	20.50 (12.25-28.00)	0.91	29 (19-34)	17.50 (11-25)	0.17
Stenosis>50%, %	0 (0)	0 (0)	-	0 (0)	0 (0)	-
Reference diameter, mm	3.05 (2.69-3.56)	3.20 (2.85-3.31)	0.91	2.81 (2.24-3.36)	3.17 (2.80-3.64)	0.03
Maximal diameter, mm	3.92 (3.06-4.29)	3.89 (3.70-4.61)	0.72	3.59 (2.84-4.14)	3.94 (3.30-4.38)	0.09
Mean diameter, mm	2.96 (2.54-3.50)	3.34 (2.87-3.61)	0.78	2.54 (2.30-3.11)	3.20 (2.78-3.57)	0.009
Distal segment						
	FFR ≤0.85 (n=90)	FFR >0.85 (n=19)	p value	Distal lesion* (n=34)	No distal lesion* (n=75)	p value
Length, mm	25.11 (17.16-36.02)	29.49 (19.17-41.18)	0.78	30.54 (21.11-41.13)	24.52 (17.17-34.76)	0.10
Minimal diameter, mm	1.37 (1.23-1.57)	1.69 (1.23-1.89)	0.59	1.39 (1.23-1.60)	1.44 (1.23-1.69)	0.82
Diameter stenosis, %	29.50 (18-38)	29 (11-37)	0.77	33.50 (28.25-43.25)	24 (13-34)	0.02
Stenosis>50%, %	5 (6%)	0 (0)	0.29	3 (9)	2 (3)	0.16
Reference diameter, mm	1.97 (1.69-2.20)	2.06 (1.76-2.55)	0.68	2.10 (1.84-2.37)	1.93 (1.63-2.16)	0.02
Maximal diameter, mm	2.43 (2.16-2.73)	2.86 (2.45-3.44)	0.51	2.51 (2.18-2.85)	2.45 (2.20-2.87)	0.90
Mean diameter, mm	1.87 (1.70-2.07)	2.13 (1.84-2.46)	0.004	1.92 (1.71-2.12)	1.90 (1.70-2.15)	0.71
In-segment						
	FFR ≤0.85 (n=104)	FFR >0.85 (n=19)	p value	>20% underexpansion* (n=62)	≤20% underexpansion* (n=61)	p value
Length, mm	33.41 (24.04-46.07)	27.74 (23.18-32.34)	0.93	33.36 (24.72-43.52)	30.29 (22.48-45.56)	0.35
Minimal diameter, mm	1.82 (1.56-2.04)	1.91 (1.69-2.31)	0.41	1.79 (1.55-1.99)	1.91 (1.63-2.18)	0.07
Diameter stenosis, %	23 (17-30)	21 (16-28)	0.65	22 (17-30)	22 (17.50-30.50)	0.82
Stenosis>50%	0 (0)	0 (0)	-	0 (0)	0 (0)	-
Reference diameter, mm	2.34 (2.11-2.70)	2.66 (2.19-2.89)	0.32	2.30 (2.03-2.57)	2.58 (2.16-2.80)	0.02
Maximal diameter, mm	3.22 (2.87-3.74)	3.34 (3.04-3.55)	0.44	3.19 (2.91-3.76)	3.30 (2.92-3.74)	0.92
Mean diameter, mm	2.61 (2.38-2.90)	2.71 (2.45-2.99)	0.32	2.59 (2.33-2.85)	2.70 (2.42-2.94)	0.19
In-stent						
	FFR ≤0.85 (n=104)	FFR >0.85 (n=19)	p value	>20% underexpansion* (n=62)	≤20% underexpansion* (n=61)	p value
Length, mm	23.77 (14.57-37.01)	17.56 (14.42-23.79)	0.96	23.78 (15.76-35.60)	21.27 (13.26-36.36)	0.31
Minimal diameter, mm	2.08 (1.86-2.47)	2.31 (2.08-2.67)	0.35	2.07 (1.83-2.41)	2.15 (1.91-2.57)	0.19
Diameter stenosis, %	15 (9-20)	13 (3-19)	<0.001	15 (8.75-19)	13 (8-21)	0.65
Stenosis>50%, %	0 (0)	0 (0)	-	0 (0)	0 (0)	-
Reference diameter, mm	2.42 (2.14-2.81)	2.80 (2.34-3.05)	0.3	2.37 (2.10-2.82)	2.65 (2.25-2.90)	0.06
Maximal diameter, mm	3.21 (2.88-3.59)	3.16 (2.97-3.54)	0.37	3.18 (2.86-3.58)	3.28 (2.98-3.65)	0.30
Mean diameter, mm	2.68 (2.43-2.99)	2.81 (2.58-3.01)	0.28	2.65 (2.43-2.97)	2.79 (2.50-3.03)	0.15

*as detected by IVUS. Values are median (IQR) or absolute numbers (%)

In brief, in the proximal segments, QCA did not reveal any significant differences in luminal dimensions in the two FFR cohorts, whereas in the distal segments diameters were significantly larger in the cohort with a post PCI FFR >0.85. As expected, in the presence either proximal- or distal focal lesions on IVUS, angiographic luminal dimensions differed significantly as compared to segments without residual lesions on IVUS. However, diameter stenosis did not exceed 50% in any of the proximal residual lesions detected by IVUS and/or FFR. In 5 cases QCA detected a diameter stenosis >50% (range 51 to 61%), corresponding to 3 cases with an IVUS detected distal focal lesion. Stented length was significantly larger in vessels with a post PCI FFR <0.85 as compared to vessels with a post PCI >0.85. Finally, QCA was not able to detect a difference in luminal dimensions of stented segments with 20% underexpansion or more.

DISCUSSION

In this IVUS sub-study of the FFR SEARCH registry we demonstrated, for the first time, that clear signs of residual luminal narrowing, including focal lesions, underexpansion and malapposition, were present in a significant amount of vessels with an impaired post PCI FFR. Findings that were not readily apparent on QCA. Several recent studies demonstrated the value of low post PCI FFR in predicting late adverse cardiac events^{3, 4}. Unfortunately, details on the actual rationale for these low PCI FFR values often remained elusive since no data on residual angiographically apparent disease were reported, nor were details presented on intravascular imaging findings. In our study meticulous intravascular ultrasound analysis revealed specific morphologic explanations for the suboptimal post PCI FFR.

First, in the low FFR cohort, we found residual focal lesions in 51% of the vessels. We found MLAs in focal proximal and distal lesions of 2.88 (2.29-3.37) mm and 2.03 (1.74-2.21) mm respectively. Several previous studies already indicated the strong correlation of IVUS derived low post PCI MLA with both low post PCI FFR values (<0.80) and worse outcome¹⁸⁻²². With QCA conversely, diameter stenosis in proximal and distal lesions were 29 (19-34) % and 33.5 (28.25-43.25) % respectively. Interestingly, in only 3 of the segments with residual focal lesions on IVUS, QCA detected a diameter stenosis >50%.

Secondly, in the low FFR cohort, we found underexpanded stents in 74% of the vessels with an FFR ≤0.85, a significantly higher percentage as would be expected post stenting in general, with expected underexpansion rates of 20-44%²³. Again,

these underexpansion figures appreciated with IVUS were not apparent with QCA. The latter might illustrate the potential of post PCI FFR to expose more severe forms of underexpansion and also fits with previous data showing a clear correlation between underexpansion and increased rates of early stent thrombosis and restenosis²⁴⁻²⁷.

Thirdly, in the low FFR cohort, malapposition was identified in 23% of the cases. Since we could not demonstrate a direct correlation between malapposition and a drop in FFR, in most cases malapposition was found in combination with underexpansion (87%), residual focal lesions or lumen compromising hematoma (52%) and only occurred isolated in one patient. Furthermore, the malapposition rate of 23% found in our study fits with previous imaging studies post DES implantation, showing rates of malapposition in 7-39% of the cases with no significant correlation to either stent thrombosis or restenosis^{24, 28-30}. Nevertheless, stent malapposition is suboptimal and is associated with stent thrombosis in intravascular imaging studies and adequate strut apposition might help to avoid long-term stent related complications³¹.

Although we only enrolled 20 cases with a post PCI FFR >0.85 as a reference a clear trend was seen towards larger minimal stent areas, a lower number of residual proximal focal lesions, less stents with malapposition and a lower incidence of diffuse disease. Additionally, the incidence of patients presenting with STEMI was significantly lower in patients with post PCI FFR <0.85 as compared to those with higher post PCI values³². Nevertheless, also in the STEMI cohort, IVUS revealed residual luminal narrowing in a significant proportion of patients.

Despite accumulating outcome data supporting the use of IVUS, its adoption in daily clinical practice remains low³³. IVUS has the reputation to be costly and time-consuming, and insufficient IVUS knowledge might hamper ad-hoc image interpretation. Conversely, FFR allows a faster and more easily interpretable assessment of the hemodynamic importance of coronary artery disease.

In the present study we attempted to link a lower than expected FFR to morphological findings by IVUS and QCA. FFR pressure drops were more pronounced in vessels with residual proximal focal lesions but not with distal lesions. Previous work already alluded to the lack of correlation between anatomic and functional severity of stenosis in small vessels, probably due to the small myocardial territory at risk³⁴. On the other hand, FFR guided PCI resulted in significantly superior outcomes as compared to angiography guided PCI also in studies focussing on small vessels³⁵. Finally, we demonstrated that milder forms of underexpansion might remain unnoticed on FFR pullbacks while larger, and perhaps more clinically relevant rates

of underexpansion might be associated with significant pressure gradients.

While the results of the FFR-REACT trial (Dutch trial register: NTR6711), assessing whether FFR directed IVUS guided PCI optimization improves patient outcomes as compared to standard clinical practice, are eagerly awaited, there is a clear need for larger prospective randomized controlled trials designed to better understand the potential benefit of FFR-guided PCI optimization with or without the focused use of IVUS.

Limitations

Several limitations need to be mentioned. First, we only enrolled 20 patients with a post PCI FFR >0.85. The absence of clear significant differences in IVUS findings between both cohorts might have been due to a lack of power. Second, the criteria for underexpansion in this study are based upon the MUSIC criteria¹⁴. Unlike in the MUSIC study in which only stents with a length of 15 mm were used, the average stented length in the present cohort was 34 mm resulting in significant differences between proximal and distal reference segments which might have impacted the calculation of the percentage underexpansion. This could have resulted in a lower mean reference LA and therefore an overestimation of the degree of expansion. Third, pressure measurements were performed with the Navvus microcatheter, which might underestimate the FFR value as compared to the wire based FFR³⁶⁻³⁸. The latter might mean that the IVUS finding from this study can also be applicable to higher post PCI values, measure with a wired base device. Fourth, maximum hyperemic conditions during continuous intravenous infusion of adenosine might fluctuate and therefore influence pullback assessment in up to 40% of the cases³⁹. Fifth, for the present study we used an FFR cut-off of 0.85. While several previous studies demonstrated a clear trend towards increased MACE rates with decreasing post PCI FFR values an exact cut-off for an optimal post PCI FFR, at present, is elusive. Finally, since the FFR SEARCH registry was developed to assess the impact of post PCI FFR measured in routine clinical practice, per protocol, no additional interventions were performed based on either FFR or IVUS findings. Whether additional treatment will optimize the longer-term results of these patients is currently being investigated in the FFR REACT trial.

CONCLUSION

In patients with a post procedural FFR ≤0.85, IVUS revealed focal signs of luminal narrowing in the majority of the cases. Only proximal focal lesions resulted in significant FFR pressure drops during pullback.

Supplementary Table 1.

	FFR ≤0.75 (n=22)	FFR ≤0.80 (n=56)	FFR ≤0.85 (n=100)	FFR > 0.85 (n=20)
Mean lumen area, mm ²	5.99 (4.53-6.78)	5.79 (4.68-6.95)	5.95 (5.01-7.03)	6.24 (5.12-8.10)
Minimal lumen area, mm ²	2.04 (1.49-2.92)	2.14 (1.59-3.17)	2.19 (1.81-3.19)	2.92 (1.96-4.10)
Minimal stent area, mm ²	3.59 (4.53-6.78)	3.87 (2.83-4.94)	4.01 (3.09-5.21)	5.11 (3.05-7.41)
Focal lesion (proximal)	10 (46)	18 (32)	29 (29)	3 (15)
MLA at proximal lesion, mm ²	3.12 (2.26-4.83)	3.00 (2.26-3.51)	2.98 (2.24-3.36)	2.60 (2.30-2.60)
Focal lesion (distal)	3 (14)	13 (23)	30 (30)	6 (30)
MLA at distal lesion, mm ²	1.71 (1.40-1.71)	2.03 (1.54-2.28)	2.01 (1.68-2.12)	2.51 (1.88-3.26)
Lumen compromising hematoma	0 (0)	1 (1.8)	3 (3)	0 (0)
MLA lumen compromising hematoma, mm ²	-	1.22	1.97 (1.22-1.97)	-
Underexpansion	18 (82)	40 (71)	74 (74)	15 (75)
Malapposition	6 (27)	17 (23)	23 (23)	1 (5)
Spasm	2 (9)	8 (14)	9 (9)	0 (0)
Diffuse diseased	2 (9)	6 (11)	8 (8)	0 (0)
Any focal lesion	11 (50)	27 (48)	51 (51)	9 (45)
Any focal lesion or lumen compromising hematoma	11 (50)	28 (50)	54 (54)	9 (45)
Any focal lesion, underexpansion, lumen compromising hematoma or malapposition	19 (86)	49 (88)	84 (84)	18 (90)

Values are median (IQR) or absolute numbers (%)

REFERENCES

1. Fearon WF, Bornschein B, Tonino PA, Gothe RM, Bruyne BD, Pijls NH, Siebert U and Fractional Flow Reserve Versus Angiography for Multivessel Evaluation Study I. Economic evaluation of fractional flow reserve-guided percutaneous coronary intervention in patients with multivessel disease. *Circulation*. 2010;122:2545-50.
2. Tonino PA, De Bruyne B, Pijls NH, Siebert U, Ikeno F, van' t Veer M, Klauss V, Manoharan G, Engstrom T, Oldroyd KG, Ver Lee PN, MacCarthy PA, Fearon WF and Investigators FS. Fractional flow reserve versus angiography for guiding percutaneous coronary intervention. *N Engl J Med*. 2009;360:213-24.
3. Wolfrum M, Fahrni G, de Maria GL, Knapp G, Curzen N, Kharbanda RK, Fröhlich GM and Banning AP. Impact of impaired fractional flow reserve after coronary interventions on outcomes: a systematic review and meta-analysis. *BMC Cardiovascular Disorders*. 2016;16:177.
4. Rimac G, Fearon WF, De Bruyne B, Ikeno F, Matsuo H, Piroth Z, Costerousse O and Bertrand OF. Clinical value of post-percutaneous coronary intervention fractional flow reserve value: A systematic review and meta-analysis. *Am Heart J*. 2017;183:1-9.
5. Kasula S, Agarwal SK, Hacioglu Y, Pothineni NK, Bhatti S, Ahmed Z, Uretsky B and Hakeem A. Clinical and prognostic value of poststenting fractional flow reserve in acute coronary syndromes. *Heart*. 2016;102:1988-1994.
6. Diletti R, van Bommel R, Masdjedi K, van Zandvoort L, Lemmert ME, Wilschut J, De Jaegere P, Boersma E, Zijlstra F, Daemen J and van Mieghem NMDA. Routine Fractional Flow Reserve Measurement after Percutaneous Coronary Intervention The FFR-SEARCH Study. *EuroPCR presentation 2017*.
7. Hanekamp CE, Koolen JJ, Pijls NH, Michels HR and Bonnier HJ. Comparison of quantitative coronary angiography, intravascular ultrasound, and coronary pressure measurement to assess optimum stent deployment. *Circulation*. 1999;99:1015-21.
8. Fearon WF, Luna J, Samady H, Powers ER, Feldman T, Dib N, Tuzcu EM, Cleman MW, Chou TM, Cohen DJ, Ragosta M, Takagi A, Jeremias A, Fitzgerald PJ, Yeung AC, Kern MJ and Yock PG. Fractional flow reserve compared with intravascular ultrasound guidance for optimizing stent deployment. *Circulation*. 2001;104:1917-22.
9. Stempfle HU, König A, Drescher E, Siebert U and Klauss V. Discrepancy between morphologic and functional criteria of optimal stent deployment using intravascular ultrasound and pressure derived myocardial fractional flow reserve. *Int J Cardiovasc Intervent*. 2005;7:101-7.
10. Pijls NH, De Bruyne B, Bech GJ, Liistro F, Heyndrickx GR, Bonnier HJ and Koolen JJ. Coronary pressure measurement to assess the hemodynamic significance of serial stenoses within one coronary artery: validation in humans. *Circulation*. 2000;102:2371-7.
11. Kim HL, Koo BK, Nam CW, Doh JH, Kim JH, Yang HM, Park KW, Lee HY, Kang HJ, Cho YS, Youn TJ, Kim SH, Chae IH, Choi DJ, Kim HS, Oh BH and Park YB. Clinical and physiological outcomes of fractional flow reserve-guided percutaneous coronary intervention in patients with serial stenoses within one coronary artery. *JACC Cardiovasc Interv*. 2012;5:1013-8.
12. Ben-Dor I, Torguson R, Deksissa T, Bui AB, Xue Z, Satler LF, Pichard AD and Waksman R. Intravascular ultrasound lumen area parameters for assessment of physiological ischemia by fractional flow reserve in intermediate coronary artery stenosis. *Cardiovasc Revasc Med*. 2012;13:177-82.
13. Ben-Dor I, Torguson R, Gaglia MA, Jr., Gonzalez MA, Maluenda G, Bui AB, Xue Z, Satler LF, Suddath WO, Lindsay J, Pichard AD and Waksman R. Correlation between fractional flow reserve and intravascular ultrasound lumen area in intermediate coronary artery stenosis. *EuroIntervention*. 2011;7:225-33.
14. de Jaegere P, Mudra H, Figulla H, Almagor Y, Doucet S, Penn I, Colombo A, Hamm C, Bartorelli A, Rothman M, Nobuyoshi M, Yamaguchi T, Voudris V, DiMario C, Makovski S, Hausmann D, Rowe S, Rabinovich S, Sunamura M and van Es GA. Intravascular ultrasound-guided optimized stent deployment. Immediate and 6 months clinical and angiographic results from the Multicenter Ultrasound Stenting in Coronaries Study (MUSIC Study). *Eur Heart J*. 1998;19:1214-23.
15. Mintz GS, Nissen SE, Anderson WD, Bailey SR, Erbel R, Fitzgerald PJ, Pinto FJ, Rosenfield K, Siegel RJ, Tuzcu EM and Yock PG. American College of Cardiology Clinical Expert Consensus Document on Standards for Acquisition, Measurement and Reporting of Intravascular Ultrasound Studies (IVUS). A report of the American College of Cardiology Task Force on Clinical Expert Consensus Documents. *J Am Coll Cardiol*. 2001;37:1478-92.
16. Koyama J, Yamagishi M, Tamai J, Kawano S, Daikoku S and Miyatake K. Comparison of vessel wall morphologic appearance a sites of focal and diffuse coronary vasospasm by intravascular ultrasound. *American Heart Journal*. 1995;130:440-445.
17. Miyao Y, Kugiyama K, Kawano H, Motoyama T, Ogawa H, Yoshimura M, Sakamoto T and Yasue H. Diffuse intimal thickening of coronary arteries in patients with coronary spastic angina. *J Am Coll Cardiol*. 2000;36:432-7.
18. Takayama T and Hodgson JM. Prediction of the physiologic severity of coronary lesions using 3D IVUS: validation by direct coronary pressure measurements. *Catheter Cardiovasc Interv*. 2001;53:48-55.
19. Briguori C, Anzuini A, Airoidi F, Gimelli G, Nishida T, Adamian M, Corvaja N, Di Mario C and Colombo A. Intravascular ultrasound criteria for the assessment of the functional significance of intermediate coronary artery stenoses and comparison with fractional flow reserve. *Am J Cardiol*. 2001;87:136-41.
20. Takagi A, Tsurumi Y, Ishii Y, Suzuki K, Kawana M and Kasanuki H. Clinical potential of intravascular ultrasound for physiological assessment of coronary stenosis: relationship between quantitative ultrasound tomography and pressure-derived fractional flow reserve. *Circulation*. 1999;100:250-5.
21. Lee SY, Shin DH, Kim JS, Kim BK, Ko YG, Choi D, Jang Y and Hong MK. Intravascular Ultrasound Predictors of Major Adverse Cardiovascular Events After Implantation of Everolimus-eluting Stents for Long Coronary Lesions. *Rev Esp Cardiol (Engl Ed)*. 2017;70:88-95.

22. Ito T, Tani T, Fujita H and Ohte N. Relationship between fractional flow reserve and residual plaque volume and clinical outcomes after optimal drug-eluting stent implantation: insight from intravascular ultrasound volumetric analysis. *Int J Cardiol.* 2014;176:399-404.
23. Mudra H, di Mario C, de Jaegere P, Figulla HR, Macaya C, Zahn R, Wennerblom B, Rutsch W, Voudris V, Regar E, Henneke KH, Schachinger V, Zeiher A and Investigators OS. Randomized comparison of coronary stent implantation under ultrasound or angiographic guidance to reduce stent restenosis (OPTICUS Study). *Circulation.* 2001;104:1343-9.
24. Choi SY, Witzendichler B, Maehara A, Lansky AJ, Guagliumi G, Brodie B, Kellett MA, Jr, Dressler O, Parise H, Mehran R, Dangas GD, Mintz GS and Stone GW. Intravascular ultrasound findings of early stent thrombosis after primary percutaneous intervention in acute myocardial infarction: a Harmonizing Outcomes with Revascularization and Stents in Acute Myocardial Infarction (HORIZONS-AMI) substudy. *Circ Cardiovasc Interv.* 2011;4:239-47.
25. Liu X, Doi H, Maehara A, Mintz GS, Costa Jde R, Jr, Sano K, Weisz G, Dangas GD, Lansky AJ, Kreps EM, Collins M, Fahy M, Stone GW, Moses JW, Leon MB and Mehran R. A volumetric intravascular ultrasound comparison of early drug-eluting stent thrombosis versus restenosis. *JACC Cardiovasc Interv.* 2009;2:428-34.
26. Fujii K, Carlier SG, Mintz GS, Yang YM, Moussa I, Weisz G, Dangas G, Mehran R, Lansky AJ, Kreps EM, Collins M, Stone GW, Moses JW and Leon MB. Stent underexpansion and residual reference segment stenosis are related to stent thrombosis after sirolimus-eluting stent implantation: an intravascular ultrasound study. *J Am Coll Cardiol.* 2005;45:995-8.
27. Sonoda S, Morino Y, Ako J, Terashima M, Hassan AH, Bonneau HN, Leon MB, Moses JW, Yock PG, Honda Y, Kuntz RE, Fitzgerald PJ and Investigators S. Impact of final stent dimensions on long-term results following sirolimus-eluting stent implantation: serial intravascular ultrasound analysis from the sirius trial. *J Am Coll Cardiol.* 2004;43:1959-63.
28. Steinberg DH, Mintz GS, Mandinov L, Yu A, Ellis SG, Grube E, Dawkins KD, Ormiston J, Turco MA, Stone GW and Weissman NJ. Long-term impact of routinely detected early and late incomplete stent apposition: an integrated intravascular ultrasound analysis of the TAXUS IV, V, and VI and TAXUS ATLAS workhorse, long lesion, and direct stent studies. *JACC Cardiovasc Interv.* 2010;3:486-94.
29. Kawamori H, Shite J, Shinke T, Otake H, Matsumoto D, Nakagawa M, Nagoshi R, Kozuki A, Hariki H, Inoue T, Osue T, Taniguchi Y, Nishio R, Hiranuma N and Hirata K-i. Natural consequence of post-intervention stent malapposition, thrombus, tissue prolapse, and dissection assessed by optical coherence tomography at mid-term follow-up. *European Heart Journal Cardiovascular Imaging.* 2013;14:865-875.
30. Guo N, Maehara A, Mintz GS, He Y, Xu K, Wu X, Lansky AJ, Witzendichler B, Guagliumi G, Brodie B, Kellett MA, Jr, Dressler O, Parise H, Mehran R and Stone GW. Incidence, mechanisms, predictors, and clinical impact of acute and late stent malapposition after primary intervention in patients with acute myocardial infarction: an intravascular ultrasound substudy of the Harmonizing Outcomes with Revascularization and Stents in Acute Myocardial Infarction (HORIZONS-AMI) trial. *Circulation.* 2010;122:1077-84.
31. Souteyrand G, Amabile N, Mangin L, Chabin X, Meneveau N, Cayla G, Vanzetto G, Barnay P, Trouillet C, Rioufol G, Range G, Teiger E, Delaunay R, Dubreuil O, Lhermusier T, Mulliez A, Levesque S, Belle L, Caussin C, Motreff P and Investigators P. Mechanisms of stent thrombosis analysed by optical coherence tomography: insights from the national PESTO French registry. *Eur Heart J.* 2016;37:1208-16.
32. Stone GW, Webb J, Cox DA, Brodie BR, Qureshi M, Kalynych A, Turco M, Schultheiss HP, Dulas D, Rutherford BD, Antonucci D, Krucoff MW, Gibbons RJ, Jones D, Lansky AJ, Mehran R, Enhanced Myocardial E and Recovery by Aspiration of Liberated Debris I. Distal microcirculatory protection during percutaneous coronary intervention in acute ST-segment elevation myocardial infarction: a randomized controlled trial. *Jama.* 2005;293:1063-72.
33. Ahn J-M, Kang S-J, Yoon S-H, Park HW, Kang SM, Lee J-Y, Lee S-W, Kim Y-H, Lee CW, Park S-W, Mintz GS and Park S-J. Meta-Analysis of Outcomes After Intravascular Ultrasound-Guided Versus Angiography-Guided Drug-Eluting Stent Implantation in 26,503 Patients Enrolled in Three Randomized Trials and 14 Observational Studies. *The American Journal of Cardiology.* 2014;113:1338-1347.
34. Costa MA, Sabate M, Staico R, Alfonso F, Seixas AC, Albertal M, Crossman A, Angiolillo DJ, Zenni M, Sousa JE, Macaya C and Bass TA. Anatomical and physiologic assessments in patients with small coronary artery disease: final results of the Physiologic and Anatomical Evaluation Prior to and After Stent Implantation in Small Coronary Vessels (PHANTOM) trial. *Am Heart J.* 2007;153:296 e1-7.
35. Puymirat E, Peace A, Mangiacapra F, Conte M, Ntarladimas Y, Bartunek J, Vanderheyden M, Wijns W, De Bruyne B and Barbato E. Long-term clinical outcome after fractional flow reserve-guided percutaneous coronary revascularization in patients with small-vessel disease. *Circ Cardiovasc Interv.* 2012;5:62-8.
36. Menon M, Jaffe W, Watson T and Webster M. Assessment of coronary fractional flow reserve using a monorail pressure catheter: the first-in-human ACCESS-NZ trial. *EuroIntervention.* 2015;11:257-63.
37. Pouillot C, Fournier S, Glasenapp J, Rambaud G, Bougrini K, Vi Fane R, Geyer C and Adedj J. Pressure wire versus microcatheter for FFR measurement: a head-to-head comparison. *EuroIntervention.* 2018;13:e1850-e1856.
38. Masdjedi K, van Mieghem NMDA, Diletti R, van Geuns RJ, de Jaegere P, Regar E, Zijlstra F, van Domburg RT and Daemen J. Navvus FFR to reduce CONTRASt, Cost and radiaTion (CONTRACT); insights from a single-centre clinical and economical evaluation with the RXi Rapid-Exchange FFR device. *Int J Cardiol.* 2017;233:80-84.
39. Johnson NP, Johnson DT, Kirkeeide RL, Berry C, De Bruyne B, Fearon WF, Oldroyd KG, Pijls NHJ and Gould KL. Repeatability of Fractional Flow Reserve Despite Variations in Systemic and Coronary Hemodynamics. *JACC Cardiovasc Interv.* 2015;8:1018-1027.

Chapter 11



Impact of intravascular ultrasound findings in patients with a post PCI fractional flow reserve ≤ 0.85 on 2 year clinical outcome

van Zandvoort LJC, Masdjedi K, Neleman T, Tovar Forero MN, Wilschut J, den Dekker WK, de Jaegere PPT, Diletti R, Zijlstra F, van Mieghem NMDA, Daemen J

*Erasmus University Medical Center, Thoraxcenter, Department of cardiology, Rotterdam,
the Netherlands*

Int J Cardiol. 2020;317:33-36

ABSTRACT

Background: Patients with a low post PCI fractional flow reserve (FFR) are at increased risk for future adverse cardiac events. The aims of the present study was to assess the impact of specific intravascular ultrasound (IVUS) findings in patients with a low post percutaneous coronary intervention (PCI) FFR on long-term clinical outcome.

Methods: In a subgroup analysis, 100 vessels with an FFR value ≤ 0.85 underwent post PCI IVUS to further assess the potential determinants for low post PCI FFR. No further action was taken to improve post PCI FFR. The primary endpoint of this study was the event free survival of target vessel failure (TVF) at two years in patients with a post PCI FFR ≤ 0.85 , which was defined as a composite of cardiac death, target vessel myocardial infarction or target vessel revascularization.

Results: In patients with a post PCI FFR ≤ 0.85 , TVF free survival rates were 88.5% vs. 95.5% for patients with versus without residual proximal lesions and 88.2% vs. 95.5% for patients with versus without residual distal lesions respectively (HR=2.53, 95% confidence interval (CI) 0.52-12.25, $p=0.25$ and HR=2.60, 95% CI 0.54-12.59, $p=0.24$ respectively). TVF free survival was 92.8% vs. 93.5% in patients with versus without stent underexpansion $>20\%$ (HR=1.01, 95% CI 0.21-4.88, $p=0.99$) and 89.3% vs. 97.8% in patients with versus without any residual focal lesion including lumen compromising hematoma (HR=4.64, 95% CI 0.55-39.22, $p=0.18$).

Conclusion: Numerically higher TVF rates were observed in patients with a post PCI FFR ≤ 0.85 and clear focal residual disease as assessed with IVUS.

BACKGROUND

FFR after stenting proved to be a strong and independent predictor for MACE¹. Unfortunately, the exact rationale behind this observation remains elusive based on angiographic findings alone let alone the impact on clinical follow-up. Fractional flow reserve (FFR) has proven to be a useful technique to address coronary physiology and the haemodynamic significance of coronary segments both pre- and post-intervention².

In the intravascular ultrasound (IVUS) sub-study of the FFR SEARCH registry we demonstrated, for the first time, that clear signs of residual luminal narrowing, including focal lesions, underexpansion and malapposition, were present in a significant amount of vessels with an impaired post percutaneous coronary intervention (PCI) FFR despite optimal angiographic results³.

Patients with a low post PCI fractional flow reserve (FFR) are at increased risk for future adverse cardiac events. The aims of the present study was to assess the impact of specific IVUS findings in patients with a low post PCI FFR on long-term clinical outcome (FFR ≤ 0.85).

METHODS

Patient selection

The FFR SEARCH (Stent Evaluated at Rotterdam Cardiology Hospital) study is a prospective single center registry in which 1000 consecutive patients underwent FFR evaluation after angiographic successful PCI with a primary endpoint to study the impact of post PCI FFR on major adverse cardiac event rates at 2 years. In a subgroup analysis, 95 consecutive patients (100 vessels) with a post PCI FFR value ≤ 0.85 and 20 patients (20 vessels) with a post PCI FFR > 0.85 underwent post PCI IVUS to further assess the potential determinants for the low post PCI FFR. No further action was taken to improve the post PCI FFR. The study was performed in accordance with the Declaration of Helsinki. The study protocol was approved by the local ethics committee. All patients provided written informed consent for the procedure and the use of anonymous datasets for research purposes in alignment with the Dutch Medical Research Act.

Specifics on angiographic measurements, FFR assessment and IVUS acquisition are discussed in the initial FFR SEARCH registry study and the IVUS sub-study report^{3,4}. In brief, a dedicated FFR Navvus MicroCatheter (ACIST Medical Systems, Inc., Eden Prairie, MN, USA) was advanced over the previously used coronary guidewire approximately 20 mm distal to the most distal stent edge. IVUS imaging was

performed with the multi frequency High Definition IVUS Kodama catheter (ACIST Medical Systems, Inc., Eden Prairie, MN, USA).

The primary endpoint of this study was the event free survival of target vessel failure (TVF) at two years, which was defined as a composite of cardiac death, target vessel myocardial infarction or target vessel revascularization.

Myocardial infarction (MI) was defined according to the fourth definition recommended by the European Society of Cardiology ⁵. Cardiac death was adjudicated if the cause of death was most probable cardiac cause or could not be identified. Clinical follow-up data were collected by hospital visit, chart review or telephone contact.

Categorical variables are reported as either counts or percentages, continuous variables are reported as mean \pm standard and compared using a generalized linear mixed model. Survival analyses were performed using the Kaplan-Meier method. In order to evaluate IVUS findings and the impact on TVF at two year follow-up, all 100 vessels were tested univariately using a Cox proportional hazards model which accounted for the multilevel nature of the data. No multivariable model was constructed due to a lack of events. Statistical analyses were performed by using SPSS 25 and R (version 3.5.1, packages: lme4, nlme, surv).

RESULTS

Baseline characteristics and IVUS findings are depicted in Table 1.

In the dedicated IVUS analyses, in patients with a post PCI FFR ≤ 0.85 , significant focal lesions proximal or distal to the treated segment were found in 29% and 30% of the vessels respectively. Underexpansion $>20\%$ was present in 50% of the vessels. In 54% of the vessels clear focal signs of luminal narrowing were found due to residual focal lesions or lumen compromising hematoma (3%). In 87% of the vessels, either a focal lesion, underexpansion ($>10\%$), a lumen compromising hematoma or malapposition were present. Baseline characteristics compared in different subgroups are depicted in supplementary Table 1.

Complete two-year follow-up was available for 100% of the patients. At two years, the cumulative survival free of TVF was 93.2% in patients with a post PCI FFR ≤ 0.85 . TVF free survival rates were 88.5% vs. 95.5% (n. events=3 vs. 3) for patients with versus without residual proximal lesions and 88.2% vs. 95.5% (n. events=3 vs. 3) for patients with versus without residual distal lesions respectively (hazard ratio (HR)=2.53, 95% confidence interval (CI) 0.52-12.25, $p=0.25$ and HR=2.60, 95% CI 0.54-12.59, $p=0.24$ respectively) (Figure 1).

Table 1. Key characteristic and IVUS findings

	FFR ≤ 0.85 (n=95) (100 vessels)	FFR > 0.85 (n=20) (20 vessels)	p value
Patient and vessel characteristic			
Age, years	65 \pm 12	66 \pm 12	0.67
Gender, male	81 (85)	19 (95)	0.29
Diabetes	24 (25)	6 (30)	0.57
Prior PCI	29 (31)	7 (35)	0.66
Indication			
Stable angina	41 (43)	9 (45)	0.80
ACS	54 (57)	11 (55)	0.80
Target vessel			
Left anterior descending artery (LAD)	81 (81)	12 (60)	0.24
Left circumflex artery (LCX)	7 (7)	3 (15)	0.25
Left main artery (LM)	3 (3)	1 (5)	0.65
Right coronary artery (RCA)	9 (9)	4 (20)	0.16
Predilatation	74 (74)	10 (50)	0.04
High pressure post dilatation (NC balloon)	74 (74)	13 (65)	0.41
Mean post PCI Pd/Pa	0.91 \pm 0.04	0.96 \pm 0.03	<0.001
Mean post PCI FFR, maximum hyperemia	0.79 \pm 0.05	0.90 \pm 0.03	<0.001
No. of stents	1 (1-2)	1 (1-1)	<0.001
Mean stent diameter, mm	3 (2.75-3.25)	3.25 (3.0-3.5)	0.13
Total stent length, mm	28 (15-46)	21 (16-25)	0.12
IVUS analysis			
Minimal lumen area, mm ²	2.19 (1.81-3.19)	2.92 (1.96-4.10)	0.02
Mean lumen area, mm ²	5.95 (5.01-7.03)	6.24 (5.12-8.10)	0.15
Minimal stent area, mm ²	4.01 (3.09-5.21)	5.11 (3.05-7.41)	0.01
Focal lesion (proximal)	29 (29)	3 (15)	0.78
MLA at proximal lesion, mm ²	2.98 (2.24-3.36)	2.60 (2.30-2.60)	0.98
Focal lesion (distal)	30 (30)	6 (30)	1.00
MLA at distal lesion, mm ²	2.01 (1.68-2.12)	2.51 (1.88-3.26)	0.02
Lumen compromising hematoma	3 (3)	0 (0)	0.69
MLA lumen compromising hematoma, mm ²	1.97 (1.22-1.97)	-	-
Underexpansion ($>10\%$)	74 (74)	15 (75)	0.93
Underexpansion ($>20\%$)	50 (50)	8 (40)	0.41
Malapposition	23 (23)	1 (5)	0.10
Spasm	9 (9)	0 (0)	0.31
Diffuse diseased	8 (8)	0 (0)	0.68
Any focal lesion	51 (51)	9 (45)	0.63
Any focal lesion or lumen compromising hematoma	54 (54)	9 (45)	0.37
Any focal lesion, underexpansion ($>10\%$), lumen compromising hematoma or malapposition	84 (84)	18 (90)	0.99

Values are n (%) or mean \pm SD, PCI = Percutaneous Coronary Artery and CABG = Coronary Artery Bypass Grafting, NSTEMI = non ST elevated myocardial infarction, STEMI =ST elevated myocardial infarction. NC = non-compliant, Pd/Pa = the Pressure in the Distal coronary artery to the Pressure in the Aorta ratio, FFR = Fractional Flow Reserve. MLA = minimal lumen area.

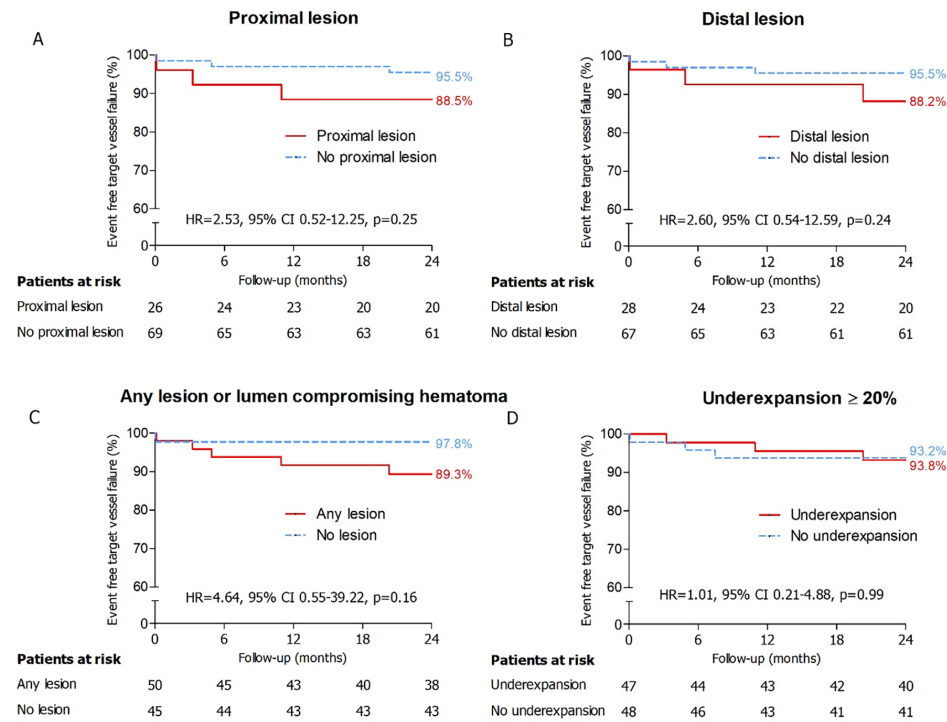


Figure 1. Kaplan-Meier curves for separated for the presence of proximal focal lesions, distal focal lesions, any lesion including lumen compromising hematoma and >20% underexpansion. Event free survival of target vessel failure (TVF).

TVF free survival was 93.8% vs. 93.2% (n. events=3 vs. 3) in patients with versus without stent underexpansion >20% (HR=1.01, 95% CI 0.21-4.88, p=0.99) and 89.3% vs. 97.8% (n. events=5 vs. 1) in patients with versus without any residual focal lesion including lumen compromising hematoma (HR=4.64, 95% CI 0.55-39.22, p=0.16). In contrast to focal residual disease, which clearly tended to impact TVF at 2 years, no events were found related to vessels with diffuse disease (n=8). TVF free survival in patients with a post PCI FFR >0.85 was 90.0% (88.9% and 90.9% in patients with versus without residual lesions or lumen compromising hematoma).

DISCUSSION

Low post PCI FFR proved to be associated with higher rates of TVF ¹. However, the practical implications of low post PCI FFR remain debated since little is known about the exact mechanisms behind the low FFR and potential consequences of further intravascular treatment.

In the FFR SEARCH IVUS study, we found a high proportion of IVUS detected anomalies including focal lesions, stent underexpansion and malapposition in vessels with a post PCI FFR ≤0.85; findings that were not readily apparent on coronary angiography ³.

The present predefined long-term follow-up analysis demonstrated a clear trend towards higher rates of TVF at two years when IVUS derived residual lesions were found.

Patients without clear residual disease on IVUS had a 2.2% risk of TVF at 2 year, despite having a post PCI FFR<0.85 (as compared to 10.7% in those with residual disease, HR 4.6).

We therefore believe that IVUS might provide significant benefit in further stratifying those at the highest risk for future adverse events (post PCI FFR<0.85) and guide further treatment optimization.

Limitations

The sample size in this sub-study of the FFR SEARCH is registry is limited. Although clear clinical trends were observed, the limited number of patients with a persistent low post PCI FFR and subsequent IVUS withheld us from providing significant hazard ratios. The current study is hypothesis generating and large randomized trials are warranted to further investigate the relation between IVUS detected anomalies and hard clinical endpoints in patients with persistent low post PCI FFR.

Finally, adverse events were adjudicated by investigators blinded to the final FFR values and IVUS findings. No dedicated independent event committee was used

CONCLUSION

At two years, the cumulative survival free of TVF in patients with a post PCI FFR ≤0.85 was 93.5%. Numerically higher TVF rates were observed in patients with clear focal residual disease as assessed with IVUS.

Supplementary table 1. Baseline characteristic and IVUS findings in vessels with and without proximal lesions, distal lesions underexpansion or any lesion (post PCI FFR ≤0.85)

	Proximal lesion			Distal lesion		
	present (n=26 patients, 29 vessels)	Not present (n=69 patients, 71 vessels)	p value	Present (n=28 patients, 30 vessels)	No Present (n=67 patients, 70 vessels)	p value
Age, years	65±14	64±12	0.633	67±12	64±13	0.559
Gender, male	15 (58)	60 (96)	<0.001	26 (93)	55 (82)	0.177
Diabetes	7 (27)	17 (25)	0.819	9 (32)	15 (22)	0.318
Prior PCI	11 (42)	18 (26)	0.126	8 (29)	21 (31)	0.789
Indication						
Stable angina	10 (39)	31 (45)	0.571	15 (54)	26 (39)	0.185
ACS	16 (61)	38 (55)	0.571	13 (46)	41 (61)	0.185
Target vessel						
Left anterior descending artery (LAD)	16 (55)	65 (92)	<0.001	24 (80)	57 (81)	0.867
Left circumflex artery (LCX)	5 (17)	2 (3)	0.048	2 (7)	5 (7)	0.932
Left main artery (LM)	1 (3)	2 (3)	0.866	1 (3)	2 (3)	0.898
Right coronary artery (RCA)	7 (24)	2 (3)	0.080	3 (10)	6 (9)	0.819
Predilatation	19 (66)	55 (78)	0.235	21 (70)	53 (76)	0.551
High pressure post dilatation (NC balloon)	16 (55)	58 (82)	0.032	23 (77)	51 (73)	0.689
Mean post PCI Pd/Pa	0.91±0.03	0.91±0.06	0.943	0.91±0.03	0.91±0.05	0.841
Mean post PCI FFR, maximum hyperemia	0.77±0.06	0.79±0.05	0.026	0.80±0.04	0.78±0.05	0.135
No. of stents	1 (1-2)	2.0 (1-2)	0.061	2 (1-2)	1 (1-2)	0.726
Mean stent diameter, mm	2.75 (2.5-3)	3 (3-3.5)	<0.001	3 (2.9-3.3)	3 (2.7-3.5)	0.528
Total stent length, mm	15 (13-35)	30 (22-52)	0.012	28 (19-42)	28 (15-47)	0.673

	>20% underexpansion			Any lesion or lumen compromising hematoma		
	Present (n=47 patients, 58 vessels)	Not present (n=48 patients, 62 vessels)	p value	Present (n=33 patients, 36 vessels)	No Present (n=80 patients, 84 vessels)	p value
Age, years	64±13	65±13	0.374	67±12	64±13	0.299
Gender, male	39 (83)	42 (88)	0.534	38 (76)	43 (96)	0.007
Diabetes	14 (30)	10 (21)	0.315	15 (30)	9 (20)	0.263
Prior PCI	15 (32)	14 (29)	0.771	16 (32)	13 (29)	0.742
Indication						
Stable angina	22 (47)	19 (40)	0.477	22 (44)	19 (42)	0.861
ACS	25 (53)	29 (60)	0.477	28 (56)	26 (58)	0.861
Target vessel						
Left anterior descending artery (LAD)	38 (76)	43 (86)	0.207	39 (72)	42 (91)	0.021
Left circumflex artery (LCX)	5 (10)	2 (4)	0.255	6 (11)	1 (2)	0.116
Left main artery (LM)	2 (4)	1 (2)	0.565	1 (2)	2 (4)	0.479
Right coronary artery (RCA)	5 (10)	4 (8)	0.727	8 (15)	1 (2)	0.057
Predilatation	37 (74)	37 (74)	0.999	38 (70)	36 (78)	0.371
High pressure post dilatation (NC balloon)	38 (76)	36 (72)	0.649	36 (67)	38 (83)	0.074
Mean post PCI Pd/Pa	0.91±0.05	0.91±0.03	0.774	0.91±0.05	0.91±0.04	0.833
Mean post PCI FFR, maximum hyperemia	0.79±0.06	0.78±0.04	0.578	0.79±0.05	0.79±0.05	0.909
No. of stents	1 (1-2)	1 (1-2)	0.363	1 (1-2)	1 (1-2)	0.308
Mean stent diameter, mm	3 (2.8-3)	3 (2.8-3.5)	0.090	3 (2.6-3)	3 (3-3.5)	0.004
Total stent length, mm	35 (18-52)	26 (15-42)	0.118	26 (14-40)	30 (20-53)	0.083

Values are n (%) or mean±SD, PCI = Percutaneous Coronary Artery and CABG = Coronary Artery Bypass Grafting, NSTEMI = non ST elevated myocardial infarction, STEMI =ST elevated myocardial infarction. NC = non-compliant, Pd/Pa = the Pressure in the Distal coronary artery to the Pressure in the Aorta ratio, FFR = Fractional Flow Reserve. MLA = minimal lumen area

REFERENCES

1. Wolfrum M, Fahrni G, de Maria GL, Knapp G, Curzen N, Kharbanda RK, et al. Impact of impaired fractional flow reserve after coronary interventions on outcomes: a systematic review and meta-analysis. *BMC Cardiovascular Disorders*. 2016;16(1):177.
2. De Bruyne B, Fearon Wf Fau - Pijls NHJ, Pijls Nh Fau - Barbato E, Barbato E Fau - Tonino P, Tonino P Fau - Piroth Z, Piroth Z Fau - Jagic N, et al. Fractional flow reserve-guided PCI for stable coronary artery disease. *N Engl J Med*. 2014(1533-4406 (Electronic)).
3. van Zandvoort LJC, Masdjedi K, Witberg K, Ligthart JMR, Tovar Forero MN, Diletti R, et al. Explanation of Postprocedural Fractional Flow Reserve Below 0.85. *Circ Cardiovasc Interv*. 2019;12(2):e007030.
4. van Bommel RJ, Masdjedi K, Diletti R, Lemmert ME, van Zandvoort L, Wilschut J, et al. Routine Fractional Flow Reserve Measurement After Percutaneous Coronary Intervention. *Circ Cardiovasc Interv*. 2019;12(5):e007428.
5. Thygesen K, Alpert JS, Jaffe AS, Chaitman BR, Bax JJ, Morrow DA, et al. Fourth universal definition of myocardial infarction (2018). *European Heart Journal*. 2018:ehy462-ehy.

Chapter 12



FFR guided PCI optimization directed by high-definition IVUS versus standard of care: Rationale and study design of the prospective randomized FFR-REACT trial

van Zandvoort LJC, Masdjedi K, Tovar Forero MN, Lenzen MJ, Ligthart JMR, Diletti R, Lemmert ME, Wilschut J, De Jaegere PPT, Zijlstra F, van Mieghem NMDA, Daemen J

Erasmus University Medical Center, Thoraxcenter, Department of cardiology, Rotterdam, the Netherlands

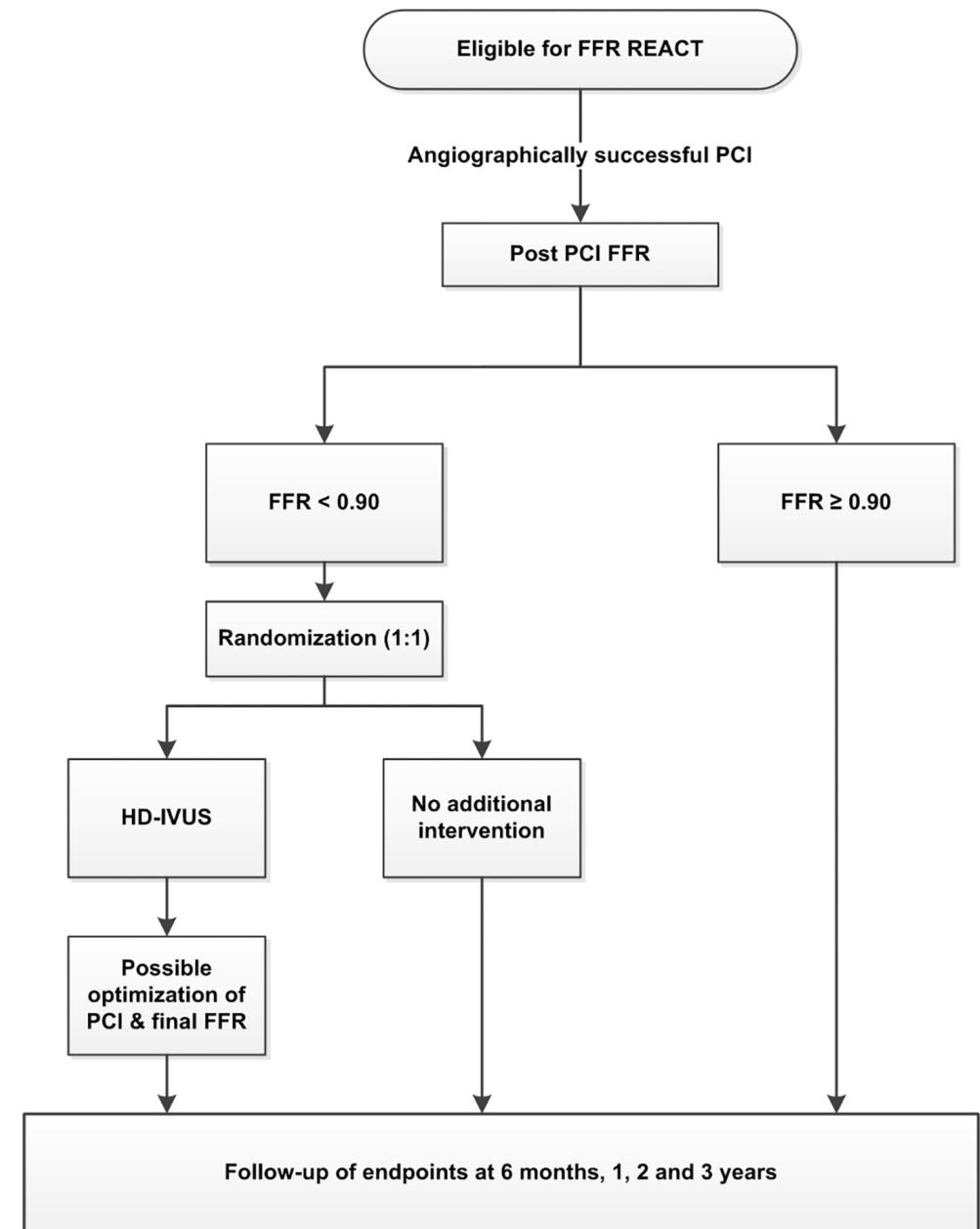
Am Heart J. 2019;213:66-72.

ABSTRACT

Background: Post percutaneous coronary intervention (PCI) fractional flow reserve (FFR) is a significant predictor of major adverse cardiac events (MACE). The rationale for low post procedural FFR values often remains elusive based on angiographic findings alone, warranting further assessment using an FFR pullback or additional intravascular imaging. It is currently unknown if additional interventions intended to improve the PCI, decrease MACE rates.

Study design: The FFR REACT trial is a prospective, single-center randomized controlled trial in which 290 patients with a post PCI FFR <0.90 will be randomized (1:1) to either standard of care (no additional intervention) or IVUS-directed optimization of the FFR (treatment arm). Eligible patients are those treated with angiographically successful PCI for (un)stable angina or non-ST elevation myocardial infarction (MI). Assuming 45% of patients will have a post PCI FFR <0.90, approximately 640 patients undergoing PCI will need to be enrolled. Patients with a post PCI FFR ≥0.90 will be enrolled in a prospective registry. The primary end point is defined as a composite of cardiac death, target vessel MI and clinically driven target vessel revascularisation (target vessel failure) at 1 year. Secondary end points will consist of individual components of the primary end point, procedural success, stent thrombosis and correlations on clinical outcome, changes in post PCI Pd/Pa and FFR and IVUS derived dimensions. All patients will be followed for 3 years.

Conclusion: The FFR-REACT trial is designed to explore the potential benefit of HD-IVUS-guided PCI optimization in patients with a post PCI FFR <0.90 (Dutch trial register: NTR6711).



Graphical abstract. Study flowchart for the FFR REACT trial

BACKGROUND

Accurate angiographic assessment of the severity and hemodynamic importance of coronary artery stenosis can be challenging and proved to be frequently unreliable^{1, 2}. Previous studies demonstrated that routine pre-procedural fractional flow reserve (FFR) in patients with multivessel coronary artery disease undergoing percutaneous coronary intervention (PCI) with drug-eluting stents significantly reduces the rate of the composite end point of death, nonfatal myocardial infarction (MI), and repeat revascularization at 1 year as compared to angiographic guided PCI³. More recently, FFR after stenting proved to be a strong and independent predictor of major adverse cardiac events (MACE) at 1 year⁴. A contemporary meta-analysis on the clinical impact of post PCI FFR values showed that an FFR <0.90 is associated with an increased risk of target vessel revascularization (TVR)⁵.

A number of factors might cause a post-PCI pressure drop over a treated segment including residual disease in the proximal or distal segment, a geographically misplaced stent, stent underexpansion, malapposition, plaque protrusion, edge dissection and plaque shift^{6, 7}. While these findings are not always readily apparent on coronary angiography alone, high definition (HD) intravascular ultrasound (IVUS) demonstrated to be a powerful tool to detect potential causes for low FFR post stenting. More specifically, these issues proved to be more frequently present in patients with low as compared to high post PCI FFR⁷. The latter adds to the substantial body of evidence on the benefit of IVUS-guided PCI as compared to angiography-guided PCI in improving long-term outcomes^{8, 9}.

While post PCI FFR is at present only rarely performed in routine clinical practice, an FFR after stenting <0.90 proved to be present in approximately 45% of the patients¹⁰. Additionally, IVUS was able to detect problems of intraluminal obstruction in up to 84% of those cases⁷. It is currently unknown if additional interventions with the intent to optimize post procedure FFR improve patient outcome.

The rationale and design of the FFR REACT trial was based on a simple and fast way of measuring post PCI FFR using a small microcatheter over the previously used coronary guidewire. Although a substantial body of evidence exists towards a pressure wire based post PCI FFR of 0.90 to predict MACE, at the moment no clear cut-off for post PCI FFR value as measured with a microcatheter to predict events has been established^{4, 5}. The potential findings and clinical implications of this study might open the door to a more frequent use of post PCI physiological assessment with the intention to further reduce the risk of future MACE with the help of IVUS.

Study aims

To assess if FFR guided PCI optimization directed by HD-IVUS in patients with an increased risk for MACE (post-PCI FFR below 0.90) will improve clinical outcome and reduce target vessel failure, a composite of cardiac death, target-vessel myocardial infarction and clinically driven TVR at 1 year.

STUDY DESIGN AND METHODS

The FFR REACT trial is a prospective, investigator initiated single-center randomized controlled trial in which 290 patients with a post PCI FFR <0.90 will

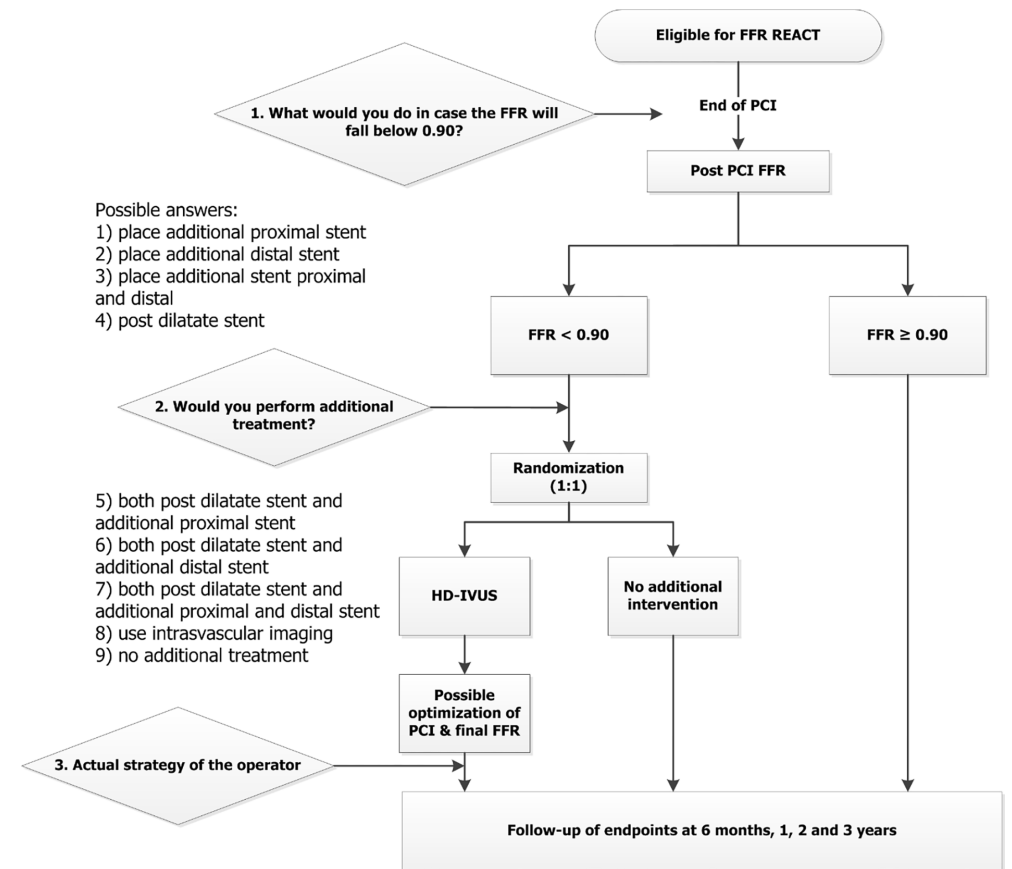


Figure 1. Study flow chart including the operator strategy questionnaire

The first two rhombuses contain the operator questions. The third rhombus is not asked but filled in according to the additional intervention. Nine possible answers are provided. FFR is fractional flow reserve, HD-IVUS is high definition intravascular ultrasound and PCI is percutaneous coronary intervention.

The study protocol was approved by our local ethical committee on the 26th of October 2017 (MEC-2017-489). Financial support is provided by ACIST Medical Systems, Inc.. The Erasmus Medical Center is totally independent from ACIST Medical Systems, Inc. regarding the conduct of the study and the medical treatment of patients and study subjects. The authors are solely responsible for the design and conduct of this study, all study analyses, the drafting and editing of the paper and its final contents. The study is in accordance with Good Clinical Practices (GCP), ISO14155 and with the Declaration of Helsinki (64th WMA General Assembly, Fortaleza, Brazil, October 2013). The study is registered at the Dutch trial register: NTR6711.

Study population

With the assumption that post PCI FFR will be <0.90 in 45% of the patients, an estimated number of 640 patients will be enrolled in order to be able to randomize 290 patients. Detailed in- and exclusion criteria are depicted in Table 1.

Table 1. In- and exclusion criteria

<p>Inclusion criteria</p> <ul style="list-style-type: none"> • Age ≥18 • Stable- or unstable angina or Non-ST segment elevation myocardial infarction • Target lesion stenosis ≥ 50% by visual estimation or QCA successfully treated by PCI and stenting • Written informed consent • The patient agrees to the follow-up <p>Exclusion criteria:</p> <ul style="list-style-type: none"> • Patients with ST-elevation myocardial infarction within the last 72 hours. • Target vessel distal reference diameter <2.25mm • Cardiogenic shock or severe hemodynamic instability • Unsuccessful stenting • PCI without stenting • Inability to perform post procedure FFR • The patient has other medical illnesses (i.e., cancer) that may cause the patient to be non-compliant with the protocol, confound the data interpretation or are associated with limited life expectancy (i.e., less than one year)

MI is myocardial infarction, FFR is fractional flow reserve, QCA is quantitative coronary angiography, PCI is percutaneous coronary intervention and IVUS is intravascular ultrasound.

Each patient must sign and date the approved informed consent form after the study has been thoroughly explained.

Study endpoints

The primary endpoint will be assessed at 1-year follow-up and is defined as target vessel failure, a composite of cardiac death, target vessel Q-wave or non-Q wave MI and clinically driven TVR.

Secondary endpoints consist of the individual components of the primary endpoint at 6 months, 1, 2 and 3 years, along with other clinical endpoints: all-cause death, any coronary revascularization, non-fatal MI, stent thrombosis (according the ARC criteria ¹¹), stroke, periprocedural complications and acute kidney injury. Procedural characteristics such as contrast medium usage, nr of stents, total stent length and procedural time will be compared between groups. Additionally, correlations between changes in post procedural FFR and Pd/Pa and luminal dimensions on IVUS due to potential optimization will be assessed. Table 2 depicts both primary and secondary endpoints. Finally, operator PCI strategy will be assessed at multiple time points.

Table 2. Primary and secondary endpoints of the FFR-REACT trial

<p>Primary endpoints</p> <ul style="list-style-type: none"> • Target vessel failure* <p>Secondary endpoints</p> <p><u>In hospital</u></p> <ul style="list-style-type: none"> • Procedural characteristics e.g. contrast medium usage, nr of stents, total stent length and procedural time • Major access site bleeding • Periprocedural MI • Acute kidney injury • Periprocedural complications • Change in post-procedural FFR after optimization therapy • Change in post-procedural Pd/Pa and FFR after optimization therapy • Correlation of the IVUS parameters and proximal VS stent VS distal FFR drop in categories of 0.05. • Correlation of FFR segmental drop and minimum luminal area on IVUS and 3D QCA • Correlation of Pd/Pa and FFR, both dependent and independent of IVUS findings • Operators PCI strategy change dependent on the information received from either FFR or IVUS <p><u>6 months and longer follow-up</u></p> <ul style="list-style-type: none"> • The individual components of the primary endpoint (cardiac death, target vessel MI, target vessel revascularization) • All-cause mortality • Cardiovascular mortality • Rehospitalisation for heart failure • Target lesion revascularization • Any coronary revascularization • Non-fatal myocardial infarction • Stent thrombosis • Periprocedural MI • Stroke • Kidney injury • Correlation of Pd/Pa, FFR and the primary endpoints components
--

* A composite of cardiac death, target-vessel myocardial infarction and clinically driven TVR at 1 year. QCA is quantitative coronary angiography, FFR is fractional flow reserve, PCI is percutaneous coronary intervention.

Blinding and randomization

Patient randomization will be initiated through a web-based application (ALEA, Formvision, Utrecht, The Netherlands). In order to prevent a disturbed allocation between treatment arms, a block randomization will be used, varying between four and six in size. Subjects will be blinded to the post procedural FFR and subsequent treatment allocation. In order to monitor the level of blinding, the perceived treatment allocation will be inquired at the 1 year clinical follow-up visit. Furthermore, the procedure report will not contain any details about post procedural FFR and subsequent treatment arm allocation. More specifically, no information will be provided on the measured vessel, post PCI FFR value and potential randomization allocation in the procedure report or discharge letter. Event adjudication at the set time points of 6 months, 1, 2 and 3 years will be performed by an independent critical event committee, not aware of the patients specific FFR values and/or randomization allocation. Patients will be unblinded at the last follow-up moment (3 years).

Investigational products

Post PCI FFR will be assessed using the Navvus® monorail microcatheter (ACIST Medical Systems, Inc., Eden Prairie, Minnesota) advanced over the previously used coronary guidewire. This monorail microcatheter precludes the need to advance a separate pressure wire along the treatment segment which will simplify and speed-up post PCI FFR measurements ¹².

Additional imaging in the intervention group will be performed using the multi frequency (40-60 MHz) Kodama® HD-IVUS catheter (ACIST Medical Systems, Inc., Eden Prairie, Minnesota). Both devices are CE marked and are currently used in regular clinical practice.

STUDY PROCEDURES

Routine care

Procedures will be performed according to standard clinical practice: angiography guided PCI and stenting with the use of periprocedural imaging, (either IVUS or OCT) and/or pre-procedural functional assessment (either iFR or FFR) left at the discretion of the operator ¹³. Angiographic success was defined as residual stenosis <30% by visual analysis in the presence of TIMI 3 grade flow. Procedural success will be identified as angiographic success in the absence of periprocedural MI. Dual antiplatelet therapy (including aspirin and a P2Y12 inhibitor) will be prescribed for at least 6 months to all patients consisting of clopidogrel in case of

stable angina, or prasugrel/ticagrelor for at least 12 months in case of an acute coronary syndrome ¹⁴.

Study measurements and interventions, if applicable, will only be performed after confirmation of angiographic success of the PCI and after administration of intracoronary nitrates.

Post procedural indices: Pd/Pa and FFR

Pd/Pa is defined as a ratio, where Pd is the distal coronary pressure derived from the tip of the Navvus® catheter and Pa stands for proximal coronary pressure (measured at the tip of the guiding system). The two values are recorded simultaneously during resting conditions. FFR is defined as mean distal coronary artery pressure divided by mean aortic pressure during maximum hyperemia achieved by continuous intravenous infusion of adenosine at a rate of 140 µg/kg/min through an antecubital vein.

Both indices will be measured approximately 20 mm from the most distal stent edge. A pullback will be performed to obtain pressure gradients on the distal and proximal stent edges. Drift will be checked at the end of each pullback. Measurements with a drift value above 0.02 will be repeated a second time ¹⁵. All vessels with a drift value above 0.05 during the second attempt will be excluded from the study. All pressure tracing will be stored in a dedicated database for off-line analyses. All tracings will be analyzed for ventricularization, dampening and drift by our academic corelab.

IVUS (Intervention Group)

IVUS-directed FFR optimization will be guided by an automated pullback with a 40-60 MHz HD-IVUS catheter at a speed of 2.5 mm/sec (24 frames/mm) starting approximately 20 mm distal from the most distal stent edge. Images will be analyzed online in order to identify potential reasons for the low post-procedural FFR. Treatment of potential anomalies will be performed through a guidance protocol initiated in order to standardize potential further treatment (Table 3) and will be based on the patient's characteristics, angiographic anatomy, distal and interval Pd/Pa and FFR and luminal IVUS dimensions. Final resting Pd/Pa and FFR will be measured at the end of the procedure if additional treatment was performed along with an IVUS pullback assessing the final treatment result.

All IVUS pullbacks will be analyzed offline using QCU-CMS (Leiden University MC, LKEB, Division of Image Processing, version 4.69). Offline analysis will be performed by three independent IVUS experts within our academic corelab. All

IVUS pullback will be divided in 4 segments, a distal segment, in stent, in segment (stent \pm 5mm) and a proximal segment. The luminal dimensions for all segments will be separately analyzed, including, but not limited to, minimal lumen area, minimal lumen diameter, minimal stent area, mean lumen diameter, mean lumen diameter and maximum plaque burden. Additionally, malapposition, stent edge dissections, underexpansion and residual lesion will be scored according to Table 3.

Table 3. Stepwise protocol after high definition intravascular ultrasound (IVUS)

Malapposition	When malapposition is present in more than 1 frame post dilatation with a balloon ≥ 0.25 mm larger than the stent balloon is recommended. Malapposition due to a non-symmetrical vessel should not be additionally dilated.
Edge dissection	Additional stenting is recommended in case a distal edge dissection of more than 90 degrees is encountered. In case of a proximal edge dissection additional stenting is left at the discretion of the operator.
Underexpansion	Underexpansion can be measured with the help of a simple calculating tool, based on the MUSIC criteria ¹⁶ . This will be done ad hoc. When the criteria of underexpansion are met, additional dilatation should be performed preferably by using a non-compliant balloon with a diameter ≥ 0.25 mm larger than the largest balloon used.
Residual lesion ¹⁷⁻²¹	<ul style="list-style-type: none"> • Measure reference vessel diameter (RVD) distally of the potential residual lesion. A residual lesion is present in case: <ul style="list-style-type: none"> • RVD is 2.5 – 3.0 mm and lesion MLA is < 2.5 mm² • RVD is 3.0 - 3.5 mm and lesion MLA is < 3.0 mm² • RVD is > 3.5 mm and lesion MLA is < 3.5 mm² • In case left main lesion: if MLA is < 6.0mm². Stent size for additional treatment should be based on lesion length and RVD.

To ensure a homogenous treatment approach post IVUS imaging of the treated segment the following guidelines have been designed.

Conservative treatment (Control Group)

No further treatment or IVUS assessment will be performed. Procedures will be concluded based on the confirmation of angiographic success according to routine clinical practice.

Operator strategy

Operator strategy will be assessed at 3 time points during the procedure based on the available information at that stage: following angiography, following first post-PCI FFR in patients with a FFR < 0.90 , and following HD-IVUS in subjects

who are randomized to the IVUS-directed FFR optimization. In the first question, the operator will be asked what he/she would do in the hypothetical case the FFR would fall below 0.90. Possible answers are: 1) place additional proximal stent 2) place additional distal stent 3) place additional stent proximal and distal 4) post dilatate stent 5) both post dilatate stent and additional proximal stent 6) both post dilatate stent and additional distal stent 7) both post dilatate stent and additional proximal and distal stent 8) perform intravascular imaging 9) no additional treatment. A similar question will be asked directly after the first FFR measurement in which the answer may be guided by the information provided by the initial post PCI Pd/Pa and FFR (pullback) analyses. The latter two answers will be compared to the actual treatment strategy based on the IVUS pullback (Figure 1). The operator strategy questions were added with the intent to further assess how the use of post PCI FFR and IVUS impact treatment strategies intended to improve PCI results.

Follow-up at 6 months, 1, 2 and 3 years follow-up

All patients will be contacted by letter and/or telephone contact at 6, 24 and 36 months. Before patient contact, survival status will be ascertained by an automated civil registry check. A clinical follow-up with ECG will be scheduled at 12 months. All possible clinical outcomes, including all-cause mortality, cardiac mortality, myocardial infarction (MI), target lesion revascularization (TLR) and TVR, any revascularization, stent thrombosis, stroke and bleeding. Additional information will be retrieved in case of event triggers from local electronic medical records, referring physicians and general practitioner.

Data management and monitoring

Registry of specific endpoints and other details will be managed through OpenClinica, an electronic, online, case report form (CRF) application. Follow-up contacts will be performed by physicians or study nurses not involved in the index procedure and blinded to the final FFR and assigned treatment arm. All data will be anonymized and handled confidentially. The key to the de-anonymization will be safeguarded by the principal investigator.

Event adjudication will be performed by an independent Clinical Events Committee (CEC) unaware of the post PCI FFR and assigned treatment arm. Specific information in the PCI report on the treatment strategy will be masked when submitting documents to the CEC.

Monitoring will verify that the rights and well-being of the patients are protected, the trial is conducted according to GCP and ISO14155, and that the protocol is

followed. The trial specific monitoring program is based on the guidelines for on-site monitoring in relationship to the estimated risk of the study (Erasmus MC version 15 November 2012). According to these guidelines a negligible risk-monitoring program was set up for the trial.

STATISTICAL CONSIDERATIONS

Statistical analysis of endpoints

Categorical variables will be expressed as percentages and counts. Differences in categorical variables between randomly allocated treatment groups will be evaluated by applying chi-square tests or Fisher's exact tests. Continuous variables will be described as mean \pm one standard deviation, or as median and interquartile range, accordingly. Shapiro-Wilk tests will be applied to evaluate normality of continuous variables. Differences in continuous variables between randomly allocated treatment groups will then be evaluated by applying Student's t-tests or Mann-Whitney tests. Parametric correlations will be assessed using the Pearson correlation coefficient while the Spearman's rank correlation coefficient is used if the correlation is non-parametric.

The operator strategy questionnaire will be evaluated using the McNemar's test.

Differences between the groups, both randomized and non-randomized, will be measured using the log-rank tests to evaluate differences in event-free survival. An univariate Cox proportional hazard regression will be used to quantify the relation between randomly allocated treatment arms and the incidence of clinical outcomes. In order to provide adjusted hazard ratios (HR), a multivariate Cox regression will be used, with adjustment for age, sex and (as far as allowed given the number of endpoint events) other confounders, possibly including stent size, previous coronary artery intervention, previous MI, multivessel disease, a history of CABG, dyslipidaemia, hypertension, smoking, diabetes mellitus and renal function. Competing risks are taken into account for the analysis. Both primary and secondary study parameters are depicted in Table 2.

All tests will be 2-tailed, and a p-value of <0.05 will be considered statistically significant. The secondary outcomes are hypothesis generating and therefore no adjustment for multiple testing will be made. We will report estimates of population parameters together with their 95% confidence interval.

Sample size calculation

A recent meta-analysis showed that the incidence of MACE (heterogenous definitions used) in patients with post PCI FFR <0.90 was 21.4% versus 5% in patients with post PCI FFR ≥ 0.90 ⁴. The average incidence of MACE in the latter study was 11%. The average incidence of MACE (comprised of cardiac death, any MI and TVR) at 1-year post PCI at the Erasmus MC is 10%. When these data are extrapolated, in the Erasmus MC patients with an FFR <0.90 will have an estimated MACE incidence of 19%. The MACE incidence of the patients who will be randomized to optimal care with IVUS is estimated at 7.5%: the average of the incidence at the EMC and the 5% that was found in the meta-analysis.

In summary, to determine the sample size we made the following assumptions/choices:

- Incidence of the study endpoint in those randomized to control/standard care: 19%
- Incidence of the study endpoint in those randomized to IVUS-directed stent placement: 7.5%
- type I error, two-sided: 0.05
- type II error: 0.2 (i.e. power 80%)
- Allocation ratio $N_2/N_1 = 1$

Then a sample size of 272 is required, 136 patients per treatment arm. The sample size should be enlarged by an additional 2-5% due to possible technical failures, lost to follow-up or unsuitable FFR or IVUS acquisition. Finally 290 patients will be randomized.

Based on results of the FFR-SEARCH registry, 45% of the patients will have a post-procedural FFR <0.90 ¹⁰. This implies that a total of approximately 640 patients need to be enrolled in order find 290 patients with a post PCI FFR <0.90 .

Potential issues of concern

The use of FFR and IVUS in daily clinical practice has been shown to be safe with a low risk of complications. In the FFR SEARCH study, focusing on the predictive value of post-procedural FFR in almost 1000 patients, no complications due to the microcatheter were observed, while in only 2 patients a severe response to the intravenous adenosine occurred¹⁰. In a study by van der Sijde et al. in which the risk of periprocedural complications due to the use of IVUS was assessed in 2476 procedures, 12 complications (0.5%) occurred²². All of these were self-limiting

after retrieval of the imaging catheter and no major adverse events due to the use of IVUS were found. Furthermore, limited evidence is available at the moment on the homogeneity of post PCI FFR values in patients presenting with stable angina as compared to patients with unstable angina or non-ST elevation MI. Additionally, pre PCI FFR assessment using the Navvus microcatheter has proven to significantly overestimated the stenosis severity as compared to pressure wire based FFR measurements^{23, 24}. However, this difference was mainly driven by a larger delta in vessels with a small minimal luminal area pre procedure. It is currently unknown if post PCI FFR assessment with the latter two methods will exemplify the same variance and direct extrapolation of the current study to pressure wire based post PCI FFR assessment and optimization is therefore not possible.

The sample size calculation presented the current study is based on a meta-analysis which included a heterogenous cohort of studies with several outdated registries⁴. The latter might result in an overestimation of the event rates and thus underpower the study design. Cumulative incidences are expected to diverge between the treatment and control group at longer follow-up if the luminal dimension and FFR can be increased, ensuring a hypothetical under-powered study at one year would be sufficiently powered at two or three years follow-up^{4, 5, 25, 26}.

Study status and timeline

The FFR REACT trial is actively enrolling patients since October 31st, 2017 and has reached the milestone of enrolling 50% of the target population October 2018. At its current pace the study is expected to complete enrolment Q4 2019.

SUMMARY

The FFR REACT study is an investigator initiated prospective, single-center randomized controlled trial conducted at the Erasmus Medical Center designed to assess if FFR guided PCI optimization directed by IVUS in patients with an increased risk for MACE (post-PCI FFR below 0.90) will decrease target vessel failure at 1 year. Inclusion started in October 2017 and enrolment is expected to be complete in Q4 2019.

Public disclosure and publication policy

Findings of the study will be submitted for publication in a peer-reviewed international cardiology journal. Publication of the data will remain in the hands of the principal investigator and steering committee. The Erasmus MC received an unrestricted institutional grant from ACIST Medical Systems, Inc..

REFERENCES

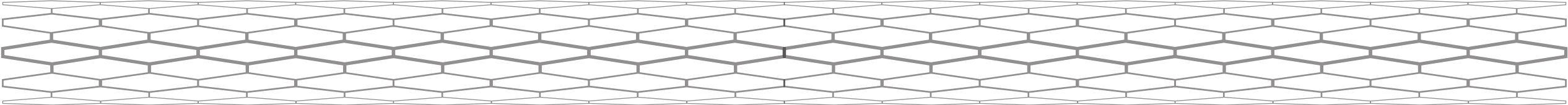
1. Cameron A, Kemp HG, Jr, Fisher LD, Gosselin A, Judkins MP, Kennedy JW, et al. Left main coronary artery stenosis: angiographic determination. *Circulation*. 1983;68(3):484-9.
2. Girasis C, Onuma Y, Schuurbiens JC, Morel MA, van Es GA, van Geuns RJ, et al. Validity and variability in visual assessment of stenosis severity in phantom bifurcation lesions: a survey in experts during the fifth meeting of the European Bifurcation Club. *Catheter Cardiovasc Interv*. 2012;79(3):361-8.
3. Tonino PA, De Bruyne B, Pijls NH, Siebert U, Ikeno F, van' t Veer M, et al. Fractional flow reserve versus angiography for guiding percutaneous coronary intervention. *N Engl J Med*. 2009;360(3):213-24.
4. Wolfrum M, Fahrni G, de Maria GL, Knapp G, Curzen N, Kharbanda RK, et al. Impact of impaired fractional flow reserve after coronary interventions on outcomes: a systematic review and meta-analysis. *BMC Cardiovascular Disorders*. 2016;16(1):177.
5. Rimac G, Fearon WF, De Bruyne B, Ikeno F, Matsuo H, Piroth Z, et al. Clinical value of post-percutaneous coronary intervention fractional flow reserve value: A systematic review and meta-analysis. *Am Heart J*. 2017;183:1-9.
6. Tonino PA, Johnson NP. Why Is Fractional Flow Reserve After Percutaneous Coronary Intervention Not Always 1.0? *JACC Cardiovasc Interv*. 2016;9(10):1032-5.
7. Zandvoort van LJC MK, Witberg K., Ligthart JMR., Tovar Forero M.N., Diletti R., Lemmert M., Wilschut J., Jaegere de P.T., Boersma E., Zijlstra F., Mieghem van N., Daemen J.,. Explanation of post procedural fractional flow reserve below 0.85: a comprehensive ultrasound analysis of the FFR Search registry. CRT meeting. 2018.
8. Ahn J-M, Kang S-J, Yoon S-H, Park HW, Kang SM, Lee J-Y, et al. Meta-Analysis of Outcomes After Intravascular Ultrasound-Guided Versus Angiography-Guided Drug-Eluting Stent Implantation in 26,503 Patients Enrolled in Three Randomized Trials and 14 Observational Studies. *The American Journal of Cardiology*. 2014;113(8):1338-47.
9. Zhang J, Gao X, Kan J, Ge Z, Han L, Lu S, et al. Intravascular Ultrasound-Guided Versus Angiography-Guided Implantation of Drug-Eluting Stent in All-Corers: The ULTIMATE trial. *J Am Coll Cardiol*. 2018.
10. Diletti R, van Bommel R, Masdjedi K, van Zandvoort L, Lemmert ME, Wilschut J, et al. Routine Fractional Flow Reserve Measurement after Percutaneous Coronary Intervention The FFR-SEARCH Study. EuroPCR presentation. 2017.
11. Cutlip DE, Windecker S, Mehran R, Boam A, Cohen DJ, van Es GA, et al. Clinical end points in coronary stent trials: a case for standardized definitions. *Circulation*. 2007;115(17):2344-51.
12. Diletti R, van Mieghem NMDA, Valgimigli M, Karanasos A, Everaert BR, Daemen J, et al. Rapid exchange ultra-thin microcatheter using fibre-optic sensing technology for measurement of intracoronary fractional flow reserve. *EuroIntervention*. 2015;11(4):428-32.
13. Authors/Task Force m, Windecker S, Kolh P, Alfonso F, Collet JP, Cremer J, et al. 2014 ESC/EACTS

- Guidelines on myocardial revascularization: The Task Force on Myocardial Revascularization of the European Society of Cardiology (ESC) and the European Association for Cardio-Thoracic Surgery (EACTS) Developed with the special contribution of the European Association of Percutaneous Cardiovascular Interventions (EAPCI). *Eur Heart J*. 2014.
14. Neumann F-J, Sousa-Uva M, Ahlsson A, Alfonso F, Banning AP, Benedetto U, et al. 2018 ESC/EACTS Guidelines on myocardial revascularization. *European Heart Journal*. 2018;ehy394-ehy.
 15. Cook Christopher M, Ahmad Y, Shun-Shin Matthew J, Nijjer S, Petraco R, Al-Lamee R, et al. Quantification of the Effect of Pressure Wire Drift on the Diagnostic Performance of Fractional Flow Reserve, Instantaneous Wave-Free Ratio, and Whole-Cycle Pd/Pa. *Circulation: Cardiovascular Interventions*. 2016;9(4):e002988.
 16. de Jaegere P, Mudra H, Figulla H, Almagor Y, Doucet S, Penn I, et al. Intravascular ultrasound-guided optimized stent deployment. Immediate and 6 months clinical and angiographic results from the Multicenter Ultrasound Stenting in Coronaries Study (MUSIC Study). *Eur Heart J*. 1998;19(8):1214-23.
 17. Waksman R, Legutko J, Singh J, Orlando Q, Marso S, Schloss T, et al. FIRST: Fractional Flow Reserve and Intravascular Ultrasound Relationship Study. *Journal of the American College of Cardiology*. 2013;61(9):917-23.
 18. Ben-Dor I, Torguson R, Deksissa T, Bui AB, Xue Z, Satler LF, et al. Intravascular ultrasound lumen area parameters for assessment of physiological ischemia by fractional flow reserve in intermediate coronary artery stenosis. *Cardiovasc Revasc Med*. 2012;13(3):177-82.
 19. Ben-Dor I, Torguson R, Gaglia MA, Jr., Gonzalez MA, Maluenda G, Bui AB, et al. Correlation between fractional flow reserve and intravascular ultrasound lumen area in intermediate coronary artery stenosis. *EuroIntervention*. 2011;7(2):225-33.
 20. Mallidi J, Atreya AR, Cook J, Garb J, Jeremias A, Klein LW, et al. Long-term outcomes following fractional flow reserve-guided treatment of angiographically ambiguous left main coronary artery disease: A meta-analysis of prospective cohort studies. *Catheter Cardiovasc Interv*. 2015;86(1):12-8.
 21. de la Torre Hernandez JM, Baz Alonso JA, Gomez Hospital JA, Alfonso Manterola F, Garcia Camarero T, Gimeno de Carlos F, et al. Clinical impact of intravascular ultrasound guidance in drug-eluting stent implantation for unprotected left main coronary disease: pooled analysis at the patient-level of 4 registries. *JACC Cardiovasc Interv*. 2014;7(3):244-54.
 22. van der Sijde JN, Karanasos A, van Ditzhuijzen NS, Okamura T, van Geuns RJ, Valgimigli M, et al. Safety of optical coherence tomography in daily practice: a comparison with intravascular ultrasound. *Eur Heart J Cardiovasc Imaging*. 2016.
 23. Pouillot C, Fournier S, Glasenapp J, Rambaud G, Bougrini K, Vi Fane R, et al. Pressure wire versus microcatheter for FFR measurement: a head-to-head comparison. *EuroIntervention*. 2018;13(15):e1850-e6.
 24. Wijntjens GW, van de Hoef TP, Kraak RP, Beijk MA, Sjauw KD, Vis MM, et al. The IMPACT Study (Influence of Sensor-Equipped Microcatheters on Coronary Hemodynamics and the Accuracy of Physiological Indices of Functional Stenosis Severity). *Circ Cardiovasc Interv*. 2016;9(12).
 25. Elgendy IY, Mahmoud AN, Elgendy AY, Bavry AA. Outcomes With Intravascular Ultrasound-Guided Stent Implantation: A Meta-Analysis of Randomized Trials in the Era of Drug-Eluting Stents. *Circ Cardiovasc Interv*. 2016;9(4):e003700.
 26. Witzembichler B, Maehara A, Weisz G, Neumann F-J, Rinaldi MJ, Metzger DC, et al. Relationship Between Intravascular Ultrasound Guidance and Clinical Outcomes After Drug-Eluting Stents The Assessment of Dual Antiplatelet Therapy With Drug-Eluting Stents (ADAPT-DES) Study. *Circulation*. 2014;129(4):463-70.

PART IV

INNOVATIONS
IN CORONARY
PHYSIOLOGY

Chapter 13



Validation of 3-Dimensional Quantitative Coronary Angiography based software to calculate vessel-Fractional Flow Reserve: Fast Assessment of STenosis severity (FAST)-study

Masdjedi K¹, van Zandvoort LJC¹, Balbi MM¹, Gijzen FJH¹, Ligthart JMR¹, Rutten MCM², Lemmert¹, Wilschut J¹ Diletti R¹ Zijlstra F¹ van Mieghem NMDA¹ Daemen J¹

¹*Erasmus University Medical Center, Thoraxcenter, Department of cardiology, Rotterdam, the Netherlands*

²*Department of Cardiovascular Biomechanics, Technical University of Eindhoven*

EuroIntervention. 2019;EIJ-D-19-00466.

ABSTRACT

Background: Fractional flow reserve (FFR) assessment requires the use of a costly pressure wire combined with the administration of a hyperemic agent, which may contribute to its low adoption rate in clinical practice. The aim of the study was to validate novel software to calculate vessel FFR (vFFR) based on three dimensional quantitative coronary angiography (3D-QCA) and to assess inter-observer variability in patients who underwent routine pre procedural FFR assessment for intermediate coronary artery stenosis.

Methods and results: Technical validation of the software (CAAS Workstation 8.0) was performed in an in vitro experimental model. Clinical validation was performed in an observational single-center cohort study. A total of 100 patients presenting with stable angina or non-ST segment elevation acute coronary syndrome and an indication to perform FFR between Jan 2016 and Oct 2016 were included. vFFR was calculated based on the aortic root pressure along with two orthogonal angiographic projections and validated against pressure wire-derived FFR.

Mean age was 64 ± 11 years and 67% were males. Mean FFR and vFFR were 0.82 ± 0.08 and 0.84 ± 0.07 respectively. A good linear correlation was found between FFR and vFFR ($r=0.89$; $p<0.001$). Assessment of vFFR had a low inter-observer variability ($r=0.95$; $p<0.001$). The diagnostic accuracy of vFFR in identifying lesions with an $FFR \leq 0.80$ was higher as compared with 3D-QCA: 93% (95% CI: 88%-97%) vs. 34% (95% CI: 23%-45%) respectively.

Conclusion: The 3D-QCA derived vFFR has a high linear correlation to invasively measured FFR, a high diagnostic accuracy to detect $FFR \leq 0.80$ and a low inter-observer variability.

INTRODUCTION

Invasive coronary angiography has served as the cornerstone for the diagnosis of patients with known or suspected coronary artery disease (CAD). Unfortunately, the technique is limited in its ability to assess the hemodynamic impact of intermediate coronary artery stenosis resulting in under- or overestimation of disease severity¹. In order to overcome this limitation, Fractional Flow Reserve (FFR) has emerged as the mainstay of functional hemodynamic assessment of coronary artery lesions and is presently regarded as the gold standard for identifying stenoses that cause myocardial ischemia²⁻⁵. Despite indisputable evidence supporting the benefit of FFR to guide clinical decision making, adoption into daily practice has been limited. FFR assessment requires the use of a (costly) dedicated guidewire or microcatheter along with the administration of a hyperemic agent associated with temporary patient discomfort⁶. Although instantaneous wave-free ratio (iFR) has emerged as an adenosine-free faster and easier method to achieve physiologic assessment, the need for a costly pressure wire remains a fact^{7,8}.

Several studies assessed the potential value of FFR derived from three-dimensional quantitative coronary angiography (3D-QCA) and blood flow simulation⁹⁻¹¹. The recently published FAVOR II China study showed promising results for online examination of quantitative flow ratio (QFR) in the diagnostic catheterization laboratory¹². The contrast flow mode, which uses a frame count method to derive contrast flow velocity from coronary angiography, was used for QFR computation. The Fast Assessment of STenosis severity (FAST) study aimed to validate a new 3D-QCA-based software to calculate vessel-FFR (vFFR) using phantom models. In addition we correlated this index with pressure wire derived FFR in a consecutive series of patients and studied inter-observer variability.

METHODS

In vitro experimental model

An in vitro experimental model was developed for technical validation of the calculation method performed by the CAAS workstation in phantoms. The experimental set-up, as described earlier by Geven et al. consists of a chamber, a water-driven systemic and coronary circulation¹³. The chamber mimics the left ventricle and artificial valves mimic the mitral- and aortic valve of the heart (Figure 1).

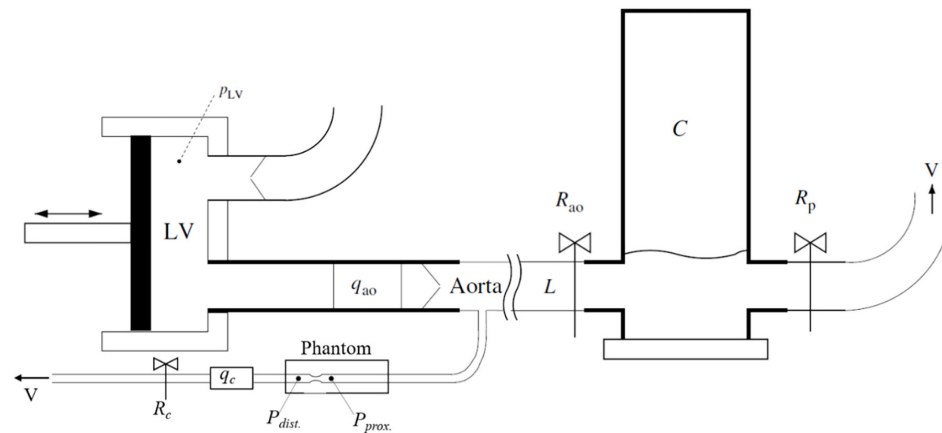


Figure 1. Schematic of the in vitro experimental model

The LV-chamber pumps water through the aorta flow probe (q_{ao}) and the artificial valve into the aorta and from the aorta into the systemic Windkessel components (R_{ao} , L , C and R_p). A tube, representing the coronary artery, branches off the aorta, passes the phantom, the coronary flow probe (q_c) towards a venous outlet (V). The pressure sensors are positioned proximal ($P_{prox.}$) and distal ($P_{dist.}$) to the lesion in the phantom, the flow (q_c) is measured at the outflow tract of the phantom. The flow through the phantom is controlled by the resistance (R_c) in the outflow tract.

The piston is powered by a computer-controlled linear motor (ETB32, Parker) creating pulsatile flow at 75 beats per minute. For non-pulsatile flow, a constant flow pump (2035, Verder) fills a higher placed reservoir, with overflow function, the output of the reservoir connects to the mitral valve. A polyurethane tube models the aorta, and input impedance characterizes the systemic circulation behaviour. Flow through the aorta was set at approximately 5 l/min and measured using an ultrasound flow probe (Transonic 28PAU, with TS 410 flowmeter). The distal systemic compliance is modelled using a Windkessel, resulting in physiological pressure conditions.

Coronary circulation

The in vitro coronary circulation comprised a tube (8mm diameter) connected to the ostium of the aorta with a phantom attached at the end of this tube. The phantom consisted of an 8mm tube with a 75% sinusoidal stenosis (Model: QA-STV, Simutec). A resistance was placed at the outflow tract of the phantom to control the amount of flow through the phantom. The diameter of the tubes in the phantom are relatively large compared to human coronary artery dimensions.¹⁴ To simulate significant pressure drop along the lesion, the average flow through the phantom was set higher as compared to physiological coronary flow, and was set to an average of 100, 200, 300 and 400 ml/min for both pulsatile flow and constant flow¹⁵. The proximal and distal pressures to the lesion were measured simultaneously with two pressure wires (Certus12006, Radi). The flow rate through the phantom was registered by an electromagnetic flow probe. The pressure drop over the lesion was obtained by calculating the difference between the measured pressures distal and proximal to the lesion. Measurement of pressures was averaged over four cycles during pulsatile flow, and the same period was used for averaging during constant flow.

Pressure drop computation methods

The pressure drop over the lesion in the phantom was computed using two different approaches: 1) Computational Fluid Dynamic (CFD) being considered a reference standard in blood flow simulations¹⁶ and 2) by using CAAS Workstation 8.0 (Pie Medical Imaging, Maastricht, the Netherlands).

A 3D surface mesh of the phantom, corresponding to the geometry between the locations of the two pressure wires, was used for calculating the pressure drop by both approaches. Within both approaches viscosity differences of water against blood were taken into consideration.

A single flow value was applied to both computational approaches, to eliminate time-variation in flow profile and pressure drop. Assuming that the average pulsatile flow has a linear relation with the average pressure drop, the application of a single flow value for the computation approaches was justified. The pressure drop obtained by both pulsatile and constant flow for the different flow values were compared to the computed pressure drop values of both the CFD approach and CAAS Workstation vFFR (Figure 2).

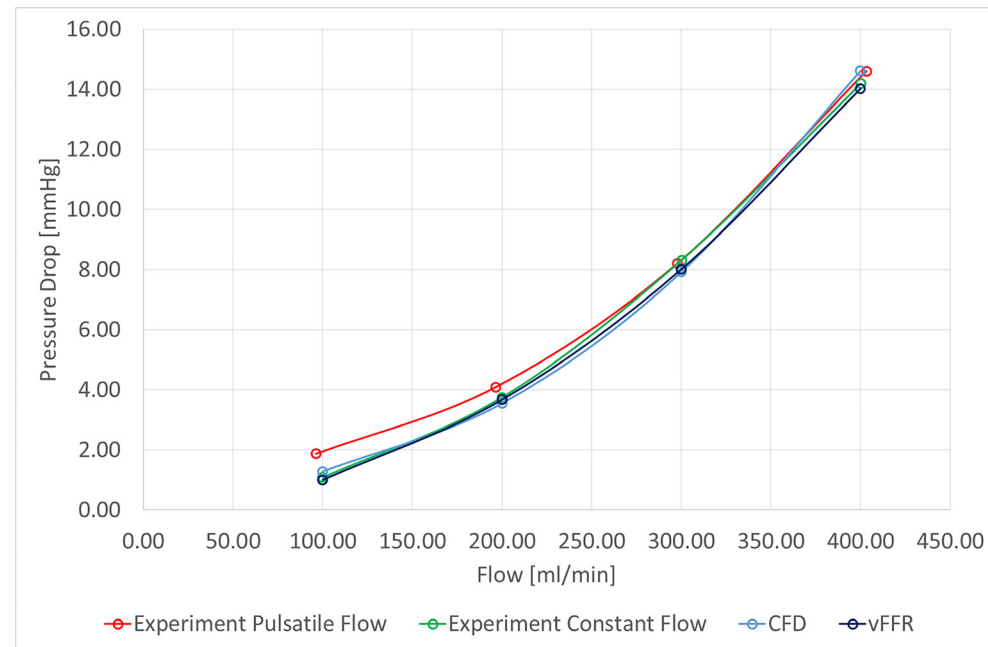


Figure 2. Pressure drop resulting from pressure measurements during pulsatile flow (red line) and constant flow (green line) as well as the computed pressure drop by the Computational Fluid Dynamic (CFD) (light blue) and CAAS Workstation vFFR (dark blue)

Clinical validation study

Study design and patient population

The FAST (Fast Assessment of STenosis severity) study is an observational, retrospective, single-center cohort study in which offline computation of vFFR as compared with conventional invasive FFR measurement using a pressure wire based FFR system (St. Jude Aeris, Abbott Vasuclar, St Paul, MA, USA) was studied. From January 2016 through October 2016, patients ≥ 18 years of age presenting with stable coronary artery disease or non-ST elevation acute coronary syndrome who underwent pre-PCI FFR assessment were eligible. Angiographic inclusion criteria were: at least one intermediate stenosis in one of the epicardial coronary arteries (diameter stenosis of 30-70% by visual assessment). Exclusion criteria were FFR measurements with damped pressure curves, patients with ST-elevation myocardial infarction (STEMI) or lesions containing thrombus, cardiogenic shock or severe hemodynamic instability and adenosine intolerance.

Procedure protocol

All procedures were performed according to standard local clinical practice. Angiographic lesion severity was assessed by two standard monoplane angiographic projections (at least 30 degrees apart, preferably orthogonal) after a bolus of 200mcg nitroglycine. Subsequently, FFR measurement were performed under maximum hyperemia achieved by continuous intravenous infusion of adenosine at a rate of 140 $\mu\text{g}/\text{kg}/\text{min}$ through an antecubital vein for at least 2 minutes. FFR was defined as mean distal coronary artery pressure divided by mean aortic pressure during maximum hyperemic condition. An additional projection was recorded with the pressure wire in situ to capture the position of the pressure wire. Angiograms and pressure waveforms were stored as DICOM image format for offline analyses. Aortic root pressure was constantly recorded. The last blood pressure measurement taken before the start of the FFR measurement was used as input in the CAAS/vFFR software.

3D-coronary reconstruction and computation of vFFR

Computation of vFFR was performed offline and assessed blinded by 2 different independent observers to assess inter-observer variability (KM, MB). A total of 3 two-dimensional images, were exported to the CAAS workstation 8.0 (Pie Medical Imaging, Maastricht, the Netherlands): Two views with at least 30 degrees differences in rotation/angulation to create a 3D reconstruction of the coronary arteries and one view to ascertain the position of the FFR pressure wire. Temporal alignment of the two orthogonal view phases in the cardiac cycle was performed automatically by ECG triggering. Contour detecting was performed semi-automatically, delineating the vessel contour from the ostium to the position at which the pressure wire sensor was positioned (3cm from the tip). The percent diameter stenosis, minimal lumen diameter, reference lumen diameter, minimal lumen area and lesion length were measured from the same 3D model as on which the vFFR was determined. The lesion segment was defined as proximal, mid, or distal. vFFR was calculated automatically incorporating the invasively measured aortic root pressure and automatically generated 3D QCA values and vFFR along entire vessel instantaneously (Figure 3).

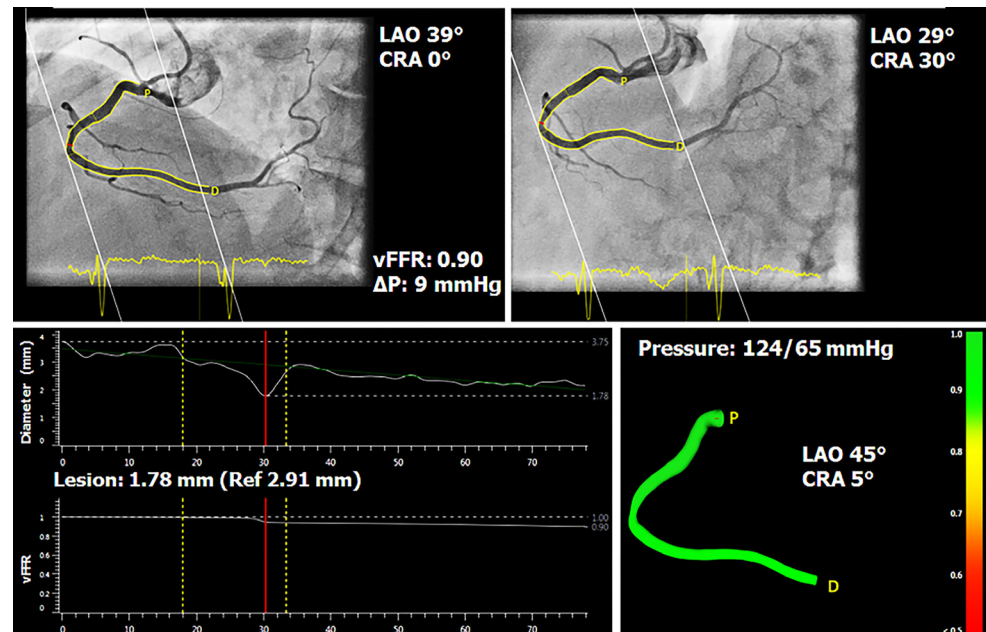


Figure 3. Three-dimensional reconstruction of coronary artery and computation of vessel-FFR, using 2 angiographic projections with at least 30 degrees apart and invasively measured aortic root pressure

Statistical analysis

Continuous variables are presented as mean \pm standard deviation. All continuous variables were normally distributed. Categorical variables are expressed as counts and percentages. All statistical tests are 2-tailed. Pearson's correlation coefficient (r) was used to assess the relationship between FFR and vFFR and to assess inter-observer variability. Agreement between the indices and the inter-observer reliability were assessed by Bland-Altman plots with corresponding 95% limits of agreement. Receiver-operating characteristic (ROC) area under the curve (AUC) analysis was used to estimate the diagnostic performance of vFFR as compared to the wire-based FFR threshold of ≤ 0.80 . Statistical analysis was carried out using the SPSS statistical package version 24 (IBM, Armonk, North Castle, New York, USA).

RESULTS

Pre-clinical data

Pressure measurements from the pulsatile flow corresponded well with the pressure drops obtained by constant flow (0.36 ± 0.37 mmHg, $r > 0.99$; $p = 0.002$), (Figure

2). This supports the assumption to apply a single flow value for the computational approaches. The CFD pressure drop results showed excellent agreement with the experimental pulsatile and constant flow (-0.36 ± 0.28 mmHg and 0.01 ± 0.38 mmHg respectively, $r > 0.99$; $p < 0.002$), as well as the CAAS Workstation vFFR pressure drop results (0.52 ± 0.28 mmHg and -0.16 ± 0.11 mmHg respectively, $r > 0.99$; $p < 0.002$). The difference between CFD and vFFR was -0.17 ± 0.34 mmHg with excellent agreement ($r > 0.99$; $p < 0.002$).

Clinical data

Patient demographics and procedural data

One hundred patients were included in the study. Baseline and procedural characteristics are summarized in Table 1.

Mean age was 64 ± 11 years and the majority of patients were male (67%). Diabetes was present in 26% of the cases. The majority of the FFR measurements were performed in the left anterior descending artery (60%). The left circumflex artery and the right coronary artery were involved in 13% and 27% of the cases respectively. Mean angiographic percent diameter stenosis (DS), lesion length and minimum lumen diameter (MLD), measured from 3D-QCA, were $37 \pm 13\%$, 20 ± 13 mm and 1.7 ± 0.3 mm respectively.

Correlation and agreement between FFR and vFFR

Mean FFR and vFFR were 0.82 ± 0.08 and 0.84 ± 0.07 respectively. A good linear correlation was found between FFR and vFFR ($r = 0.89$; $p < 0.001$). Assessment of vFFR had a low inter-observer variability ($r = 0.95$; $p < 0.001$) (Figure 4). vFFR had a good accuracy in the identification of patients with significant FFR values ≤ 0.80 (AUC of 0.93 [95% CI: 0.88–0.97]) (Figure 5). The diagnostic accuracy of 3D-QCA, based on percentage diameter stenosis was lower, (AUC of 0.34 [95% CI: 0.23–0.45]).

Table 1. Baseline characteristics

Total, n = 100	
Age, y, mean±SD	64±11
Male gender, n (%)	67 (67)
<u>Cardiovascular risk factors, n (%)</u>	
Hypertension	70 (70)
Hyperlipidemia	59 (59)
Diabetes Mellitus	26 (26)
Current smoker	25 (25)
Peripheral artery disease	10 (10)
<u>Medical history and co-morbidity, mean±SD</u>	
eGFR, ml/min	88±30
Hemoglobine, (mmol/L)	8.2±1.4
BMI	28±5
<u>Lesions location and characteristics, n (%)</u>	
Left anterior descending artery	60 (60)
Left circumflex artery	13 (13)
Right coronary artery	27 (27)
Tortuous vessels	28 (28)
Tandem lesions	7 (7)
Moderate or severe calcification	36 (36)
Bifurcation lesions	21 (21)
<u>Coronary angiography indication, n (%)</u>	
Stable coronary artery disease	60 (60)
Unstable coronary artery disease	14 (14)
NSTEMI	26 (26)
<u>3D- Quantitative Coronary Angiography, mean±SD</u>	
Lesion length, mm	20±13
Minimal lumen diameter, mm	1.7±0.33
Minimal lumen area, mm ²	2.3±0.96
Diameter stenosis, %	37±13
Reference vessel diameter, mm	2.8±0.5
<u>Indices, mean±SD</u>	
FFR	0.82±0.08
vFFR	0.84±0.07

Values are n, mean±SD of n (%); BMI= Body Mass Index; eGFR= estimated glomerular filtration rate; FFR= Fractional Flow Reserve; NSTEMI= Non-ST-segment elevation myocardial infarction; vFFR= vessel Fractional Flow Reserve

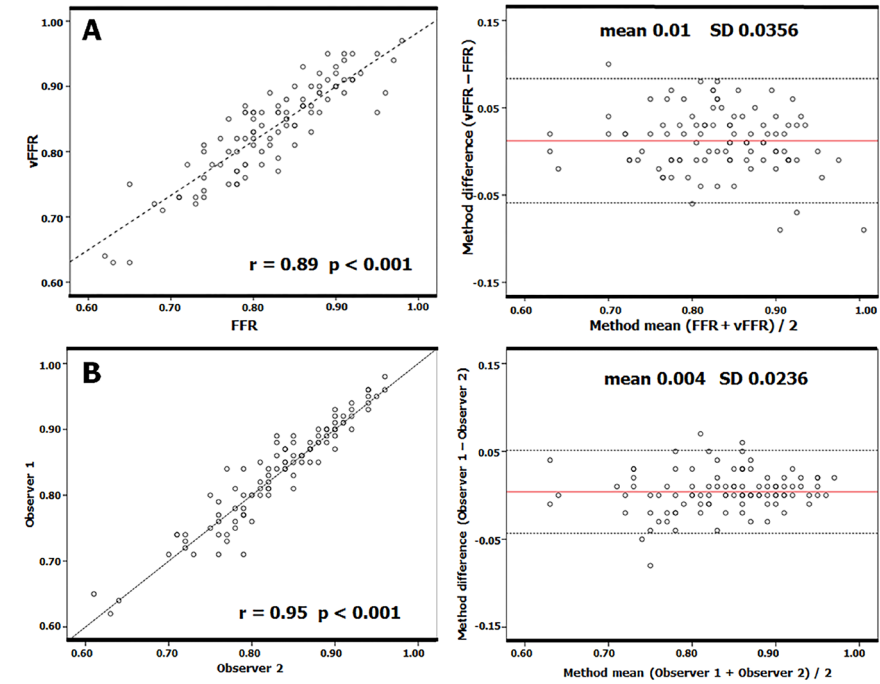


Figure 4. Scatter Plots showing the relationship between vFFR vs. wire-based FFR (A) and inter-observer variability (B) and Bland- Altman plots of differences against the means. The mean bias is represented by the solid red line and the 95% confidence interval is represented by the dashed lines.

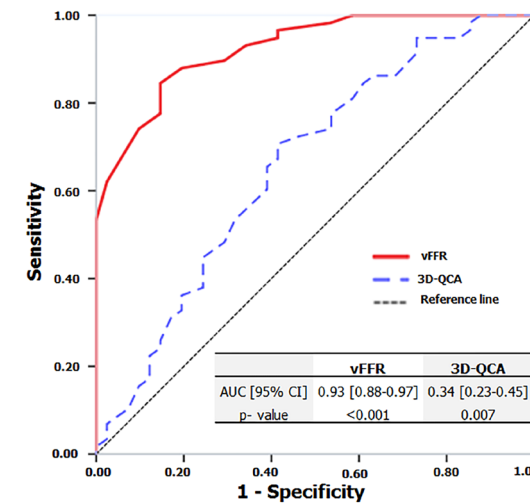


Figure 5. ROC Curves for vFFR and 3D-QCA. Comparison is made with a wire-based FFR at a cut point of 0.80

DISCUSSION

The FAST study confirmed the feasibility of a novel 3D-QCA based software tool to calculate FFR without the use of a pressure wire or microcatheter. In the pre-clinical technical validation model, vFFR proved to have a strong correlation with CFD and invasively measured flow parameters. In our clinical validation study, we confirmed an excellent agreement and high diagnostic value of vFFR compared to invasively measured FFR using a dedicated pressure wire under maximum hyperemia. Finally, we showed that vFFR had a low inter-observer variability.

Angiography guided coronary revascularization has been the cornerstone of routine PCI since its first introduction in September 1977¹⁷. In the past decade a wealth of data has become available demonstrating pitfalls of angiographic lesion assessment and the superiority of FFR guided PCI as compared to angiography guided PCI^{4, 18-20}.

Based on these compelling data, the use of FFR received strong recommendations in current revascularization guidelines^{18, 20}. Even though the use of FFR proved to be contrast saving, cost effective and associated with improved quality of life, FFR is still not being performed in the vast majority of cases^{5, 19, 21, 22}. The latter has been hypothesized to be due to the need for (in some countries) expensive hyperemic agents with known adverse events as dyspnea and arrhythmias and or intolerance due to pulmonary disease and the use of a costly pressure wire^{7, 8}. More recently, the adenosine free index iFR proved to be a valuable alternative to FFR in several large scale randomized controlled clinical trials which demonstrated the non-inferiority of iFR as compared to FFR^{7, 8}. However, iFR still requires the use of a costly pressure wire. For these reasons, the search for cheaper, faster and more patient-friendly methods to assess coronary physiology remains imperative.

Several recent studies assessed the potential value of FFR derived from 3D-QCA and blood flow simulation^{9, 10}. In the VIRTU-1 study²³, Morris et al. developed a computer model that accurately predicted virtual FFR from angiographic images alone assuming 3D reconstruction, using a Philips workstation. The authors showed a good correlation ($r = 0.84$) of virtual FFR values with FFR measured invasively. However, in this 3D-QCA-based FFR study, FFR was calculated based on lengthy CFD analysis hampering direct clinical applicability^{9, 10, 23, 24}. In our in-vitro models we simulated flow by using Navier-Stokes equations (Kratos, Multi-Physics 5, version 20), on a finite element mesh derived from the 3D surface mesh of the phantom. The measured flow was used to generate a parabolic velocity profile at the inlet. No-slip boundary conditions were used at the wall, and stress-free outflow was prescribed²⁵. We demonstrated an excellent correlation between

CFD based experimental pulsatile and constant flow and CAAS Workstation vFFR pressure drop results.

More recently published studies validated easier methods using contrast flow models to calculate 3D-QCA-based FFR by using frame counting^{11, 12}. In the FAVOR Pilot Study, Tu and coworkers assessed the diagnostic accuracy of quantitative flow ratio (QFR) as measured offline in three different ways, based on the different mean hyperemic flow velocities¹¹: 1) fixed empiric hyperemic flow velocity (fQFR) 2) modeled hyperemic flow velocity derived from angiography without drug-induced hyperemia (cQFR) and 3) measured hyperemic flow velocity derived from angiography during adenosine-induced hyperemia (aQFR). The authors observed a good agreement with FFR for all three QFR values with mean differences of 0.003 ± 0.068 ; 0.001 ± 0.059 and 0.001 ± 0.065 respectively. The diagnostic accuracy for identifying a positive FFR ($FFR < 0.80$) was 80%, 85% and 87% for fQFR, cQFR and aQFR respectively. Comparable results were recently presented by Xu et al. in the FAVOR II China Study in which the authors demonstrated that even when performed online, QFR has high feasibility and accuracy in identifying hemodynamically significant coronary artery stenosis¹². In both studies, QFR was performed using a prototype software package (QAngio XA 3D prototype, Medis Medical Imaging System, Leiden, the Netherlands). However, despite the apparently good correlation of QFR to invasively measured FFR, the contrast flow models (cQFR and aQFR) have several limitations. Coronary flow velocity is a highly sensitive variable. It is well known, that coronary perfusion occurs mainly during diastole. This implies that coronary velocity is not constant during the entire cardiac cycle and therefore passage of contrast agent might be different in systole and diastole.

In addition, there are phasic changes in resistance as well. The perfusion of the left coronary artery (LCA) is predominantly diastolic while the perfusion of right coronary artery (RCA) is both systolic and diastolic, due to lower pressure in the right ventricle as compared with the left ventricle. Therefore, one could assume differences while using frame count methods to obtain pressure gradients in the left vs. the right coronary artery. Furthermore, administration of contrast for performing coronary angiography is usually performed using manually contrast injections. The pressure used for contrast injection intrinsically influences coronary flow velocity and frame count measurements. In case contrast injection was indeed performed manually, larger variations might be expected in inter-study variability. Unfortunately, no data is available thus far on the reproducibility of QFR. In contrast, in the present study, we demonstrated an excellent inter-observer variability ($r = 0.95$; $p < 0.001$). Assessment of inter-observer variability

was based on redo the analysis of one time acquisition. The mean QCA-based diameter stenosis in the FAVOR II China Study was 46.5% and about 34% of the measured lesions had an FFR ≤ 0.80 . In the present study, we selected the intermediate coronary stenosis by visual assessment. The mean QCA-based diameter stenosis was 37%. However, despite relatively low diameter stenosis, 42% of the patients had an FFR ≤ 0.80 .

Furthermore, we used a more simplified method for computation of 3D-QCA-based FFR by using CAAS Workstation 8.0 (Pie Medical Imaging, Maastricht, the Netherlands). Based on well-validated 3D coronary reconstruction^{26, 27}, CAAS Workstation generated a 3D coronary reconstruction using 2 angiographic projections with at least 30 degrees apart. vFFR was calculated instantaneously by utilizing a proprietary algorithm which incorporates the morphology of the 3D coronary reconstruction and routinely measured patient specific aortic pressure. The CAAS Workstation 8.0 used for the in vitro experimental model was adapted to allow importing a 3D geometry of the phantom. In the FAST study, we demonstrated a high diagnostic accuracy of vFFR in the identification of patients with significant FFR as well, (AUC of 0.93 [95% CI: 0.88 – 0.97]).

In addition, this is the first validation study of this novel software with a limited sample size and offline assessment of vFFR. There is room for improvement in terms of diversity in study population and procedural and angiographic characteristics like tandem lesions and bifurcations. Clinical outcome studies should be obtained to assess the value of vFFR measured by CAAS Workstation for the hemodynamic assessment of lesion severity into daily clinical practice.

Limitations

Our study has several limitations. First, it is a single center experience in which we restricted our analyses to those recordings with undamped pressure wave forms. Previous work showed the high prevalence of suboptimal FFR curves in clinical practice (up to 30%) suggesting an additional benefit when using techniques based on angiography and simplified flow models²⁸. Second, the software's accuracy in complex vessels, e.g. bifurcations and diffusely diseased vessels, remains to be determined in larger patient cohorts. Furthermore, as mentioned in the methods section, contour detection was performed semi-automatically.

CONCLUSION

vFFR based on 3D-QCA as determined using novel software has a high linear correlation to invasively measured FFR, a high diagnostic accuracy to detect FFR ≤ 0.80 along with a low inter-observer variability.

REFERENCES

1. Lindstaedt M, Spiecker M, Perings C, Lawo T, Yazar A, Holland-Letz T, Muegge A, Bojara W and Germing A. How good are experienced interventional cardiologists at predicting the functional significance of intermediate or equivocal left main coronary artery stenoses? *Int J Cardiol.* 2007;120:254-61.
2. Authors/Task Force m, Windecker S, Kolh P, Alfonso F, Collet JP, Cremer J, Falk V, Filippatos G, Hamm C, Head SJ, Juni P, Kappetein AP, Kastrati A, Knuuti J, Landmesser U, Laufer G, Neumann FJ, Richter DJ, Schauerte P, Sousa Uva M, Stefanini GG, Taggart DP, Torracca L, Valgimigli M, Wijns W and Witkowski A. 2014 ESC/EACTS Guidelines on myocardial revascularization: The Task Force on Myocardial Revascularization of the European Society of Cardiology (ESC) and the European Association for Cardio-Thoracic Surgery (EACTS) Developed with the special contribution of the European Association of Percutaneous Cardiovascular Interventions (EAPCI). *Eur Heart J.* 2014;35:2541-619.
3. De Bruyne B, Pijls NH, Kalesan B, Barbato E, Tonino PA, Piroth Z, Jagic N, Mobius-Winkler S, Rioufol G, Witt N, Kala P, MacCarthy P, Engstrom T, Oldroyd KG, Mavromatis K, Manoharan G, Verlee P, Frobert O, Curzen N, Johnson JB, Juni P, Fearon WF and Investigators FT. Fractional flow reserve-guided PCI versus medical therapy in stable coronary disease. *N Engl J Med.* 2012;367:991-1001.
4. Pijls NH, van Schaardenburgh P, Manoharan G, Boersma E, Bech JW, van't Veer M, Bar F, Hoorntje J, Koolen J, Wijns W and de Bruyne B. Percutaneous coronary intervention of functionally nonsignificant stenosis: 5-year follow-up of the DEFER Study. *J Am Coll Cardiol.* 2007;49:2105-11.
5. Tonino PA, De Bruyne B, Pijls NH, Siebert U, Ikeno F, van't Veer M, Klauss V, Manoharan G, Engstrom T, Oldroyd KG, Ver Lee PN, MacCarthy PA, Fearon WF and Investigators FS. Fractional flow reserve versus angiography for guiding percutaneous coronary intervention. *N Engl J Med.* 2009;360:213-24.
6. Toth GG, Toth B, Johnson NP, De Vroey F, Di Serafino L, Pyxaras S, Rusinaru D, Di Gioia G, Pellicano M, Barbato E, van Mieghem C, Heyndrickx GR, De Bruyne B and Wijns W. Revascularization decisions in patients with stable angina and intermediate lesions: results of the international survey on interventional strategy. *Circ Cardiovasc Interv.* 2014;7:751-9.
7. Davies JE, Sen S, Dehbi HM, Al-Lamee R, Petraco R, Nijjer SS, Bhindi R, Lehman SJ, Walters D, Sapontis J, Janssens L, Vrints CJ, Khashaba A, Laine M, van Belle E, Krackhardt F, Bojara W, Going O, Harle T, Indolfi C, Niccoli G, Ribichini F, Tanaka N, Yokoi H, Takashima H, Kikuta Y, Erglis A, Vinhas H, Canas Silva P, Baptista SB, Alghamdi A, Hellig F, Koo BK, Nam CW, Shin ES, Doh JH, Brugaletta S, Alegria-Barrero E, Meuwissen M, Piek JJ, van Royen N, Sezer M, Di Mario C, Gerber RT, Malik IS, Sharp ASP, Talwar S, Tang K, Samady H, Altman J, Seto AH, Singh J, Jeremias A, Matsuo H, Kharbanda RK, Patel MR, Serruys P and Escaned J. Use of the Instantaneous Wave-free Ratio or Fractional Flow Reserve in PCI. *N Engl J Med.* 2017;376:1824-1834.
8. Gotberg M, Christiansen EH, Gudmundsdottir IJ, Sandhall L, Danielewicz M, Jakobsen L, Olsson SE, Ohagen P, Olsson H, Omerovic E, Calais F, Lindroos P, Maeng M, Todt T, Venetsanos D, James SK, Karegren A, Nilsson M, Carlsson J, Hauer D, Jensen J, Karlsson AC, Panayi G, Erlinge D, Frobert O and i FRISI. Instantaneous Wave-free Ratio versus Fractional Flow Reserve to Guide PCI. *N Engl J Med.* 2017;376:1813-1823.
9. Tu S, Barbato E, Koszegi Z, Yang J, Sun Z, Holm NR, Tar B, Li Y, Rusinaru D, Wijns W and Reiber JH. Fractional flow reserve calculation from 3-dimensional quantitative coronary angiography and TIMI frame count: a fast computer model to quantify the functional significance of moderately obstructed coronary arteries. *JACC Cardiovasc Interv.* 2014;7:768-77.
10. Papafaklis MI, Muramatsu T, Ishibashi Y, Lakkas LS, Nakatani S, Bourantas CV, Ligthart JMR, Onuma Y, Echavarría-Pinto M, Tsirka G, Kotsia A, Nikas DN, Mogabgab O, van Geuns RJ, Naka KK, Fotiadis DI, Brilakis ES, Garcia-Garcia HM, Escaned J, Zijlstra F, Michalis LK and Serruys PW. Fast virtual functional assessment of intermediate coronary lesions using routine angiographic data and blood flow simulation in humans: comparison with pressure wire - fractional flow reserve. *EuroIntervention.* 2014;10:574-83.
11. Tu S, Westra J, Yang J, von Birgelen C, Ferrara A, Pellicano M, Nef H, Tebaldi M, Murasato Y, Lansky A, Barbato E, van der Heijden LC, Reiber JH, Holm NR, Wijns W and Group FPTS. Diagnostic Accuracy of Fast Computational Approaches to Derive Fractional Flow Reserve From Diagnostic Coronary Angiography: The International Multicenter FAVOR Pilot Study. *JACC Cardiovasc Interv.* 2016;9:2024-2035.
12. Xu B, Tu S, Qiao S, Qu X, Chen Y, Yang J, Guo L, Sun Z, Li Z, Tian F, Fang W, Chen J, Li W, Guan C, Holm NR, Wijns W and Hu S. Diagnostic Accuracy of Angiography-Based Quantitative Flow Ratio Measurements for Online Assessment of Coronary Stenosis. *J Am Coll Cardiol.* 2017;70:3077-3087.
13. Geven MC, Bohte VN, Aarnoudse WH, van den Berg PM, Rutten MC, Pijls NH and van de Vosse FN. A physiologically representative in vitro model of the coronary circulation. *Physiol Meas.* 2004;25:891-904.
14. Dodge JT, Jr, Brown BG, Bolson EL and Dodge HT. Lumen diameter of normal human coronary arteries. Influence of age, sex, anatomic variation, and left ventricular hypertrophy or dilation. *Circulation.* 1992;86:232-46.
15. Li S, Chin C, Thondapu V, Poon EKW, Monty JP, Li Y, Ooi ASH, Tu S and Barlis P. Numerical and experimental investigations of the flow-pressure relation in multiple sequential stenoses coronary artery. *Int J Cardiovasc Imaging.* 2017;33:1083-1088.
16. Morris PD, Narracott A, von Tengg-Kobligh H, Silva Soto DA, Hsiao S, Lungu A, Evans P, Bressloff NW, Lawford PV, Hose DR and Gunn JP. Computational fluid dynamics modelling in cardiovascular medicine. *Heart.* 2016;102:18-28.
17. Gruntzig AR, Senning A and Siegenthaler WE. Nonoperative dilatation of coronary-artery stenosis: percutaneous transluminal coronary angioplasty. *N Engl J Med.* 1979;301:61-8.

18. Levine GN, Bates ER, Blankenship JC, Bailey SR, Bittl JA, Cercek B, Chambers CE, Ellis SG, Guyton RA, Hollenberg SM, Khot UN, Lange RA, Mauri L, Mehran R, Moussa ID, Mukherjee D, Nallamothu BK and Ting HH. 2011 ACCF/AHA/SCAI Guideline for Percutaneous Coronary Intervention: a report of the American College of Cardiology Foundation/American Heart Association Task Force on Practice Guidelines and the Society for Cardiovascular Angiography and Interventions. *Circulation*. 2011;124:e574-651.
19. Siebert U, Arvandi M, Gothe RM, Bornschein B, Eccleston D, Walters DL, Rankin J, De Bruyne B, Fearon WF, Pijls NH and Harper R. Improving the quality of percutaneous revascularisation in patients with multivessel disease in Australia: cost-effectiveness, public health implications, and budget impact of FFR-guided PCI. *Heart Lung Circ*. 2014;23:527-33.
20. Windecker S, Kolh P, Alfonso F, Collet JP, Cremer J, Falk V, Filippatos G, Hamm C, Head SJ, Juni P, Kappetein AP, Kastrati A, Knuuti J, Landmesser U, Laufer G, Neumann FJ, Richter DJ, Schauerte P, Uva MS, Stefanini GG, Taggart DP, Torracca L, Valgimigli M, Wijns W, Witkowski A, Grupa Robocza Europejskiego Towarzystwa K, Europejskie Stowarzyszenie Chirurgii Serca i Klatki Piersiowej do spraw rewaskularyzacji miesnia s and European Association for Percutaneous Cardiovascular I. [2014 ESC/EACTS Guidelines on myocardial revascularization]
21. Wytoczne ESC/EACTS dotyczące rewaskularyzacji miesnia sercowego w 2014 roku. *Kardiol Pol*. 2014;72:1253-379.
22. Fearon WF, Bornschein B, Tonino PA, Gothe RM, Bruyne BD, Pijls NH, Siebert U and Fractional Flow Reserve Versus Angiography for Multivessel Evaluation Study I. Economic evaluation of fractional flow reserve-guided percutaneous coronary intervention in patients with multivessel disease. *Circulation*. 2010;122:2545-50.
23. van Nunen LX, Zimmermann FM, Tonino PA, Barbato E, Baumbach A, Engstrom T, Klaus V, MacCarthy PA, Manoharan G, Oldroyd KG, Ver Lee PN, van't Veer M, Fearon WF, De Bruyne B, Pijls NH and Investigators FS. Fractional flow reserve versus angiography for guidance of PCI in patients with multivessel coronary artery disease (FAME): 5-year follow-up of a randomised controlled trial. *Lancet*. 2015;386:1853-60.
24. Morris PD, Ryan D, Morton AC, Lycett R, Lawford PV, Hose DR and Gunn JP. Virtual fractional flow reserve from coronary angiography: modeling the significance of coronary lesions: results from the VIRTU-1 (VIRTUal Fractional Flow Reserve From Coronary Angiography) study. *JACC Cardiovasc Interv*. 2013;6:149-57.
25. Poon EK, Hayat U, Thondapu V, Ooi AS, Ul-Haq MA, Moore S, Foin N, Tu S, Chin C, Monty JP, Marusic I and Barlis P. Advances in three-dimensional coronary imaging and computational fluid dynamics: is virtual fractional flow reserve more than just a pretty picture? *Coron Artery Dis*. 2015;26 Suppl 1:e43-54.
26. Wentzel JJ, Gijzen FJ, Schuurbiens JC, Krams R, Serruys PW, De Feyter PJ and Slager CJ. Geometry guided data averaging enables the interpretation of shear stress related plaque development in human coronary arteries. *J Biomech*. 2005;38:1551-5.
27. Girasis C, Schuurbiens JC, Muramatsu T, Aben JP, Onuma Y, Soekhradj S, Morel MA, van Geuns RJ, Wentzel JJ and Serruys PW. Advanced three-dimensional quantitative coronary angiographic assessment of bifurcation lesions: methodology and phantom validation. *EuroIntervention*. 2013;8:1451-60.
28. Schuurbiens JC, Lopez NG, Ligthart JMR, Gijzen FJ, Dijkstra J, Serruys PW, van der Steen AF and Wentzel JJ. In vivo validation of CAAS QCA-3D coronary reconstruction using fusion of angiography and intravascular ultrasound (ANGUS). *Catheter Cardiovasc Interv*. 2009;73:620-6.
29. Matsumura M, Johnson NP, Fearon WF, Mintz GS, Stone GW, Oldroyd KG, De Bruyne B, Pijls NHJ, Maehara A and Jeremias A. Accuracy of Fractional Flow Reserve Measurements in Clinical Practice: Observations From a Core Laboratory Analysis. *JACC Cardiovasc Interv*. 2017;10:1392-1401.

Chapter 14



**Validation of novel 3-Dimensional Quantitative
Coronary Angiography based software to
calculate Vessel Fractional Flow Reserve
(vFFR) post stenting: Fast Assessment of
STenosis severity POST stenting, The FAST
POST-study**

Masdjedi K, van Zandvoort LJC, Balbi MM, Ligthart JMR, Nuis RJ, Vermaire A,
Lemmert ME, Wilschut J, Diletti R, De Jaegere PPT, Zijlstra F, van Mieghem
NMDA, Daemen J

*Erasmus University Medical Center, Thoraxcenter, Department of cardiology, Rotterdam,
the Netherlands*

Catheter Cardiovasc Interv. (Accepted)

ABSTRACT

Objectives: To validate novel dedicated 3D-QCA based software to calculate post PCI vessel-FFR (vFFR) in a consecutive series of patients and to assess the diagnostic accuracy and to assess inter-observer variability.

Background: Low post percutaneous coronary intervention (PCI) Fractional Flow Reserve (FFR) predicts future adverse cardiac events. However, FFR assessment requires the insertion of a pressure wire in combination with the use of a hyperemic agent.

Methods: FAST POST study is an observational, retrospective, single-center cohort study. One hundred patients presenting with stable angina or non ST-elevation myocardial infarction, who underwent post PCI FFR assessment using a dedicated microcatheter were included. Two orthogonal angiographic projections were acquired to create a 3D reconstruction of the coronary artery using CAAS workstation 8.0. vFFR was subsequently calculated using the aortic root pressure.

Results: Mean age was 65±12 years and 70% was male. Mean microcatheter based FFR and vFFR were 0.91±0.07 and 0.91±0.06 respectively. A good linear correlation was found between FFR and vFFR ($r = 0.88$; $p < 0.001$). vFFR had a higher accuracy in the identification of patients with FFR values < 0.90 , AUC 0.98 (95% CI: 0.96-1.00) as compared to 3D-QCA AUC 0.62 (95% CI: 0.94-0.74). Assessment of vFFR had a low inter-observer variability ($r = 0.95$; $p < 0.001$).

Conclusion: 3D-QCA derived post PCI vFFR correlates well with invasively measured microcatheter based FFR and has a high diagnostic accuracy to detect FFR < 0.90 with low inter-observer variability.

INTRODUCTION

In contrast to fractional flow reserve (FFR), coronary angiography has limited ability to accurately assess the hemodynamic significance of coronary stenosis¹⁻⁶. Furthermore, FFR post PCI is a strong and independent predictor of major adverse cardiac events (MACE) up to 2 years⁷⁻⁹. However, despite unequivocal evidence supporting the use of FFR to guide clinical decision-making, adoption into routine practice has been limited and in particular FFR assessment after stenting is rarely performed. The latter illustrates the need for tools that allow simple and fast post PCI physiological assessment without the need for a pressure wire and hyperemic agent.

Vessel FFR (vFFR) as assessed by three-dimensional quantitative coronary angiography (3D-QCA) proved to have a high correlation with FFR and a high diagnostic accuracy to detect FFR ≤ 0.80 and a low inter-observer variability¹⁰.

The aim of the present study was to validate 3D-QCA based vFFR with microcatheter based FFR post stenting in a consecutive series of patients, assess the diagnostic accuracy to detect an FFR < 0.90 and determine inter-observer variability.

MATERIALS AND METHODS

The FAST POST (Fast Assessment of STenosis severity POST PCI) study is an observational, single-center cohort study with the aim to assess the diagnostic accuracy of offline post PCI vFFR assessment as compared to invasively measured FFR using the Acist Navvus™ rapid exchange FFR (ACIST Medical Systems) microcatheter.

Based on the findings of the FAST I trial ($n=100$), a sample of 100 patients was selected from the FFR SEARCH registry to validate post PCI vFFR. FFR SEARCH registry was a prospective registry in which FFR measurements were routinely performed after angiographically successful PCI in 1000 consecutive patients between March 2016 and May 2017. Patients referred for coronary angiography with at least one hemodynamically significant stenosis who underwent PCI with stenting were eligible. Inclusion criteria for the present study were age ≥ 18 years and presentation with either stable- or unstable angina or non ST-elevation myocardial infarction. Angiographic inclusion criteria study were: at least one significant stenosis in one of the epicardial coronary arteries (diameter stenosis of $> 70\%$ on QCA or hemodynamically significant stenosis defined as FFR ≤ 0.80). Exclusion criteria were patients with ST-elevation myocardial infarction (STEMI), coronary bypass grafts (CABG), cardiogenic shock or severe hemodynamic

instability and adenosine intolerance. The sample of 100 patients for the present study was derived from a consecutive cohort of the 200 most recent patients in the FFR SEARCH registry. The majority of the patients were excluded due to STEMI. Furthermore, patients with inadequate pressure waveform or lack of two adequate orthogonal view to create a 3D reconstruction of the vessel, were excluded.

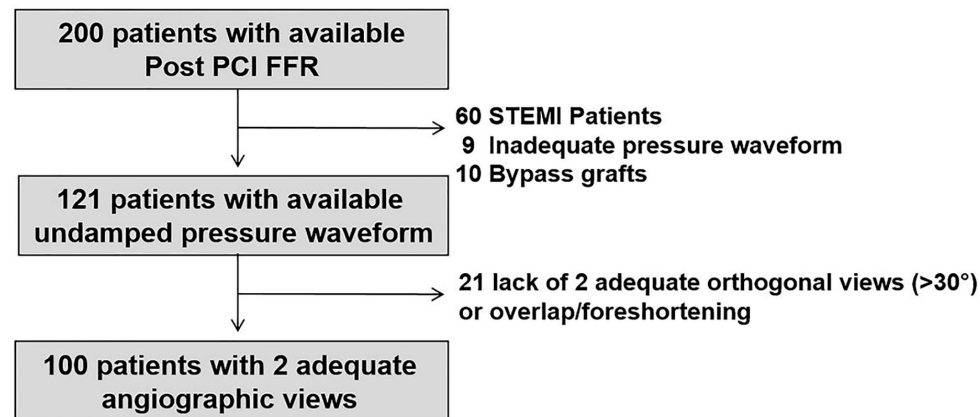


Figure 1. Flowchart of all included and excluded patients

The significant percentage of cases that had to be excluded due to a lack of qualifying angiograms should be put into perspective to procedures that were performed in routine practice with a lack of focus on post PCI vFFR.

All procedures were performed according to standard local routine clinical practice. FFR was defined as mean distal coronary artery pressure divided by mean aortic pressure during maximum hyperemia achieved by continuous intravenous infusion of adenosine at a rate of 140 µg/kg/min through an antecubital vein. Post PCI FFR assessment was performed using the Acist Navvus microcatheter, 2 cm distal from the most distal stent-edge. Subsequently, two standard monoplane angiographic projections (at least 30 degrees apart, preferably orthogonal) were performed after a bolus of 200mcg nitroglycine. An additional projection was recorded with the Navvus catheter in situ to capture the position of the device. Aortic root pressure was constantly recorded, the pressure measurement taken before the start of the FFR measurement was used as input in the CAAS/vFFR software. Angiograms and pressure waveforms were stored as DICOM image format for offline analyses.

We recently reported the methodology of vFFR calculation¹⁰. vFFR computation was performed offline by 2 independent observers, blinded to the invasive post PCI FFR measurement, in order to assess inter-observer variability (KM, MB).

A total of three 2D images, were exported to the CAAS workstation 8.0 (Pie Medical Imaging, Maastricht, the Netherlands) that used the same algorithms for vFFR computation as previously described¹⁰. Two views with at least 30 degrees differences in rotation/angulation to create a 3D reconstruction of the coronary arteries and one view to determine the position of the FFR pressure wire. Within CAAS Workstation vFFR the pressure drop is calculated instantaneously by applying physical laws including viscous resistance and separation loss effects present in coronary flow behavior, as described by Gould and Kirkeeide^{11, 12}. The methods however are based on a single angiographic projection. Within CAAS vFFR, the geometry of the coronary artery is derived from well-validated 3D reconstructions^{13, 14} which reduces the effects of foreshortening, out of plane magnification and non-symmetric coronary lesions.

The two independent observers used the same cine-images for the calculation of vFFR. Although temporal alignment of the cardiac cycle between the two angiograms was performed automatically by ECG triggering, manual frame selection was allowed. Contour detecting was performed semi-automatically, delineating the vessel contour from the ostium to the most distal position of the Navvus catheter. The percent diameter stenosis, minimal lumen diameter, reference lumen diameter, minimal lumen area and lesion length were measured from the same 3D model as in which the vFFR was determined. vFFR was calculated automatically integrating the invasively measured aortic root pressure and the automatically generated 3D QCA dimensions. Based on well-validated 3D coronary reconstruction^{13, 14}, CAAS Workstation generated a 3D coronary reconstruction using 2 different angiographic projections. vFFR was calculated instantaneously with a proprietary algorithm which incorporates the morphology of the 3D coronary reconstruction and routinely measured real-time aortic pressure.

Statistical analysis

Continuous variables are presented as mean ± standard deviation. All continuous variables were normally distributed. Categorical variables are expressed as counts and percentages. All statistical tests are 2-tailed. Pearson's correlation coefficient (r) was used to assess the relationship between FFR and vFFR and to assess inter-observer variability. Agreement between the indices and the inter-observer variability were assessed by Bland-Altman plots with corresponding 95% limits of agreement. Receiver-operating characteristic (ROC) area under the curve (AUC) analysis was used to estimate the diagnostic performance of both vFFR and 3D QCA-based diameter stenosis as compared to the microcatheter-based FFR with a threshold of <0.90 which has been used in previous studies as an arbitrary cut-off

value to predict clinical outcome^{1,5,8}. Statistical analysis was carried out using the SPSS statistical package version 24 (IBM, Armonk, North Castle, New York, USA).

RESULTS

Baseline and procedural characteristics are summarized in Table 1. Mean age was 65±12 years and the majority of patients were male (70%). Diabetes was present in 21% of the cases. A prior myocardial infarction (MI) or PCI was present in 26% and 33% of the patients respectively. In 50 % of the cases, the FFR measurement was performed in the left anterior descending artery. Mean 3D QCA-based diameter stenosis post PCI was 11±15% with a reference vessel diameter of 3.0±0.6 mm.

Mean distal coronary artery pressure to mean aortic pressure in the resting state during the whole cardiac cycle (Pd/Pa) was 0.96 ±0.04. Mean FFR and vFFR were 0.91±0.07 and 0.91±0.06 respectively, Table 1. A good linear correlation was found between FFR and vFFR (r =0.88; p<001), Figure 2. Assessment of vFFR had a low inter-observer variability (r =0.95; p<0.001), Figure 3. vFFR had a higher accuracy in the identification of patients with FFR values <0.90, AUC 0.98 (95% CI: 0.96-1.00) as compared to 3D-QCA AUC 0.62 (95% CI: 0.94-0.74), Figure 4.

A vFFR threshold of <0.90 was associated with a sensitivity and specificity of 80% and 97% respectively to identify FFR <0.90. The positive predictive value (PPV) and negative predictive value (NPV) were 94 % and 88% respectively.

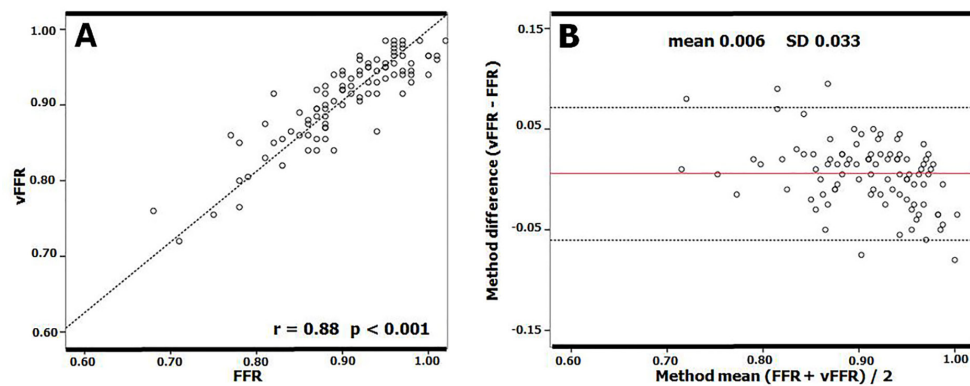


Figure 2. Scatter Plot showing the relationship between vessel-FFR (vFFR) and invasive measured FFR using a rapid exchange microcatheter (FFR) (A) and Bland- Altman plots of differences against the means (B).

The mean bias is represented by the solid red line and the 95% confidence interval is represented by the dashed lines. FFR = Fractional Flow Reserve; vFFR = Vessel Fractional Flow Reserve.

Table 1. Baseline characteristics

	Total, n=100
Age, y, mean±SD	65±12
Male sex, n (%)	70 (70)
<u>Cardiovascular risk factors, n (%)</u>	
Hypertension	59 (59)
Hyperlipidemia	53 (53)
Diabetes Mellitus	21 (21)
Current Smoker	30 (30)
<u>Medical history and co-morbidity</u>	
Prior ACS, n (%)	26 (26)
Prior PCI, n (%)	33 (33)
Peripheral artery disease, n (%)	8 (8)
Creatinin, µmol/L, µmol/L, Mean±SD	99 (84)
Hemoglobine, (mmol/L), Mean±SD	8.7 (1.0)
BMI, Mean±SD	24 ± 4
<u>Measured vessel, n (%)</u>	
Left main stem	6 (6)
Left anterior descending artery	50 (50)
Left circumflex artery	22 (22)
Right coronary artery	22 (22)
<u>3D- Quantitative Coronary Angiography, mean±SD</u>	
Lesion length, mm	10.5±10
Minimal lumen diameter, mm	2.7±0.7
Reference vessel diameter, mm	3.0±0.6
Diameter stenosis, %	11±15
<u>Indices, mean±SD</u>	
Pd/Pa	0.96 (0.04)
FFR	0.91 (0.07)
vFFR	0.91 (0.06)

Values are n, mean±SD of n (%); ACS =Acute coronary syndrome; BMI= Body Mass Index; FFR= Fractional Flow Reserve; PCI = Percutaneous coronary intervention; SD = Standard deviation; vFFR= vessel Fractional Flow Reserve.

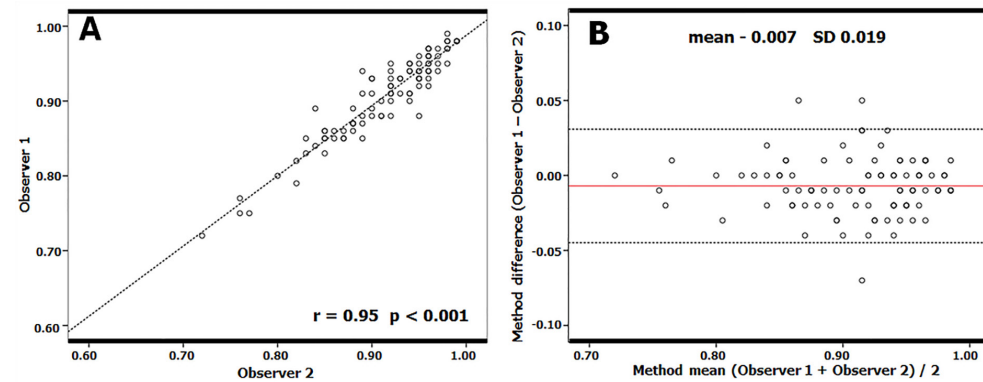


Figure 3. Scatter Plot (A) and Bland-Altman Analysis of inter-observer variability (B). The mean bias is represented by the solid red line and the 95% confidence interval is represented by the dashed lines.

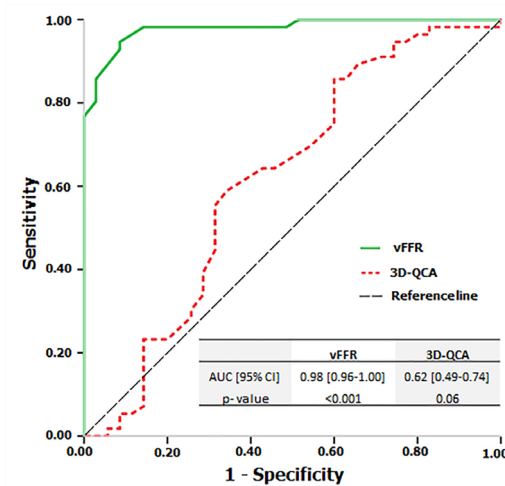


Figure 4. ROC Curves for vFFR and 3D-QCA. Comparison is made with an FFR at a cut point of 0.89. 3D-QCA = Three dimensional quantitative coronary angiography; vFFR = Vessel Fractional Flow Reserve.

DISCUSSION

The main findings of the FAST POST study can be summarized as follows: 1) vFFR allows to identify post PCI FFR <0.90 with a high diagnostics accuracy 2) vFFR, showed good correlation and agreement with post PCI FFR as measured using a dedicated microcatheter and 3) post PCI vFFR computation has a low inter-observer variability.

Pre-PCI FFR has become an important tool in detecting hemodynamically significant lesions in patients with stable and unstable coronary artery disease and FFR-guided PCI proved to significantly improve PCI outcomes as compared to angiography guided PCI alone ^{4, 5, 15-17}.

There has been increasing interest in the assessment of post PCI FFR since several studies demonstrated an increased risk of MACE in patient with low pressure wire- based post-PCI FFR. In contrast to the generally accepted pre PCI FFR cut off of 0.80, there is at present no generally accepted number related to post PCI assessment. Previous studies however demonstrated that the optimal threshold to predict clinical outcome appeared to be around 0.90 ¹⁸⁻²⁶. The clinical relevance of the latter was recently strengthened by the results of the FFR-SEARCH registry, the largest microcatheter-based post PCI FFR study thus far, demonstrating that up to 56% of the patients had at least one lesion with a post PCI FFR ≤0.90 despite adequate angiographic result ²⁷. Almost 11% of the patients had at least one lesion with a post PCI FFR ≤0.80, a number that confirmed previous studies showing post PCI FFR rates ≤0.80 in 6 to 9.5% of the cases but was significantly higher as compared to findings from the DK-CRUSH VII study (4%) ^{18, 22, 28}. Differences in these rates have been explained by differences in baseline characteristics and linked to more complex lesion phenotypes like bifurcations, extensive calcification, CTO, LAD lesions or in-stent restenosis (low post PCI FFR) and prior MI, presence of diabetes or presentation with ACS (higher post PCI FFR).

A dedicated IVUS substudy of FFR-SEARCH demonstrated that residual proximal or distal lesions, or stent related problems including underexpansion, malapposition and edge dissections or hematomas were present in 84% of the patients with a post PCI FFR ≤0.85, despite adequate angiographic results ²⁹.

Nevertheless, despite strong recommendations and increasing evidence on the cost-effectiveness of FFR in case of pre-treatment lesion assessment, FFR is still underused in clinical practice ^{30, 31}. This reality has been linked to reimbursement issues, the need for hyperemic agents like adenosine and possible concomitant adverse events like dyspnea, chest pain, rhythm disturbances and hypotension ^{32, 33}. Although, the use of post PCI iFR has emerged as a non-hyperemic faster and easier method to evaluate post stenting physiological results, the need for a pressure wire remains a fact ³⁴. Moreover, pressure wires that are used pre procedurally might get damaged and are often replaced during the course of the PCI which mitigates their user-friendliness in a post PCI setting. While the use of FFR microcatheters might solve part of this issue, the search towards less invasive methods to assess coronary physiology continues and several studies assessed

the potential value of FFR derived from three-dimensional quantitative coronary angiography (3D-QCA) and computational flow modeling^{35, 36}.

In the FAST I study we recently demonstrated a good correlation between vFFR using CAAS 8.0 and pre PCI FFR measured using a conventional pressure wire along with a low inter-observer variability¹⁰. Similar results were found in the FAVOR studies using computational approaches to derive FFR from diagnostic coronary angiography (QFR) based on frame counting and contrast flow models as well as FFR_{angio} (CathWorks) which allows functional angiographic mapping of the entire coronary tree³⁷⁻³⁹. The PIONEER QFR substudy assessed the difference of QFR immediately post stenting and at nine months follow up between two different drug eluting stents and reported that the QFR did not differ between the groups⁴⁰. The HAWKEYE study investigated the prognostic value of post PCI QFR and reported that lower values of post stenting QFR predict clinical outcome⁴¹. However, in none of both studies pressure wire or microcatheter based FFR data were available as a reference. The present study is the first to validate vFFR against microcatheter based FFR in a post PCI setting. In the present study we were able to show an excellent correlation between vFFR and invasively measured FFR using a dedicated microcatheter and a high diagnostic accuracy to detect post PCI FFR <0.90. Interestingly, given the fact that the present population solely consisted of patients with optimal angiographic results, vFFR proved to be <0.90 in 41% of the cases. The present findings are at clear odds with recently reported data by Pizzato et al. who reported a weak correlation between vFFR and pressure wire based FFR⁴². However, several methodological and anatomic differences between both studies should be highlighted. At first, vFFR computation is based on aortic pressure. No mentioning about this step was made by Pizzato et al. It is unlikely the authors were able to retrospectively retrieve accurate real-time aortic pressures from >50 centers. If inadequate, a poorer correlation could be explained. Second, angiographic lesion severity was clearly different in both studies (53% vs. 37% in FAST I). The latter is however less likely to explain potential differences in accuracy.

Based on the results of the present study, the calculation of post stenting vFFR using the CAAS Workstation could be a useful tool to identify and potentially optimize the outcomes of patients at higher risk for future adverse cardiac events. Previous studies have shown that post stenting FFR reclassified 20% of angiographically satisfactory lesions, which required further intervention thereby providing an opportunity for complete functional optimization at the time of the index procedure⁴³. Larger clinical outcome studies are warranted to assess the practicalities and value of angiography based post PCI FFR and its potential to

optimize long-term outcomes.

Limitations

Our study reflects a single-center experience with a relatively small patient sample size. The vFFR was compared to FFR using the Acist Navvus microcatheter. Microcatheter based FFR correlated well with conventional pressure-wire wire based FFR. The latter findings should be interpreted in the light of a known overestimation of microcatheter based FFR as compared to routine pressure wire based FFR recordings of approximately 0.03 reported in previous studies that was mainly linked to larger differences in smaller caliber vessels^{44, 45}. Furthermore, vFFR calculation was performed off-line by two independent observers, there was no independent core-lab involved. Both online and independent corelab adjudication of vFFR will be performed in the ongoing international multicenter FAST II study (ClinicalTrials.gov ID: NCT03791320). Furthermore, the accuracy of the technique is strongly dependent on the quality of the angiographic cine-images. Image acquisition should meet the criteria of non-overlapping images with at least 30 degrees differences in angulation. Although these are pre-requisites that theoretically should be fulfilled in all pre procedural angiographies, previous studies showed that up to 65% of routine angiograms are of insufficient quality to be used in angiography-based FFR software due to insufficient luminal contrast opacification, overlap or lack of adequate orthogonal views. Also costs of angio based FFR are currently a topic of debate between software vendors, hospitals and health care reimbursement plans. No definitive universal pricing models have been made for the different software packages available. Finally, the average FFR in the present cohort was relatively high, directly related to the post PCI nature of the patient cohort. Yet, still 41% had a post PCI vFFR of <0.90.

CONCLUSION

The 3D-QCA derived vFFR post PCI correlates well with invasively measured microcatheter based FFR and has a high diagnostic accuracy to detect FFR <0.90 with low inter-observer variability.

REFERENCES

1. De Bruyne B, Pijls NH, Kalesan B, Barbato E, Tonino PA, Piroth Z, Jagic N, Mobius-Winkler S, Rioufol G, Witt N and others. Fractional flow reserve-guided PCI versus medical therapy in stable coronary disease. *N Engl J Med* 2012;367(11):991-1001.
2. Lindstaedt M, Spiecker M, Perings C, Lawo T, Yazar A, Holland-Letz T, Muegge A, Bojara W, Germing A. How good are experienced interventional cardiologists at predicting the functional significance of intermediate or equivocal left main coronary artery stenoses? *Int J Cardiol* 2007;120(2):254-61.
3. Neumann FJ, Sousa-Uva M, Ahlsson A, Alfonso F, Banning AP, Benedetto U, Byrne RA, Collet JP, Falk V, Head SJ and others. 2018 ESC/EACTS Guidelines on myocardial revascularization. *Eur Heart J* 2018.
4. Pijls NH, van Schaardenburgh P, Manoharan G, Boersma E, Bech JW, van't Veer M, Bar F, Hoortje J, Koolen J, Wijns W and others. Percutaneous coronary intervention of functionally nonsignificant stenosis: 5-year follow-up of the DEFER Study. *J Am Coll Cardiol* 2007;49(21):2105-11.
5. Tonino PA, De Bruyne B, Pijls NH, Siebert U, Ikeno F, van't Veer M, Klauss V, Manoharan G, Engstrom T, Oldroyd KG and others. Fractional flow reserve versus angiography for guiding percutaneous coronary intervention. *N Engl J Med* 2009;360(3):213-24.
6. Tu S, Echavarría-Pinto M, von Birgelen C, Holm NR, Pyxaras SA, Kumsars I, Lam MK, Valkenburg I, Toth GG, Li Y and others. Fractional flow reserve and coronary bifurcation anatomy: a novel quantitative model to assess and report the stenosis severity of bifurcation lesions. *JACC Cardiovasc Interv* 2015;8(4):564-74.
7. Wolfrum M, Fahrni G, de Maria GL, Knapp G, Curzen N, Kharbanda RK, Fröhlich GM, Banning AP. Impact of impaired fractional flow reserve after coronary interventions on outcomes: a systematic review and meta-analysis. *BMC Cardiovascular Disorders* 2016;16(1):177.
8. Rimac G, Fearon WF, De Bruyne B, Ikeno F, Matsuo H, Piroth Z, Costerousse O, Bertrand OF. Clinical value of post-percutaneous coronary intervention fractional flow reserve value: A systematic review and meta-analysis. *Am Heart J* 2017;183:1-9.
9. Kasula S, Agarwal SK, Hacioglu Y, Pothineni NK, Bhatti S, Ahmed Z, Uretsky B, Hakeem A. Clinical and prognostic value of poststenting fractional flow reserve in acute coronary syndromes. *Heart* 2016;102(24):1988-1994.
10. Masdjedi K, van Zandvoort LJC, Balbi MM, Gijsen FJH, Ligthart JMR, Rutten MCM, Lemmert ME, Wilschut J, Diletti R, De Jaegere P and others. Validation of 3-Dimensional Quantitative Coronary Angiography based software to calculate Fractional Flow Reserve: Fast Assessment of STenosis severity (FAST)-study. *EuroIntervention* 2019.
11. Gould KL, Kelley KO, Bolson EL. Experimental validation of quantitative coronary arteriography for determining pressure-flow characteristics of coronary stenosis. *Circulation* 1982;66(5):930-7.
12. Kirkeeide R. Coronary obstructions, morphology and physiologic significance. 1991:229-44.
13. Girasis C, Schuurbijs JC, Muramatsu T, Aben JP, Onuma Y, Soekhradj S, Morel MA, van Geuns RJ, Wentzel JJ, Serruys PW. Advanced three-dimensional quantitative coronary angiographic assessment of bifurcation lesions: methodology and phantom validation. *EuroIntervention* 2013;8(12):1451-60.
14. Schuurbijs JC, Lopez NG, Ligthart JMR, Gijsen FJ, Dijkstra J, Serruys PW, van der Steen AF, Wentzel JJ. In vivo validation of CAAS QCA-3D coronary reconstruction using fusion of angiography and intravascular ultrasound (ANGUS). *Catheter Cardiovasc Interv* 2009;73(5):620-6.
15. Berger A, Botman KJ, MacCarthy PA, Wijns W, Bartunek J, Heyndrickx GR, Pijls NH, De Bruyne B. Long-term clinical outcome after fractional flow reserve-guided percutaneous coronary intervention in patients with multivessel disease. *J Am Coll Cardiol* 2005;46(3):438-42.
16. Pijls NH, Fearon WF, Tonino PA, Siebert U, Ikeno F, Bornschein B, van't Veer M, Klauss V, Manoharan G, Engstrom T and others. Fractional flow reserve versus angiography for guiding percutaneous coronary intervention in patients with multivessel coronary artery disease: 2-year follow-up of the FAME (Fractional Flow Reserve Versus Angiography for Multivessel Evaluation) study. *J Am Coll Cardiol* 2010;56(3):177-84.
17. Sels JW, Tonino PA, Siebert U, Fearon WF, van't Veer M, De Bruyne B, Pijls NH. Fractional flow reserve in unstable angina and non-ST-segment elevation myocardial infarction experience from the FAME (Fractional flow reserve versus Angiography for Multivessel Evaluation) study. *JACC Cardiovasc Interv* 2011;4(11):1183-9.
18. Pijls NH, Klauss V, Siebert U, Powers E, Takazawa K, Fearon WF, Escaned J, Tsurumi Y, Akasaka T, Samady H and others. Coronary pressure measurement after stenting predicts adverse events at follow-up: a multicenter registry. *Circulation* 2002;105(25):2950-4.
19. Johnson NP, Toth GG, Lai D, Zhu H, Acar G, Agostoni P, Appelman Y, Arslan F, Barbato E, Chen SL and others. Prognostic value of fractional flow reserve: linking physiologic severity to clinical outcomes. *J Am Coll Cardiol* 2014;64(16):1641-54.
20. Ishii H, Kataoka T, Kobayashi Y, Tsumori T, Takeshita H, Matsumoto R, Shirai N, Nishioka H, Hasegawa T, Nakata S and others. Utility of myocardial fractional flow reserve for prediction of restenosis following sirolimus-eluting stent implantation. *Heart Vessels* 2011;26(6):572-81.
21. Nam CW, Hur SH, Cho YK, Park HS, Yoon HJ, Kim H, Chung IS, Kim YN, Kim KB, Doh JH and others. Relation of fractional flow reserve after drug-eluting stent implantation to one-year outcomes. *Am J Cardiol* 2011;107(12):1763-7.
22. Agarwal SK, Kasula S, Almomani A, Hacioglu Y, Ahmed Z, Uretsky BF, Hakeem A. Clinical and angiographic predictors of persistently ischemic fractional flow reserve after percutaneous revascularization. *Am Heart J* 2017;184:10-16.
23. Doh JH, Nam CW, Koo BK, Lee SY, Choi H, Namgung J, Kwon SU, Kwak JJ, Kim HY, Choi WH and others. Clinical Relevance of Poststent Fractional Flow Reserve After Drug-Eluting Stent Implantation. *J Invasive Cardiol* 2015;27(8):346-51.
24. Kimura Y, Tanaka N, Okura H, Yoshida K, Akabane M, Takayama T, Hirayama A, Tada T, Kimura T, Takano H and others. Characterization of real-world patients with low fractional flow reserve

- immediately after drug-eluting stents implantation. *Cardiovasc Interv Ther* 2016;31(1):29-37.
25. Leesar MA, Satran A, Yalamanchili V, Helmy T, Abdul-Waheed M, Wongpraparut N. The impact of fractional flow reserve measurement on clinical outcomes after transradial coronary stenting. *EuroIntervention* 2011;7(8):917-23.
 26. Wolfrum M, Fahrni G, de Maria GL, Knapp G, Curzen N, Kharbanda RK, Frohlich GM, Banning AP. Impact of impaired fractional flow reserve after coronary interventions on outcomes: a systematic review and meta-analysis. *BMC Cardiovasc Disord* 2016;16(1):177.
 27. van Bommel RJ, Masdjedi K, Diletti R, Lemmert ME, van Zandvoort L, Wilschut J, Zijlstra F, de Jaegere P, Daemen J, van Mieghem NMDA. Routine Fractional Flow Reserve Measurement After Percutaneous Coronary Intervention. *Circ Cardiovasc Interv* 2019;12(5):e007428.
 28. Li SJ, Ge Z, Kan J, Zhang JJ, Ye F, Kwan TW, Santoso T, Yang S, Sheiban I, Qian XS and others. Cutoff Value and Long-Term Prediction of Clinical Events by FFR Measured Immediately After Implantation of a Drug-Eluting Stent in Patients With Coronary Artery Disease: 1- to 3-Year Results From the DKCRUSH VII Registry Study. *JACC Cardiovasc Interv* 2017;10(10):986-995.
 29. van Zandvoort LJC, Masdjedi K, Witberg K, Ligthart JMR, Tovar Forero MN, Diletti R, Lemmert ME, Wilschut J, de Jaegere PPT, Boersma E and others. Explanation of Postprocedural Fractional Flow Reserve Below 0.85. *Circ Cardiovasc Interv* 2019;12(2):e007030.
 30. Siebert U, Arvandi M, Gothe RM, Bornschein B, Eccleston D, Walters DL, Rankin J, De Bruyne B, Fearon WF, Pijls NH and others. Improving the quality of percutaneous revascularisation in patients with multivessel disease in Australia: cost-effectiveness, public health implications, and budget impact of FFR-guided PCI. *Heart Lung Circ* 2014;23(6):527-33.
 31. van Nunen LX, Zimmermann FM, Tonino PA, Barbato E, Baumbach A, Engstrom T, Klaus V, MacCarthy PA, Manoharan G, Oldroyd KG and others. Fractional flow reserve versus angiography for guidance of PCI in patients with multivessel coronary artery disease (FAME): 5-year follow-up of a randomised controlled trial. *Lancet* 2015;386(10006):1853-60.
 32. Gotberg M, Christiansen EH, Gudmundsdottir IJ, Sandhall L, Danielewicz M, Jakobsen L, Olsson SE, Ohagen P, Olsson H, Omerovic E and others. Instantaneous Wave-free Ratio versus Fractional Flow Reserve to Guide PCI. *N Engl J Med* 2017;376(19):1813-1823.
 33. Davies JE, Sen S, Dehbi HM, Al-Lamee R, Petraco R, Nijjer SS, Bhindi R, Lehman SJ, Walters D, Sapontis J and others. Use of the Instantaneous Wave-free Ratio or Fractional Flow Reserve in PCI. *N Engl J Med* 2017;376(19):1824-1834.
 34. Jeremias A, Davies JE, Maehara A, Matsumura M, Schneider J, Tang K, Talwar S, Marques K, Shammam NW, Gruberg L and others. Blinded Physiological Assessment of Residual Ischemia After Successful Angiographic Percutaneous Coronary Intervention: The DEFINE PCI Study. *JACC Cardiovasc Interv* 2019;12(20):1991-2001.
 35. Tu S, Barbato E, Koszegi Z, Yang J, Sun Z, Holm NR, Tar B, Li Y, Rusinaru D, Wijns W and others. Fractional flow reserve calculation from 3-dimensional quantitative coronary angiography and TIMI frame count: a fast computer model to quantify the functional significance of moderately obstructed coronary arteries. *JACC Cardiovasc Interv* 2014;7(7):768-77.
 36. Papafaklis MI, Muramatsu T, Ishibashi Y, Lakkas LS, Nakatani S, Bourantas CV, Ligthart JMR, Onuma Y, Echavarría-Pinto M, Tzirka G and others. Fast virtual functional assessment of intermediate coronary lesions using routine angiographic data and blood flow simulation in humans: comparison with pressure wire - fractional flow reserve. *EuroIntervention* 2014;10(5):574-83.
 37. Tu S, Westra J, Yang J, von Birgelen C, Ferrara A, Pellicano M, Nef H, Tebaldi M, Murasato Y, Lansky A and others. Diagnostic Accuracy of Fast Computational Approaches to Derive Fractional Flow Reserve From Diagnostic Coronary Angiography: The International Multicenter FAVOR Pilot Study. *JACC Cardiovasc Interv* 2016;9(19):2024-2035.
 38. Xu B, Tu S, Qiao S, Qu X, Chen Y, Yang J, Guo L, Sun Z, Li Z, Tian F and others. Diagnostic Accuracy of Angiography-Based Quantitative Flow Ratio Measurements for Online Assessment of Coronary Stenosis. *J Am Coll Cardiol* 2017;70(25):3077-3087.
 39. Fearon WF, Achenbach S, Assali TEA, Jeremias RSA, Fournier S, Kirtane AJ, Kornowski R, Greenberg G, Jubeh R, Kolansky DM and others. Accuracy of Fractional Flow Reserve Derived From Coronary Angiography. *Circulation* 2018.
 40. Asano T, Katagiri Y, Collet C, Tenekecioglu E, Miyazaki Y, Sotomi Y, Amoroso G, Aminian A, Brugaletta S, Vrolix M and others. Functional comparison between the BuMA Supreme biodegradable polymer sirolimus-eluting stent and a durable polymer zotarolimus-eluting coronary stent using quantitative flow ratio: PIONEER QFR substudy. *EuroIntervention* 2018;14(5):e570-e579.
 41. Biscaglia S, Tebaldi M, Brugaletta S, Cerrato E, Erriquez A, Passarini G, Ielasi A, Spitaleri G, Di Girolamo D, Mezzapelle G and others. Prognostic Value of QFR Measured Immediately After Successful Stent Implantation: The International Multicenter Prospective HAWKEYE Study. *JACC Cardiovasc Interv* 2019;12(20):2079-2088.
 42. Ely Pizzato P, Samdani AJ, Vergara-Martel A, Palma Dallan LA, Tensol Rodrigues Pereira G, Zago E, Zimin V, Grando Bezerra H. Feasibility of coronary angiogram-derived vessel fractional flow reserve in the setting of standard of care percutaneous coronary intervention and its correlation with invasive FFR. *Int J Cardiol* 2020;301:45-49.
 43. Agarwal SK, Kasula S, Hacioglu Y, Ahmed Z, Uretsky BF, Hakeem A. Utilizing Post-Intervention Fractional Flow Reserve to Optimize Acute Results and the Relationship to Long-Term Outcomes. *JACC Cardiovasc Interv* 2016;9(10):1022-31.
 44. Beygui F, Lemaitre A, Bignon M, Wain-Hobson J, Briet C, Ardouin P, Sabatier R, Parienti JJ, Blanchart K, Roule V. A head-to-head comparison of three coronary fractional flow reserve measurement technologies: The fractional flow reserve-device study. *Catheter Cardiovasc Interv* 2019.
 45. Menon M, Jaffe W, Watson T, Webster M. Assessment of coronary fractional flow reserve using a monorail pressure catheter: the first-in-human ACCESS-NZ trial. *EuroIntervention* 2015;11(3):257-63.

Chapter 15



Coronary physiology assessment in a cardiac transplant patient

van Zandvoort LJC, Masdjedi K, Tovar Forero MN, Manintveld O, Daemen J,.

Erasmus University Medical Center, Thoraxcenter, Department of cardiology, Rotterdam, the Netherlands

Neth Heart J. 2019;27(7-8):385-6.

A 39-year-old male received a coronary angiography, 14 years after cardiac allograft transplantation, indicating a significant lesion in the left coronary artery (LAD). Coronary angiography revealed an intermediate lesion in the LAD, for which further physiological assessment was considered necessary. (Figure 1). Subsequent pressure wire based FFR_{pw} was 0.87, suggesting a non-significant lesion, however non-hyperemic 3D based quantitative coronary angiography based vessel fractional flow reserve (vFFR) was 0.74 (Figure 1B). Given the discrepancies, optical coherence tomography was performed showing a fibrofatty plaque with a minimal lumen area (MLA) of 1.70mm^2 . The LAD was subsequently treated with a $3.0 \times 15\text{mm}$ stent. There has been ongoing debate on the validity of using FFR in denervated hearts due to high rates of microvascular dysfunction and an unreliable hyperemic response¹. Anatomical based assessment might be the preferable choice to assess the significance of intermediate coronary lesions in denervated hearts^{2,3}.

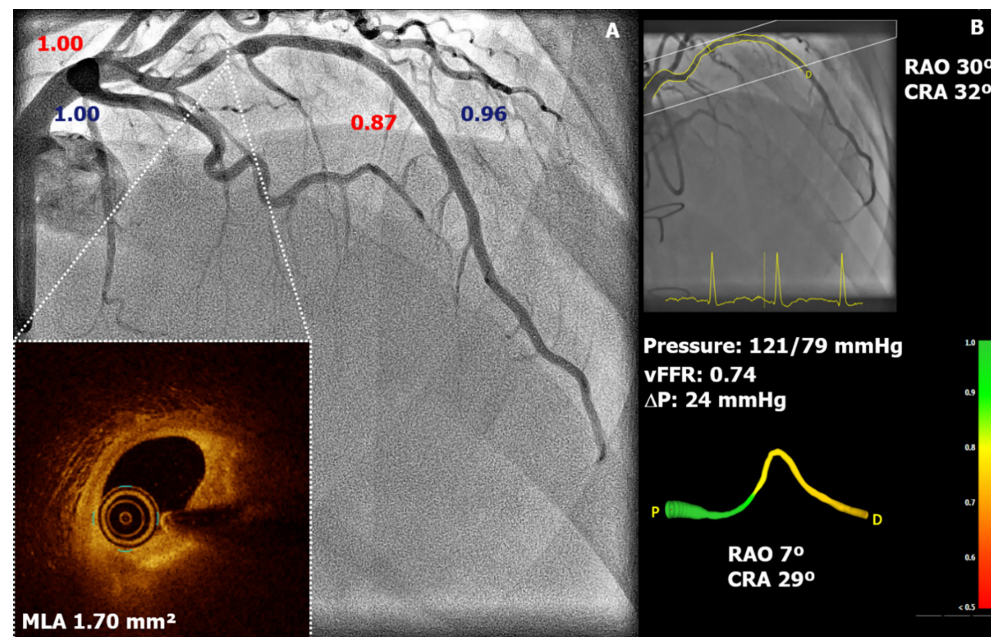


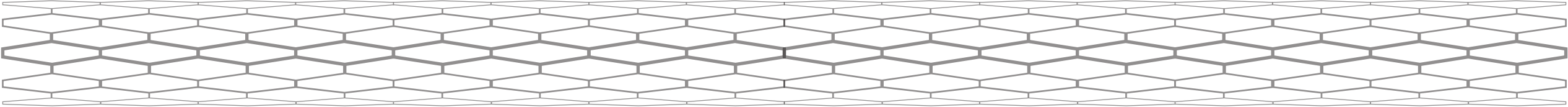
Figure 1.

A: Coronary angiography of a patient, 14 years after allograft cardiac transplant. The LAD shows an angiographic intermediate stenosis in the mid segment, Pd/Pa values in blue and FFR values in red. Optical coherence tomography of the LAD shows a 15 mm lesion with a minimal lumen area (MLA) of 1.70mm^2 and appropriate landing zones. B: Vessel fractional flow reserve (vFFR) of the LAD. The vFFR is 0.74, which indicates a significant lesion (threshold ≤ 0.80).

REFERENCES

1. De Bruyne B, Fearon WF, Pijls NHJ, et al. Fractional flow reserve-guided PCI for stable coronary artery disease. *N Engl J Med.* 2014;1533-4406.
2. Douglas PS, Pontone G, Hlatky MA, Patel MR, et al. Clinical outcomes of fractional flow reserve by computed tomographic angiography-guided diagnostic strategies vs. usual care in patients with suspected coronary artery disease: the prospective longitudinal trial of FFR(CT): outcome and resource impacts study. *European Heart Journal.* 2015;36(47):3359-67.
3. Masdjedi K. Validation of novel three-dimensional quantitative coronary angiography based software to calculate vessel FFR: the FAST study. *Novel approaches to coronary physiology.* Oral presentation. EuroPCR, Paris: 2018.

Chapter 16



Validation of Resting Diastolic Pressure Ratio Calculated by a Novel Algorithm and Its Correlation With Distal Coronary Artery Pressure to Aortic Pressure, Instantaneous Wave-Free Ratio, and Fractional Flow Reserve, The dPR Study

Ligthart JMR*, Masdjedi K*, Witberg K, Mastik F, van Zandvoort LJC, Lemmert ME, Wilschut J, Diletti R, de Jaegere PPT, Zijlstra F, Kardys I, van Mieghem NMDA, Daemen J

* Both authors contributed equally to this paper

Erasmus University Medical Center, Thoraxcenter, Department of cardiology, Rotterdam, the Netherlands

Circ Cardiovasc Interv. 2018;11(12):e006911.

ABSTRACT

Background: Instantaneous wave free ratio (iFR) offers a reliable non-hyperemic assessment of coronary physiology but requires dedicated proprietary software with a fully automated algorithm. We hypothesized that diastolic pressure ratio (dPR), calculated with novel universal software, has a strong correlation with iFR, similar diagnostic accuracy relative to resting Pd/Pa and Fractional Flow Reserve (FFR).

Methods and results: An observational, prospective, single-center cohort study including patients who underwent iFR or FFR. Dedicated software was used to calculate the dPR from DICOM pressure waveforms. The “flat” period on the dP/dt signal was used to detect automatically the period, where the resistance is low and constant, and to calculate the dPR, which is an average over five consecutive heartbeats.

The software was validated by correlating iFR results with dPR. Software validation was done by comparing 78 iFR measurements in 44 patients who underwent iFR. Mean iFR and dPR were 0.91 ± 0.10 and 0.92 ± 0.10 respectively, with a significant linear correlation ($R=0.997$; $p<0.001$). Diagnostic accuracy was tested in 100 patients who underwent FFR. Mean FFR, resting Pd/Pa and dPR were 0.85 ± 0.09 ; 0.94 ± 0.05 ; 0.93 ± 0.07 respectively. There was a significant linear correlation between dPR and FFR ($R = 0.77$; $p<0.001$). Both Pd/Pa and dPR had good diagnostic accuracy in the identification of lesions with an FFR ≤ 0.80 (AUC 0.84 (95% CI: 0.76-0.92) and 0.86 (95% CI: 0.78 to 0.93) respectively).

Conclusion: dPR, calculated by a novel validated software tool, showed a strong linear correlation with iFR. dPR correlated well with FFR with a good diagnostic accuracy to identify positive FFR.

INTRODUCTION

As compared to angiography guided percutaneous coronary intervention (PCI), Fractional Flow Reserve (FFR) guided PCI has been shown to significantly improve patient outcomes and cost-effectiveness and is currently considered the gold standard to identify the hemodynamic severity of coronary artery stenosis ¹⁻⁶. However, the concept of FFR which is based on maximum hyperemic conditions requiring intracoronary or intravenous hyperemic agents with potential side effects like dyspnea, chest pain and arrhythmias ⁷.

In recent years, non-hyperemic pressure ratios (NHPR), such as the instantaneous wave-free ratio (iFR) and resting distal coronary artery pressure/aortic pressure (Pd/Pa), were introduced as alternative invasive indices to assess the severity of coronary artery stenosis ^{8,9}. While Pd/Pa presents the ratio from the mean resting distal pressure to aortic coronary pressure during the whole cardiac cycle, iFR is based on the same ratio measured during the so-called “wave-free period”, a period during diastole in which the microvascular resistance is low, and constant. As compared to FFR, the diagnostic accuracy of iFR has been assumed to be slightly better than Pd/Pa ¹⁰. While Pd/Pa can be calculated from any type of pressure wire or microcatheter, the algorithm of iFR belongs to the iFR core laboratory (Imperial College, London, United Kingdom) and its use is restricted to the proprietary software of a single vendor (Philips Volcano)

The aim of this study was to validate the diastolic pressure ratio (dPR), calculated using novel software applicable to any type of pressure wire or microcatheter, to assess the correlation of dPR with iFR and to assess the diagnostic accuracy of dPR as compared to FFR and resting Pd/Pa.

METHODS

Study design and patient population

Dedicated software was developed in the Erasmus Medical Center (Erasmus MC) (FM, JL, KW). The software was designed to calculate a dPR from DICOM pressure tracings generated by any type of pressure wire or catheter using either electrical (Piezo-Resistive) or optical sensors and from spreadsheet data (csv file), provided by the S5i console (Volcano Corporation, Rancho Cordova, California; FFR software version 2.4.1.2723) offline. The dPR study consisted of two parts: 1) validation of the dPR software with original iFR results and 2) assessment of the correlation of dPR with FFR and its diagnostic accuracy for identification of positive FFR.

For the purpose of this retrospective study patients were not subjected to study

interventions, neither was any mode of behavior imposed, otherwise than as part of their regular treatment. Therefore according to Dutch law, no formal approval was required. This study was conducted according to the privacy policy of the Erasmus MC and to the Erasmus MC regulations for the appropriate use of data in patient orientated research, which are based on international regulations, including the declaration of Helsinki. All patients consented to the use of their data for scientific research.

The data, analytic methods, and study materials will not be made available to other researchers for purposes of reproducing the results or replicating the procedure.

Coronary angiography and calculation of dPR

All procedures were performed according to standard local clinical practice. Pressure measurements were performed after an intracoronary bolus of nitrates (100-200 μg), in case there was doubt regarding the hemodynamic significance of intermediate coronary artery lesions. Pd/Pa was defined as the ratio of mean distal coronary artery pressure to mean aortic pressure in the resting state during the whole cardiac cycle. FFR was defined as lowest ratio of mean distal coronary artery pressure divided by mean aortic pressure during maximum hyperemia achieved by continuous intravenous infusion of adenosine at a rate of 140 $\mu\text{g}/\text{kg}/\text{min}$ through an antecubital vein. The dPR was defined by the ratio between the mean diastolic pressure distal to the stenosis and the mean diastolic aortic pressure in resting conditions. The diastolic period used to calculate the dPR was automatically delineated based on the dP/dt curve of the aortic pressure at the point at which the resistance was low, constant and stable. The dP/dt curve represents the increase and decrease of the pressure over time during the heart cycle. dP is the pressure difference between sample points and dt is the time difference between the same sample points. The "flat line" of the dP/dt tracing was used as trigger for the software to detect the "wave-free period" within the range of 60-80% of the cardiac phase as a first default. Because of this range the wave-free period detected by dP/dt tracing can be shorter than the wave-free period detected by original iFR. Both original iFR and calculated dPR values were stored in a spreadsheet, created by the dPR software and from each measurement a graphic representation was provided in PDF format (Figure 1), showing the pressure and dP/dt tracings together with the triggered regions and region of interest (ROI) to calculate dPR.

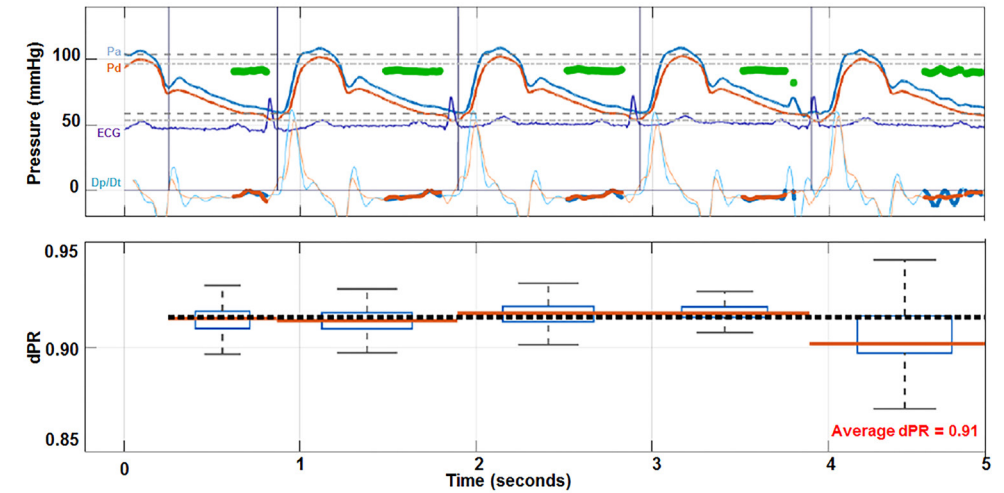


Figure 1. Sample tracing of the ECG, Aortic Pressure and dP/dt with the effect of different periods in the heart cycle

Calculation of the index (dPR) during diastole by automatically indicating the "flat" period of the dP/dt signal in 5 consecutive heartbeats.

Validation with iFR

A total of 78 iFR measurements from 44 patients were used for the validation step. iFR measurements were performed using the Verrata[®] pressure wire along with the original proprietary software (Philips Volcano). The csv spreadsheet files were imported in the software. The spreadsheet values of the reference aortic pressure and the wire pressure signals were used by the software to automatically analyze the dP/dt tracing and calculate the corresponding dPR based on 5 consecutive heart beats.

Validation with FFR

From April 2017 through September 2017, patients referred for coronary angiography for stable or unstable coronary artery disease and an indication to perform FFR, were included. A consecutive cohort of 100 patients with adequate pressure tracings was enrolled. DICOM recorded tracings derived from either a Pressure Wire (Pressure Wire[™] X, Abbott Vascular, Santa Clara, CA, USA) or micro catheter (Navvus, ACIST Medical Systems, Eden Prairie, MN, USA) were eligible. Pressure waveforms were automatically exported to Siemens Sensis[®], converted to DICOM and stored in a local hospital database.

Statistical analysis

Continuous variables are presented as mean ±standard deviation. All continuous variables were normally distributed. Categorical variables are expressed as frequencies (n) and percentages (%). All statistical tests are 2-tailed. Pearson’s correlation coefficient (R) was used to assess the relationship between the several indices. Agreement between the indices and the inter-observer variability were assessed by Bland-Altman plots with corresponding 95% limits of agreement. Receiver-operating characteristic (ROC) area under the curve (AUC) analysis was used to estimate the diagnostic accuracy of dPR as compared to FFR with a threshold of ≤0.80. Statistical analysis was carried out using the SPSS statistical package version 21 (IBM, Armonk, North Castle, New York, USA).

RESULTS

Validation with iFR

A total of 44 patients (age 70±10, 70% male) presenting with stable or unstable coronary artery disease underwent iFR measurements in 78 vessels (LAD n=38, LCX n=22, RCA n=18). Baseline characteristics of the iFR cohort are summarized in Table 1. Mean iFR and dPR were 0.91±0.10 and 0.92±0.10 respectively. An excellent correlation was found between both indices; (R = 0.997; p<0.001); Mean bias -0.0016±0.084), (Figure 2).

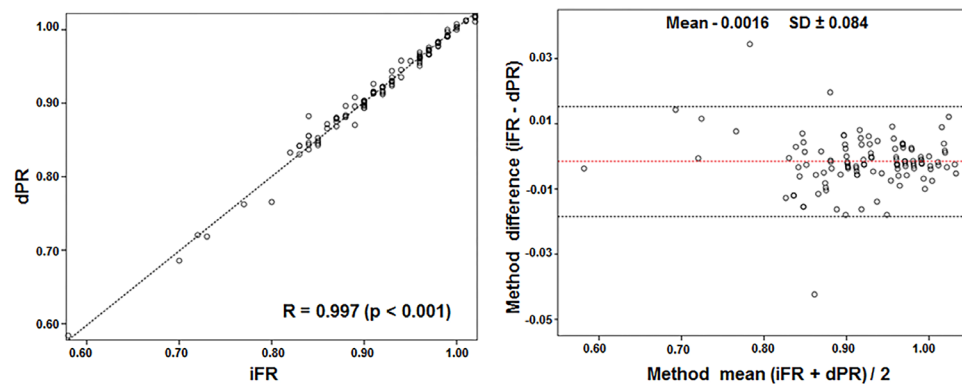


Figure 2. Scatter Plot showing the relationship between the iFR and dPR (left panel) and Bland- Altman plots of difference against the mean (right panel)

The mean bias is represented by the solid red line and the 95% confidence interval is represented by the dashed lines. Abbreviations as in Table 1.

Table 1. Baseline characteristics iFR cohort

	Total (N=48)
Age, y mean (±SD)	70 (10)
Male sex, n (%)	31 (70)
<u>Clinical indication procedure, n (%)</u>	
Stable angina	32 (67)
Unstable angina	2 (4)
Non ST segment elevation MI	14 (29)
<u>Cardiovascular risk factors, n (%)</u>	
Hypertension	23 (52)
Hyperlipidemia	17 (38)
Diabetes Mellitus	14 (32)
Smoker	8 (18)
Family history of CVD	16 (36)
<u>Co-morbidity, mean (±SD)</u>	
Creatinine µmol/L	111 (46)
Hemoglobine (mmol/L)	8.1 (1.2)
BMI	27 (4)
<u>Measured vessel Lesions, n (%)</u>	
Left anterior descending artery	38 (49)
Left circumflex artery	22 (28)
Right coronary artery	18 (23)
<u>Indices, mean (±SD)</u>	
iFR	0.91 (0.10)
dPR	0.92 (0.10)

Values are n, mean±SD of n (%); BMI =Body Mass Index; CVD =cardiovascular disease; dPR =resting diastolic pressure ratio; iFR =instantaneous wave-free ratio; MI =myocardial infarction.

Patient demographics and procedural data of the FFR cohort

Baseline and procedural characteristics of the FFR cohort are summarized in Table 2.

Table 2. Baseline characteristics of FFR cohort

	Total cohort	FFR _{MC} (N=50)	FFR _{PW} (N=50)	p value
Age, y mean (±SD)	66 (11)	67 (13)	66 (8)	0.94
Male sex, n (%)	80 (80)	39 (78)	41 (82)	0.62
<u>Clinical indication procedure, n (%)</u>				
Stable angina	56 (56)	20 (40)	36 (72)	0.001
Unstable angina	11 (11)	7 (14)	4 (8)	0.34
Non ST segment elevation MI	33 (33)	23 (46)	10 (20)	0.01
<u>Cardiovascular risk factors, n (%)</u>				
Hypertension	65 (65)	34 (68)	31 (62)	0.53
Hyperlipidemia	55 (55)	26 (52)	29 (58)	0.55
Diabetes Mellitus	22 (22)	12 (24)	10 (20)	0.63
Smoker	18 (18)	11 (22)	7 (14)	0.30
Family history of CVD	27 (27)	17 (34)	10 (20)	0.12
<u>Co-morbidity, mean (±SD)</u>				
Creatinine µmol/L	96 (46)	96 (40)	97 (50)	0.94
Hemoglobine (mmol/L)	8.5 (1.1)	8.6 (1.0)	8.3 (1.1)	0.27
BMI	28 (4)	28 (5)	27 (4)	0.25
<u>Measured vessel Lesions, n (%)</u>				
Left anterior descending artery	67 (67)	34 (68)	33 (66)	0.83
Left circumflex artery	14 (14)	6 (12)	8 (16)	0.57
Right coronary artery	19 (19)	10 (20)	9 (18)	0.80
<u>Indices, mean (±SD)</u>				
Resting Pd/Pa	0.94 (0.05)	0.94 (0.05)	0.94 (0.05)	0.73
FFR	0.85 (0.09)	0.85 (0.08)	0.85 (0.09)	1.00
dPR	0.93 (0.07)	0.93 (0.06)	0.92 (0.07)	0.87

Values are n, mean ±SD of n (%); BMI= Body Mass Index; CVD =cardiovascular disease; dPR =resting diastolic pressure ratio; FFR =Fractional Flow Reserve; FFR_{PW} =FFR measured by pressure wire system; FFR_{MC} =FFR measured by the Acist FFR wire system; MI =myocardial infarction; Pd/Pa =resting distal to aortic coronary pressure.

Mean age was 66 years and the majority of patients were male (80%). Clinical presentation was stable angina (56%), unstable angina (11%) and non ST segment elevation myocardial infarction (33%). Diabetes was present in 22% of the cases. The majority of the FFR measurements were performed in the left anterior descending artery (67%). The left circumflex artery and the right coronary artery were measured in 14% and 19% of the cases respectively.

Relationship between dPR, Pd/Pa and FFR

Mean FFR, resting Pd/Pa and dPR were 0.85±0.09, 0.94±0.05 and 0.93±0.07 respectively (Table 2). A good linear correlation was found between dPR and FFR (R = 0.77; p<0.001) (Figure 3). The linear correlation between FFR and Pd/Pa was 0.81 (p<0.001). The correlation between FFR as measured using the Navvus system (FFR_{MC}) and dPR was higher as compared to pressure wire based FFR (FFR_{PW}) and dPR (R =0.81 vs R =0.76 respectively). dPR showed to have good diagnostic accuracy in the identification of patients with FFR values ≤0.80 (AUC of 0.86 [95% CI: 0.78-0.93]). Comparable results applies to Pd/Pa as well (AUC of 0.84 [95% CI: 0.76 – 0.92]) (Figure 4). The optimal cutoff value for an FFR ≤0.80 derived from the ROC analyses was 0.91 for dPR and 0.92 for Pd/Pa.

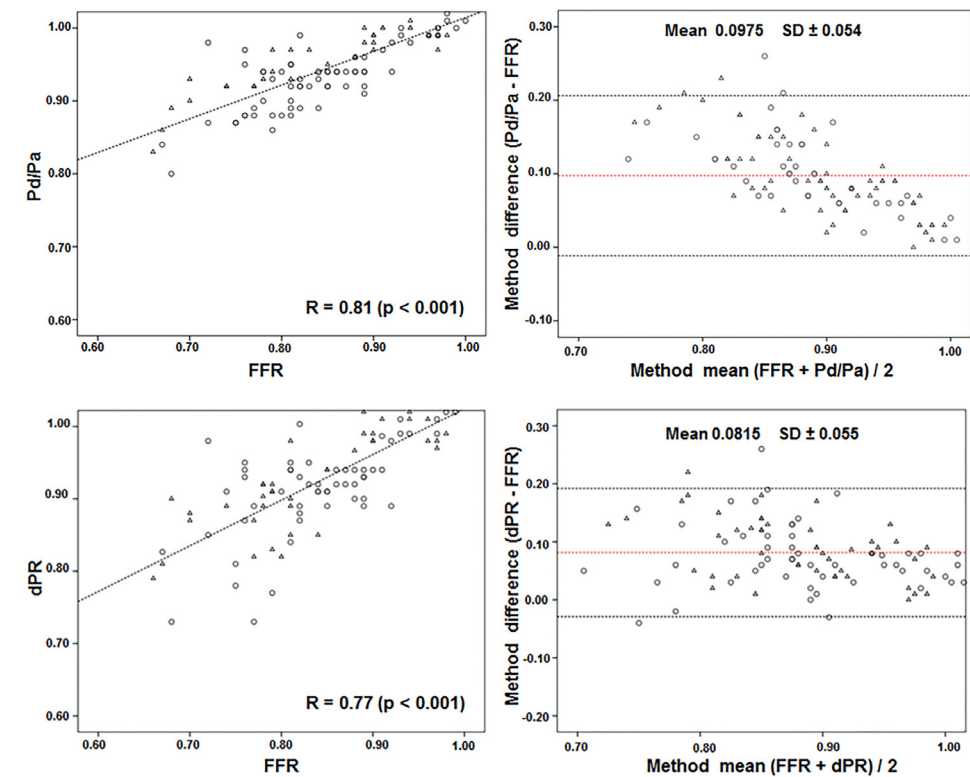


Figure 3. Scatter Plot showing the relationship between FFR and two different resting indices (Pa/Pa and dPR) and Bland- Altman plots of difference against the mean

The mean bias is represented by the solid red line and the 95% confidence interval is represented by the dashed lines. Abbreviations as in Table 1 and 2. Δ represents FFR measurements as measured using the Navvus system (FFR_{MC}) and O represents pressure wire based FFR measurements (FFR_{PW})

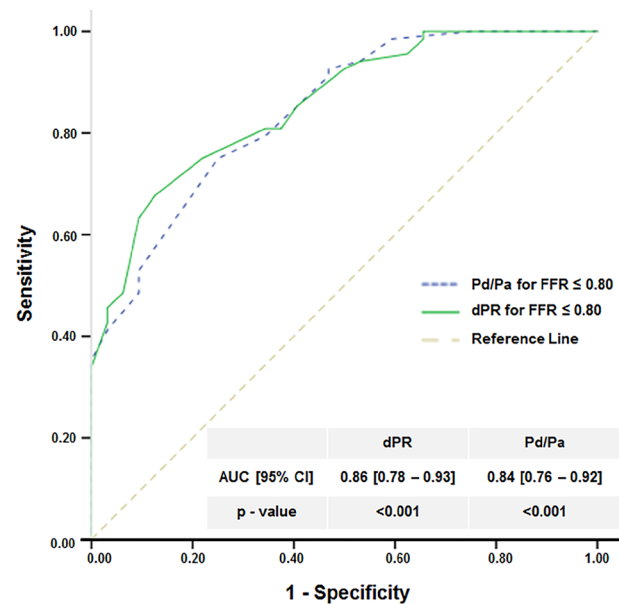


Figure 4. ROC Curves for dPR and Pd/Pa. Comparisons are made with an FFR at a cut point of 0.80. Abbreviations as in Table 1.

DISCUSSION

In the present study, we demonstrated the feasibility of using a non-hyperemic pressure ratio, the dPR, calculated using novel software applicable to any type of pressure wire or microcatheter. dPR had an excellent linear correlation with iFR and a strong diagnostic accuracy in identifying lesions with an FFR ≤ 0.80 .

FFR has become the gold standard to determine the severity of epicardial coronary stenoses and myocardial ischemia based on studies demonstrating significantly better outcomes with FFR-guided PCI as compared to angiography guided PCI^{5, 4, 6, 11, 12}. Nevertheless, despite strong guideline recommendations and increasing evidence on its cost-effectiveness, the adoption of FFR in routine clinical practice remains low¹³⁻¹⁶. The latter has been linked to reimbursement issues and the need for hyperemic agents. Hyperemic agents like intravenous adenosine might provoke transient dyspnea, chest pain, vomiting, rhythm disturbances and hypotension in up to 37.5% of the cases^{8, 9}. For these reasons the search for cheaper, faster and more patient-friendly methods remains relevant and several studies assessed the concept of the adenosine-independent index iFR as an alternative method to assess lesion severity. As mentioned, the concept of FFR

is based on maximum hyperemic conditions necessitating the use of intravenous hyperemic agents. Nevertheless, even during hyperemia, intracoronary resistance is not static but instead fluctuates in a phasic pattern throughout the cardiac cycle with the lowest resistance during diastole due to decompression of the microvasculature and due to the lowest difference in pressure between the aorta and the coronary artery during diastole¹⁷. The iFR concept relies on the theory that intracoronary resistance is naturally low, constant and stable during the “wave-free” period precluding the need for hyperemic agents¹⁸. iFR had a high diagnostic accuracy to predict positive or negative FFR values. More recently, iFR guided PCI demonstrated to be non-inferior to FFR in reducing a composite of death from any cause, nonfatal myocardial infarction or unplanned revascularization within 12 months^{8, 9}. However, in a pooled meta-analysis of this two trials, a numeric excess in the incidence of death and myocardial infarction was found in the iFR group¹⁹. Although no large scale randomized outcome studies are available on the efficacy of Pd/Pa as compared to FFR-guided revascularization, iFR appeared more sensitive than Pd/Pa to differentiate stenosis severity and showed a lower maximum difference in estimated major adverse cardiac event risk influenced by the measurement variability compared with resting Pd/Pa¹⁰. The latter supports the concept of applying the diastolic period to calculate pressure gradients when refraining from the use of hyperemic agents. At present, the use of iFR is restricted to the use of a single device and software (Philips Volcano) whereas a large variety of pressure wires and microcatheters are available to measure Pd/Pa and FFR. In the current study, we demonstrated the feasibility of a fast, simple and reproducible method of measuring a dPR based on non-hyperemic DICOM pressure waveforms derived from either PW or microcatheter devices which could open up the field for a more widespread use of diastolic pressure gradients in real world clinical practice. By using a simple software tool to automatically detect the flat period in the dP/dt curve that indicates the so called “wave-free” period we found that the resultant dPR correlated nearly perfect with the original iFR output of Phillips Volcano ($r=0.997$, $p<0.001$). Subsequently, our results showed a correlation between dPR and FFR ($r=0.77$) in line with previous results from the VERIFY study demonstrating a correlation coefficient r of 0.789 between iFR and FFR²⁰. Additionally, dPR showed a high diagnostic accuracy in the identification of patients with FFR values ≤ 0.80 (AUC of 0.86 (95% CI: 0.78-0.93)) while the AUC was 0.84 (95% CI: 0.76 – 0.92) for Pd/Pa. Also these results are in line with previous findings as published in the Resolve study in which the AUC was 0.81 and 0.82 for iFR and Pd/Pa respectively²¹. In the present study, we used the flat period of the dP/dt signal to identify the “wave free period”. While during this period in diastole there is the least amount of pressure variation between aortic and

distal pressures, it allowed us to develop software using the same methodology in any pressure-wire or microcatheter. It is likely that using either period during diastole to compute the dPR would result in equal results. van 't Veer et al. looked at the correlation between iFR and resting indices during different parts of the diastole by using a simple Matlab algorithm and concluded that all diastolic resting indices were identical to iFR²². Therefore, any diastolic resting index can be used with the same advantages and disadvantages inherent within iFR. However, in our validation cohort of 78 iFR measurements we found two cases with a bias beyond the 95% confidence interval. Analysis of these cases (Figure 5) showed that the dP/dt triggered a shorter “wave-free” period, resulting in a shorter ROI, in one case positioned earlier in the heart sequence, resulting in a lower dPR ratio compared to iFR, in the other case positioned later in the heart sequence, resulting in a higher dPR as compared to iFR. In conclusion, the length of the interval used in the present algorithm depends on the length of the flat line on dP/dt waveform which might slightly differ per cardiac cycle. Conclusions about accuracy of iFR versus dPR and correlation to FFR cannot be drawn based on these two cases but warrant further research.

Kobayashi et al. looked at the influence of lesion location on the diagnostic accuracy of resting indices contrast FFR (cFFR), iFR and Pd/Pa and found that this three resting indices are less accurate in left main and proximal ramus descendens artery lesions as compared to other lesion locations²³. The authors in the VERIFY 2 study, hypothesized that in comparison with FFR, revascularization decisions based on either binary cutoff values for iFR and Pd/Pa or hybrid strategies incorporating iFR or Pd/Pa will result in similar levels of disagreement. They found that binary cutoff values for iFR and Pd/Pa result in misclassification of 1 in 5 lesions²⁴. We know that perfusion of the left coronary artery is predominantly diastolic while the perfusion of right coronary artery is both systolic and diastolic, due to lower pressure in the right ventricle as compared to the left ventricle.

While the diagnostic accuracy of NHPR in predicting positive FFR in general might differ between left and right sided assessments, we do not see any reason to believe that any difference might be expected in the diagnostic accuracy of dPR as compared to iFR.

Thereby, our study population is too small to analyze the differences between different lesion locations and between right (19%) vs left coronary artery (81%) (Table 2). However, we think there is no reason to believe that the dPR calculated based on dP/dt has superior diagnostic accuracy as any of the other resting indices. Finally, small previous studies demonstrated a good correlation

between FFR_{MC} and FFR_{PW} however also suggested an overestimation of FFR with FFR_{MC} compared to FFR_{PW} by approximately 1%²⁵. While in the present study mean FFR_{MC} and FFR_{PW} were similar, the correlation between FFR_{MC} and dPR was higher as compared to FFR_{PW} and dPR ($R=0.81, p<0.001$ and $R=0.76, p<0.001$ respectively). We assume that the fact that the microcatheter was used merely for post-PCI FFR measurements, with subsequently lower pressure gradient, might have impacted our findings. Larger studies are needed to confirm any differences in optimal cut-off values for both devices.

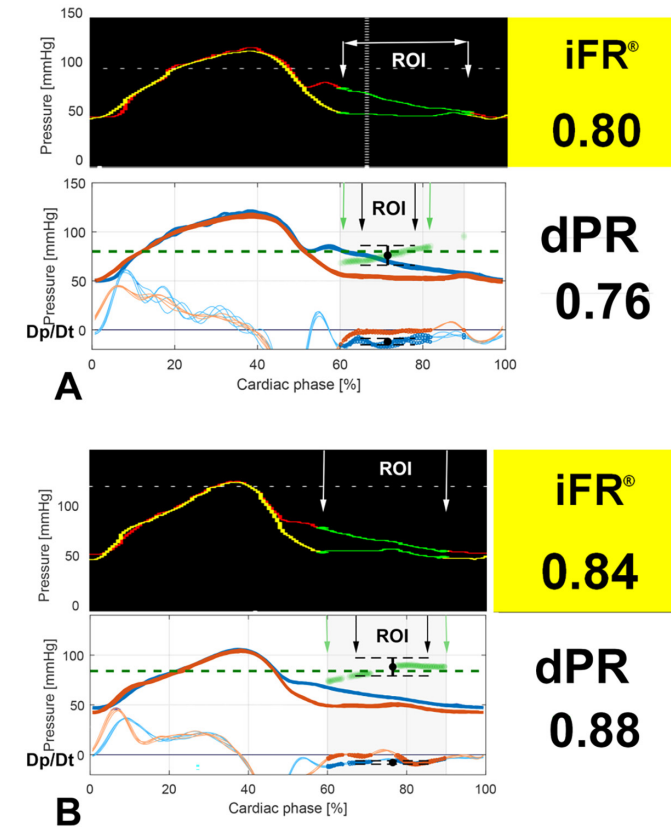


Figure 5. Explanation of discrepancy between iFR and dPR

Two cases with a bias beyond the 95% confidence. Compared to iFR, dPR software triggers a shorter region of interest (ROI). Depending on the position of the ROI in the sequence this may result in a higher or lower Pd/Pa ratio compared to iFR. Case A: iFR includes a region with a “lump” in the distal pressure, dPR detected a “lump” in Dp/Dt and did not include the region beyond this “lump”, positioned the ROI earlier in the sequence, resulting in a lower ratio. Case B: dPR ignored a steeper region in the Dp/Dt signal, positioned the ROI later in middle of the sequence, resulting in a higher Pd/Pa ratio compared to iFR.

Limitations

The present results are based on a single center experience in which we restricted our analyses to those recordings with undamped pressure wave forms. The latter could have artificially influenced our results since recent core laboratory study data, assessing the prevalence of erroneous or suboptimal FFR measurements in clinical practice, demonstrated that in up to 30% of the recordings, pressure signals were inadequate²⁶. In order not to be biased by measurements and results based on dampening pressure waveforms which might have biased the final FFR, iFR or Pd/Pa we scrutinized the pressure waveforms from tracings in the cases selected. In order to be able to mitigate to amount of bias caused by dampened pressure waveforms, we only selected cases in which pressure tracings and waveforms were adequate. Furthermore, Navvus microcatheter may confound the relationship with stenosis severity, which may be relevant when considering relationships between Pd/Pa and FFR. However, all included vessels in the present study were >2.5mm and that makes the comparison more reliable.

CONCLUSION

Resting diastolic pressure ratio (dPR), calculated by a novel algorithm, had an excellent correlation with iFR, a high linear correlation to both Pd/Pa and FFR and a better diagnostic accuracy as compared to Pd/Pa.

Acknowledgement

We would like to thank Rutger den Boer for his careful revision of the manuscript and help in developing the modified version of the RUBO software application to test our concept. A manual calculation method of dPR is implemented in the RuboMed DICOM viewer (Rubo Medical Imaging BV, Aerdenhout, the Netherlands: www.rubomedical.com).

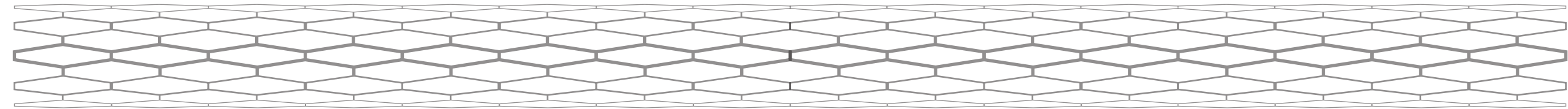
REFERENCES

1. De Bruyne B, Fearon WF, Pijls NH, Barbato E, Tonino P, Piroth Z, Jagic N, Mobius-Winckler S, Rioufol G, Witt N, Kala P, MacCarthy P, Engstrom T, Oldroyd K, Mavromatis K, Manoharan G, Verlee P, Frobert O, Curzen N, Johnson JB, Limacher A, Nuesch E, Juni P and Investigators FT. Fractional flow reserve-guided PCI for stable coronary artery disease. *N Engl J Med*. 2014;371:1208-17.
2. Authors/Task Force m, Windecker S, Kolh P, Alfonso F, Collet JP, Cremer J, Falk V, Filippatos G, Hamm C, Head SJ, Juni P, Kappetein AP, Kastrati A, Knuuti J, Landmesser U, Laufer G, Neumann FJ, Richter DJ, Schauerte P, Sousa Uva M, Stefanini GG, Taggart DP, Torracca L, Valgimigli M, Wijns W and Witkowski A. 2014 ESC/EACTS Guidelines on myocardial revascularization: The Task Force on Myocardial Revascularization of the European Society of Cardiology (ESC) and the European Association for Cardio-Thoracic Surgery (EACTS) Developed with the special contribution of the European Association of Percutaneous Cardiovascular Interventions (EAPCI). *Eur Heart J*. 2014;35:2541-619.
3. De Bruyne B, Pijls NH, Kalesan B, Barbato E, Tonino PA, Piroth Z, Jagic N, Mobius-Winkler S, Rioufol G, Witt N, Kala P, MacCarthy P, Engstrom T, Oldroyd KG, Mavromatis K, Manoharan G, Verlee P, Frobert O, Curzen N, Johnson JB, Juni P, Fearon WF and Investigators FT. Fractional flow reserve-guided PCI versus medical therapy in stable coronary disease. *N Engl J Med*. 2012;367:991-1001.
4. Pijls NH, van Schaardenburgh P, Manoharan G, Boersma E, Bech JW, van't Veer M, Bar F, Hoorntje J, Koolen J, Wijns W and de Bruyne B. Percutaneous coronary intervention of functionally nonsignificant stenosis: 5-year follow-up of the DEFER Study. *J Am Coll Cardiol*. 2007;49:2105-11.
5. Tonino PA, De Bruyne B, Pijls NH, Siebert U, Ikeno F, van't Veer M, Klauss V, Manoharan G, Engstrom T, Oldroyd KG, Ver Lee PN, MacCarthy PA, Fearon WF and Investigators FS. Fractional flow reserve versus angiography for guiding percutaneous coronary intervention. *N Engl J Med*. 2009;360:213-24.
6. Pijls NH, Fearon WF, Tonino PA, Siebert U, Ikeno F, Bornschein B, van't Veer M, Klauss V, Manoharan G, Engstrom T, Oldroyd KG, Ver Lee PN, MacCarthy PA, De Bruyne B and Investigators FS. Fractional flow reserve versus angiography for guiding percutaneous coronary intervention in patients with multivessel coronary artery disease: 2-year follow-up of the FAME (Fractional Flow Reserve Versus Angiography for Multivessel Evaluation) study. *J Am Coll Cardiol*. 2010;56:177-84.
7. Toth GG, Toth B, Johnson NP, De Vroey F, Di Serafino L, Pyxaras S, Rusinaru D, Di Gioia G, Pellicano M, Barbato E, van Mieghem C, Heyndrickx GR, De Bruyne B and Wijns W. Revascularization decisions in patients with stable angina and intermediate lesions: results of the international survey on interventional strategy. *Circ Cardiovasc Interv*. 2014;7:751-9.
8. Davies JE, Sen S, Dehbi HM, Al-Lamee R, Petraco R, Nijjer SS, Bhindi R, Lehman SJ, Walters

- D, Sapontis J, Janssens L, Vrints CJ, Khashaba A, Laine M, van Belle E, Krackhardt F, Bojara W, Going O, Harle T, Indolfi C, Niccoli G, Ribichini F, Tanaka N, Yokoi H, Takashima H, Kikuta Y, Erglis A, Vinhas H, Canas Silva P, Baptista SB, Alghamdi A, Hellig F, Koo BK, Nam CW, Shin ES, Doh JH, Brugaletta S, Alegria-Barrero E, Meuwissen M, Piek JJ, van Royen N, Sezer M, Di Mario C, Gerber RT, Malik IS, Sharp ASP, Talwar S, Tang K, Samady H, Altman J, Seto AH, Singh J, Jeremias A, Matsuo H, Kharbanda RK, Patel MR, Serruys P and Escaned J. Use of the Instantaneous Wave-free Ratio or Fractional Flow Reserve in PCI. *N Engl J Med*. 2017;376:1824-1834.
9. Gotberg M, Christiansen EH, Gudmundsdottir IJ, Sandhall L, Danielewicz M, Jakobsen L, Olsson SE, Ohagen P, Olsson H, Omerovic E, Calais F, Lindroos P, Maeng M, Todt T, Venetsanos D, James SK, Karegren A, Nilsson M, Carlsson J, Hauer D, Jensen J, Karlsson AC, Panayi G, Erlinge D, Frobert O and iFRSI. Instantaneous Wave-free Ratio versus Fractional Flow Reserve to Guide PCI. *N Engl J Med*. 2017;376:1813-1823.
 10. Lee JM, Park J, Hwang D, Kim CH, Choi KH, Rhee TM, Tong Y, Park JJ, Shin ES, Nam CW, Doh JH and Koo BK. Similarity and Difference of Resting Distal to Aortic Coronary Pressure and Instantaneous Wave-Free Ratio. *J Am Coll Cardiol*. 2017;70:2114-2123.
 11. Berger A, Botman KJ, McCarthy PA, Wijns W, Bartunek J, Heyndrickx GR, Pijls NH and De Bruyne B. Long-term clinical outcome after fractional flow reserve-guided percutaneous coronary intervention in patients with multivessel disease. *J Am Coll Cardiol*. 2005;46:438-42.
 12. Sels JW, Tonino PA, Siebert U, Fearon WF, van't Veer M, De Bruyne B and Pijls NH. Fractional flow reserve in unstable angina and non-ST-segment elevation myocardial infarction experience from the FAME (Fractional flow reserve versus Angiography for Multivessel Evaluation) study. *JACC Cardiovasc Interv*. 2011;4:1183-9.
 13. Levine GN, Bates ER, Blankenship JC, Bailey SR, Bittl JA, Cercek B, Chambers CE, Ellis SG, Guyton RA, Hollenberg SM, Khot UN, Lange RA, Mauri L, Mehran R, Moussa ID, Mukherjee D, Nallamothu BK and Ting HH. 2011 ACCF/AHA/SCAI Guideline for Percutaneous Coronary Intervention: a report of the American College of Cardiology Foundation/American Heart Association Task Force on Practice Guidelines and the Society for Cardiovascular Angiography and Interventions. *Circulation*. 2011;124:e574-651.
 14. Windecker S, Kolh P, Alfonso F, Collet JP, Cremer J, Falk V, Filippatos G, Hamm C, Head SJ, Juni P, Kappetein AP, Kastrati A, Knuuti J, Landmesser U, Laufer G, Neumann FJ, Richter DJ, Schauerte P, Uva MS, Stefanini GG, Taggart DP, Torracca L, Valgimigli M, Wijns W, Witkowski A, Grupa Robocza Europejskiego Towarzystwa K, Europejskie Stowarzyszenie Chirurgii Serca i Klatki Piersiowej do spraw rewaskularyzacji miesnia s and European Association for Percutaneous Cardiovascular I. [2014 ESC/EACTS Guidelines on myocardial revascularization]
 15. Siebert U, Arvandi M, Gothe RM, Bornschein B, Eccleston D, Walters DL, Rankin J, De Bruyne B, Fearon WF, Pijls NH and Harper R. Improving the quality of percutaneous revascularisation in patients with multivessel disease in Australia: cost-effectiveness, public health implications, and budget impact of FFR-guided PCI. *Heart Lung Circ*. 2014;23:527-33.
 16. van Nunen LX, Zimmermann FM, Tonino PA, Barbato E, Baumbach A, Engstrom T, Klauss V, McCarthy PA, Manoharan G, Oldroyd KG, Ver Lee PN, van't Veer M, Fearon WF, De Bruyne B, Pijls NH and Investigators FS. Fractional flow reserve versus angiography for guidance of PCI in patients with multivessel coronary artery disease (FAME): 5-year follow-up of a randomised controlled trial. *Lancet*. 2015;386:1853-60.
 17. Davies JE, Whinnett ZI, Francis DP, Manisty CH, Aguado-Sierra J, Willson K, Foale RA, Malik IS, Hughes AD, Parker KH and Mayet J. Evidence of a dominant backward-propagating "suction" wave responsible for diastolic coronary filling in humans, attenuated in left ventricular hypertrophy. *Circulation*. 2006;113:1768-78.
 18. Sen S, Escaned J, Malik IS, Mikhail GW, Foale RA, Mila R, Tarkin J, Petraco R, Broyd C, Jabbour R, Sethi A, Baker CS, Bellamy M, Al-Bustami M, Hackett D, Khan M, Lefroy D, Parker KH, Hughes AD, Francis DP, Di Mario C, Mayet J and Davies JE. Development and validation of a new adenosine-independent index of stenosis severity from coronary wave-intensity analysis: results of the ADVISE (ADenosine Vasodilator Independent Stenosis Evaluation) study. *J Am Coll Cardiol*. 2012;59:1392-402.
 19. Berry C, McClure JD and Oldroyd KG. Meta-Analysis of Death and Myocardial Infarction in the DEFINE-FLAIR and iFR-SWEDEHEART Trials. *Circulation*. 2017;136:2389-2391.
 20. Berry C, van 't Veer M, Witt N, Kala P, Bocek O, Pyxaras SA, McClure JD, Fearon WF, Barbato E, Tonino PA, De Bruyne B, Pijls NH and Oldroyd KG. VERIFY (VERification of Instantaneous Wave-Free Ratio and Fractional Flow Reserve for the Assessment of Coronary Artery Stenosis Severity in EverydaY Practice): a multicenter study in consecutive patients. *J Am Coll Cardiol*. 2013;61:1421-7.
 21. Jeremias A, Maehara A, Genereux P, Asrress KN, Berry C, De Bruyne B, Davies JE, Escaned J, Fearon WF, Gould KL, Johnson NP, Kirtane AJ, Koo BK, Marques KM, Nijjer S, Oldroyd KG, Petraco R, Piek JJ, Pijls NH, Redwood S, Siebes M, Spaan JAE, van 't Veer M, Mintz GS and Stone GW. Multicenter core laboratory comparison of the instantaneous wave-free ratio and resting Pd/Pa with fractional flow reserve: the RESOLVE study. *J Am Coll Cardiol*. 2014;63:1253-1261.
 22. van't Veer M, Pijls NHJ, Hennigan B, Watkins S, Ali ZA, De Bruyne B, Zimmermann FM, van Nunen LX, Barbato E, Berry C and Oldroyd KG. Comparison of Different Diastolic Resting Indexes to iFR: Are They All Equal? *J Am Coll Cardiol*. 2017;70:3088-3096.
 23. Kobayashi Y, Johnson NP, Berry C, De Bruyne B, Gould KL, Jeremias A, Oldroyd KG, Pijls NHJ, Fearon WF and Investigators CS. The Influence of Lesion Location on the Diagnostic Accuracy of Adenosine-Free Coronary Pressure Wire Measurements. *JACC Cardiovasc Interv*. 2016;9:2390-2399.
 24. Hennigan B, Oldroyd KG, Berry C, Johnson N, McClure J, McCartney P, McEntegart MB, Eteiba H, Petrie MC, Rocchiccioli P, Good R, Lindsay MM, Hood S and Watkins S. Discordance Between Resting and Hyperemic Indices of Coronary Stenosis Severity: The VERIFY 2 Study (A Comparative Study of Resting Coronary Pressure Gradient, Instantaneous Wave-Free Ratio and Fractional Flow Reserve in an Unselected Population Referred for Invasive Angiography).

Circ Cardiovasc Interv. 2016;9.

25. Menon M, Jaffe W, Watson T and Webster M. Assessment of coronary fractional flow reserve using a monorail pressure catheter: the first-in-human ACCESS-NZ trial. *EuroIntervention.* 2015;11:257-63.
26. Matsumura M, Johnson NP, Fearon WF, Mintz GS, Stone GW, Oldroyd KG, De Bruyne B, Pijls NHJ, Maehara A and Jeremias A. Accuracy of Fractional Flow Reserve Measurements in Clinical Practice: Observations From a Core Laboratory Analysis. *JACC Cardiovasc Interv.* 2017;10:1392-1401.



PART V



INNOVATIONS IN
INTRAVASCULAR
POLARIMETRY
ASSESSMENT

Chapter 18



Intravascular Polarimetry in Patients With Coronary Artery Disease

Otsuka K¹, Villiger M¹, Karanasos A^{2,3}, van Zandvoort LJC², Doradla P¹, Ren J¹, Lippok N¹, Daemen J², Diletti R², van Geuns RJ², Zijlstra F², van Soest G², Dijkstra J⁴, Nadkarni SK¹, Regar E^{2,5}, Bouma BE^{1,2,6}

¹*Wellman Center for Photomedicine, Massachusetts General Hospital, Harvard Medical School, Boston, MA USA*

²*Erasmus University Medical Center, Thoraxcenter, Department of cardiology, Rotterdam, the Netherlands*

³*1st Department of Cardiology, Hippokration Hospital, University of Athens, Greece*

⁴*Division of Image Processing, Department of Radiology, Leiden University Medical Center, Leiden, The Netherlands*

⁵*Heart Center, University Hospital Zurich, Zurich, Switzerland*

⁶*Institute for Medical Engineering and Science, Massachusetts Institute of Technology, Cambridge, Massachusetts, USA*

JACC Cardiovasc Imaging. 2020;13(3):790-801

ABSTRACT

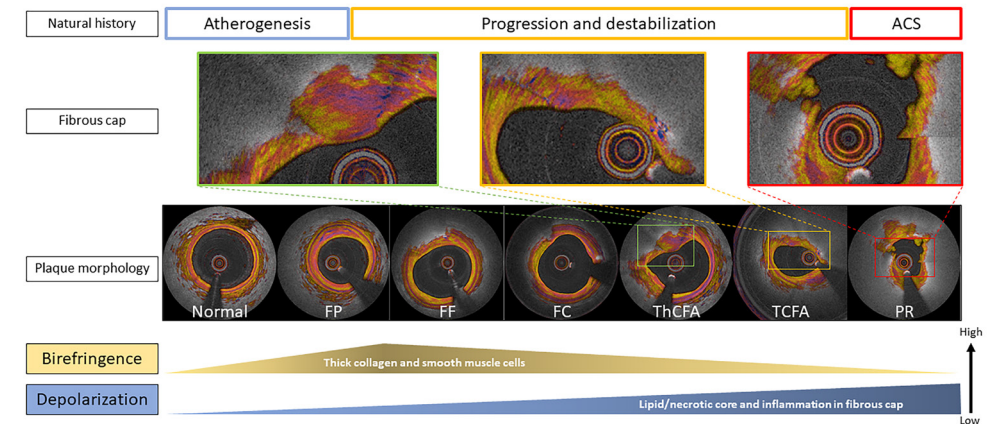
Background: Polarization-sensitive (PS-) optical frequency domain imaging (OFDI) measures polarization properties of tissue together with conventional cross-sectional OFDI images of subsurface microstructure.

Objectives: This first-in-human pilot study of intravascular polarimetry aimed to investigate birefringence and depolarization features of coronary plaques in patients and to examine the relationship of these features with established structural characteristics available to conventional OFDI and with clinical presentation.

Methods: 30 patients undergoing PS-OFDI (acute coronary syndrome; ACS, n=12 and stable angina pectoris; SAP, n=18) participated in this study. 342 cross-sectional images evenly distributed along all imaged coronary arteries were classified into one of seven plaque categories according to conventional OFDI. Polarization features averaged over the entire intimal area of each cross-section were compared between plaque types and with structural parameters. Further, we assessed the polarization properties in the fibrous caps of ACS and SAP culprit lesions and compared them with structural features using a generalized linear model.

Results: The median birefringence and depolarization showed statistically significant differences among plaque types (both $p < 0.001$, one-way ANOVA). Depolarization significantly differed between individual plaque types ($p < 0.05$), except between fibro-fatty and fibro-calcified plaques. Caps of ACS lesions and ruptured caps exhibited lower birefringence than caps of SAP lesions ($p < 0.01$). In addition to clinical presentation, cap birefringence also associated with macrophage accumulation as assessed by normalized standard deviation.

Conclusion: Intravascular polarimetry provides quantitative metrics that help to characterize coronary arterial tissues and may offer refined insight into coronary arterial atherosclerotic lesions in patients.



Central illustration. Polarization properties in plaque progression and destabilization

In a less advanced stage of atherogenesis, birefringence and depolarization increase along with the proliferation of thick collagen, smooth muscle cells and lipid content (atherogenesis and progression). Birefringence of the plaques declines in hand with the reduction of interstitial collagen, and the development of the lipid/necrotic core, which in turn leads to a significant increase in depolarization, corresponding to the transition of pathological intimal thickening (FP and FF) to a fibroatheroma (progression and destabilization). Abbreviations as in Figure 2 and 4.

INTRODUCTION

Plaque morphology and composition have been implicated in the pathogenesis of acute coronary syndromes (ACS) ¹⁻². The high resolution of optical coherence tomography (OCT) and optical frequency domain imaging (OFDI) has enabled identification of several structural features of plaque instability ³⁻⁶. Despite much progress, prospective identification of rupture-prone plaques, which would be crucial to stratify risk and improve patient management, remains elusive ⁷⁻¹⁰. Current OCT/OFDI imaging modalities rely on subjective interpretation and fall short of providing an objective and quantitative assessment of plaque morphology and composition ¹¹⁻¹⁴.

Recently, we have introduced intravascular polarimetry by using polarization-sensitive optical frequency domain imaging (PS-OFDI) in combination with standard intravascular OFDI catheters ¹⁵⁻¹⁷. Intravascular polarimetry complements the high-resolution imaging of subsurface microstructures known from OCT and OFDI with polarimetric measurements of tissue birefringence and depolarization ^{15, 16}. Tissue with fibrillar architecture, such as interstitial collagen or layered arrays of

arterial smooth muscle cells, exhibits birefringence, which can serve to assess collagen and smooth muscle cell content^{16, 18}. Depolarization corresponds to the randomization of the detected polarization states¹⁹ caused by the propagation of light through tissue containing lipid particles, macrophage accumulation, or cholesterol crystals¹⁶. In our previous study comparing intravascular polarimetry with histopathology, we showed that tissue birefringence and depolarization provide useful compositional information and offer advanced tissue characterization¹⁶. The present study aimed to investigate, for the first time, the polarization properties of atherosclerotic plaques in patients with coronary artery disease. We explored how the quantitative polarization metrics evaluated in entire cross-sections vary between different types of plaques, classified by conventional OFDI according to established qualitative structural criteria (plaque analysis). Moreover, we compared the polarization properties measured locally in the fibrous caps of culprit lesions between patients with ACS and SAP (cap analysis).

METHODS

Study population

This first-in-human pilot study of intravascular polarimetry enrolled 30 non-consecutive patients (ACS, n = 12 and stable angina pectoris; SAP, n = 18) undergoing percutaneous coronary intervention at Erasmus University Medical Center (Erasmus MC) between December 2014 and July 2015. The ethics committee at Erasmus MC approved the protocol and each patient gave written informed consent before inclusion into the study, which was conducted in compliance with the protocol and the Declaration of Helsinki. PS-OFDI was performed using commercial intravascular catheters (FastView™, Terumo Corp., Tokyo, Japan) with a custom-built PS-OFDI system (Supplementary methods), as previously described in detail¹⁵⁻¹⁷. Imaging in the 30 patients yielded a total of 36 pullbacks, performed either before the procedure (n = 15, whereof culprit/target vessel, n = 13, and non-culprit/non-target vessel, n = 2) or after the procedure (n = 21). Patient characteristics are summarized in Table 1.

Study design

The present study comprises a plaque analysis evaluating entire cross-sections evenly distributed along all imaged coronary arteries and a cap analysis focusing solely on the fibrous cap of culprit lesions (Figure 1A). For the plaque analysis, all pullbacks were uniformly divided into segments of 5 mm length, progressing distally and proximally from the culprit lesion (Figure 1B). From the resulting total of 508 segments, comprising 2540 mm pullback length, 166 segments were

excluded from the analysis due to the following criteria: 1) containing a stent or from within 5 mm proximal or distal to an implanted stent (n = 150); 2) subject to pre-dilatation (n = 2); and, 3) poor image quality due to insufficient blood clearing (n = 14). In each of the retained 342 segments, the cross section with the smallest lumen area was identified for further analysis. Cross-sections containing a side branch of diameter > 1.5 mm were replaced with another section from the same segment. For fibroatheromas, instead of the smallest lumen area, the cross-section with the thinnest fibrous cap thickness (FCT) was used for analysis. For the cap analysis, we identified the culprit lesion in patients with ACS (n = 4) and SAP (n = 9) who underwent PS-OFDI imaging prior to percutaneous coronary intervention (Figure 1A). ACS culprit lesions were identified based on invasive coronary angiography, electrocardiographic ST-segment alterations, and/or regional wall motion abnormality on echocardiographic assessment. SAP target lesions were determined on the basis of left ventricular wall motion abnormalities, nuclear scan, stress test, and coronary angiographic findings. For the cap analysis, we identified the cross section with the smallest luminal area in the culprit/target lesion of each patient (Figure 1B). Every other cross-sectional image up to 5 mm both proximally and distally, if featuring a lipid arc exceeding > 90 degree, was included into the analysis, resulting in a total of 244 cross-sections.

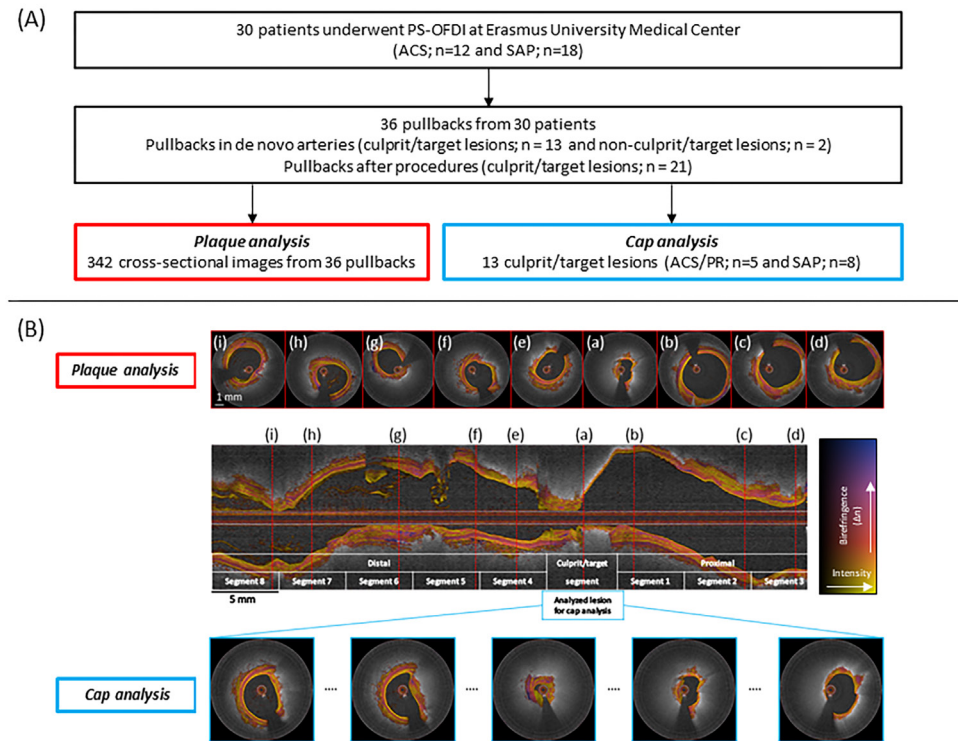


Figure 1. Study population, design and lesion selection

(A) Study population and data analysis. (B) PS-OFDI pullbacks were divided into 5 mm segments, centered on the culprit segment for the plaque analysis. Red broken lines indicate the selected cross-sectional images within each 5 mm segment, corresponding to the cross-section with the smallest luminal area. The cap analysis focused on the culprit/target segment centered around the cross section with the smallest luminal area in the culprit lesion of each patient. Cross-sectional images were analyzed every 2 frames both proximally and distally up to 5 mm, as long as the lipid arc exceeded > 90 degrees. Scale bars measure 1 mm for cross-sectional images (white) and 5 mm for the longitudinal image (black), respectively. ACS = acute coronary syndrome, PR = plaque rupture, SAP = stable angina pectoris, and PS-OFDI = polarization-sensitive optical frequency domain imaging.

Conventional OFDI analysis

Two independent investigators (A.K. and L.Z.) analyzed the conventional OFDI appearance of the selected images using QCU-CMS viewing software (Leiden University Medical Center, Leiden, The Netherlands). Conventional OFDI analysis was performed blinded to the polarimetric signals. Luminal area was measured in all cross-sections. Percent area stenosis was calculated as previously reported ⁸, taking the mean of the largest lumen within 5 mm proximal and distal to the lesion containing the current cross-section as the reference.

Each selected cross-section was then categorized as either of normal artery, fibrous plaque (FP), fibro-fatty plaque (FF), fibro-calcified plaque (FC), thick cap fibroatheroma (ThCFA), thin cap fibroatheroma (TCFA), or plaque rupture (PR), based on the conventional OFDI signal (Figure 2 A1 to G1). Briefly, a vessel with a tunica intima thinner or similar in thickness to the tunica media was labelled as normal artery (Figure 2 A1). FP was defined as a plaque with high backscattering and relatively homogeneous OFDI signal (Figure 2 B1). Plaques with calcium, that appears as signal-poor or heterogeneous region with a sharply delineated border within fibrous tissue, were classified as FC (Figure 2 D1) ⁹. A plaque with a lipid arc of more than 90 degrees was defined as a fibroatheroma. A lipid-rich plaque with a lipid arc extending less than 90 degrees was categorized as FF, to appreciate the optical properties of the small lipid-rich area (Figure 2 C1). In fibroatheromas, the FCT was measured around its thinnest part 3 times by each observer and then the averaged value was calculated. If the FCT was <65 μm the plaque was categorized as TCFA and as ThCFA otherwise. PR was defined as a plaque featuring intimal disruption and cavity formation (Figure 2 E1 to G1). In cases of discordance between the observers, a third investigator (B.B.) acted as referee to achieve consensus classification.

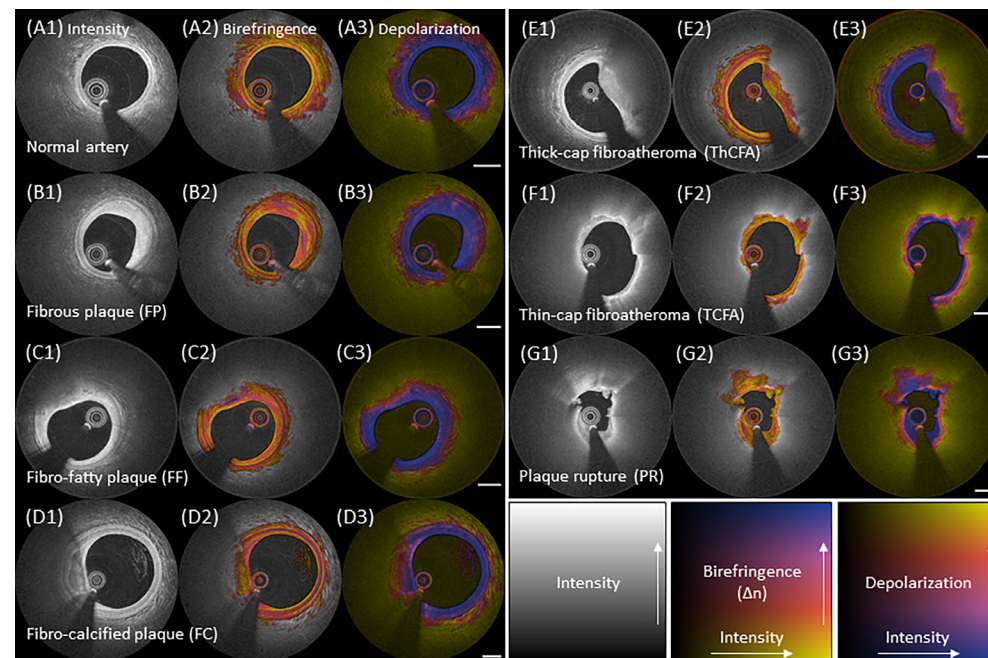


Figure 2. Representative PS-OFDI for all plaque types

(A1 to G1) Typical intensity images, (A2 to G2) birefringence images, and (A3 to G3) depolarization images of all plaque types. Rows show representative images of normal artery (A1 to A3), FP (B1 to B3), FF (C1 to C3), FC (D1 to D3), ThCFA (E1 to E3), TCFA (F1 to F3), and PR (G1 to G3), respectively. (A2 and A3) Normal artery feature very low birefringence and low depolarization in the intima. The media features high birefringence, independent of the lesion type, and is clearly visible in normal arteries. (B2 and B3) Fibrous tissue in FP exhibits heterogeneous patterns of birefringence and relatively homogeneous, low depolarization. (C2 and C3) Fibrous regions covering the lipid-pools of FF generally present with high birefringence. The Lipid-rich areas cause pronounced depolarization. (D2 and D3) Calcifications in FC show rather low birefringence and moderate depolarization. Depolarization of calcifications increases with the presence of lipid. (E2 and E3) Fibrous caps of ThCFA exhibit heterogeneous birefringence. (F2 and F3) Fibrous caps of TCFA typically reveal low birefringence. Depolarization in the diffuse border of the cap promptly transitions from low to high. (G2 and G3) The caps of PR have low birefringence. The most intimal layer from 3 to 9 o'clock in the intensity image displays relatively high and heterogeneous birefringence compared to the fragments of white thrombus at 1 and 11 o'clock. White bar = 1 mm. FC = fibro-calcified plaque, FF = fibro-fatty plaque, FP = fibrous plaque, PR = plaque rupture, PS-OFDI = polarization-sensitive optical frequency domain imaging, TCFA = thin cap fibroatheroma, and ThCFA = thick cap fibroatheroma.

Quantitative birefringence and depolarization analysis

PS-OFDI analysis was performed at Massachusetts General Hospital blinded to the conventional OFDI measurements and clinical information. Co-registration between conventional OFDI and polarimetric signals is intrinsic, since they are computed from the exact same raw data. For the plaque analysis, we segmented the intimal layer of each cross-section using custom-written software in MATLAB (The MathWorks, Inc., Natick, Massachusetts). In addition to the lumen, we segmented the internal elastic lamina (IEL), whenever visible, using the birefringence map to leverage from the improved visibility of the media in the birefringence map¹⁶. In areas where the IEL segmentation was unattainable, typically in lipid-rich areas of advanced lesions, an automatic outer border corresponding to a tissue depth of 1 mm from the lumen surface was used. We also segmented calcifications and areas of thrombus. To compute the average birefringence of cross-sections, we evaluated the median of the birefringence in the area bounded by the lumen and the IEL or outer border segmentation, excluding the guidewire shadow, and featuring a depolarization of ≤ 0.2 as previously reported¹⁷. The median depolarization was computed within the entire segmented area after masking the guidewire shadow.

For the cap analysis, the border between the fibrous caps of the culprit fibroatheromas and the underlying lipid/necrotic core was drawn manually, together with the lipid arc angle extending from the center of the lumen (total cap analysis). Mean and thinnest FCT were automatically calculated from the segmented fibrous cap in MATLAB. Furthermore, to investigate the features of fibrous caps at their thinnest part (focal cap analysis), we also defined a narrower arc angle, centered on the thinnest part of each cap (29° on average). In addition, we evaluated the normalized standard deviation (NSD) within the fibrous caps, which has been shown to correlate with macrophage infiltration^{3, 12}. NSD was computed by first evaluating the standard deviation of the linear-scale backscatter intensity data within elliptical regions of interest, extending by $80 \mu\text{m}$ in depth and 12° in the circumferential direction and moved across the entire cap area. These values were then normalized with the difference between the maximum and the minimum intensity within each fibrous cap.

Statistical analysis

Continuous outcome measures were reported as mean \pm SD. For the plaque analysis, the mean polarimetry signals of the different plaque types were compared with one-way analysis of variance. Pairwise comparison was performed with a generalized linear model using a generalized estimating equation (GEE), since cross-sectional images are clustered within each pullback and within each patient.

For comparison with clinical presentation in the cap analysis, the one PR lesion in the SAP group was classified together with the ACS lesions into an ACS and/or PR group. Differences in the means between the two groups were analyzed with an unadjusted generalized linear model using a GEE. The relationship between polarization properties and clinical and conventional OFDI parameters were determined by a univariate generalized linear model using a GEE to take into consideration the intra-subject correlations among multiple cross-sectional images from individual patients. β and 95% confidence interval (CI) for birefringence are given in units of $\times 10^{-3}$ throughout the manuscript. A p -value of <0.05 was considered to indicate statistical significance, and all tests were two-sided. SPSS 22.0 was used for all analyses (IBM Corp., Armonk, NY, USA).

RESULTS

Polarization properties of individual plaque types

Table 1 summarizes patient characteristics and OFDI parameters for the overall study population.

The selected 342 cross-sectional images representing all imaged vessels were classified into normal artery ($n = 31$), FP ($n = 84$), FF ($n = 45$), FC ($n = 81$), ThCFA ($n = 88$), TCFA ($n = 11$), and plaque rupture ($n = 2$) based on conventional OFDI. Intra- and interobserver kappa coefficients for overall plaque classification were 0.95 and 0.89, respectively. For the sub-classification of fibroatheromas into ThCFA, TCFA and PR, intra- and interobserver were 0.96 and 0.91, respectively. Figure 3 shows significant differences in median birefringence and depolarization among the 7 plaque types ($p < 0.001$ for both, One-way ANOVA). Comparing individual plaque types, normal arteries were significantly less birefringent than all other plaque types ($p < 0.01$), except for PR ($p = 0.408$). FPs featured the highest birefringence ($p < 0.05$), followed by FFs, FCs, ThCFAs, TCFA and PRs in decreasing order (Figure 3A), but without statistical significance between most categories. Normal arteries also featured the lowest depolarization. Plaque rupture showed the highest depolarization among the 7 plaque types. Except FF versus FC, all plaque types had statistically significant differences in depolarization when compared individually (Figure 3B).

Table 1. Patient and OFDI lesion characteristics

	Overall (n = 30)
<u>Patient characteristics</u>	
Age, years	63 \pm 9
Male	24 (80)
Hypertension	12 (40)
Diabetes Mellitus	5 (17)
Dyslipidemia	13 (43)
STEMI	1 (3.3)
NSTEMI	5 (17)
Unstable angina	6 (20)
Previous myocardial infarction	8 (27)
Previous PCI	14 (47)
Previous CABG	4 (13)
<u>Imaged vessel (n=36)</u>	
LAD	18 (50)
LCX	6 (17)
RCA	12 (33)
<u>OFDI lesion characteristics</u>	
Analyzed frames	342
Luminal area, mm ²	6.1 \pm 3.3
Percent area stenosis, %	40 \pm 20
<u>Plaque morphology</u>	
AIT	31 (9.1)
FP	84 (25)
FF	45 (13)
FC	81 (24)
ThCFA	88 (26)
TCFA	11 (3.2)
PR	2 (0.6)
Lipid arc, degree	57 \pm 72
Calcium arc, degree	73 \pm 50
Minimum fibrous cap thickness, μ m	140 \pm 81
<u>Polarization properties</u>	
Birefringence, $\times 10^{-3}$	0.50 \pm 0.11
Depolarization	0.12 \pm 0.09

Variables are expressed as mean \pm SD or n, (%).

ACS = acute coronary syndrome, AIT = adaptive intimal thickening, CABG = coronary artery bypass graft, CAD = coronary artery disease, FC = fibro-calcified plaque, FF = fibro-fatty plaque, FP = fibrous plaque, PCI = percutaneous coronary intervention, LAD = left anterior descending coronary artery, LCX = left circumflex coronary artery, NSTEMI = non-ST-segment elevation myocardial infarction, PCI = percutaneous coronary intervention, PR = plaque rupture, RCA = right coronary artery, SAP = stable angina pectoris, STEMI = ST-segment elevation myocardial infarction, TCFA = thin cap fibroatheroma, ThCFA = thick cap fibroatheroma, and OFDI = optical frequency domain imaging.

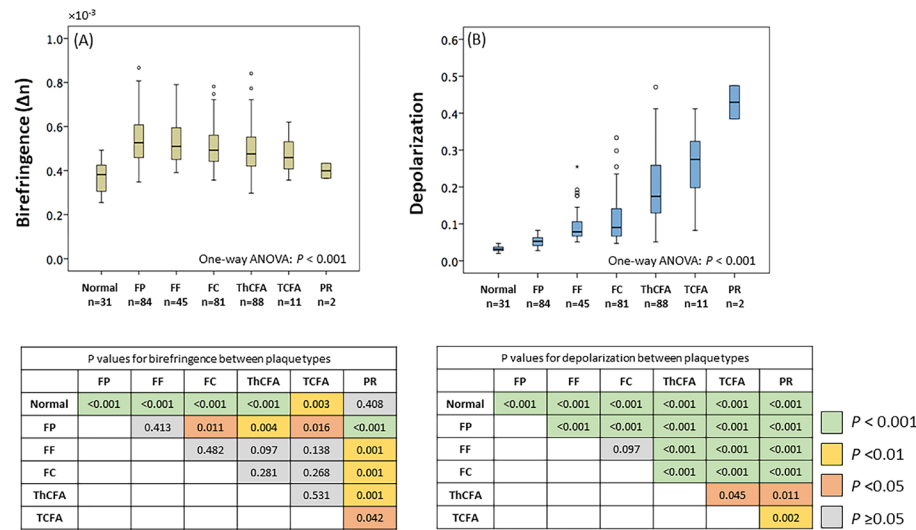


Figure 3. Plaque characterization and polarization properties
 (A) The differences between individual groups were significant with the exception of normal artery versus PR; FP versus FF; FF versus FC, ThCFA, and TCFA; ThCFA versus TCFA. (B) A significant gradual variation in depolarization was observed among plaque types ($p < 0.001$, $p < 0.05$ for ThCFA versus TCFA and PR, TCFA versus PR) except for FF versus FC. Normal indicates normal artery and other abbreviations as in Figure 2.

Calcifications featured low birefringence and low depolarization (Supplementary Figure S1 A and B). Calcifications located in fibrous tissue exhibited lower birefringence and depolarization than those in lipid-rich lesions (both $p < 0.001$), as shown in Supplementary Figure S1 C and D. Thrombus (white thrombus) presented very low birefringence and depolarization (Supplementary Figure S2 A and B).

Polarization properties of fibrous caps in culprit lesions

The lipid arc and minimum FCT differed with statistical significance between the ACS/PR and the SAP group, as shown in Table 2.

When comparing the polarimetric signals of the fibrous caps in the culprit lesions we found a lower birefringence in the ACS/PR group than in SAP patients ($p = 0.002$), but comparable depolarization ($p = 0.772$) (Figure 4A and B). Table 3 shows GEE model parameters for the relationship between polarization properties, clinical presentation, and conventional OFDI parameters, when analyzing the entire cap.

Table 2. OFDI and polarimetry lesion characteristics in culprit/target lesion

	ACS/PR group (n = 5)	SAP group (n = 8)	p value
Analyzed frames	88	156	
OFDI lesion characteristics			
Luminal area, mm ²	3.7 ± 2.1	3.8 ± 2.2	0.871
Percent area stenosis, %	56 ± 23	55 ± 22	0.934
Lipid arc, degree	219 ± 88	171 ± 72	0.045
Calcium arc, degree	95 ± 36	100 ± 62	0.951
Minimum fibrous cap thickness, μm	219 ± 109	291 ± 146	0.027
Mean fibrous cap thickness, μm	377 ± 124	406 ± 125	0.506
NSD in total cap	2.0 ± 1.5	2.2 ± 1.6	0.596
NSD in focal cap	4.4 ± 3.2	3.9 ± 3.2	0.533
Polarization properties			
Birefringence (plaque), ×10 ⁻³	0.44 ± 0.07	0.52 ± 0.08	0.001
Birefringence (total cap), ×10 ⁻³	0.42 ± 0.10	0.53 ± 0.16	0.002
Birefringence (focal cap), ×10 ⁻³	0.38 ± 0.10	0.49 ± 0.18	<0.001
Depolarization (plaque)	0.28 ± 0.12	0.21 ± 0.12	0.034
Depolarization (total cap)	0.10 ± 0.04	0.10 ± 0.03	0.772
Depolarization (focal cap)	0.11 ± 0.05	0.11 ± 0.04	0.845

Variables are expressed as ± standard deviation. P-values were obtained by generalized linear models using GEE. GEE = generalized estimating equation and NSD = normalized standard deviation. Other abbreviations as in Table 1.

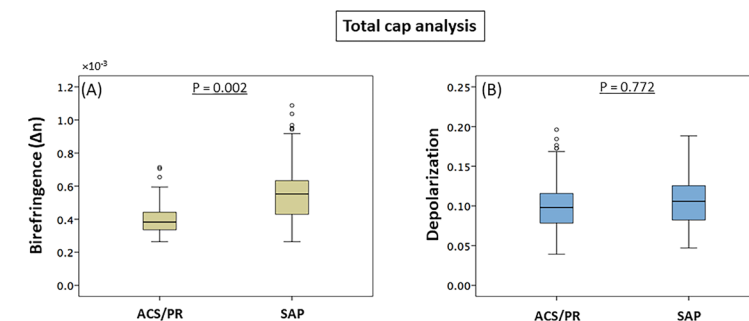


Figure 4. Polarization properties in caps of culprit/target lesions
 (A and B) Difference in birefringence (A) and depolarization (B) between patients with ACS/PR and SAP. Fibrous caps in ACS/PR patients exhibited significantly lower birefringence compared to SAP patients. ACS = acute coronary syndrome, PR = plaque rupture, and SAP = stable angina pectoris.

Table 3. Relationships between polarization properties in total fibrous cap, clinical presentation, and OFDI parameters

Total cap analysis						
	Birefringence			Depolarization		
	β	p value	95% CI Lower Upper	β	p value	95% CI Lower Upper
Age (per 5 years increase)	0.003	0.813	-0.019 0.024	0.001	0.782	-0.007 0.009
ACS/PR	-0.156	0.002	-0.254 -0.058	0.003	0.772	-0.014 0.019
FCT, mean (per 10 μ m increase)	0.002	0.264	-0.001 0.005	-0.001	< 0.001	-0.002 -0.001
Lipid arc (per 10° increase)	-0.004	0.109	-0.008 0.001	0.001	0.001	0.0005 0.0021
Percent area stenosis (per 10% increase)	0.006	0.643	-0.018 0.030	0.001	0.647	-0.002 0.004
Calcium arc (per 10° increase)	0.003	0.339	-0.004 0.011	0.001	0.477	-0.001 0.003
NSD	-0.021	0.013	-0.037 -0.004	0.005	0.062	-0.0002 0.0092

The relationship between polarization properties and clinical and OFDI parameters were determined by unadjusted generalized linear model using a GEE to take into consideration the intra-subject correlations among multiple cross-sectional images from individual patients. β and 95% CI for birefringence are given in units of $\times 10^{-3}$. CI = confidence interval, GEE = generalized estimating equation, and other abbreviations as in Table 1.

Table 4. Associations of polarization properties in focal fibrous cap and OFDI parameters

Focal cap analysis						
	Birefringence			Depolarization		
	β	p value	95% CI Lower Upper	β	p value	95% CI Lower Upper
ACS/PR	-0.138	< 0.001	-0.211 -0.065	0.002	0.845	-0.022 0.027
FCT, thinnest (per 10 μ m increase)	0.005	0.001	0.002 0.008	-0.001	0.005	-0.0016 -0.0003
NSD	-0.012	0.001	-0.020 -0.005	0.004	< 0.001	0.002 0.006

The relationship between polarization properties and clinical and OFDI parameters were determined by unadjusted generalized linear model using a GEE to take into consideration the intra-subject correlations among multiple cross-sectional images from individual patients. β and 95% CI for birefringence are given in units of $\times 10^{-3}$. Abbreviations as in Table 1 and Table 3.

Birefringence of the total cap was negatively correlated with ACS/PR ($\beta = -0.156$; $p = 0.002$) and NSD ($\beta = -0.021$; $p = 0.013$). Depolarization of the total cap was negatively associated with mean FCT ($\beta = -0.001$; $p < 0.001$) and positively with lipid arc ($\beta = 0.001$; $p = 0.001$) and tended to be correlated with NSD ($\beta = 0.005$; $p = 0.062$). Further, we analyzed narrow regions of interest centered on the thinnest part of each fibrous cap (Table 4).

The generalized linear model using GEE showed that ACS/PR ($\beta = -0.138$; $p < 0.001$), thinnest FCT ($\beta = 0.005$; $p = 0.001$) and NSD ($\beta = -0.012$; $p = 0.001$) were associated with birefringence. Factors associated with depolarization were thinnest FCT ($\beta = -0.001$; $p = 0.005$) and NSD ($\beta = 0.004$; $p < 0.001$).

DISCUSSION

This first-in-human pilot study of intravascular polarimetry demonstrates how it augments conventional OFDI plaque characterization with quantitative polarization properties, measured through standard intravascular OFDI catheters simultaneously with the conventional OFDI signal. The polarization features offer refined insight into tissue composition, consistent with our current understanding of the mechanisms involved in plaque progression and destabilization. The major finding of this study is that fibrous caps in ACS culprit lesions and ruptured plaques exhibit lower birefringence compared to the caps of target lesions in SAP patients within our limited study cohort. Compared to the interpretation of conventional OFDI, which relies on subjective identification of qualitative features, polarimetry offers quantitative metrics, leading a way to objective and automated characterization of atherosclerotic plaques. The improved assessment of plaque composition afforded by the polarization features may provide novel insight into the mechanism of plaque progression and instability in human coronary atherosclerosis.

Polarimetric plaque characterization

Smooth muscle cells and collagen are known to influence the polarization of near infrared light¹⁸. Our recent study of intravascular PS-OFDI in cadaveric human hearts revealed that normal intimal tissue exhibits low birefringence compared to intimal tissue in fibrous, early, and advanced atherosclerotic lesions¹⁶. In the present study, we observed significant differences in birefringence and depolarization among all plaque types, despite analyzing the entire manually segmented intimal layer, comprising both the angle subtended by the plaque and the remainder of the cross-section. Depolarization featured significant

differences even between individual plaque types, whereas birefringence was less distinguishing. These observations suggest that PS-OFDI provides insight into biological aspects of plaque progression and destabilization, complementary to the structural information available to conventional OFDI. Combined analysis of birefringence and depolarization in more refined automatically segmented regions of interest may offer automated tissue characterization. Moreover, accurate diagnosis of TCFA by OCT/OFDI remains challenging¹³, and future studies are warranted to investigate the polarization features of thin and thick fibrous caps and early and late necrotic cores in detail.

Polarization properties in fibrous caps

Within our limited patient cohort, we observed that the fibrous cap of the culprit lesion in ACS/PR patients exhibited significantly lower birefringence than in the caps of target lesions in SAP patients. Fibrillar collagen is the primary extracellular matrix molecule imparting both birefringence and mechanical stability to the fibrous cap overlying an atheroma²⁰. Histopathological studies showed that ruptured fibrous caps lack layered smooth muscle cells and feature different collagen phenotypes than intact caps²⁰, which offers an explanation for the low birefringence observed in the fibrous caps of ACS/PR patients. In addition to cap birefringence, minimum FCT and lipid arc angle also featured statistically significant differences between these two patient groups. Yet, FCT alone is insufficient to identify caps that are prone to rupture^{4, 5, 8, 9}. The polarization metrics available to intravascular polarimetry complement these structural features and may advance our understanding of the pathogenesis of ACS with or without fibrous cap rupture^{10, 21}.

Furthermore, birefringence and depolarization of the fibrous cap were associated with increased NSD, suggesting macrophage accumulation. Inflammation is a known mechanism of plaque destabilization^{2, 22, 23}. Macrophages release enzymes including matrix-metalloproteinases that destroy the extracellular matrix and weaken the cap²². Our observations suggest that the presence of active macrophages may increase depolarization, whereas the effect of their presence causes a reduction in birefringence. The physical mechanism inducing depolarization in atherosclerosis remains to be elucidated. We speculate that lipid droplets exceeding the size of the wavelength used for OFDI and small cholesterol crystals, which have been postulated to be a crucial factor in the initiation of inflammatory response in atherosclerosis²⁴, are the origin of the observed depolarization.

The few occurrences of white thrombus in the present study had minimal impact on the underlying polarization signatures. However, the stronger attenuation of

red thrombus may lead to an apparent increase in depolarization that would impair interpretation of the underlying vessel wall, similar to conventional OFDI imaging.

Study limitations

First, our study consists of a small number of patients from a cohort of nonconsecutive patients and was cross-sectional in design. Considering potential selection bias of patients, our findings should be interpreted with caution, although we included all patients imaged with intravascular polarimetry. Furthermore, the limited number may lead to a potential over-estimation of the differences between polarization features when performing multiple pairwise comparisons and prevented multivariate analysis. Owing to its compatibility with clinical OFDI imaging catheters, intravascular polarimetry can be readily applied to any patient eligible for conventional OFDI imaging, and future well-designed studies are needed to ascertain our current findings. Second, our plaque classification corresponds well to the current understanding of plaque subtypes in OFDI⁶ and could be readily performed on the conventional OFDI signal, yet conventional OFDI has limited ability to classify lesion types, especially in advanced lesions^{11,14}. Although lipid-rich plaques offer some prognostic implication⁸, clear identification of fibroatheromas with OCT/OFDI remains debatable. Combination of intravascular ultrasound and OCT/OFDI has been shown to improve diagnostic accuracy of identifying fibroatheromas¹³. Future histopathological validation studies are needed to inspect the ability of polarization properties to distinguish between different plaque types and potentially enable automated plaque classification. Third, we observed that NSD was associated with depolarization in the focal fibrous caps but not in the entire caps. Macrophage infiltration frequently occurs very locally and averaging the signals across entire caps carries less meaning than across a local region of interest. Moreover, the required normalization of the NSD depends delicately on the ROI, and evidence supporting the NSD metric remains scant. We suspect that both NSD and depolarization capture aspects of macrophage infiltration, but validation studies with histology are needed to identify how depolarization relates to macrophage infiltration. Finally, no patient in the current study presented plaque erosion, the second most common cause of ACS.

CONCLUSION

This study presents polarization properties of coronary atherosclerotic lesions in patients with coronary artery disease. The fibrous caps of culprit lesions in ACS/PR patients featured lower birefringence than in SAP patients. When averaged across

entire cross-sections, the polarimetric signals varied among distinct morphological plaque subtypes. Quantitative assessment of plaque polarization properties by intravascular polarimetry may open new avenues for studying plaque progression and detecting high-risk patients. Prospective studies in larger populations are needed to evaluate how polarization metrics could translate into improved patient outcomes and optimized medical therapy compared to utilizing only the structural features available to conventional OFDI.

Clinical Competencies

Modification of the optical frequency domain imaging (OFDI) apparatus along with recently developed image reconstruction methods enabled measurements of polarization properties of the coronary arterial wall. Intravascular polarimetry permits quantitative assessment of polarization properties through standard intravascular OFDI catheters simultaneously with intensity image cross-sections. This first-in-human pilot study of intravascular polarimetry demonstrated that polarization properties differ between culprit lesions of acute coronary syndrome or plaque rupture and stable angina pectoris, and also among different morphological plaque subtypes.

Translational Outlook

Quantitative assessment of plaque structure and composition by intravascular polarimetry may open new avenues for studying coronary atherosclerosis and may contribute to advancing our understanding of plaque progression and destabilization in patients. Future well-designed studies are needed to investigate how the risk of future acute coronary events may manifest in the polarization properties of coronary atherosclerotic lesions at an early timepoint.

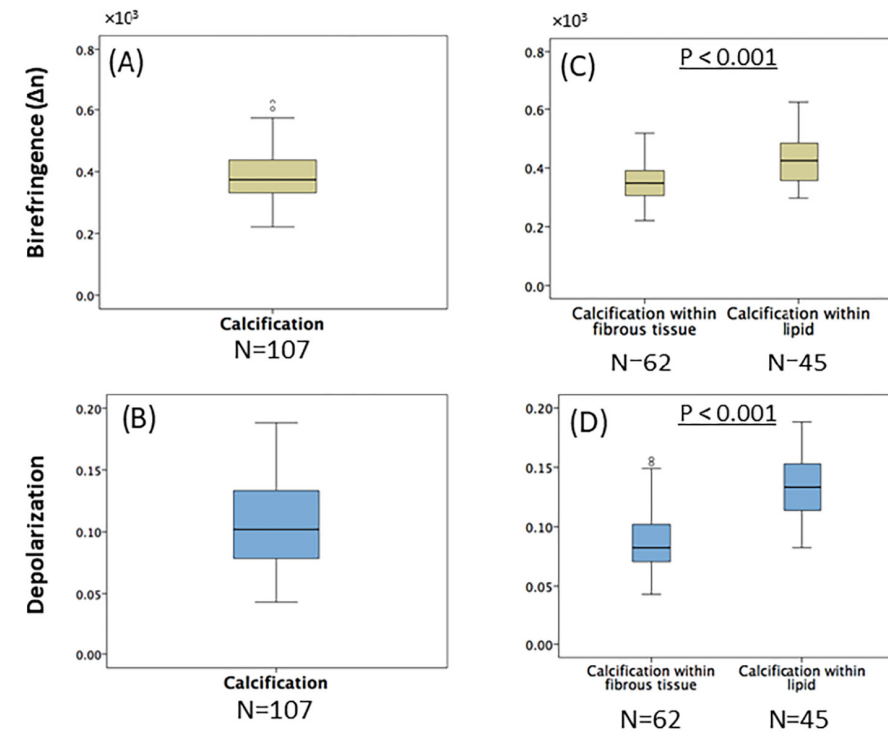
Funding: This work was supported by the National Institutes of Health (grants P41EB-015903 and R01HL-119065) and by Terumo Corporation. Dr. Bouma was supported in part by the Professor Andries Querido visiting professorship of the Erasmus University Medical Center in Rotterdam.

Acknowledgements: The authors sincerely thank Dr. Peter Libby of Brigham and Women's Hospital and Harvard Medical School for fruitful discussion and feedback on this manuscript. Dr. Hang Lee, Biostatistics Center, Massachusetts General Hospital, Harvard Medical School, provided invaluable guidance with respect to the statistical analyses of this work. Dr. Otsuka acknowledges partial support from the Japan Heart Foundation / Bayer Yakuhin Research Grant Abroad, the Uehara Memorial Foundation Postdoctoral Fellowship, and the Japan Society for the Promotion of Science Overseas Research Fellowship.

Supplementary Methods

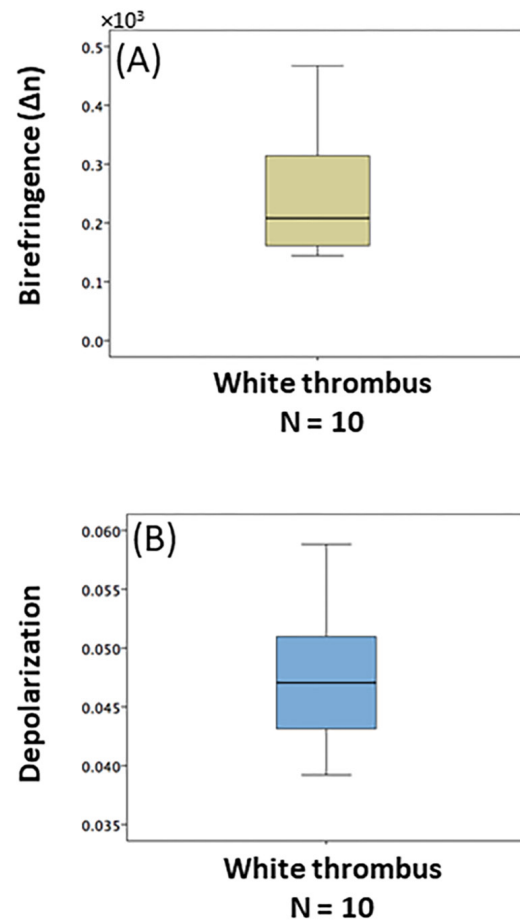
Intravascular PS-OFDI

All procedures were performed according to standard practice in the Erasmus MC catheterization laboratory ¹. Briefly, the imaging system operated at a center wavelength of 1300 nm with a wavelength scanning range of 110 nm, corresponding to a radial resolution of 9.4 μm , assuming a refractive index of 1.34. The intravascular catheter was pulled back at a rate of 20 mm/s with continuous injection of non-ionic contrast solution at a rate of 3-4 mL/s, and images were acquired at a rate of 100 frames/s, each consisting of 1024 radial scans. Intravascular PS-OFDI offers insight into tissue composition by quantifying birefringence and depolarization through standard intravascular imaging catheters, as described in detail previously ². In short, the imaging system employed a polarization diverse receiver to determine the polarization state of the light scattered by the tissue, and an electro-optic polarization modulator to vary the polarization state of the light illuminating the vessel wall between consecutive radial scans. Polarimetric analysis was performed offline with spectral binning to reconstruct maps of tissue birefringence and depolarization ³. Birefringence is the unitless ratio of change in retardation (phase delay between two principle polarization states) per propagation distance traveled by light. It corresponds to the difference of the refractive indices experienced by light polarized parallel and orthogonal to the fibrillary components, such as collagen fibers and layered smooth muscle cells ⁴. In the present study, birefringence is displayed in the range of $0-1.8 \times 10^{-3}$. Depolarization corresponds to a randomization of the detected polarization states, induced by propagation and scattering of light inside tissue ^{2,5}. As a measure of tissue depolarization, we computed the complement to 1 of the degree of polarization. ³ Depolarization ranges from 0 for completely polarized light without any randomness to 1 for completely depolarized, i.e. randomized light. Comparison of polarization properties with plaque burden and stenosis severity to investigate the association of polarization properties with stenosis severity, we examined the correlation of birefringence and depolarization with percent area stenosis. Plaque cross-sectional area (CSA) was defined as IEL CSA minus lumen CSA and computed only in normal artery and FP. Percent plaque CSA (%CSA_{plaque}) was calculated as plaque CSA divided by the IEL CSA. The GEE approach was employed to determine the relationship between polarization properties, percent area stenosis for all plaque types and %CSA_{plaque} for normal artery and FP, respectively.



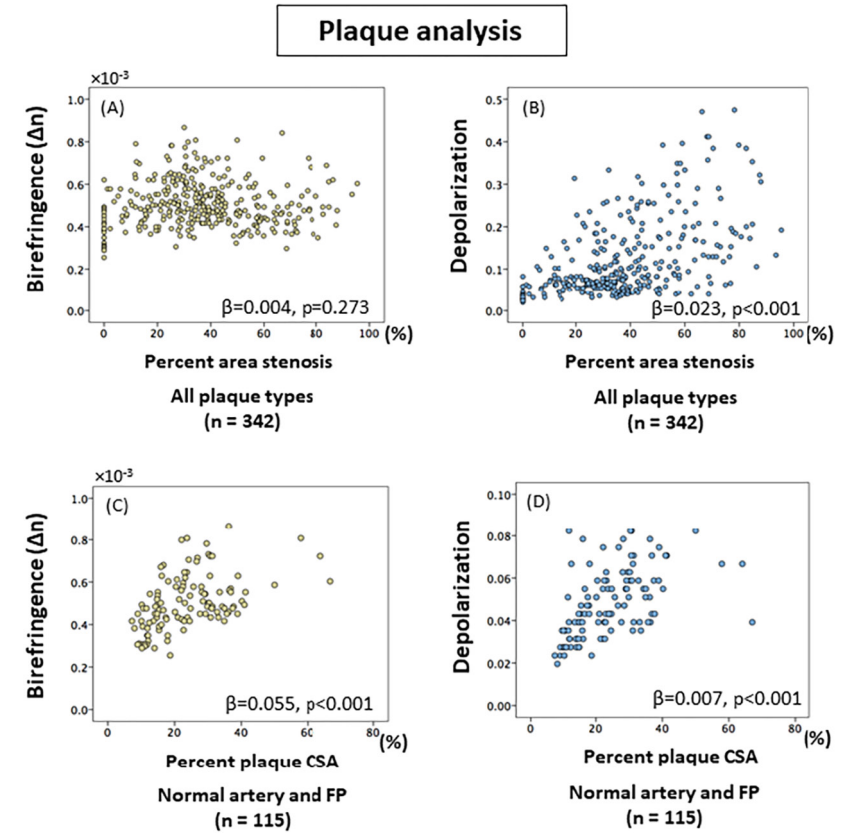
Supplementary Figure S1. Polarization properties of calcification

Median birefringence and depolarization were measured in calcifications, manually segmented in the intensity images of the 342 cross-sectional images of the plaque analysis. Calcifications were classified into 2 groups according to the presence or absence of lipid in the surrounding lesion (calcification within fibrous tissue or calcification within lipid). Calcifications exhibit low birefringence (A) and low depolarization (B). C and D show comparisons of polarization properties of calcifications with and without lipid (fibrous tissue). (C) Calcifications in fibrous tissue exhibit lower birefringence compared to those in a lipid-rich lesion ($p < 0.001$). (D) Higher depolarization was observed in calcifications in lipid-rich tissue than in those located in fibrous tissue ($p < 0.001$). Association was tested by unadjusted generalized linear model using GEE. GEE = generalized estimating equation.



Supplementary Figure S2. Polarization properties of white thrombus

The plaque and cap analysis combined contained a total of 10 cross-sectional images with white thrombus. Based on intensity signal in conventional optical frequency domain imaging (OFDI), all the thrombus was classified as white thrombus. Manual segmentation, performed by tracing the boundary of the thrombus, revealed very low birefringence (A) and depolarization (B) in white thrombus.



Supplementary Figure S3. Associations between polarization properties and percent plaque Cross-sectional area

(A and B) Association between percent area stenosis and polarization properties for all crosssections. (C and D) Association between percent plaque area and polarization properties in normal artery and FP. Association was tested by unadjusted generalized linear model using GEE. The percent area stenosis in all plaque types combined was significantly associated with depolarization ($\beta = 0.023$; $p < 0.001$), but not with birefringence ($\beta = 0.004$; $p = 0.273$) (Supplementary Figure 3A and 3B). Since %CSA_{plaque} can only be accurately calculated in normal artery and FP where the IEL is reliably identified in OFDI imaging, we also compared the polarization properties and %CSA_{plaque} in normal artery and FP. Birefringence ($\beta = 0.055$; $p < 0.001$) and depolarization ($\beta = 0.007$; $p < 0.001$) correlated positively with %CSA_{plaque} (Supplementary Figure S3-C and -D). CSA = cross-sectional area, FP = fibrous plaque, and GEE = generalized estimating equation.

REFERENCES

1. Virmani R, Burke AP, Farb A, Kolodgie FD. Review 2006 pathology of coronary vulnerable plaque. *J Am Coll Cardiol* 2006;47:C13-8.
2. Narula J, Nakano M, Virmani R, et al. Histopathologic characteristics of atherosclerotic coronary disease and implications of the findings for the invasive and noninvasive detection of vulnerable plaques. *J Am Coll Cardiol* 2013;61:1041-1051.
3. Tearney GJ, Yabushita H, Houser SL, et al. Quantification of macrophage content in atherosclerotic plaques by optical coherence tomography. *Circulation* 2003;107:113-119.
4. Toutouzas K, Karanasos A, Tsiamis E, et al. New insights by optical coherence tomography into the differences and similarities of culprit ruptured plaque morphology in non-ST-elevation myocardial infarction and ST-elevation myocardial infarction. *Am Heart J* 2011;161:1192-1199.
5. Yonetsu T, Kakuta T, Lee T, et al. In vivo critical fibrous cap thickness for rupture-prone coronary plaques assessed by optical coherence tomography. *Euro Heart J* 2011;32:1251-1259.
6. Tearney GJ, Regar E, Akasaka T, et al. Consensus standards for acquisition, measurement, and reporting of intravascular optical coherence tomography studies: A report from the International Working Group for Intravascular Optical Coherence Tomography Standardization and Validation. *J Am Coll Cardiol* 2012;59:1058-1072.
7. Arbab-Zadeh A, Fuster V. The myth of the "vulnerable plaque": Transitioning from a focus on individual lesions to atherosclerotic disease burden for coronary artery disease risk assessment. *J Am Coll Cardiol* 2015;65:846-855.
8. Xing L, Higuma T, Wang Z, et al. Clinical Significance of Lipid-Rich Plaque Detected by Optical Coherence Tomography: A 4-Year Follow-Up Study. *J Am Coll Cardiol* 2017;69:2502-2513.
9. Zhang BC, Karanasos A, Gnanadesigan M, et al. Qualitative and quantitative evaluation of dynamic changes in non-culprit coronary atherosclerotic lesion morphology: A longitudinal OCT study. *EuroIntervention* 2018;13:e2190-e2200.
10. Garcia-Garcia HM, Jang IK, Serruys PW, Kovacic JC, Narula J, Fayad ZA. Imaging plaques to predict and better manage patients with acute coronary events. *Circulation Research* 2014;114:1904-1917.
11. Manfrini O, Mont E, Leone O, et al. Sources of error and interpretation of plaque morphology by optical coherence tomography. *Am J Cardiol* 2006;98:156-159.
12. Phipps JE, Vela D, Hoyt T, et al. Macrophages and intravascular OCT bright spots: A quantitative study. *J Am Coll Cardiol Img* 2015;8:63-72.
13. Nakano M, Yahagi K, Yamamoto H, et al. Additive Value of Integrated Backscatter IVUS for Detection of Vulnerable Plaque by Optical Frequency Domain Imaging: An Ex Vivo Autopsy Study of Human Coronary Arteries. *J Am Coll Cardiol Img* 2016;9:163-172.
14. Phipps JE, Hoyt T, Vela D, et al. Diagnosis of Thin-Capped Fibroatheromas in Intravascular Optical Coherence Tomography Images: Effects of Light Scattering. *Circ Cardiovasc interventions* 2016;9.
15. van der Sijde JN, Karanasos A, Villiger M, Bouma BE, Regar E. First-in-man assessment of plaque rupture by polarization-sensitive optical frequency domain imaging in vivo. *Euro Heart J* 2016;37:1932.
16. Villiger M, Otsuka K, Karanasos A, et al. Coronary Plaque Microstructure and Composition Modify Optical Polarization. A New Endogenous Contrast Mechanism for Optical Frequency Domain Imaging. *J Am Coll Cardiol Img* 2018;11:1666-1676.
17. Villiger M, Otsuka K, Karanasos A, et al. Repeatability Assessment of Intravascular Polarimetry in Patients. *IEEE Transactions on Medical Imaging* 2018;37:1618-1625.
18. Nadkarni SK, Pierce MC, Park BH, et al. Measurement of Collagen and Smooth Muscle Cell Content in Atherosclerotic Plaques Using Polarization-Sensitive Optical Coherence Tomography. *J Am Coll Cardiol* 2007;49:1474-1481.
19. Lippok N, Villiger M, Albanese A, et al. Depolarization signatures map gold nanorods within biological tissue. *Nature Photonics* 2017;11:583-588.
20. Yahagi K, Kolodgie FD, Otsuka F, et al. Pathophysiology of native coronary, vein graft, and in-stent atherosclerosis. *Nat Rev Cardiol* 2016;13:79-98.
21. Niccoli G, Montone RA, Di Vito L, et al. Plaque rupture and intact fibrous cap assessed by optical coherence tomography portend different outcomes in patients with acute coronary syndrome. *Euro Heart J* 2015;36:1377-1384.
22. Galis ZS, Sukhova GK, Lark MW, Libby P. Increased expression of matrix metalloproteinases and matrix degrading activity in vulnerable regions of human atherosclerotic plaques. *J Clin Invest* 1994;94:2493-2503.
23. Ridker PM, Everett BM, Thuren T, et al. Antiinflammatory Therapy with Canakinumab for Atherosclerotic Disease. *N Engl J Med* 2017;NEJMoa1707914.
24. Duewell P, Kono H, Rayner KJ, et al. NLRP3 inflammasomes are required for atherogenesis and activated by cholesterol crystals. *Nature* 2010;464:1357-1361.

Supplementary References

1. Sijde JN Van Der, Karanasos A, Ditzhuijzen NS Van, Okamura T, Geuns RJ Van, Valgimigli M, Ligthart JMR, Witberg KT, Wemelsfelder S, Fam JM, Zhang BC, Diletti R, Jaegere PP De, Mieghem NM Van, Soest G Van, Zijlstra F, Domburg RT Van, Regar E. Safety of optical coherence tomography in daily practice: A comparison with intravascular ultrasound. *Euro Heart J Cardiovasc Imaging* 2017;18:467-474.
2. Villiger M, Otsuka K, Karanasos A, Doradla P, Ren J, Lippok N, Shishkov M, Daemen J, Diletti R, Geuns R-J van, Zijlstra F, Soest G van, Libby P, Regar E, Nadkarni SK, Bouma BE. Coronary Plaque Microstructure and Composition Modify Optical Polarization. A New Endogenous Contrast Mechanism for Optical Frequency Domain Imaging. *J Am Coll Cardiol Img* 2017
3. Villiger M, Zhang EZ, Nadkarni SK, Oh W-Y, Vakoc BJ, Bouma BE. Spectral binning for mitigation

of polarization mode dispersion artifacts in catheter-based optical frequency domain imaging. *Optics Express* 2013;21:16353.

4. Nadkarni SK, Pierce MC, Park BH, Boer JF de, Whittaker P, Bouma BE, Bressner JE, Halpern E, Houser SL, Tearney GJ. Measurement of Collagen and Smooth Muscle Cell Content in Atherosclerotic Plaques Using Polarization-Sensitive Optical Coherence Tomography. *J Am Coll Cardiol* 2007;49:1474–1481.
5. Lippok N, Villiger M, Albanese A, Meijer EFJ, Chung K, Padera TP, Bhatia SN, Bouma BE. Depolarization signatures map gold nanorods within biological tissue. *Nature Photonics*; 2017;11:583–588.

Chapter 19



Intracoronary polarimetry of a honeycomb-like structure

van Zandvoort LJC¹, Otsuka K², Bouma BE^{2, 3}, Daemen J¹

¹*Erasmus University Medical Center, Thoraxcenter, Department of cardiology, Rotterdam, the Netherlands*

²*Wellman Center for Photomedicine, Massachusetts General Hospital, Harvard Medical School, Boston, Massachusetts*

³*Institute for Medical Engineering and Science, Massachusetts Institute of Technology, Cambridge, Massachusetts, USA*

EuroIntervention. 2019;EIJ-D-19-00431

Case presentation

A 69 year old female patient was admitted to our institution for potential treatment of a non-ST segment elevation myocardial infarction after 8 days of intermittent pain. Angiography showed an unusual filling defect in the mid right coronary artery with TIMI III flow and moderate stable disease in the left coronary system. Optical frequency domain imaging (OFDI) revealed a honeycomb-like structure with multiple intraluminal microchannels confirming the presence of recanalized thrombus (Figure 1). Fresh thrombus (<1 day) comprises platelet aggregates, erythrocytes, and fibrin. Lytic thrombus (1 to 5 days), containing areas of necrosis and granulocytes, transforms into organized thrombus (>5 days) characterized by the presence of smooth muscle cells (SMCs), homogeneous or hyalin fibrin, and depositions of connective tissue and capillary ingrowth¹. The patient was included in the POLARIS-I registry, designed to assess the added value of measuring birefringence with polarization sensitive OFDI in ACS patients. Collagen and SMCs have been shown to display higher birefringence than other tissue components in the vessel wall². In the present case (Figure 1, right panel), high birefringence signals can be appreciated in connective tissue between the microchannels suggesting the presence of collagen and SMCs.

To date, the progression and consistency of thrombus can only be reliably assessed using histopathological examination, which has no place in an acute setting. PS-OFDI may be of value to study age, stability and morphometric characteristics of coronary thrombus.

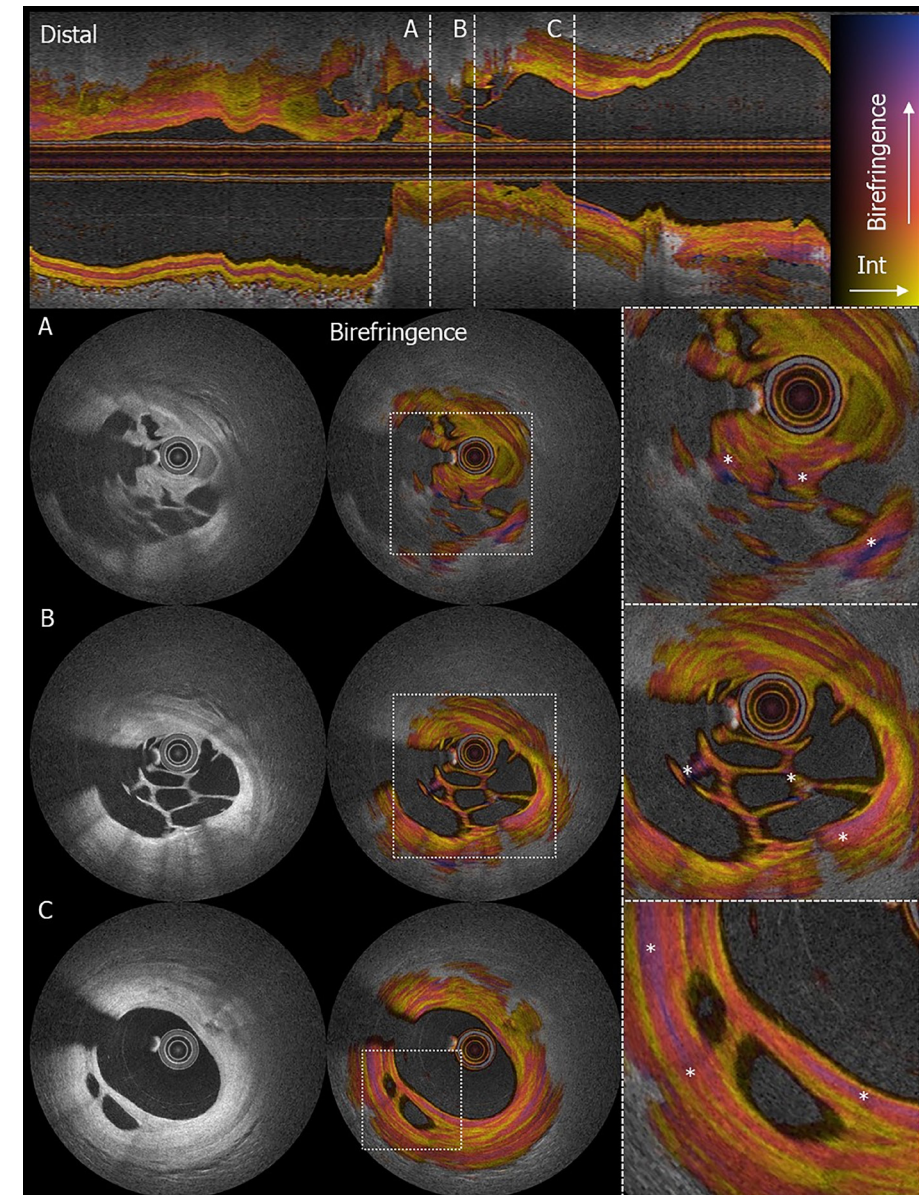
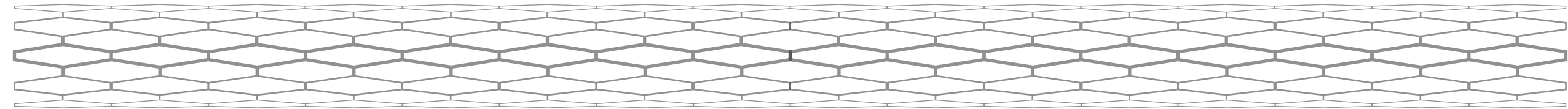


Figure 1. Conventional intensity and polarimetric properties of organized thrombus with microchannels. Upper panel: longitudinal view of the right coronary artery. The dashed white lines denote the cross-sectional locations for A, B and C. (A,B,C) Three locations with clear recanalization in organized thrombus; from left to right: Conventional OFDI intensity, birefringence, magnified birefringence (* denotes zones of high birefringence surrounding microchannels).

REFERENCES

1. Silvain J, Collet J-P, Nagaswami C, Beygui F, Edmondson KE, Bellemain-Appaix A, Cayla G, Pena A, Brugier D, Barthelemy O, Montalescot G and Weisel JW. Composition of coronary thrombus in acute myocardial infarction. *Journal of the American College of Cardiology*. 2011;57:1359-1367.
2. Villiger M, Otsuka K, Karanasos A, Doradla P, Ren J, Lippok N, Shishkov M, Daemen J, Diletti R, van Geuns RJ, Zijlstra F, van Soest G, Libby P, Regar E, Nadkarni SK and Bouma BE. Coronary Plaque Microstructure and Composition Modify Optical Polarization: A New Endogenous Contrast Mechanism for Optical Frequency Domain Imaging. *JACC Cardiovasc Imaging*. 2018.



Chapter 21



Summary & conclusion
Samenvatting & conclusie

Summary and conclusion

Both physiological assessment and intravascular imaging have emerged as excellent tools to improve angiographic lesion classification and their implementation proved to significantly improve short- and long-term outcomes of PCI. Nevertheless, despite significant improvements in plaque modification technologies and stent design over the past 3 decades, the risk of future adverse cardiac event rates remains substantial. The aim of the present thesis was to address the specific benefits of intravascular imaging and physiology when used in a post PCI setting to provide more insights into the details of target vessel failure and subsequent patient outcome.

In part one, this thesis starts with a review of the current literature supporting the clinical application of intravascular imaging and physiology in a post procedural setting. In chapter 3-5 we specifically evaluated the use of post PCI FFR and looked into the distribution, predictors and long-term clinical outcome related to post procedural FFR in a real-world patient population (FFR-SEARCH).

In part two, chapter 6-9, we addressed the specific benefit of (post) PCI intravascular imaging in procedural planning and evaluation. As such we proposed a more detailed approach to assess OCT detected stent edge dissections in the largest clinical outcome study on the topic to date and provided further details on the normal dimension of left main coronary arteries in order to better guide physicians confronted with left main stenting. Secondly, we illustrated the importance of post PCI intravascular imaging in two clinical studies assessing the performance of novel bioresorbable scaffolds.

In part three, chapter 10-12, we assessed the potential of a synergistic use of post procedural physiology (as a simple gatekeeper) and intravascular imaging (IVUS) to provide further mechanistic insights into the rationale of the low post PCI FFR. In the FFR SEARCH IVUS study we demonstrated for the first time that focal residual disease can be frequently found in patients with a low post PCI FFR providing a rationale for post PCI optimization in a specific group of patients that proved to be at higher risk of future adverse events. The latter formed the basis for the design of the FFR REACT trial.

In part four, chapter 13-17, we introduced several simplified and faster methods to assess post PCI physiology (3D-QCA based FFR and dPR).

Finally, in part five (chapter 18-20), we collaborated with the Massachusetts General Hospital and Wellman Center for Photomedicine to develop and validate

a novel imaging modality (PS-OFDI) to increase our understanding of plaque morphology in both stable and unstable coronary artery disease.

PART I VALUE OF POST PCI PHYSIOLOGY

In **chapter 2**, we present a general overview of the current literature with regard to post procedural treatment evaluation. Although clinical outcomes after PCI are gradually improving, several subpopulations still perform worse. Recent studies demonstrated that with the use of conventional intravascular imaging and physiology, clinical outcomes can be improved, while also newer modalities like angiography based fractional flow reserve and hybrid imaging catheters are entering the stage. Nevertheless, merely using these modalities is not enough and in order to truly improve patient outcome, optimal intravascular dimensions with minimal vascular injury should be targeted. When assessing post PCI results using either type of physiological or imaging technology, a broad spectrum of stent and vessel related anomalies can be expected, such as malapposition, underexpansion, stent edge dissections, side branch jailing and residual disease. Since not all of these issues warrant treatment, and can or should be improved, a profound knowledge of what to expect, how to recognize and when to treat these intraluminal problems is needed. The present review provides a detailed assessment of the incidences and impact of anatomic predictors of PCI failure reflected against the use of conventional and novel diagnostic tools with a specific focus on improving post PCI outcome.

The FFR SEARCH registry is the largest prospective study investigating the prognostic value and determinants of post PCI FFR. A total of 1000 patients were included in this single centre registry in Rotterdam in whom the FFR was measured after a successful PCI in 959 patients. While the primary endpoint consisted of clinical outcomes after two years, the initial study report in **chapter 3** provides readers with the post PCI FFR distribution and 30 day outcome figures. The FFR SEARCH registry illustrated that post PCI FFR assessment using a dedicated microcatheter is a safe and feasible method to measure the physiological status of a coronary artery after stent placement. The average additional time to measure the FFR was 5 minutes and no complications related to the microcatheter occurred. The FFR was measured at the ostium of the artery, at the proximal stent edge, distal stent edge and ± 20 mm distal of the most distal stent edge. The mean Pd/Pa in resting condition was 0.96 ± 0.04 , while the mean post PCI FFR under maximal hyperemia was 0.90 ± 0.07 . Although a satisfactory angiographic result was achieved, post PCI FFR remained ≤ 0.80 in 78 lesions (9.8%). Conversely,

post PCI FFR was >0.90 in 396 lesions (50%). Several factors were associated with a low post-PCI FFR, including bifurcations or calcified lesions. Furthermore, patients with diabetes mellitus or peripheral arterial disease were more likely to have ≥ 1 lesion with a post PCI FFR ≤ 0.90 . Finally, post-PCI FFR did not correlate with clinical events at 30 days.

In order to provide a decisive answer as to what are the predictors of post procedural fractional flow reserve values, **chapter 4**, was designed. We identified several independent patient and vessel related variables which predicted the post PCI FFR. In a LME-model, adjusting for independent predictors of post PCI FFR, females had a significantly higher mean post PCI FFR as compared to men (adjusted $\beta=0.013$, CI [0.005 to 0.02], $p=0.001$, R^2 for the complete model=0.54). The vessel in which the physiological measurements were taken was the strongest predictor, resulting in an average of 0.06 lower post PCI FFR value in LAD vessels. Additionally, type A lesions, in-stent restenosis, CTO's, post PCI MLD and pre – and post dilatation were significant predictors for post PCI FFR.

In the main paper of the FFR SEARCH register, **chapter 5**, the two year clinical results are discussed. On a patient level, post PCI FFR < 0.90 was not associated with MACE (HR 1.08, [95% CI, 0.73-1.60] $p=0.707$). On a vessel level however, FFR < 0.90 post PCI resulted into a higher rate of target vessel revascularizations (HR 0.52 [95% CI, 0.27-1.00] $p=0.049$) and a trend towards higher rate of stent thrombosis (HR 0.35 [95% CI, 0.11-1.13] $P=0.079$).

PART II UTILITY OF (POST PCI) INTRAVASCULAR IMAGING

Chapter 6 assessed the impact of untreated stent edge dissections (SEDs) as detected by OCT and potential predictors for device orientated clinical events (DOCE) at one year. The main findings of this study, representing the largest cohort of patients with SEDs as assessed by OCT, could be summarized as follows: 1) one-year cardiac event rates potentially attributable to the presence of untreated SEDs were 6.7%; 2) in patients with untreated SEDs, dissection length was the only independent predictor for DOCE at 1 year while cavity depth and reference lumen area where the only predictors for distal and proximal SEDs respectively; 3) follow-up OCT indicated (early) spontaneous healing in the majority of SEDs.

In **Chapter 7** we aimed to investigate the luminal integrity 6 to 9 months after implantation of the *Fantom* bioresorbable scaffold (BRS) with the use of IVUS. In this sub-study of the FANTOM II study we confirmed the efficacy of the *Fantom* BRS in patients with stable coronary artery disease by successfully

inhibiting neointimal hyperplasia at 6 and 9 months as assessed by IVUS. With a backbone that is designed to be absorbed within 4 to 5 years, our results show minimal obstruction volumes both at 6 and 9 months respectively, strengthening the recently published clinical and angiographic finding. Although the *Fantom* II study only represents the performance of the scaffold in highly selected cases, the obstruction volumes found are comparable to contemporary metallic DES like *Resolute Onyx*.

The results from **chapter 8** suggest that the latest magnesium BRS iteration, the *Magmaris*, suffers from premature dismantling with subsequent loss of vessel support. Together with incomplete distal device expansion, this could have contributed to a higher than expected lumen loss. Our results revealed a significant decrease in patent struts with a heterogeneous resorption pattern as soon as 4–5 months post implantation. The latest was demonstrated by an important reduction of attenuation and backscattering indices. Offline OCT at follow-up demonstrated a decrease in minimal lumen area (MLA) by $43.44 \pm 28.62\%$ ($p=0.042$), along with a significant decrease in scaffold area at the site of the MLA by $38.20 \pm 25.74\%$ ($p=0.043$). While our findings need to be confirmed in a randomized fashion, it seems imperative to follow the European working group recommendations on BRS and limiting their use to clinical trials or registries with adequate follow-up. Finally, our results suggest that clinical and angiographic follow-up alone might not be sufficient to establish the safety and long-term efficacy of new BRS, and warrants the use of serial intravascular coronary imaging at baseline and follow-up.

In **chapter 9** we assessed the luminal dimensions of non-obstructive left main coronary arteries (LMCA) with the use of IVUS in a large real world cohort. We demonstrated for the first time how non-diseased LMCA dimensions and length vary within the population and how women display smaller luminal dimensions compared to men. No clinically relevant predictors were found for both LMCA mean lumen area and length as correlation coefficients were low. These findings might guide physicians in deciding on stent- and post dilatation balloon sizing, and support the use of intravascular imaging in LMCA stenting. Given the structural undersizing based on QCA, IVUS helps in correctly identifying the exact LMCA length and area and thereby improves outcomes of complex LMCA PCI. More specifically, we demonstrated that 19% of the patients presented with IVUS derived mean luminal dimensions of >5 mm, requiring post dilatation with balloons up to 5 mm along with the use of stents with sufficient post dilatation margins.

PART III SYNERGISTIC USE OF INTRACORONARY IMAGING AND PHYSIOLOGY

Several recent studies demonstrated the value of low post PCI FFR in predicting late adverse cardiac events. Unfortunately, details on the actual rationale for these low PCI FFR values often remain elusive since no data on residual angiographically apparent disease were reported, nor were details presented on intravascular imaging findings. In the IVUS sub-study of the FFR SEARCH registry (**Chapter 10**) we demonstrated, for the first time, that clear signs of residual luminal narrowing, including focal lesions, underexpansion and malapposition, were present in a significant amount of vessels with an impaired post PCI FFR. Findings that were not readily apparent on QCA or post PCI angiography. The study included 95 patients (100 vessels) with an FFR value ≤ 0.85 and 20 with an FFR value above 0.85. In the low FFR cohort, residual focal lesions, underexpansion or malapposition was present in up to 87% of the vessel. Additionally, in the present study FFR pressure drops were more pronounced in vessels with residual proximal focal lesions but not with distal lesions.

In the succeeding follow-up study, **chapter 11**, of the IVUS cohort we assessed two year clinical events. We demonstrated a clear trend towards worse clinical outcomes at two years when IVUS derived residual lesions and underexpansion are present in patients with a post PCI FFR ≤ 0.85 . In order to answer the subsequent question, as to why then post procedural FFR remain low with good clinical outcome, we identified several independent patient and vessel related variables which predicted the post PCI FFR. In a GLME-model, adjusting for independent predictors of post PCI FFR, females had a significantly higher mean post PCI FFR as compared to men (adjusted $\beta=0.013$, CI [0.005 to 0.02], $p=0.001$, R^2 for the complete model=0.54). The vessel in which the physiological measurements were taken was the strongest predictor, resulting in an average of 0.06 lower post PCI FFR value in LAD vessels. Additionally, a history of smoking, type A lesions, in-stent restenosis, CTO's, pre procedural lesion length and pre - and post dilatation were significant predictors for post PCI FFR.

In **chapter 12** we elaborated on the FFR REACT study design. The FFR REACT study is an investigator initiated prospective, single-center randomized controlled trial conducted at the Erasmus Medical Center designed to assess if FFR guided PCI optimization directed by IVUS in patients with an increased risk for MACE (post PCI FFR below 0.90) will decrease target vessel failure at 1 year. Up to 290 patients with a post PCI FFR < 0.90 will be randomized (1:1) to either standard

of care (no additional intervention) or IVUS-directed optimization of the FFR (treatment arm). Inclusion started in October 2017 and enrolment is expected to be complete in Q1 2020. All patients will be followed for 3 years.

PART IV INNOVATIONS IN CORONARY PHYSIOLOGY

Based on previously performed research, the use of FFR received strong recommendations in current revascularization guidelines. Even though the use of FFR proved to be contrast saving, cost effective and associated with improved quality of life, FFR is still not being performed in the vast majority of cases. The latter has been hypothesized to be due to the need for (in some countries) expensive hyperemic agents with known adverse events as dyspnea and arrhythmias and or intolerance due to pulmonary disease and the use of a costly pressure wire. The FAST study (**chapter 13**) confirmed the feasibility of a novel 3D-QCA based software tool to calculate FFR without the use of a pressure wire or microcatheter (vessel FFR, vFFR). In the pre-clinical technical validation model, vFFR proved to have a strong correlation with computation fluid dynamics and invasively measured flow parameters. In our clinical validation study we confirmed an excellent agreement and high diagnostic value of vFFR compared to invasively measured FFR using a dedicated pressure wire under maximum hyperemia. Finally, we showed that vFFR had a low inter-observer variability.

In the subsequent study on vFFR, we utilized the FFR SEARCH database in order to assess the feasibility of vFFR in a post procedural setting (**Chapter 14**). The main findings of the study could be summarized as follows: vFFR allows to identify post PCI FFR < 0.90 with a high sensitivity and specificity; vFFR showed good correlation and agreement with post PCI FFR as measured using the dedicated Navvus microcatheter and post PCI vFFR computation remained to have a low inter-observer variability. Based on the results of this study, calculation of post stenting vFFR using CAAS workstation, could be a useful and easy to use tool to identify and potentially optimize the outcomes of patients at higher risk for future adverse cardiac events. Larger clinical outcome studies should be obtained to assess the value of post stenting vFFR to optimize PCI outcomes.

In **chapter 15** we proposed another potential group of patients whom might benefit from 3D-QCA based vFFR: patients with possible epicardial disease after a cardiac transplant. In the early years after cardiac transplantation, both negative remodeling of the epicardial arteries as well as a decrease in microvascular resistance (IMR) are common findings. At the longer term however,

IMR substantially increases, decreasing the maximum achievable flow down the epicardial vessels. FFR has proven to be a useful tool to identify the hemodynamic severity of intermediate coronary artery lesions. However, there has been ongoing debate on its validity in denervated hearts. Recent studies therefore suggested to measure IMR in order to appreciate the status of the allograft in order to be able to better interpret the FFR.

The recently validated software that calculates vFFR might offer a solution to the problem. In order to illustrate the latter we presented a case of a 39 year old male patient, 14 years after allograft cardiac transplantation with a suspected significant lesion. Invasive assessment using conventional intracoronary physiology assessment using FFR showed a significant discrepancy with findings on OCT and the vFFR. Illustrated by the present case, we believe that a strong argument can be made towards to use of these novel technologies that might potential be superior to conventional assessment in the routine follow-up of these high risk patients.

Another method to assess the hemodynamic severity of a coronary lesion without the need for a hyperemic agent lies in the instantaneous wave free ratio (iFR). iFR offers a reliable assessment of coronary physiology but requires dedicated proprietary software with a fully automated algorithm. **Chapter 16** comprises of the pivotal study investigating the feasibility of a non-hyperemic pressure ratio, the dPR, calculated using a novel software applicable to any type of pressure wire or microcatheter. dPR had an excellent linear correlation with iFR and a strong diagnostic accuracy in identifying lesions with an FFR ≤ 0.80 . The dPR assessment proved to be a fast, simple and reproducible non-hyperemic ratio based on DICOM pressure waveforms which could open up the field for a more widespread use of diastolic pressure gradients in real world clinical practice. By using a simple software tool to automatically detect the flat period in the dP/dt curve that indicates the so called "wave-free" period we found that the resultant dPR correlated nearly perfect with the original iFR output of Phillips Volcano ($r=0.997$, $p<0.001$). Subsequently, our results showed a correlation between dPR and FFR ($r=0.77$) in line with previous results from the VERIFY study demonstrating a correlation coefficient r of 0.789 between iFR and FFR.

Despite the unequivocal evidence supporting the use of pre PCI physiological lesion assessment, the use of the technology in a post PCI setting is still rare. Instead, post PCI results are routinely assessed by visual angiographic assessment, a technique that showed to correlate poorly with functional assessment in the vast majority of cases. The importance of the latter was illustrated by a growing body

of evidence showing the strong predictive value of post PCI FFR for future adverse events. However, at present little is known about the use of post PCI dPR and its independent predictors.

Chapter 17 discusses the results of the post hoc analysis of the FFR SEARCH registry with the applied dPR algorithm. The study showed that despite optimal angiographic PCI results 15% of the patients and 13% of the vessels end with a post PCI dPR of ≤ 0.89 . Second, LAD lesions, diabetes, stent diameter, in-stent restenosis, pre and post reference diameter proved to be independent predictors of post PCI dPR and finally, there was a strong trend towards higher rates future adverse events in case post PCI dPR was ≤ 0.89 .

PART V INNOVATIONS IN INTRAVASCULAR POLARIMETRY ASSESSMENT

At this stage, intravascular polarimetry had been investigated as a basis for assessing coronary atherosclerosis in both cadaveric human coronary arteries and patients with mainly stable coronary disease, yet it is currently unknown what added value the polarimetric measurements might have in patients with unstable coronary artery disease. In order to investigate the latter, the POLARIS-I study was initiated with the aim to include up to 35 patients with unstable coronary artery disease (unstable angina or non ST elevated myocardial infarction) and a clinical indication for plaque characterization with OCT/OFDI.

The first-in-human pilot study of intravascular polarimetry in **chapter 18** demonstrated how the technology could strengthen conventional OFDI plaque characterization with quantitative polarization properties, measured through standard intravascular OFDI catheters simultaneously with the conventional OFDI signal. The polarization features offer refined insight into tissue composition, consistent with our current understanding of the mechanisms involved in plaque progression and destabilization. The major finding of this study is that fibrous caps in culprit lesions and ruptured plaques of patients presenting with an acute coronary syndrome exhibit lower birefringence as compared to the caps of target lesions in patients with stable disease. Compared to the interpretation of conventional OFDI, which relies on subjective identification of qualitative features, polarimetry offers quantitative metrics, leading a way to objective and automated characterization of atherosclerotic plaques. The improved assessment of plaque composition offered by the polarization features may provide novel insight into the mechanism of plaque progression and instability in human coronary atherosclerosis.

In **chapter 19** we elaborate on the potential added value of PS-OFDI to study thrombus. A 69 year old female patient was admitted to our institution for potential treatment of a non-ST segment elevation myocardial infarction after 8 days of intermittent pain. Angiography showed an unusual filling defect in the mid right coronary artery with TIMI III flow and moderate stable disease in the left coronary system. PS-OFDI revealed a honeycomb-like structure with multiple intraluminal microchannels confirming the presence of recanalized thrombus. Collagen and smooth muscle cells have been shown to display higher birefringence, evidently PS-OFDI may be of value to study age, stability and morphometric characteristics of coronary thrombus

The final chapter of this dissertation, **chapter 20**, discusses the POLARIS-I registry to focus on the polarization properties of intracoronary thrombus in patients presenting with ACS as assessed with PS-OFDI. We were able to demonstrate, for the first time, a significantly higher birefringence in healing coronary thrombus as compared to fresh thrombus. Additionally, we found that birefringence is dependent on the age of the thrombus when using the time until intravascular imaging as approach of measuring. Finally, no difference in birefringence was found between the fibrous caps of ruptured plaques and remote fibroatheromas. To date, the composition and progression of thrombus can only be reliably assessed using histopathological examination, which has no place in an acute setting. PS-OFDI might be a valuable new imaging modality to help further study age, stability and morphometric characteristics of coronary thrombus.

Future perspectives

The future of interventional cardiology would most probable coincide with several transitions with regard to intravascular imaging and physiology. Contemporary academic research already illustrates a glimpse of these transitions which might happen simultaneously. Although the three transitions that I envision might be developed separately in different institutions or medical companies, at some point they all need to be brought together in the catheterization laboratory to help the clinician in improving patient outcome.

First, intravascular imaging, primarily IVUS and OCT, should be used in a higher proportion of cases. Large clinical trials have already shown that target vessel failure can be reduced using IVUS when optimal luminal dimension are reached. Clinical interventional cardiologists need a better understanding on when to use intravascular imaging and how to interpret it. Post PCI evaluation using imaging is a critical step in the treatment of a patient presenting with coronary artery disease

and any interventional cardiologist should at least consider this option. At present intravascular imaging catheters are expensive and not reimbursed in all countries. The latter will also need to change in order to increase the adoption rates.

Second, a more simplistic interpretation with the use of (intravascular) physiology should be developed to assess the hemodynamic significance of a coronary segment. Important steps have already been made using both hyperemic and non-hyperemic indexes. Even more simplified models are studied at the moment, precluding the need for a pressure wire, where coronary physiology is assessed using angiography and assumptions based on simplified computational fluid dynamics. Future studies should test these novel physiological modalities in randomized controlled trials, while also including post procedural assessment, tandem lesions and patients with impaired microvascular resistance.

Finally, novel imaging modalities should not merely provide the operators with more information and additional intergrated images, but support neural networks, with the aim to automatically assess clinical relevant segments that warrant additional treatment. Contemporary acoustic – and photo medicine evolves at such a rapid pace that topical familiarity on the most recent body of research and well-advised implementation is hard. At the moment, cumulative evidence is being presented on the novel applicability of hybrid imaging and their ability to provide a unique insight in plaque vulnerability in unstented segments to identify lesions that are prone to rupture. Although basic interpretation of conventional imaging modalities such as IVUS and OCT is key, state of the art hybrid imaging catheters should provide the operator with treatment recommendations, rather than images that require extensive knowledge and training to fully appreciate their underlying information.

Conclusion

Clinical outcomes after PCI are gradually improving, although several subpopulations still perform worse. Recent research demonstrated that with the use of conventional intravascular imaging and physiology, clinical outcomes can be enhanced and also newer modalities, for instance angiography based FFR and hybrid imaging catheters are entering the stage. Nevertheless, merely using these modalities is not enough and in order to truly improve patient outcome, optimal intravascular dimensions with minimal vascular injury is warranted. Procedural success can be suboptimal due to several factors, including stent related anomalies like malapposition, stent underexpansion, stent edge dissections, jailed side branches, or residual focal disease, missed on angiography. Although some

of latter might truly increase target vessel failure on the long run, some on the other hand have proven to be self-resolving and a well-balanced decision needs to be made concerning potential treatment. Each intravascular modality, able to assess procedural success, has its own perks and drawbacks, warranting academic research and clinical experience to rightfully select the appropriate modality.

With this dissertation, we aimed to contribute to the body of evidence supporting the clinical application of intravascular imaging and physiology. We were able to assess the feasibility of conventional intravascular imaging and physiology strategies in a post procedural setting. We identified post procedural anomalies with the use of OCT, IVUS and FFR and assessed their impact on clinical outcome. Finally, we implemented novel imaging and physiology modalities to gain further insight in plaque morphology and simplify hemodynamic coronary assessment. We hope this dissertation contributes towards the next step in clinical PCI evaluation and therefore improve patient outcome.

Samenvatting en conclusie

Zowel fysiologische metingen als intravasculaire beeldvorming blijken een excellente manier om angiografische laesies te classificeren en het gebruik van deze modaliteiten verbetert significant korte en lange resultaten na een dotterbehandeling. Desalniettemin is er ondanks aanzienlijke verbetering in plaque modifierende technologie en stentontwerp in de laatste 3 decennia nog steeds een aanzienlijk risico op cardiale problemen en stent falen. Het doel van dit proefschrift was om de specifieke voordelen van intravasculaire beeldvorming en fysiologie na een dotterprocedure te onderzoeken en meer inzicht te krijgen in de details voor het falen van een kransslagader en de daarbij behorende slechte uitkomst voor een patiënt

In deel één begint dit proefschrift met een overzicht van de huidige literatuur ter ondersteuning van de klinische toepassing van intravasculaire beeldvorming en fysiologie in een post procedurele setting. In hoofdstuk 3-5 hebben we specifiek het gebruik van post-PCI FFR geëvalueerd en gekeken naar de distributie, voorspellers en klinische uitkomsten op lange termijn gerelateerd aan post-procedurele FFR in patiëntenpopulatie die lijkt op de klinische praktijk (FFR-SEARCH).

In deel twee, hoofdstuk 6-9, hebben we de specifieke voordelen van intravasculaire beeldvorming (na een dotterbehandeling) onderzocht. Zodanig hebben we een meer gedetailleerde benadering voorgesteld om OCT-gedetecteerde dissecties op een stent rand te beoordelen in de grootste klinische studie over dit onderwerp tot nu toe. Daarnaast hebben we onderzoek gedaan naar de afmetingen van hoofdstam kransslagaders om interventiecardiologen beter te kunnen begeleiden. Verder hebben we het belang van intravasculaire beeldvorming na een procedure geïllustreerd in twee klinische onderzoeken die nieuwe biologisch afbreekbare stent evalueerden.

In deel drie, hoofdstuk 10-12, hebben we het potentieel van synergetisch gebruik van fysiologie na een behandeling (als een eenvoudige poortwachter) en intravasculaire beeldvorming (IVUS) onderzocht om verdere inzichten te verschaffen over de oorzaken van een lage FFR na een behandeling. In de FFR SEARCH IVUS-studie hebben we voor het eerst aangetoond dat focale residuele ziekte vaak kan worden aangetroffen bij patiënten met een lage post-PCI FFR, wat het opstapje vormt voor optimalisatie middels IVUS na een procedure met een lage post procedurele FFR. Dit laatste vormde de basis voor het ontwerp van de FFR REACT-studie.

In deel vier, hoofdstuk 13-17, hebben we verschillende vereenvoudigde en snellere

methoden geïntroduceerd om post-PCI-fysiologie te beoordelen (FFR gebaseerd op 3D-QCA en dPR).

Ten slotte werkten we in deel vijf (hoofdstuk 18-20) samen met het Massachusetts General Hospital en het Wellman Center for Photomedicine om een nieuwe beeldvormingsmodaliteit (PS-OFDI) te ontwikkelen en te valideren om ons begrip van plaquemorfologie in zowel stabiele als onstabiele kransslagaders te vergroten.

DEEL I FYSIOLOGIE NA EEN DOTTERBEHANDELING

In **hoofdstuk 2** presenteren we een overzicht van de huidige literatuur met betrekking tot post procedurele behandeling evaluatie. Hoewel klinische resultaten na een dotterbehandeling geleidelijk verbeteren, presteren verschillende subpopulaties nog steeds suboptimaal. Recente studies laten zien dat met het gebruik van conventionele intravasculaire beeldvorming en fysiologie, klinische resultaten kunnen worden verbeterd. Daarnaast beginnen ook nieuwere modaliteiten zoals op angiografie gebaseerde FFR en hybride beeldvormende katheters aan een opmars. Desondanks is alleen het gebruik van deze modaliteiten niet voldoende om klinische resultaten te verbeteren en zal men moeten streven naar optimale intravasculaire dimensies met minimaal vaatletsel. Bij het beoordelen van het resultaat na een dotterbehandeling met behulp van fysiologie en beeldvorming, kan een breed spectrum aan stent- en vaatgerelateerde afwijkingen worden verwacht, zoals stents die niet tegen de vaatwand liggen (malappositie), onvolledig geëxpandeerde stents, scheurtjes aan de stentrand, zijtak vernauwing en residuele ziekte. Aangezien niet al deze kwesties kunnen of dienen behandeld te worden, is grondige kennis nodig over wat men kan verwachten, hoe men dit kan herkennen en wanneer het behandeld dient te worden. Dit hoofdstuk biedt een gedetailleerd overzicht van de incidentie en impact van vaatgerelateerde afwijkingen met het gebruik van conventionele en nieuwe diagnostische hulpmiddelen. We richten ons hierbij specifiek op het verbeteren van de resultaten na een dotterbehandeling.

Het FFR SEARCH register is het grootste prospectieve onderzoek naar de prognostische waarde en determinanten van FFR na een dotterbehandeling. In totaal zijn 1000 patiënten geïnccludeerd in dit register uit Rotterdam, bij wie in 959 gevallen de FFR werd gemeten na een succesvolle dotterbehandeling. Hoewel het primaire eindpunt bestond uit de klinische resultaten na twee jaar, omvat het eerste onderzoeksrapport in **hoofdstuk 3** de distributie van de FFR waarden na een dotterbehandeling en de 30 dagen klinische uitkomsten. Het FFR

SEARCH register illustreerde dat FFR na een dotterbehandeling een veilige en reële methode is om de fysiologische status van kransslagaders na stentplaatsing te meten met behulp van de Navvus rapid exchange monorail microcatheter. De gemiddelde tijd om de FFR te meten was 5 minuten boven de normale procedure tijd en daarnaast zijn er geen complicaties opgetreden dankzij de microcatheter. De FFR werd gemeten aan de opening van de kransslagader, aan de proximale stentrand, distale stentrand en ± 20 mm distaal van de meest distale stentrand. De gemiddelde Pd / Pa in rusttoestand was 0.96 ± 0.04 , terwijl de gemiddelde FFR na de dotterbehandeling onder maximale hyperemie 0.90 ± 0.07 was. Hoewel in alle gevallen een acceptabel angiografisch resultaat werd bereikt, bleef de FFR na de dotterbehandeling ≤ 0.80 in 78 laesies (9.8%). Omgekeerd zijn de FFR na de behandeling > 0.90 in 396 laesies (50%). Verschillende factoren waren geassocieerd met een lage post procedurele FFR, waaronder bifurcaties en verkalkte laesies. Bovendien hadden patiënten met diabetes mellitus of perifere arteriële ziekte meer kans op het hebben van ≥ 1 laesie met een FFR ≤ 0.90 . Tot slot correleerde FFR na een dotterbehandeling niet met klinische uitkomsten op 30 dagen.

Om een definitief antwoord te geven op de vraag, wat de voorspellers zijn van post procedurele FFR waarden, hebben we **hoofdstuk 4**, ontworpen. We hebben verschillende onafhankelijke patiënt en vaat gerelateerde variabelen geïdentificeerd die de post PCI FFR voorspelden. In een LME-model, gecorrigeerd voor onafhankelijke voorspellers van post PCI FFR, hadden vrouwen een significant hogere post PCI FFR vergeleken met mannen (gecorrigeerde $\beta = 0.013$, CI [0.005 tot 0.02], $p = 0.001$, R^2 voor het volledige model = 0.54). Het vat waarin de fysiologische metingen werden verricht, was de sterkste voorspeller, wat resulteerde in een post procedurele FFR van 0.06 lager in LAD vaten. Andere voorspellers voor een lagere post procedurele FFR waren, type A laesies, in-stent restenose, CTO's, post procedurele MLD en en pre- en postdilatie.

In het concluderende artikel van het FFR SEARCH register, **hoofdstuk 5**, worden de klinische resultaten na twee jaar besproken. Op patiëntniveau was de post procedurele FFR < 0.90 niet geassocieerd met meer cardiale complicaties (HR 1.08, [95% CI, 0.73-1.60] $p = 0.707$). Op vatniveau resulteerde een FFR < 0.90 na een dotterbehandeling echter in een hoger percentage revascularisaties van het gemeten vat (HR 0.52 [95% CI, 0.27-1.00] $p = 0.049$). Tot slot werd er een trend gezien met een hoger percentage stenttrombose (HR 0.35 [95 % CI, 0.11-1.13] $P = 0.079$).

DEEL II GEBRUIK VAN INTRAVASCULAIRE BEELDVORMING (NA EEN DOTTERBEHANDELING)

In **hoofdstuk 6** is onderzocht wat de invloed van onbehandelde stentrand dissecties (SEDs), geïdentificeerd met OCT en potentiële voorspellers voor klinische gebeurtenissen gerelateerd aan deze dissecties (DOCE) na één jaar zijn. De belangrijkste bevindingen van deze studie, die het grootste cohort van patiënten met OCT gedetecteerde SEDs bevat, kunnen als volgt worden samengevat: 1) cardiale incidenten die mogelijk te wijten zijn aan de aanwezigheid van onbehandelde SEDs traden op 6.7%; 2) bij patiënten met onbehandelde SEDs was de dissectielengte de enige onafhankelijke voorspeller voor DOCE na 1 jaar, terwijl de diepte van de SED en de referentie lumen oppervlakte de enige voorspellers waren voor respectievelijk distale en proximale SEDs; 3) een herhaling van de OCT tijdens een vervolg katheterisatie toonden (vroeg) spontane genezing in een grote meerderheid van de SEDs.

In **hoofdstuk 7** hebben we getracht de vaatwand integriteit te onderzoeken, 6 en 9 maanden na het plaatsen van een *Fantom* oplosbare stent met behulp van IVUS. In deze sub studie van de FANTOM II-studie bevestigden we de werkzaamheid van de *Fantom* oplosbare stent bij patiënten met een stabiel kransslagader lijden. We toonden dit aan door succesvolle inhibitie van nieuwe vaatwand vernauwing op 6 en 9 maanden na het plaatsen van de stent. De *Fantom* oplosbare stent heeft een geraamte dat ontworpen is om binnen 4-5 jaar op te lossen en met de huidige studie hebben we aangetoond dat er na zowel 6 als 9 maanden minimale obstructie volumes te zien zijn. Dit laatste onderstreept de goede klinische resultaten in de recent gepubliceerde studie. Ondanks dat de FANTOM II- studie alleen zeer geselecteerde patiënten bevat, zijn de obstructie volumes vergelijkbaar met de hedendaagse metalen stents zoals de Resolute Onyx.

De resultaten van **hoofdstuk 8** suggereren dat de nieuwste oplosbare magnesium stent iteratie, de Magmaris, lijdt aan voortijdige ontmanteling met daaropvolgend verminderde vaat ondersteuning. Samen met een suboptimale distale stent expansie, heeft dit bijgedragen aan een hoog verlies van lumenoppervlakte. Onze resultaten lieten een significante afname van intacte stent struts zien met een heterogeen resorptiepatroon, 4-5 maanden na de implantatie. Dit laatste werd onderstreept door een opmerkelijke reductie van helderheid en achterwaartse lichtverstrooiing van de struts. Een herhaling van de OCT tijdens een vervolg katheterisatie toont een afname van de minimale lumenoppervlakte aan van $43.44 \pm 28.62\%$ ($p = .042$), samen met een significante afname van het stentoppervlakte van

$38.20 \pm 25.74\%$ ($p = 0.043$) op de locatie van de minimale lumenoppervlakte. Hoewel onze bevindingen op gerandomiseerde wijze moeten worden bevestigd, lijkt het absoluut noodzakelijk om de aanbevelingen van de Europese werkgroep voor oplosbare stents op te volgen en het gebruik ervan te beperken tot enkel klinische proeven en registers met adequate vervolging. Tot slot suggereren onze resultaten dat vervolging door middel van intravasculaire beeldvorming van de kransslagader tijdens de initiële plaatsing en tijdens een herhaal katheterisatie aan te raden is en dat enkel klinische en angiografische vervolging niet voldoende zou zijn om de veiligheid en de lange termijn werkzaamheid van deze nieuwe oplosbare stents vast te stellen.

In **hoofdstuk 9** hebben we de kransslagader afmeting en volumes van niet-obstructieve hoofdstamkransslagaders (LMCA) onderzocht met behulp van IVUS in een groot "real world" cohort. We hebben voor de eerste keer aangetoond dat niet-zieke LMCA dimensies en lengtes binnen een populatie variëren en hoe vrouwen kleinere vaat dimensies hebben in vergelijking met mannen. Er werden geen klinisch relevante voorspellers gevonden, omdat de correlatiecoëfficiënten laag waren. Desondanks kunnen deze bevindingen artsen helpen bij het bepalen van de grootte van de stents en de grootte van post dilatatie ballonen. Verder geeft dit nogmaals aan hoe belangrijk intravasculaire IVUS is bij de behandeling van LMCA vernauwingen. Gezien de structurele onderschatting van LMCA dimensies op basis van kwantitatieve angiografie helpt IVUS bij het correct identificeren van de exacte LMCA-lengte en oppervlakte en verbetert daardoor de uitkomsten van complexe percutane LMCA behandelingen. Tot slot toonden we aan dat 19% van de patiënten, op basis van IVUS, een gemiddelde vaat diameter hadden van >5 mm, wat aangeeft dat dilatatie na het plaatsen van een stent met een 5 mm ballon nodig zou zijn in combinatie met een stent die deze marge aankan.

DEEL III SYNERGETISCH GEBRUIK VAN INTRACORONAIRE BEELDVORMING EN FYSIOLOGIE

Recente studies tonen aan dat een lage FFR na een procedure een goede voorspeller is voor toekomstige kransslagader problemen en heropnames. Wanneer men alleen kijkt naar de angiografische resultaten, dan blijkt het vaak onduidelijk waarom patiënten met een lage FFR deze problemen ontwikkelen, mede omdat eerdere studies geen IVUS resultaten presenteerden bij patiënten met een lage FFR na de behandeling. In de IVUS sub-studie van het FFR SEARCH register (**hoofdstuk 10**) hebben we voor de eerste keer aan kunnen tonen dat patiënten met een lage FFR na een procedure veelal tekenen vertoonden van focale

vatvernaauwing, malapposition en stents die niet volledig geëxpandeerd waren. Deze resultaten waren met kwantitatieve angiografie niet detecteerbaar. In de studie waren 100 patiënten met een FFR na de procedure van ≤ 0.85 geïnccludeerd en 20 met een FFR > 0.85 . In de lage FFR groep zagen we in 87% van de vaten focale vernauwingen, onvolledige stent expansie of malappositie. Verder zagen we in de huidige studie dat een FFR verval over een proximaal segment vaker voorkwam bij vaten met een focale proximale vernauwing, dit was niet het geval voor distale vernauwingen.

In het vervolg op de bovenstaande studie, **hoofdstuk 11**, beoordeelden we de klinische resultaten, na twee jaar van het IVUS cohort. We zagen een duidelijke trend van afnemende klinische resultaten na twee jaar wanneer residuele laesies en onderexpansie van stents op IVUS aanwezig waren bij patiënten met een post-PCI FFR ≤ 0.85 .

In **hoofdstuk 12** zetten we het studieontwerp van de FFR REACT uiteen. De FFR REACT studie is een door de wetenschap geïnitieerde prospectieve, single-center gerandomiseerd gecontroleerde studie uitgevoerd in het Erasmus Medisch Centrum. De studie is ontworpen om te onderzoeken of een dotterbehandeling verbeterd kan worden door te kijken naar de FFR en IVUS in patiënten die een verhoogd risico hebben op additionele kransslagader problematiek (FFR na dotterbehandeling < 0.90) en of dit een kransslagader probleem na 1 jaar verminderd. In totaal zullen 290 patiënten met een FFR na de dotterbehandeling < 0.90 worden gerandomiseerd (1:1) in ofwel de standaardbehandeling (geen extra interventie) of optimalisatie van de FFR met IVUS (behandelarm). De studie is gestart in oktober 2017 en de inclusie zal naar verwachting in Q1 2020 voltooid zijn. Alle patiënten zullen gedurende 3 jaar worden vervolgd.

DEEL IV INNOVATIES IN KRANSSLAGADER FYSIOLOGIE

Op basis van eerder onderzoek krijgt het gebruik van FFR een duidelijke aanbeveling in de huidige richtlijnen voor kransslagader dotterbehandelingen. Hoewel het gebruik van FFR kosteneffectief is en zorgt voor minder contrast gebruik en de levenskwaliteit na een behandeling verbetert, wordt het in meerderheid van de gevallen nog steeds niet gebruikt. Dit is waarschijnlijk te wijten aan de hoge kosten van hyperemische middelen in sommige landen, nadelige bijwerkingen zoals kortademigheid en hartritmestoornissen, intolerantie vanwege longziekten en het gebruik van een kostbare druk draad. De FAST studie (**hoofdstuk 13**) illustreert de toepasbaarheid van een nieuwe programma, gebaseerd op 3D-QCA,

om de FFR te berekenen zonder het gebruik van een drukdraad of microkatheter (vat FFR, vFFR). In het preklinische technische validatiemodel bleek vFFR een sterke correlatie te hebben met toegepaste vloeistofdynamica en invasief gemeten stromingsparameters. In onze klinische validatiestudie bevestigden we een uitstekende overeenkomst en een goede diagnostische nauwkeurigheid tussen vFFR en de FFR, die invasief was gemeten onder maximale hyperemie met behulp van een drukdraad. Tot slot toonden we aan dat vFFR een lage variabiliteit heeft tussen verschillende onderzoekers.

In de vervolg studie over vFFR hebben we de FFR SEARCH database gebruikt om de toepasbaarheid van vFFR na een dotterbehandeling te beoordelen (**hoofdstuk 14**). De belangrijkste bevindingen van het onderzoek kunnen als volgt worden samengevat: vFFR maakt het mogelijk om een post procedurele FFR < 0.90 te identificeren met een hoge sensitiviteit en specificiteit; vFFR liet een goede correlatie met invasief gemeten post procedurele FFR zien, zoals gemeten met de Navvus microkatheter en tot slot had de berekening van de post procedurele FFR wederom een lage inter-observer variabiliteit. Op basis van de huidige resultaten zou de berekening van vFFR na het plaatsen van een stent een nuttig en gemakkelijk te gebruiken hulpmiddel kunnen zijn om de uitkomsten van patiënten met een hoog cardiaal risicoprofiel te identificeren en mogelijk te optimaliseren. Grotere klinische onderzoeken zullen de waarde van vFFR na het plaatsen van een stent verder moeten beoordelen en evalueren of klinische resultaten verbeterd kunnen worden door eventuele vFFR optimalisatie.

In **hoofdstuk 15** hebben we een nieuwe potentiële groep patiënten geïdentificeerd die mogelijk baat zou kunnen hebben bij de op 3D-QCA gebaseerde vFFR: patiënten met potentieel epicardiaal kransslagaderlijden na een harttransplantatie. In de eerste jaren na een harttransplantatie wordt het lumen van de epicardiale slagaders kleiner en is er een afname van de weerstand in de capillairvaten (IMR). Op de langere termijn neemt de IMR echter aanzienlijk toe, waardoor de maximaal haalbare doorstroming door de epicardiale bloedvaten afneemt. FFR is nuttig gebleken om de ernst van vernauwingen in de epicardiale kransslagaderen te bepalen. Er is echter nog steeds discussie over de validiteit ervan in getransplanteerde harten. Recente studies suggereerden daarom de IMR te meten en zo de gezondheid van het getransplanteerde hart te bepalen om de FFR beter te kunnen interpreteren.

De recentelijk gevalideerde vFFR biedt mogelijk een oplossing voor dit probleem. Om dit laatste te illustreren presenteerden we de casus van een 39-jarige mannelijke patiënt, 14 jaar na allograft-harttransplantatie met een vermoedelijke

significante vernauwing. De conventionele invasief gemeten FFR verschilde aanzienlijk met de resultaten van de OCT en de vFFR. Geïllustreerd door middel van deze casus, zijn wij van mening dat deze nieuwe technologie mogelijk superieur is aan de conventionele methodes bij het routinematige opvolgen van deze hoog risicopatiënten.

De directe golfvrije ratio (*Instantaneous wave free ratio; iFR*) is een andere methode om de hemodynamische ernst van een kransslagader vernauwing te bepalen zonder een hyperemisch middel toe te dienen. iFR geeft een betrouwbare meting van de kransslagader fysiologie, maar is enkel te berekenen met een gepatenteerde software. **Hoofdstuk 16** beschrijft een studie die de uitvoerbaarheid en nauwkeurigheid van een niet-hyperemische ratio, de dPR, heeft onderzocht door middel van een nieuwe software die te gebruiken is met zowel drukdraden als kleine drukkatheters. dPR liet een excellente correlatie met iFR zien en een hoge diagnostische nauwkeurigheid voor het identificeren van een FFR ≤ 0.80 . dPR is een snelle, simpele en reproduceerbare niet-hyperemische ratio gebaseerd op DICOM drukgolven, die de mogelijkheid biedt voor een hoger gebruik van diastolische drukgradiënten in de klinische praktijk. Door een eenvoudige software programma te gebruiken dat automatisch de vlakke periode in de dp/dt-curve detecteert, de zogenaamde "golfvrije" periode, vonden we dat de dPR bijna perfect correleerde met de oorspronkelijke iFR resultaten van Phillips Volcano ($r = 0.997$), $p < 0.001$). Verder toonden onze resultaten een correlatie tussen dPR en FFR die in lijn is met de resultaten van de VERIFY studie ($r=0.77$ voor dPR vs. FFR en $r=0.79$ voor iFR vs. FFR respectievelijk).

Ondanks concreet bewijs dat het gebruik van een fysiologische meting voor het plaatsen van een stent aanraadt, worden deze metingen na de behandeling niet vaak gedaan. Evaluatie van de behandeling wordt vaak verricht op basis van angiografie, een methode die een bewezen slechte correlatie heeft met fysiologie. Dit laatste is benadrukt door verschillende studies die illustreerden hoe belangrijk FFR na behandeling is als indicator voor succes van de behandeling. Op dit moment is er echter weinig bekend over de waarde en voorspellers van de dPR na een dotterbehandeling.

In **hoofdstuk 17** worden de resultaten besproken van de post hoc analyse van het FFR SEARCH register waar het dPR algoritme op toegepast is. De studie laat zien dat ondanks goed angiografisch resultaat, 15% van de patiënten en 13% van vaten na een behandeling nog steeds een dPR ≤ 0.89 hebben. Ten tweede bleken metingen in de LAD, patiënten met diabetes, stent diameter, in-stent restenose en referentie diameters voor en na de behandeling onafhankelijke voorspellers te

zijn voor de dPR na een behandeling. Tot slot is er een trend gezien waarbij een dPR ≤ 0.89 zorgde voor meer heropnames na de behandeling.

DEEL V INNOVATIES IN INTRAVASCULAIRE POLARISATIE METINGEN

De eerste op mensen geteste studie (**hoofdstuk 18**) die polariteit meet in de kransslagaderen liet zien hoe dit de conventionele OFDI plaque karakterisatie versterkt door het kwantitatief meten van polarisatie. Dit werd gemeten met een standaard OFDI katheter die gelijktijdig het conventionele OFDI-signaal toonde. De polarisatiemetingen bieden een verfijnd inzicht in de samenstelling en consistentie van het weefsel in de kransslagaderen en is in lijn met ons huidige begrip van de mechanismen die betrokken zijn bij plaque progressie en destabilisatie. De belangrijkste bevinding van deze studie is dat de fibreuze kap van patiënten die zich presenteren met een acuut coronair syndroom een lagere *birefringence* toonde in vergelijking met fibreuze plaque kappen in patiënten met stabiel kransslagader lijden. Terwijl de interpretatie van conventionele OFDI berust op subjectieve identificatie van kwalitatieve kenmerken, biedt polarisatie kwantitatieve metingen die kunnen leiden naar een objectieve en automatische karakterisering van atherosclerotische plaques. De verbeterde beoordeling van de plaque samenstelling dankzij de polarisatiemetingen kunnen nieuw inzicht verschaffen in de mechanisme van plaque progressie en destabilisatie van menselijk kransslagaderlijden.

Op dit moment is intravasculaire polariteit gebruikt in zowel humane kadavers als in patiënten om voornamelijk stabiele atherosclerose te bestuderen, maar het is tot op heden onbekend of polariteit van toegevoegde waarde kan zijn in patiënten met onstabiel kransslagaderlijden. Om dit te onderzoeken is de POLARIS-I studie opgezet met als doel om maximaal 35 patiënten te includeren met instabiel kransslagaderlijden (onstabiele angina of een hartinfarct zonder ST elevatie) en een klinische indicatie voor kransslagader onderzoek met OCT/OFDI.

Tijdens de inclusie periode van de POLARIS-I studie presenteerde er zich een unieke patiënt in ons ziekenhuis. Geïllustreerd met de casus beschrijving van deze patiënt trachten we in **hoofdstuk 19** de waarde van de PS-OFDI te illustreren om trombus te bestuderen. Een 69 jaar oude, vrouwelijke, patiënt was verwezen naar ons ziekenhuis voor mogelijke behandeling van een hartinfarct zonder ST elevatie na 8 dagen van variërende pijn. De angiografie toonde een abnormale vulling in het midden van de rechter kransslagader met TIMI III vulling en een matig

stabiele ziekte in de linker kransslagaders. De PS-OFDI toonde een beeld dat gelijkenis toonde met een honinggraat met meerdere intraluminale microkanalen, dit bevestigde dat er een gekanaliseerde trombus aanwezig was. Eerder onderzoek liet zien dat collageen en gladde spiercellen een hoge birefringence hebben en mogelijk kunnen we de PS-OFDI daarom gebruiken om de leeftijd, stabiliteit en andere karakteristieken van kransslagader trombus te bestuderen.

In het laatste hoofdstuk van dit proefschrift, **hoofdstuk 20**, hebben we gebruik gemaakt van het POLARIS-I register om de polarisatie eigenschappen van kransslagadertrombus bij patiënten die zich presenteren met een acuut hart infarct te beoordelen met PS-OFDI. In deze studie hebben we voor het eerst aan kunnen tonen dat de birefringence in genezende kransslagadertrombus significant hoger is wanneer dit vergeleken wordt met verse trombus. Bovendien hebben we geconstateerd dat birefringence afhankelijk is van de leeftijd van de trombus wanneer de tijd tot intravasculaire beeldvorming als parameter wordt gebruikt. Tenslotte werd geen verschil in birefringence gevonden tussen in de kappen van gescheurde plaques en afgelegene vetrijke kransslagader plaques. Tot op heden kon de samenstelling en progressie van trombus alleen betrouwbaar worden beoordeeld met behulp van histopathologisch onderzoek. Histopathologisch onderzoek kan echter niet gebruikt worden in acute situaties. PS-OFDI kan een waardevolle nieuwe beeldvormingsmodaliteit zijn om de leeftijd, stabiliteit en structurele kenmerken van coronaire trombus verder te bestuderen.

Toekomstperspectief

De toekomst van de interventie cardiologie zal waarschijnlijk samen gaan met een aantal veranderingen met betrekking tot intravasculaire beeldvorming en fysiologie. Recente onderzoeken tonen ons mogelijk al aan hoe deze verandering er uit gaat zien. Hoewel de drie overgangen die ik voor ogen heb, afzonderlijk kunnen worden ontwikkeld, in verschillende instellingen of medische bedrijven, uiteindelijk zullen ze bijeen gebracht dienen te worden in het katheterisatielaboratorium om de arts en patiënt te helpen.

Ten eerste moet intravasculaire beeldvorming, voornamelijk IVUS en OCT, vaker gebruikt worden. Grote klinische studies hebben al aangetoond dat nieuwe dotterbehandeling in hetzelfde vat minder vaak nodig zijn wanneer optimale vat dimensies worden bereikt met behulp van IVUS. Verder is het belangrijk dat

interventie cardiologen een beter begrip ontwikkelen over wanneer ze intravasculaire beeldvorming moeten gebruiken en hoe ze dit kunnen interpreteren. Evaluatie na een dotterbehandeling met behulp van beeldvorming is hierbij een cruciale stap en dient zeker overwogen te worden bij patiënten met kransslagaderlijden. Op dit moment zijn intravasculaire beeldvormende katheters duur en worden ze niet in alle landen vergoed. Dit laatste zal ook moeten veranderen als we het gebruik willen verhogen.

Ten tweede zal een meer simplistische interpretatie van (intravasculaire) fysiologie nodig zijn om de hemodynamische significantie van een kransslagadersegment te beoordelen. Er zijn al belangrijke stappen gezet met behulp van zowel hyperemische als niet-hyperemische indexen. Op dit moment worden zelfs vereenvoudigde fysiologische modellen bestudeerd zonder het gebruik van een drukdraad, puur door het gebruik van angiografie en versimpelde vloeistofdynamica aannames. Toekomstige studies zouden deze nieuwe fysiologische modellen in grote gerandomiseerde studies moeten testen, waarbij ook post procedurele beoordeling, bifurcatie vernauwingen en patiënten met verminderde micro vasculaire weerstand bestudeerd dienen te worden.

Ten slotte zullen nieuwe beeldvormingsmodaliteiten de cardiologen niet alleen meer informatie geven met extra geïntegreerde beelden, maar ook complexe computer modellen ondersteunen, met als doel automatisch klinisch relevante segmenten te identificeren die een aanvullende behandeling vereisen. Hedendaagse intravasculaire beeldvorming ontwikkelt zich in een hoog tempo, zodat actuele en klinische kennis over de nieuwste onderzoeken en goed geadviseerde implementatie lastig is. Op dit moment wordt er cumulatief bewijs verzameld over de nieuwe toepasbaarheid van hybride beeldvorming technieken en het vermogen van deze modaliteiten om inzicht te geven in de kwetsbaarheid van onbehandelde kransslagadersegmenten. Hoewel de basisinterpretatie van conventionele beeldvormingsmodaliteiten, zoals IVUS en OCT vooral van belang is, moeten geavanceerde hybride beeldvormingskatheters de cardioloog behandelingsaanbevelingen bieden in plaats van beelden die veel kennis, training en expertise nodig hebben om ze te begrijpen.

Conclusie

De klinische resultaten na een dotterbehandeling verbeteren geleidelijk, hoewel verschillende subpopulaties nog steeds ondermaats presteren. Recent onderzoek toonde aan dat met het gebruik van conventionele intravasculaire beeldvorming en fysiologie, klinische resultaten verbeterd kunnen worden. Ook

nieuwe modaliteiten, bijvoorbeeld op angiografie gebaseerde FFR en hybride beeldvormingskatheters doen een intreden. Desalniettemin is alleen het gebruik van deze modaliteiten niet voldoende om de klinische resultaten voor een patiënt te verbeteren en is het nodig om optimale intravasculaire dimensies met minimaal vaatletsel na te streven. Een behandeling kan suboptimaal zijn als gevolg van verschillende factoren, waaronder stent gerelateerde afwijkingen, zoals malappositie, stent onderexpansie, stentrand scheurtjes, afgesloten zijtakken of resterende geïsoleerde kransslagadervernauwingen. Hoewel sommige afwijkingen negatieve gevolgen kunnen hebben met als resultaat een herkatheterisatie of een hartinfarct, herstellen sommige afwijkingen vanzelf en zal er dus een goed overwogen beslissing moeten worden genomen met betrekking tot mogelijke behandeling. Elke intravasculaire modaliteit, die in staat is om het succes van een behandeling te beoordelen, heeft zijn eigen voordelen en nadelen, waarbij academisch onderzoek en klinische ervaring er voor zal zorgen dat de juiste wordt gekozen op het juiste moment.

Dit proefschrift draagt bij aan de onderbouwing voor het klinische gebruik van intravasculaire beeldvorming en fysiologie. We zijn in staat geweest om de haalbaarheid te onderzoeken voor het post procedureel gebruik van conventionele intravasculaire beeldvormings- en fysiologiestrategieën. We identificeerden post procedurele afwijkingen met het gebruik van OCT, IVUS en FFR en beoordeelden hun impact op de klinische uitkomst. Tot slot hebben we nieuwe beeldvormings- en fysiologiemodaliteiten geïmplementeerd om verder inzicht te krijgen in de samenstelling van plaques en hemodynamische kransslagaderbeoordeling te vereenvoudigen. We hopen dat dit proefschrift bijdraagt aan de volgende stap in de evaluatie van kransslagaderbehandelingen en daarmee de kwaliteit van leven voor de patiënt verbetert.

Epilogue



Phd portefolio

List of publications

Dankwoord/Acknowledgements

About the author

Phd Portfolio

Name PhD student:	Laurens Joannes Cornelis van Zandvoort
Erasmus MC department:	Interventional Cardiology
Research school:	Cardiovascular Research School (COEUR)
PhD period:	March 2018 – June 2020
Title thesis:	Improving PCI Outcomes using Post Procedural Physiology and Intravascular Imaging
Promotors:	Prof. dr. F. Zijlstra
Co-promotor	Dr. J. Daemen

General academic research courses	Year	Workload (ECTS)
Principles of Research in Medicine and Epidemiology (ESP01)	2016	0.7
Clinical Trials (ESP14)	2016	0.7
Fundamentals of Medical Decision Making (ESP70)	2016	0.7
Methods of Clinical Research (ESP10)	2016	0.7
The Practice of Epidemiologic Analysis (ESP65)	2016	0.7
Health Economics (ESP25)	2016	0.7
English Language (SC01)	2016	1.4
Study Design (CC01)	2016	4.3
Biostatistical Methods I: Basic Principles (CC02)	2016	5.7
Methodologic Topics in Epidemiologic Research (EP02)	2016	1.4
Clinical Epidemiology (CE02)	2016	5.7
Biostatistical Methods II: Classical Regression Models (EP03)	2016	4.3
Principles of epidemiologic data analysis	2018	0.7
Advanced topics in clinical trials (EWP10)	2018	1.9
Scientific writing in English (SC07)	2018	2.0
Advanced analysis of prognosis studies (EWP13)	2018	0.9
Pharmaco-epidemiology and drug safety (EWP03)	2018	1.9
Research Seminars (SEM)	2018	0.8

Elective research courses	Year	Workload (ECTS)
Survival Analysis for Clinicians (EWP24)	2017	1.9
Courses for the Quantitative Researcher (SC17)	2017	1.4
Repeated Measurements in Clinical Studies (CE08)	2017	1.4
Cardiovascular Imaging and diagnostics part II	2017	0.5
NIRS-IVUS trainings session	2017	1.0
Missing Values in Clinical Research (EP16)	2017	0.7
Cardiovascular Epidemiology (EP20)	2017	0.9
Methods of Health Services Research (ESP42)	2017	0.7
History of Epidemiologic Ideas (ESP53)	2017	0.7
Erasmus Summer Lectures	2017	0.4
Causal Mediation Analysis (ESP69)	2017	0.7
BROK course	2017	1.5

Oral presentation	Year	Workload (ECTS)
CRT 2018	2018	0.6
Euro PCR 2018	2018	0.6
TCT 2018	2018	0.6

Poster presentation	Year	Workload (ECTS)
CRT 2018	2018	0.6
TCT 2018	2018	0.6

Supervising	Year	Workload (ECTS)
Mentorship for 1 st year medical students	2018	0.6
Supervising 2 nd year medical students in writing a systematic review	2018	0.6

International conferences	<i>Year</i>	<i>Workload (ECTS)</i>
Optics in Cardiology 2017	2017	0.6
CRT 2018	2018	1.5
Euro PCR 2018	2018	1.5
TCT 2018	2018	1.5

Extracurricular activities		<i>Workload (ECTS)</i>
Board member De Geneeskundestudent, representative of Rotterdam	2017-2018	
Organiser Burn-out meeting medical students	2017	
Vice president Talking Medicine congress	2019	

Grants & prizes		<i>Workload (ECTS)</i>
Queridobeurs/Gerrit Jan Mulder Travel Grant 2018-2019	2018-2019	
Erasmus Trustfonds	2018-2019	
Total		56.3

List of publications

- van Zandvoort LJC**, van Kranenburg M, Karanasos A, van Mieghem N, Ouhlous M, van Geuns RJ, et al. Serial quantitative magnetic resonance angiography follow-up of renal artery dimensions following treatment by four different renal denervation systems. *EuroIntervention*. 2017;12(18):e2271-e7.
- Daemen J, Feyz L, **van Zandvoort LJC**, van Mieghem NMDA. Redo renal denervation using a multi-electrode radiofrequency system in patients with persistent therapy-resistant hypertension. *Neth Heart J*. 2017;25(6):359-64.
- Staudacher, II, den Uil C, Jewbali L, **van Zandvoort LJC**, Zijlstra F, van Mieghem N, et al. Timing of coronary angiography in survivors of out-of-hospital cardiac arrest without obvious extracardiac causes. *Resuscitation*. 2018;123:98-104.
- Feyz L, El Faquir N, Lemmert ME, Misier KR, **van Zandvoort LJC**, Budde RPJ, et al. Prevalence and consequences of noncardiac incidental findings on preprocedural imaging in the workup for transcatheter aortic valve implantation, renal sympathetic denervation, or MitraClip implantation. *Am Heart J*. 2018;204:83-91.
- van Zandvoort LJC**, Tovar Forero MN, Masdjedi K, Lemmert ME, Diletti R, Wilschut J, et al. References for left main stem dimensions: A cross sectional intravascular ultrasound analysis. *Catheter Cardiovasc Interv*. 2019;93(2):233-8.
- Ligthart JMR, Masdjedi K, Witberg K, Mastik F, **van Zandvoort LJC**, Lemmert ME, et al. Validation of Resting Diastolic Pressure Ratio Calculated by a Novel Algorithm and Its Correlation With Distal Coronary Artery Pressure to Aortic Pressure, Instantaneous Wave-Free Ratio, and Fractional Flow Reserve. *Circ Cardiovasc Interv*. 2018;11(12):e006911.
- van Zandvoort LJC**, Dudek D, Weber-Albers J, Abizaid A, Christiansen EH, Muller DWM, et al. Intravascular ultrasound findings of the Fantom sirolimus-eluting bioresorbable scaffold at six- and nine-month follow-up: the FANTOM II study. *EuroIntervention*. 2018;14(11):e1215-e23.

8. **van Zandvoort LJC**, Masdjedi K, Witberg K, Ligthart JMR, Tovar Forero MN, Diletti R, et al. Explanation of Postprocedural Fractional Flow Reserve Below 0.85. *Circ Cardiovasc Interv.* 2019;12(2):e007030.
9. **van Zandvoort LJC**, Masdjedi K, Tovar Forero MN, Lenzen MJ, Ligthart JMR, Diletti R, et al. Fractional flow reserve guided percutaneous coronary intervention optimization directed by high-definition intravascular ultrasound versus standard of care: Rationale and study design of the prospective randomized FFR-REACT trial. *Am Heart J.* 2019;213:66-72.
10. Doradla P, Otsuka K, Nadkarni A, Villiger M, Karanasos A, **van Zandvoort LJC**, et al. Biomechanical Stress Profiling of Coronary Atherosclerosis: Identifying a Multifactorial Metric to Evaluate Plaque Rupture Risk. *JACC Cardiovasc Imaging.* 2020;13(3):804-16.
11. Tovar Forero MN, **van Zandvoort LJC**, Masdjedi K, Diletti R, Wilschut J, de Jaegere PP, et al. Serial invasive imaging follow-up of the first clinical experience with the Magmaris magnesium bioresorbable scaffold. *Catheter Cardiovasc Interv.* 2020;95(2):226-31.
12. van Bommel RJ, Masdjedi K, Diletti R, Lemmert ME, **van Zandvoort LJC**, Wilschut J, et al. Routine Fractional Flow Reserve Measurement After Percutaneous Coronary Intervention. *Circ Cardiovasc Interv.* 2019;12(5):e007428.
13. Masdjedi K, **van Zandvoort LJC**, Balbi MM, Gijsen FJH, Ligthart JMR, Rutten MCM, et al. Validation of 3-Dimensional Quantitative Coronary Angiography based software to calculate Fractional Flow Reserve: Fast Assessment of STenosis severity (FAST)-study. *EuroIntervention.* 2019;EIJ-D-19-00466.
14. **van Zandvoort LJC**, Masdjedi K, Tovar Forero MN, Manintveld O, Daemen J. Coronary physiology assessment in a cardiac transplant patient. *Neth Heart J.* 2019;27(7-8):385-6.
15. **van Zandvoort LJC**, van Bommel RJ, Masdjedi K, Tovar Forero MN, Lemmert MM, Wilschut J, et al. Long-term outcome in patients treated with first- versus second-generation drug-eluting stents for the treatment of unprotected left main coronary artery stenosis. *Catheter Cardiovasc Interv.* 2020;95(6):1085-91.
16. **van Zandvoort LJC**, Otsuka K, Bouma BE, Daemen J. Intracoronary polarimetry of a honeycomb-like structure. *EuroIntervention.* 2019;EIJ-D-19-00431
17. Otsuka K, Villiger M, Karanasos A, **van Zandvoort LJC**, Doradla P, Ren J, et al. Intravascular Polarimetry in Patients With Coronary Artery Disease. *JACC Cardiovasc Imaging.* 2020;13(3):790-801.
18. Tovar Forero MN, Scarparo P, den Dekker WK, Balbi M, Masdjedi K, **van Zandvoort LJC**, et al. Revascularization Strategies in Patients Presenting With ST-Elevation Myocardial Infarction and Multivessel Coronary Disease. *Am J Cardiol.* 2020;125(10):1486-91.
19. **van Zandvoort LJC**, Tomaniak M, Tovar Forero MN, Masdjedi K, Visseren L, Witberg K, et al. Predictors for Clinical Outcome of Untreated Stent Edge Dissections as Detected by Optical Coherence Tomography. *Circ Cardiovasc Interv.* 2020;13(3):e008685.
20. **van Zandvoort LJC**, Masdjedi K, Neleman T, Tovar Forero MN, Wilschut J, den Dekker WK, et al. Impact of intravascular ultrasound findings in patients with a post PCI fractional flow reserve ≤ 0.85 on 2 year clinical outcome. *Int J Cardiol.* 2020;317:33-36
21. Tovar Forero MN, Zanchin T, Masdjedi K, **van Zandvoort LJC**, Kardys I, Zijlstra F, et al. Incidence and predictors of outcomes after a first definite coronary stent thrombosis. *EuroIntervention.* 2020;16(4):e344-e50.
22. Tomaniak M, Masdjedi K, **van Zandvoort LJC**, Neleman T, Tovar Forero MN, Vermaire A, et al. Correlation between 3D-QCA based FFR and quantitative lumen assessment by IVUS for left main coronary artery stenoses. *Catheter Cardiovasc Interv.* 2020.
23. Otsuka K, Villiger M, **van Zandvoort LJC**, Neleman T, Karanasos A, Dijkstra J, et al. Polarimetric Signatures of Vascular Tissue Response to Drug-Eluting Stent Implantation in Patients. *JACC Cardiovasc Imaging.* 2020;13(3):790-801
24. **van Zandvoort LJC**, Masdjedi K, Neleman T, Tovar Forero MN, Wilschut J, den Dekker WK, et al. Predictors of post procedural fractional flow reserve – insights from the FFR-SEARCH study. *REC Interv Cardiol.* 2020. (Accepted).

25. Diletti R, Masdjedi K, Daemen J, **van Zandvoort LJC**, Neleman T, Wilschut J, et al. Impact of Post-Stenting Fractional Flow Reserve on Long Term Clinical Outcomes The FFR-SEARCH study. *Circ Cardiovasc Interv*. 2020. (Accepted).
26. Neleman T , Masdjedi K, **van Zandvoort LJC**, Tomaniak M, Ligthart JMR, Witberg K, Vermaire A, Boersma H, van Mieghem NMDA, Daemen J. Extended validation of novel 3D-QCA based software to calculate vessel Fractional Flow Reserve (vFFR). *JACC Cardiovasc Imaging* 2020 (Accepted).
27. Masdjedi K, **van Zandvoort LJC**, Balbi MM, Ligthart JMR, Nuis RJ, Vermaire A, et al. Validation of novel 3-Dimensional Quantitative Coronary Angiography based software to calculate Vessel Fractional Flow Reserve (vFFR) post stenting: Fast Assessment of STenosis severity POST stenting, The FAST POST-study. *Catheter Cardiovasc Interv* 2020. (Accepted).
28. Masdjedi K, **van Zandvoort LJC**, Neleman T, Tovar Forero MN, Kardys I, et al. Validation of post procedural Resting Diastolic Pressure Ratio, Its Correlation With Distal Coronary Artery Pressure to Aortic Pressure, and Fractional Flow Reserve. (Submitted).
29. **van Zandvoort LJC**, Ali Z, Kern M, Mintz G, Daemen J. Improving PCI Outcomes using Post Procedural Physiology and Intravascular Imaging. (Submitted).
30. **van Zandvoort LJC**, Otsuka K, Villiger M, Neleman T, Zijlstra F, et al. Polarimetric properties of coronary thrombus in patients with acute coronary syndrome. (Submitted).

Dankwoord

Promotor Prof. dr. Felix Zijlstra, beste professor Zijlstra, allereerst zou ik u willen bedanken voor alle begeleiding die u me heeft gegeven in de afgelopen jaren. Tijdens de coronaire interventies, maar ook de gesprekken die wij voerden naderhand, bewonderde ik altijd hoe u met een algehele kalmte en vanzelfsprekendheid te werk gaat. Deze uitzonderlijke werkwijze zorgde ervoor dat ik me als jonge student niet overweldigd hoefde te voelen. Uw kennis op het gebied van de cardiologie en de interne geneeskunde heeft mij geleerd dat we de patiënt als geheel moeten zien. Uw deur stond altijd open. Door uw uitnodigende houding heb ik nooit geschroomd om langs te komen. Graag wil ik u bedanken voor het vertrouwen dat u mij al in deze vroege fase van mijn studie hebt gegeven.

Copromotor dr. Joost Daemen, beste Joost, bedankt! Bedankt voor je toewijding, je expertise en de steun die je me hebt gegeven tijdens het promotieonderzoek dat wij samen neer hebben gezet. Het was in mijn tweede jaar van geneeskunde dat ik het geluk heb gehad dat Ron mij bij jou plaatste. Eigenlijk besef ik me nu pas, vele jaren later, hoe onze samenwerking daarin verliep. De eerste versie van ons manuscript leverde ik aan 2 kolommen per pagina, want zo deden ze dat ook in de tijdschriften. Al vanaf ons eerste project stak je enorm veel tijd in mijn leerproces en daar ben ik je ontzettend dankbaar voor. De passie die jij hebt voor je beroep als arts reflecteerde zich in de manier waarop je me begeleidde. Je wist abstracte principes op een elegante en begrijpbare manier uit te leggen. De vele uren die we samen hebben doorgebracht, sparend, reviserend, zullen me altijd inspireren. Je leerde me conceptueel denken over wat ik wil onderzoeken en het vervolgens bondig en zorgvuldig formuleren in een manuscript. Naast de academische vaardigheden die je me hebt bijgebracht ben ik je ook dankbaar voor alle levenslessen die je met me hebt gedeeld. Ik heb het volste vertrouwen dat je nog vele promovendi zult opleiden. Afgezien van de grote stappen die ik heb gemaakt in het academische veld, heb ik nog een lange weg te gaan. Jouw expertise in het cathlab en professionaliteit met patiënten zullen hopelijk altijd een drijfveer voor me blijven. Bedankt voor alles!

Secretaris Prof. Eric Boersma, beste professor Boersma, graag zou ik u willen bedanken voor de lessen tijdens mijn research master en uw expertise op het gebied van de biostatistiek. Verder stel ik het op prijs dat u bereid was om de rol van secretaris op u te nemen.

Beste Prof. dr. Nicolas van Mieghem, allereerst mijn welgemeende dank voor de ervaringen die ik de afgelopen jaren in en rondom het EMC met u heb mogen opdoen. De gedachten aan het charisma waarmee je klinisch patiënten helpt, het

cathlab leidt en onderzoekers vormt, zal mijn ambitie altijd blijven aanwakkeren. Verder zou ik u willen bedanken voor het vertrouwen dat u mij, de Roemeen, al vroeg gaf om de interventiecardiologen te assisteren met de interpretatie van IVUS en OCT.

Dear Prof. Brett Bouma, thank you for the trust in me to start the Polaris-I in Rotterdam. I am truly grateful for the opportunity you gave me to work on this project with your team at the Massachusetts General Hospital. It has been an amazing experience as a researcher and needless to say, as a person.

Verder zou ik de interventie cardiologen van het EMC, Prof. dr. Peter de Jaegere, dr. Roberto Diletti, dr. Jeroen Wilschut, dr. Miguel Lemmert, dr. Wijnand den Dekker willen bedanken. Beste professor de Jaegere, uw immer goede humeur, doch realistische blik in zowel het cathlab als daarbuiten zijn zeer waardevol gebleken. Roberto, Mr. 92%*, bedankt voor je expertise en de samenwerking in een aantal belangrijke projecten. Jeroen, graag wil ik je bedanken voor het aanstekelijke enthousiasme dat jij uit het vak haalt. Iedere keer als je na een procedure nog eens de angio's door zat te nemen en tegen mij zei: "Kom hier eens kijken, dit is uniek!" Miguel, bedankt voor je professionele doch vriendschappelijke houding, jouw zelfverzekerdheid in het cathlab en je parate kennis over de nieuwste literatuur zorgde er altijd voor dat ik het volste vertrouwen had in de procedures. Beste Wijnand, dank voor je hulp bij verscheidene projecten en de hardloopwedstrijd langs de Parijse Seine.

*CTO succes percentages ondervinden mogelijk fluctuatie

Dr. Peter van Hal, uw inspirerende houding om door middel van onderzoek ziekteprocessen te doorgronden en patiënten beter te maken, zijn de start geweest van mijn academische vorming tijdens Junior Med School, dit zal ik nooit vergeten!

Dr. Klootwijk, dankzij uw colleges in mijn eerste jaar van geneeskunde is mijn passie voor het hart ontstaan.

Jurgen en Karen, jullie hebben me bij het begin van dit traject bij de hand genomen, ik kon zo vaak langskomen als nodig was. Die aandacht die jullie me gegeven hebben, heeft ervoor gezorgd dat ik met vertrouwen en zelfverzekerdheid het cathlab in durfde te gaan. Jullie kennis en bereidheid alles te delen t.a.v. intravasculaire beeldvorming en de gang van zaken in dit ziekenhuis, heeft mij enorm geholpen als onderzoeker, maar ook zeker als toekomstig arts.

Dr. Jouke Dijkstra, bedankt voor uw bijdrage aan verschillende projecten en alle

ondersteuning die u geboden heeft.

Dr. Kaneshka Masdjedi, beste Ken, graag zou ik je willen bedanken voor de tweede helft van dit proefschrift, zonder jou was dit boek zeker 50% dunner geweest. Ik ben je enorm dankbaar voor je complementaire karakter, we vormden een perfect duo waarin we fysiologie en beeldvorming konden combineren. Jouw klinische blik bleek een essentieel onderdeel in mijn ontwikkeling en die van dit proefschrift, de chapli kebab niet. Verder zul je altijd een voorbeeld voor me blijven als dokter. De elegantie waarmee jij je vorming tot interventiecardioloog combineert met de fulltime baan als familieman blijft me verbazen, je elfje kan trots zijn. Ik zal altijd met veel plezier terugkijken op onze volledig herschreven epistels, de congressen en onze vriendschap.

Dr. Maria Natalia Tovar Forero, dear Natalia, when you say something too often, it may lose its value, therefore I would like to put it into writing. You are the best! Your Spanish-Colombian temperament and your fear of bicycles gave you a unique personality. You are the one I could always go to, for either clinical, research or personal advice. The limitless motivation and your passionate character will undoubtedly make you one of the best interventional cardiologists. Thank you for everything!

Beste Tara, graag zou ik je willen bedanken voor al je hulp vanuit Rotterdam toen ik aan de andere kant van de wereld was. De hele afdeling, maar voornamelijk Joost, mag van geluk spreken dat je nu onderdeel uitmaakt van het team.

Daarnaast zou ik graag mijn collega onderzoekers van de interventie cardiologie willen bedanken. Lida, wat heb ik een bewondering voor je! Er is niemand die zo consciëntieus en met zoveel toewijding aan een promotie bezig was als jij. Voor niemand is jouw doorzettingsvermogen onopgemerkt gebleven gezien jouw immens lange dagen, zelfs na een paar tegenslagen. Het is echter vooral je liefdevolle karakter dat mij altijd zal bijblijven. Mannen, beste Herbert, Maarten en Joris, bedankt voor de mooie tijd op de afdeling. Vooral bedankt voor de gezelligheid, jullie goede humeur, de borrels en congressen.

Dear Francesca, Paula, Mariusz and Marcello, I am very grateful for the time we spent together in Rotterdam. Thank you for the continuous amusement at lunchtime and the congresses we visited together. Your unique personalities and cultural backgrounds made me realize even more that the world is bigger than just Holland. It is not always easy to work in a foreign country for such a long time, but I truly admire your passion and perseverance.

Francesca, thank you for your never ending smile and your Italian temper. Paula,

you went back to Italy just to take over a few nightshifts at your local hospital. Thank you for showing me what true passion for your work and colleagues is. Mariusz, thank you for the honor to work with you on several projects, we made a great team! Marcello, thank you for your inspiring and hardworking ambition.

Verder zou ik graag de klinische fellows van de interventie-cardiologie willen bedanken: Dr. Koen Ameloot, Dr. Matthew Mercieca Balbi, Dr. Pieter Vriesendorp en Dr. Rutger-Jan Nuijs. Dankzij jullie passie voor het vak heb ik me geweldig op mijn plek gevoeld tijdens mijn periode op de afdeling. Beste Koen, ik bewonder enorm hoe jij je gezinsleven, je baan in Genk en je klinische fellowship hebt weten te combineren. Beste Pieter en Rutger-Jan, bedankt voor jullie enthousiasme en inzet om me onderdeel te laten voelen van het team. Matthew, thank you for your kindness, your knowledge and the ability to combine the latter two to answer all my basal questions that seem so obvious now.

Daarnaast zou ik graag alle technici en verpleegkundige van de interventie cardiologie willen bedanken. Beste John, Angelique, Elco, Alise, Quinten, Thom, Martin en Anne-Marie, graag zou ik jullie willen bedanken voor jullie vermogen om iedere nieuwe onderzoeker de kneepjes van het vak uit te leggen. Hopelijk mag de eierwekker jullie nog jaren wakker houden.

Beste Marianne, Houda, Peggy, Danielle, Shurenska, Alexander en Stefan, allereerst mijn welgemeende excuses voor alle herrie die het PS-OFDI apparaat maakte. Daarnaast zou ik jullie willen bedanken voor al jullie hulp toen ik me als student de interventiecardiologie eigen moest maken. Tot slot waardeer ik jullie adaptieve vermogen om constant interesse te tonen in de nieuwste onderzoeken.

Verder zou ik graag het trialbureau van de cardiologie willen bedanken. Arno en Nico, jullie kennis over de gang van zaken in dit ziekenhuis heeft me enorm geholpen tijdens mijn onderzoeksperiode. Mattie, dank voor al je kennis, expertise en journal clubs. Reon en Dirk, bedankt voor jullie inzet voor de FFR REACT studie. Ik heb het volste vertrouwen dat jullie geweldige academische klinici worden.

Beste Anja, ik ben je enorm dankbaar voor je flexibiliteit, ondanks onze vele verzoeken. De cardiologen mogen in hun handen knijpen dat jij er bent!

My warmest gratitude goes out to the team from MGH who so kindly hosted me during my stay in Boston, Massachusetts. Jian, Taylor, Norman, Szu-yu, Martin, Kenichiro, Nestor, Natalie, Pelham and Boy, thank you for your hospitality. Dear Kenichiro and Martin, the two of you in particular made my stay in Boston productive and enjoyable and I would like to thank you for the opportunity to gain more insight in the technical aspects of optical imaging.

Mannen van het goede leven, Jaap, Flores, Andries, Luca, Kristian, Joshua, George en Steven. Het begon allemaal tijdens de Eureka-week, de daarop volgende periode bij Skadi en natuurlijk onze studie geneeskunde. Met enige weemoed denk ik af en toe terug aan de tijd dat SBL volhing met foto's van onze epische avon(d)turen. Wat hebben we een mooie dingen beleefd en wat ben ik blij dat ik jullie mijn vrienden kan noemen.

Gedurende onze studie geneeskunde en mijn promotietraject heb ik getracht te leven met het motto: doe iets waar je je passie in kwijt kunt, want dat werkt aanstekelijk. Op dit moment zouden we allemaal al in opleiding kunnen zijn tot specialist of zelfs volleerd advocaat kunnen zijn, maar toch heeft iedereen zijn eigen passie gevolgd en dat waardeer ik enorm aan jullie. Of het nu ging om een bestuursjaar, de wereld rondreizen, intensief sporten of jezelf te verbreden in de ruimste zin van het woord, jullie deden het stuk voor stuk en dat maakt jullie uniek.

Liefste huisgenoten, Olivier, Koen, Lennart, Ton, Nadia, Caroline en Tessa, graag zou ik jullie bedanken als huisgenoten tijdens de beste jaren van mijn studietijd. We zijn een prachtig dynamische groep die verbazingwekkend goed bij elkaar past.

Heerendispuut De NUL, het is mij een ware eer jullie als eerste te mogen bedanken in een proefschrift. Jullie hebben me geleerd het leven niet voor lief te nemen, het niet te onderschatten. Het principe, waarmee deze groep heren bij elkaar is gekomen, vind ik nog steeds een prachtig initiatief en ik stel het enorm op prijs hoe we als diverse heren een gedeelde passie kunnen hebben voor het vak geneeskunde.

Beste Hugo, Felix, Michiel en Nino, ik wil jullie bedanken voor jullie verbredende en provocerende karakters. De uitdagende discussies die we altijd voeren, iets wat we op Beekvliet hebben geleerd, zijn een essentieel onderdeel gebleken van dit proefschrift en daar ben ik jullie zeer erkentelijk voor. Al jaren lang zorgen jullie ervoor dat ik niet opgesloten blijf in een geneeskunde bubbel. Ik hoop onze vriendschap nog jaren te kunnen koesteren.

Nog verder terug naar de basis zou ik graag Thijs, Kees, Elske, Floor, Pim, Jannes en Ton willen bedanken. Als jullie dit boek in handen krijgen, zal het waarschijnlijk de eerste keer zijn dat jullie erachter komen waar ik me de afgelopen jaren mee bezig heb gehouden. Dit maakt jullie echter niet minder waardevol in mijn leven. De vriendschap die wij al ruim 20 jaar delen is er eentje die terug gaat naar de essentie, een vriendschap zonder het oordeel van volwassen mensen. Jullie

plezier in het leven maakt mij een beter mens.

Lieve multipotentialist, architect, bachelor, botonist, boulderaar, brouwer, ceremoniemeester, chef, dichter, grafisch ontwerper, kalf, pedaleur, schilder, sous-chef, stoker, thigmofiel, zus, 旅行者, bedankt voor al je hulp en vriendschap!

Liefste Sjoukje, ik heb je leren kennen toen ik aan de voet van de Rinjani dit boek reviseerde. Sinds die tijd help je me met kritische vragen en oprechte interesse. Je onuitputtelijke motivatie en geduld de laatste maanden bleken onmisbaar om het uiteindelijk te finaliseren. Ik ben gefascineerd door je vermogen om me vol vertrouwen door het leven te laten gaan en de rust en balans te vinden die soms essentieel is. Ons samenzijn maakt alle facetten van het leven wonderlijk.

Tot slot zou ik graag mijn ouders willen bedanken, Pap, Mam, een kind kan geen beter paar ouders wensen. Zoals het goede ouders betaamd hebben jullie je minstens zoveel zorgen gemaakt over dit proefschrift en de daarbij behorende sores als ikzelf. Al van jongs af aan hebben jullie geprobeerd me de normen en waarden bij te brengen die voor jullie belangrijk zijn. Ik bewonder enorm hoe jullie je eigen belang volledig weg kunnen cijferen voor anderen en hoe jullie problemen met elegantie tegemoet treden. Eigenschappen die ik ook heb moeten tonen om dit proefschrift tot een goed einde te kunnen brengen. Bedankt voor de onvoorwaardelijke liefde, overgave en steun, jullie favoriete zoon.

About the author



Laurens Joannes Cornelis van Zandvoort was born 14th of January 1995 in 's-Hertogenbosch. He underwent his preparatory scientific education at the categorial gymnasium Beekvliet in Sint-Michielsgestel. Clinical research has been a central theme throughout his bachelor in medicine and even before that. Finishing Junior Med School in 2013 during high school and successfully finalizing his first research project about renal disfunction after a lung-transplantation gave him the opportunity to be admitted to Erasmus MC and it convinced him of his career choice. During the first year of medical school he became a junior research assistant at Erasmus MC dept. of Intervention Cardiology and was involved in several research projects, focusing on renal artery denervation and coronary stents. With the motivation to combine clinical medicine with academic research he applied for the research master in Health Science at the Netherlands Institute for Health Sciences (NIHES) after finishing the bachelor in medicine in 2016. The master program prepared him for an epidemiologic approach to clinical problem within his field of interest – Interventional Cardiology.

The last three years he thrived in several key projects within the interventional cardiology department, all focusing on intracoronary imaging and physiology. In this period he combined the fundamental courses of the research master simultaneously with the research for his dissertation. In 2018 he was granted with the Erasmus Trustfonds and the Gerrit Jan Mulder Prize which allowed him perform additional in-depth research on the polarization sensitive optical frequency domain imaging system, at the Massachusetts General Hospital in Boston, USA. The latter opportunity allowed him to incorporate a technical facet to his biostatistical and clinical research devotion.

Although, research has been a constant factor throughout his medical education, he was able to pursue other interests on relevant topics as well. Already from on his first year in medicine and throughout his masters, he worked as a student assistant, doing weekly shifts at Sophia Children's Hospital, dept. of pediatric oncology. Furthermore, he developed organizing skills through board membership with 'De Geneeskundestudent', where he was able to organize multiple national events for future doctors, such as the personal leadership meeting in Utrecht, the Burnout convention in Rotterdam and finally 'Talking Medicine' in January 2019, a large scale congress in the Jaarbeurs in Utrecht on the future of medicine.

In July 2020 he started his internships for medical school.

Financial support for the publication of this thesis was generously provided by the department of Cardiology Erasmus MC, Acist Medical, Pie Medical and REVA Medical

